SEDIMENTOLOGICAL AND GEOCHEMICAL EVIDENCE FOR LATE QUATERNARY ENVIRONMENTAL CHANGES IN SOUTHERN AFRICA: A CASE STUDY OF THE MUDBELT DEPOSITS OFF NAMAQUALAND

MOLEFI ELLIOT MABOTE

June 1997

SEDIMENTOLOGICAL AND GEOCHEMICAL EVIDENCE FOR LATE QUATERNARY ENVIRONMENTAL CHANGES IN SOUTHERN AFRICA: A CASE STUDY OF THE MUDBELT DEPOSITS OFF NAMAQUALAND

A thesis submitted to the Faculty of Science in Candidacy for the Degree of Master of Science

MOLEFI ELLIOT MABOTE

Supervisors: Associate Professor M. E. Meadows
Department of Environmental and Geographical Sciences

Dr. J. Rogers
Department of Geological Sciences
University of Cape Town

June 1997

Frontispiece : A corer which was used to retrieve cores used in this study

This thesis is dedicated to my mother, 'Mamolefi Mpono Elizabeth Mabote

ABSTRACT

This thesis is comprised of sedimentological and geochemical studies of seven 7m core sediments retrieved from the Namaqualand Mudbelt, South Africa. The purpose of this research is to contribute to the evidence for environmental change during the late Quaternary in the southern Africa from the analyses of continental shelf sediments and more specifically, to examine feasibility of using Namaqualand mudbelts as a key to understanding late environmental dynamics of both terrestrial and marine environment.

Namaqualand mudbelts seem to have been deposited during the last 10 000 years. Chrono- and lithostratigraphy, coarse-fraction and geochemical analyses suggest the following sedimentary development on the Namaqualand offshore:-
An early period of deposition dominated by marine conditions off the coast, but with significant input in the north (Orange Delta) and south (off Kleinsee).

There is a fining upcore sequence from the Orange Prodelta southward to the inner shelf (off Kleinsee). This fining-upward sequence is generally indicative of shoreward transgression of the sea (rising sea-level). As sea-level rises (shoreward transgression), finer-grained deeper water deposits migrate landward and are deposited over shallower water deposits.

While the Orange River might be a major source of sediments on the Orange River Delta, marine contribution is increasingly important far south of the Orange Delta (off Kleinsee). In addition, berg winds and local ephemeral Namaqualand rivers are also increasingly important.

Acknowledgments

It is impossible to acknowledge adequately and specifically the assistance and encouragement rendered by friends and to many people here unmentioned who have contributed, to all of you, I wish to tender my sincere thanks.

I am indebted to my supervisors Associate Professor M. E. Meadows and Dr. J. Rogers for their academic and moral support, advice, patience and considerable time that they have dedicated to this study. I also take this opportunity to thank Associate Professor M. E. Meadows for his permission to present some of his work (Radiocarbon dates) in this research. I would like to acknowledge the financial assistance of a Foundation for Research Development Special Programme grant which facilitated the study. Dr. C. Buhrmann of Institute of Soil, Climate and Weather (Pretoria) deserves special mention for her assistance in the analyses of clay minerals. I gratefully acknowledge the help of the following people at various stages of this research:- Dr. I. K. McMillan of De Beers Marine for identification of foraminifera and constructive criticism of the section dealing with foraminifera; Mr. J. Pether of De Beers Marine for identifying shells and constructive criticism of the section dealing with mollucs; Dr. M. V. Fey of the Department of Geological Sciences at the University of Cape Town for reviewing and constructive critisisms of Chapter Six; the HODSA team, for their fruitful discussion and stimulating insights into this project; Associate Professor J. P. Willis, Mrs S. Govender and Mrs F. Pocock, all from the

Department of Geological Sciences at the University of Cape Town for their analytical work on elements; Mrs S. Sayers for draughting numerous diagrams; Mr C. Mellem for his technical assistance; Mr and Mrs M. Kantoro for communicating to my sponsor on my behalf while I was in Cape Town; my friend, Mr J. Sebakiso for taking care of my various family projects at home while I was away. I also wish to thank my colleagues Ms J. Irving and Ms C. Gray for their support throughout the duration of this research. My best friend, Seboka Mpe is thanked for writing and phoning while I was in Cape Town.

I should like to thank my sisters-in-law, 'Mamosebatho and Polo Kantoro, and my niece Ntaoleng Mabote for their sense of humour which kept me going particularly at critical stages of this research. My brother David Mabote and his family and my sister Motselisi Mabote are all thanked for their moral support during the development of my career.

The most important acknowledgments go to my mother, to whom this thesis is dedicated and my wife, 'Mamohato. I thank my mother for the many years of financial and moral support she has given me. 'My heartfelt thanks go to 'Mamohato who gave me invaluable support and encouragement without which the completion of this thesis could have been impossible.

TABLE OF CONTENTS

LIST OF FIGURES

List of Plates

List of Tables

CHAPTER ONE

INTRODUCTION

1.1 Introduction and Background to the Study

The elucidation of environmental change globally is increasingly regarded as an important goal, since only through knowledge of the way environmental conditions have fluctuated over time may we effectively manage the contemporary environment. Analysis of, for example, pollen in sediments is a most useful tool in the study of environmental changes, and can extend our knowledge of environmental systems and help to establish the sequence of events and the amplitude of the environmental changes that took place in the past. In addition, Meadows (1995) notes that, although environmental changes impact on both terrestrial and marine environments, much data on the nature of the past fluctuations in climate (and their resultant impact on other components of ecosystems) stems from research conducted only in the terrestrial situation. However, because of its general semi-aridity and seasonal climates, records of past environmental changes are relatively sparse in southern Africa and there are comparatively few sites where long continuous sequences of sediments have accumulated and facilitate a detailed reconstruction of environmental history. The continental shelves on the other hand, appear to offer genuine opportunities for tracing environmental change through the late Quaternary through investigations of sediments which have accumulated, derived ultimately from the terrestrial situation. It is against this background that it was found logical to seek new insights into the scale and nature

of past environmental changes in the sediments, derived from the major fluvial systems of the sub-continent and deposited on the continental shelf.

1.2 Namaqualand Mudbelt

As it has been mentioned earlier, the continental shelf sediments derived from fluvial systems of the subcontinent offer opportunities for the reconstruction of palaeoenvironments, and Namaqualand Mudbelt is particularly important because it represents the thickest and the most permanent fine-grained deposits on the west coast of southern Africa. In addition, it is representative of muddy sedimentary bodies supplied by a nearby Orange River.

The study area lies off the northern part of the west coast of South Africa. It constitutes part of a feature known variously as the Namaqualand , Orange River or simply west coast mudbelt (Birch *et al.*, 1986) (Figure 1.1). It extends from the Orange Prodelta to the inner-shelf mudbelt, between the Orange and Buffels River (Figure 1.2). A number of palaeoenvironmental research opportunities manifest themselves within this region:

- The Orange River has been discharging vast quantities of sediment onto the continental margin for about 125 million years, i.e. since West Gondwanaland rifted apart from East Gondwanaland, in the Early Cretaceous (Dingle and Hendey, 1984; Bremner *et al.*, 1990).
- A thickness of over 7 km of sediment has accumulated in this region (Orange Basin) since the Early Cretaceous (Dingle and Hendey, 1984).

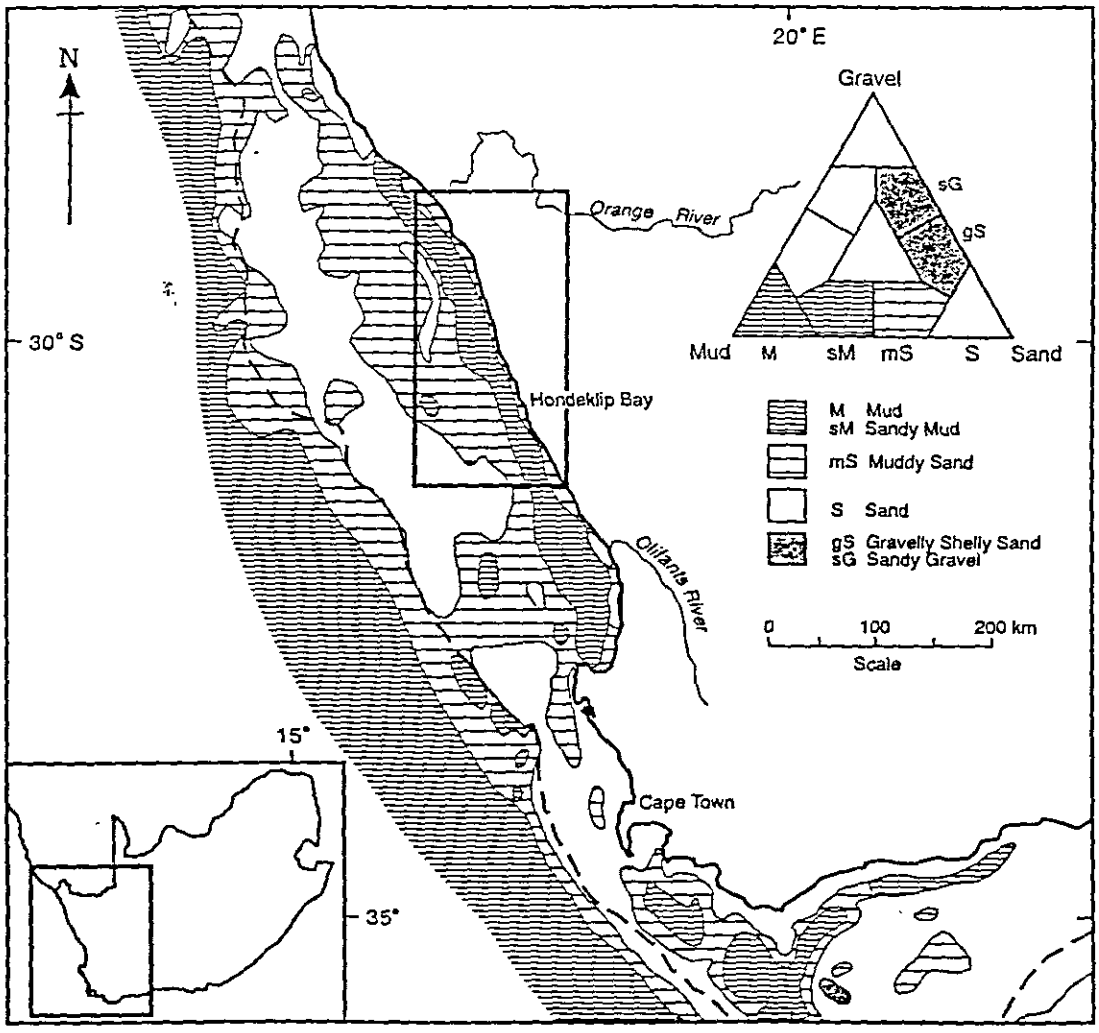

Figure 1.1 - The sediments of the continental shelf off the west coast of South Africa (after Rogers and Bremner, 1990, from Meadows *et al.*, 1997)

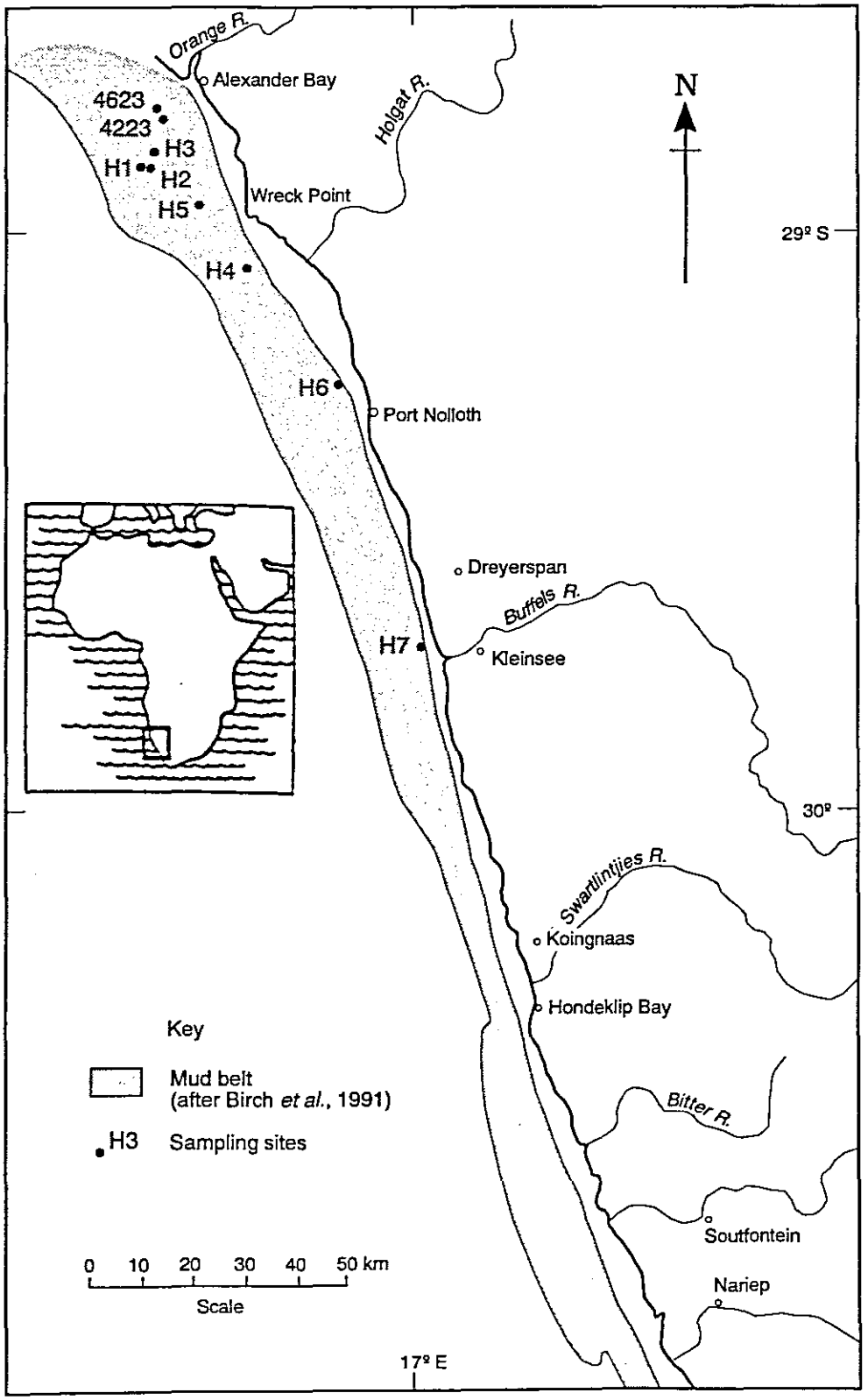

Figure 1.2 Location of sampling sites (From Mabote *et al.*, 1997; Meadows *et al.*, 1997).

- The Orange River drains approximately forty percent of southern Africa's land surface (Dingle *et al.,* 1987), and the west coast mudbelt arguably forms a very important sink for soil eroded from large areas of this sub-continent, in particular, from the Orange River catchment (Rogers, 1977).

It has therefore been assumed that the west coast or Orange River mudbelt represents an ideal source of information on Quaternary environmental changes and landscape dynamics (Meadows *et al.*, 1997).

1.3 Previous Investigations

Although the Namaqualand Coast has attracted scientists of many disciplines since the discovery of diamonds seventy years ago, most earlier regional investigations of the continental margin were undertaken in response to the discovery of diamonds between the Orange River and Kleinsee (Figure 1.2) and at the Groen River Mouth (Hoyt *et. al.,* 1965; 1969) and were mainly concerned with economically interesting gravel (>2 mm) fraction. This resulted in the dearth of information about the fine-grained sediments. Amongst the early researchers in this region are Wagner and Merensky (1928) who took the lead by describing the geology of the deposits exposed in the early prospects along the coast. This was followed by detailed studies by the Marine Diamond Corporation (MDC, now known as De Beers Marine) in 1961. Bedrock topography, sediment distribution and sediment composition on the inner shelf and the Quaternary development of the shelf were studied in detail during MDC's marine prospecting in diamond concession areas (Wright, 1964; Hoyt, *et al*, 1965; Hoyt *et al.*,

1969; Murray, 1969; Murray *et al.*, 1970; O'Shea, 1971). Carrington and Kensley (1969) also made a valuable contribution to the understanding of the mollusc-rich stratigraphy of Namaqualand coastal deposits.

Information on the composition, distribution and deposition of Holocene sediments on the continental margin of southern Africa is provided by several workers. Amongst those who made a significant input to the understanding of production, dispersal and deposition of the Holocene sediments, as well as their significance in the reconstruction of palaeoclimates on the continental margin are Dingle (1973a; 1973b; 1973c), Birch (1975), Rogers (1975), Birch *et al.* (1976), Rogers (1977), Tankard and Rogers (1978), Embley and Morley (1980), Siesser and Dingle (1981), Pether (1983), and Dingle and Hendey (1984).

Recent research off the Namaqualand Coast includes De Decker's (1987) study of the geology of the inner shelf between the Orange River and Wreck Point (Figure 1.2). The continental-shelf sediment provenances, deep-ocean basin sediment patterns, tectono-sedimentary features and the bathymetry of both the South-East Atlantic and South-West Indian Oceans were summarized by Dingle *et al.*, (1987). Verfaille (1987) focused on the innershelf mudbelts, off South Africa, focusing on the Orange River mudbelt. In his Honours Project, Verfaille (1987) characterized sediments in these mudbelts and identified their dispersal patterns. Bremner *et al.* (1990) investigated the dispersal of sediments deposited on the Orange Delta during the major flood of the Orange River in 1988.

A review of the marine-geological data available for the sea floor beneath the Benguela Ecosystem was undertaken by Rogers and Bremner (1991). Woodborne (1991) described the geology and Late-Quaternary history of the inner shelf just north of the Buffels River off Namaqualand.

Most recent research on the continental shelf, relevant to this study, are the works of Bremner and Willis (1993), who investigated the mineralogy and geochemistry of the sediments from the Namibian continental shelf, just north of the study area. Pether (1994) presented a record of the sedimentology, palaeontology and stratigraphy of coastal-plain deposits of the western margin of southern Africa obtained from diamond-mine excavations at Hondeklip Bay (Fig. 1.2).

Gray (1996) conducted a preliminary palynological investigation of the surficial terrigenous sediments of the Namaqualand deltaic mudbelt with the aim of establishing whether the upper sediment of the mudbelt is modern. Her results implied that indeed, the upper sediment is modern. Mabote *et al.*, (1997) presented a summary of the preliminary results of the present research, and related sedimentary structures, texture and composition of mudbelt deposits to depositional and post-depositional processes.

This lack of knowledge, in particular of the <63μm fraction presents the opportunity for further palaeoenvironmental research (Beltagy *et al.*, 1972; Diester-Haass, 1975 and 1976; Johnson, 1979; Lever and McCave, 1983; Pokras and Mix, 1985) within the subdisciplines of sedimentology and geochemistry. Hydraulic-size analysis of the

<63μm fraction in particular, would prove useful in the interpretation of sediment dynamics in the predominantly muddy areas (Felhaber, 1984).

1.4 Aims and Objectives

The broader aim of this research is to contribute to the evidence for environmental change during the late Quaternary in the southern Africa from the analysis of continental shelf sediments. More specifically, to examine feasibility of using Namaqualand Mudbelts as a key to understanding late Quaternary environmental dynamics of both terrestrial and marine environment. The late Quaternary period is the most recent geological time period and therefore the one which most records are clearest and most complete. It is presumed that the amount and type of terrigenous material which is transported from the continent to the ocean reflects changes in the terrestrial environment (Diester-Haass, 1976) which are integrated with fluctuations in the marine situation.

By applying a philosophy of the present approach to environmental analysis, which is basically traditional in the sense that modern depositional environments provide the 'key to the past' in examining stratigraphic successions preserved in the geological record (Leeder, 1982), and principles of sedimentological and geochemical analysis, it is hoped that the following objectives will be realised:

- To establish a detailed chronostratigraphy and test or confirm the Holocene age of the superficial deposits of the mudbelt,
- To establish a detailed lithostratigraphy of the superficial deposits of the mudbelt,

- To examine particle size distribution and composition of the mudbelt sediments,
- To determine and interpret various sedimentary properties which are found in the terrigenous sediments of the Orange Shelf,
- To relate these sedimentary properties to environmental changes, processes in the depositional environment and anthropogenic activities or influence,
- To see whether the muds found on both the Orange Prodelta and the inner shelf of Namaqualand are part of the same modern depositional event or whether they represent different periods of deposition with possibly different mineralogical and geochemical compositions and,
- To investigate the origin of Orange Shelf sediments and where possible, palaeoclimate of the source area and conditions at the environment of deposition through mineralogical, geochemistry and biogenic analyses.

The terms, "terrigenous", "biogenic" and "authigenic" particles are frequently used in this study. Whenever used, the terms should be interpreted as follows:-

- Terrigenous sediments refer to all particles derived from land and transported as solids to depositional basins (Boggs, 1995),
- Biogenic sediments refer to sediments of organic origin, and
- Authigenesis is a general name for the growth of minerals in sediments (Leeder, 1982). It includes both growth of minerals initially present in the sediment and formation of new minerals. Such minerals are termed authigenic minerals.

In summary, this chapter provides a general outline of the aims of this research project which eventually translate themselves into more specific objectives. Generally, the

aim of this research is to deduce environmental changes in the southern Africa from the analysis of continental shelf sediments, with specific reference to the Namaqualand mudbelt. It is proposed in this chapter that the Orange River (or Namaqualand) mudbelt represents an ideal source of information for the reconstruction of late Quaternary environmental changes. Chapter Two now places the Namaqualand mudbelt into its wider regional context.

CHAPTER TWO

REGIONAL SETTING

2.1 Introduction

The nature and style of sediments result primarily from a combination of two phenomena viz. climate (terrestrial and oceanographic), and continental-shelf physiography (Dingle *et al.* 1987). These phenomena need to be outlined as a prerequisite for understanding dispersal and sedimentation on the continental shelf.

2.2 Climate

The climate on the West Coast of southern Africa dictates the quantity and relative proportions of terrigenous, biogenic and authigenic material potentially available for deposition in the sea. Moreover, their discharge, dispersal and sedimentation on the continental shelf are strongly influenced by seasonal and regional variations in meteorological and oceanographical climate. In addition to this, Rogers (1977) notes that long-term meteorological observations of climatic patterns enables one to speculate on possible palaeoclimatic patterns.

A general description of these complex climates, derived from Schulze (1965), is presented in this section, whereas the effect of climate on dispersal and sedimentation of shelf sediments will be discussed in the following chapters.

The climate on the West Coast is largely influenced by meteorological forces that originate offshore in the Atlantic and Southern Oceans (De Decker, 1987).

A stable South Atlantic Anticyclone (high-pressure region) usually lies relatively close to the West Coast, forming anticyclonic conditions at about 30°S, whereas cyclonic cells form in the belt of Westerlies, between 35°S and 40°S (Figure 2.1). These pressure regions experience seasonal shifting (Schulze, 1965; Shannon, 1985; De Decker, 1987; Woodborne 1991).

During summer, the South Atlantic Anticyclone shifts polewards to about 35°S. This shifting causes the sequence of southerly gales, coastal upwelling, fog and arid climate along the west coast (Schulze, 1965). The presence of low-pressure cells travelling south along the west coast during summer increases the pressure gradient at the coast and hence powerful gales result.

During winter, when the South Atlantic Anticyclone has shifted about 5° equatorwards, cyclonic lows travelling eastwards in the Westerlies are able to encroach more directly upon the west coast, with periods of three to six days, creating storm conditions and gale-force northwesterly winds that usually last for several hours (Nelson and Hutchings, 1983). Cyclonic winter rain is precipitated orographically on

the Western Cape mountains and on the Great Escarpment as far north as the Orange River, where it falls as a gentle drizzle.

The aridity of the west coast is primarily due to the lack of summer rains that reach the region from the east coast, the presence of a temperature inversion at 600 to 1800 m and the presence of cold upwelled water at the coast (Taljaard and Schumann, 1940).

The cold upwelled water has an aridifying effect on the coast by condensing the overlying moist sea air, and forming coastal fog banks. This condensation limits coastal moisture capacity and enhances the stability of the inversion. The aridity of the Namaqualand coastal plain is evident in the low undulating topography of Pleistocene and Holocene parabolic and brachanoid dunes (Tankard and Rogers 1978), stabilised by xerophytic scrub cover (Strandveld) that attest to the persistence of strong desiccating southerly winds and suggest greater aridity during Pleistocene hypothermals (glacials).

2.2.1 Winds

The climate of the West Coast is also influenced by winds which affect the dispersal and deposition of sediments off the coast. The significance of winds (through climatic changes) on the discharge, dispersal and deposition of terrigenous sediments onto the continental shelf cannot be over-emphasized.

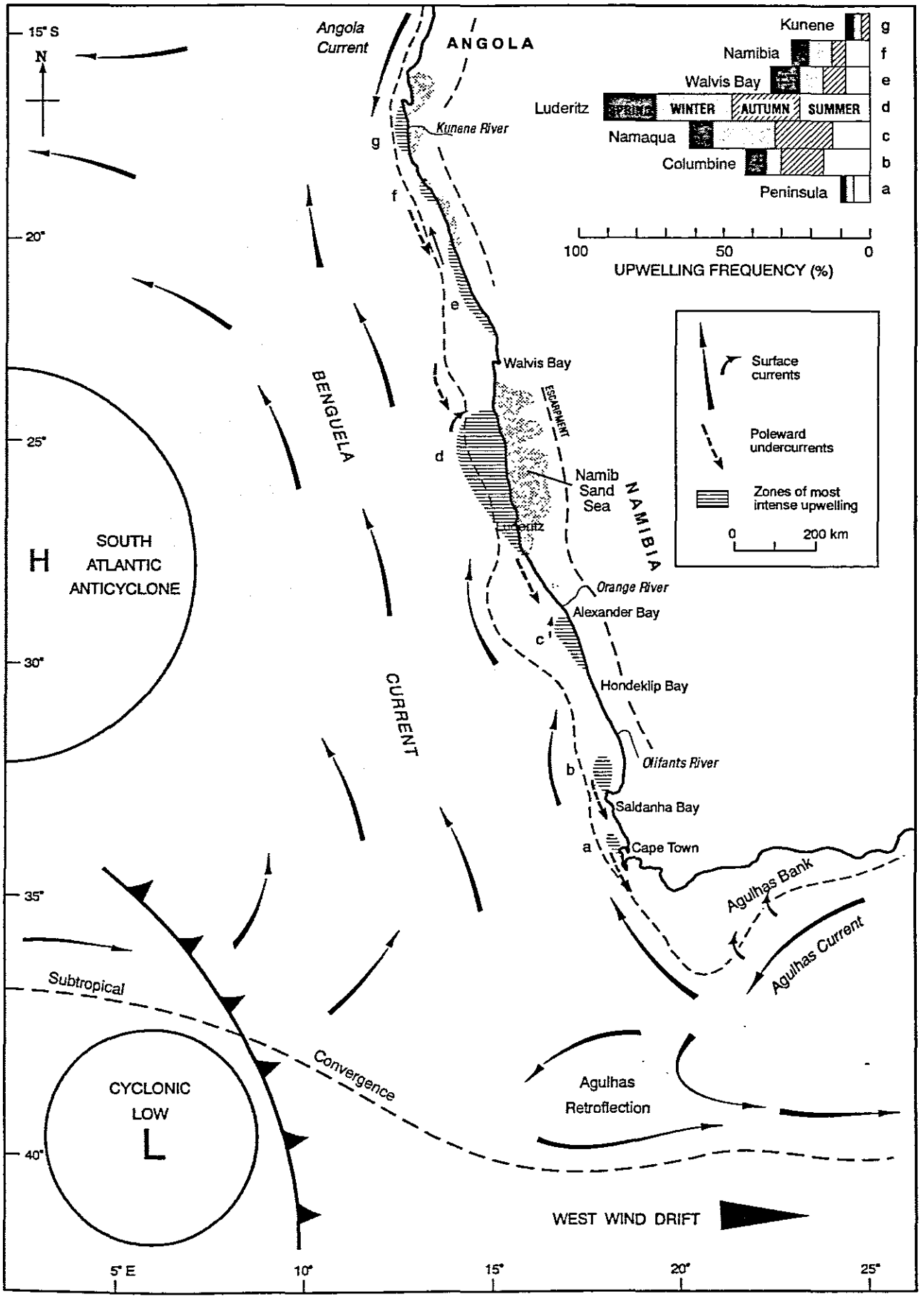

Figure 2.1 Synoptic and meteorology of the west coast of Southern Africa. Inset histogram shows frequency of upwelling cells a - g (after Pether 1994).

During summer, the West Coast is affected by strong southerly winds in the form of a curved anticyclonic flow associated with the South Atlantic High (Figure 2.1). This curved anticyclonic flow is guided by the coastline, because of the aridity of the coastal plain acts as a thermal barrier to cross flow (Nelson and Hutchings, 1983) and by orography of the continental escarpment.

The climatology of the West Coast is further affected by warm, offshore winds known as "bergwinds" and the passages of coastal low-pressure cells. Bergwinds occur most commonly during autumn and spring.

A large high-pressure system forms periodically over the interior of the subcontinent (southern Africa) as stated by Shannon and Anderson (1982). This high-pressure system causes air to move offshore from the interior, warming in the process. These adiabatically-warmed bergwinds entrain large volumes of sediment and hence make a significant sediment contribution to the shelf (Shannon and Anderson, 1982; Woodborne, 1991). Shannon and Anderson (1982) give an estimate of 50 x 10^6 tonnes for a single event and this is of the same order of magnitude as Bremner *et al.* 1990; Bremner and Willis (1993) estimate (60x 10^6 tonnes) of the Orange River'smean annual sediment input to the sea.

Shannon and Anderson (1982) found, from Lansat -3 satellite images, that plumes of wind-blown sediment may extend up to 150 km offshore, in a southwestward direction, halfway across the continental shelf. The direction of these plumes is determined by the climatic conditions giving rise to bergwinds and the orientation of

dry river beds. These winds, which migrate as coastal lows, form between Alexander Bay and Lúderitz at the approach of Westerlies cyclones (low-pressure cells) and travel down the coast (Kamstra, 1985) at a speed of about 750 km per day (Taljaard *et al.*, 1961). These coastal lows are confined by the escarpment and by subsidence inversion. The warm offshore flow occurs ahead of the low, while cool, onshore flow and foggy conditions follow the passage of the calm centre. The coastal fog, which is a common occurrence, due to the strong land/sea thermal contrast, plays an important role in the ecology of the plants in the Namib, including the Namaqualand coastal plain, as it supplements the meagre winter precipitation in the form of "mist rain", which usually condenses and falls during the night.

Namaqualand coastal winds intensify during the day, due to the sea-breeze effect as the land warm up and veer towards the south or southwest depending on location and season (Shannon, 1985). This author notes that winds are generally strongest during summer and Kamstra (1985) reports an annual average wind speed of 5-6m/s at Port Nolloth, in the study area.

2.2.2 Rainfall

Rainfall is responsible for erosion more particularly in the Upper Orange catchment (including Lesotho) and this enables the Orange River to discharge vast quantities of sediment onto the western continental margin of southern Africa. Rainfalls of both the Namaqualand coast and in the effective Orange River catchment are discussed in this section.

(a) Namaqualand Coast

Wellington (1933) describes the Namaqualand coast as an arid winter-rainfall desert. An average annual rainfall of 62mm is reported at Port Nolloth (Woodborne, 1991), which is the rainfall station within the study area. This low precipitation is supplemented by advective sea fog which occurs frequently on the coast and falls in the form of "mist rain" as mentioned above.

(b) Vaal-Orange Catchment (Effective Catchment)

The Orange River, which drains a major portion of southern Africa (Hoyt *et al.*, 1969; Embley and Morley, 1980), discharges large quantities of sediments onto the western continental margin of southern Africa and has been doing so for the last 125 million years (i.e. since Africa separated from South America, there was no South Atlantic Ocean before that) (Dingle and Hendey, 1984; Bremner *et al.*, 1990).

In order to gain an insight into the origin, erosion and dispersal of sediments transported by the Orange River, attention must be given to the rainfall of the effective catchment. Rainfall is one of the major factors that control sediment production (Mabote, 1994). A brief analysis of the rainfall pattern in the effective Orange River catchment is presented, to provide a background for understanding the erosional and depositional processes that are active in the catchment as well as around the river-mouth area and the Orange Delta. This section is derived chiefly from Rogers (1977), who gave a comprehensive review of rain formation in the Orange River catchment area.

The Orange River is one of the world's major rivers (Rogers, 1977) and it is the only river in the subcontinent to receive its rainfall on the eastern side of the continent and to discharge via the west coast (Bremner *et al.*, 1990) (Figure 2.2). The Lesotho headwater is always considered the main source of the Orange River, with its source in the Drakensberg Highlands of the Eastern Lesotho at the Mont aux Sources (2926m above sea level) (Wellington, 1955; Bremner *et al.*, 1990; Bremner and Willis, 1993).

The Orange River is 2 173 km long if measured from its spring near Mont aux Sources to its mouth at Alexander Bay (Bremner *et al.*, 1990). The total catchment area of the Orange River drainage basin is estimated to be 953 200 km^2 (Dingle and Hendey, 1984), but of this, only about 35% (i.e. approx. 333 620 km^2) has a significant runoff (McMillan, 1987). This is due to the fact that much of the northern part of the catchment lies in the Namib and Kalahari Deserts, whereas portions of the southern part are situated in the semi-arid Karoo. Like other subtropical rivers, the Orange River has a highly erratic discharge fed by summer rainfall (Rogers, 1977) and, when considered together with its main tributary, the Vaal, it delivers a mean annual runoff of 11.1 x $10^9 m^3$ and 17 x $10^6 m^3$ of sediment to the South Atlantic Ocean (Bremner *et al.*, 1990).

The Orange River is divided into the Upper Orange, above the Vaal confluence, the Middle Orange between the Vaal confluence and Aughrabies Falls and the Lower Orange between the Falls and the sea (Wellington, 1955) (Figure 2.2).

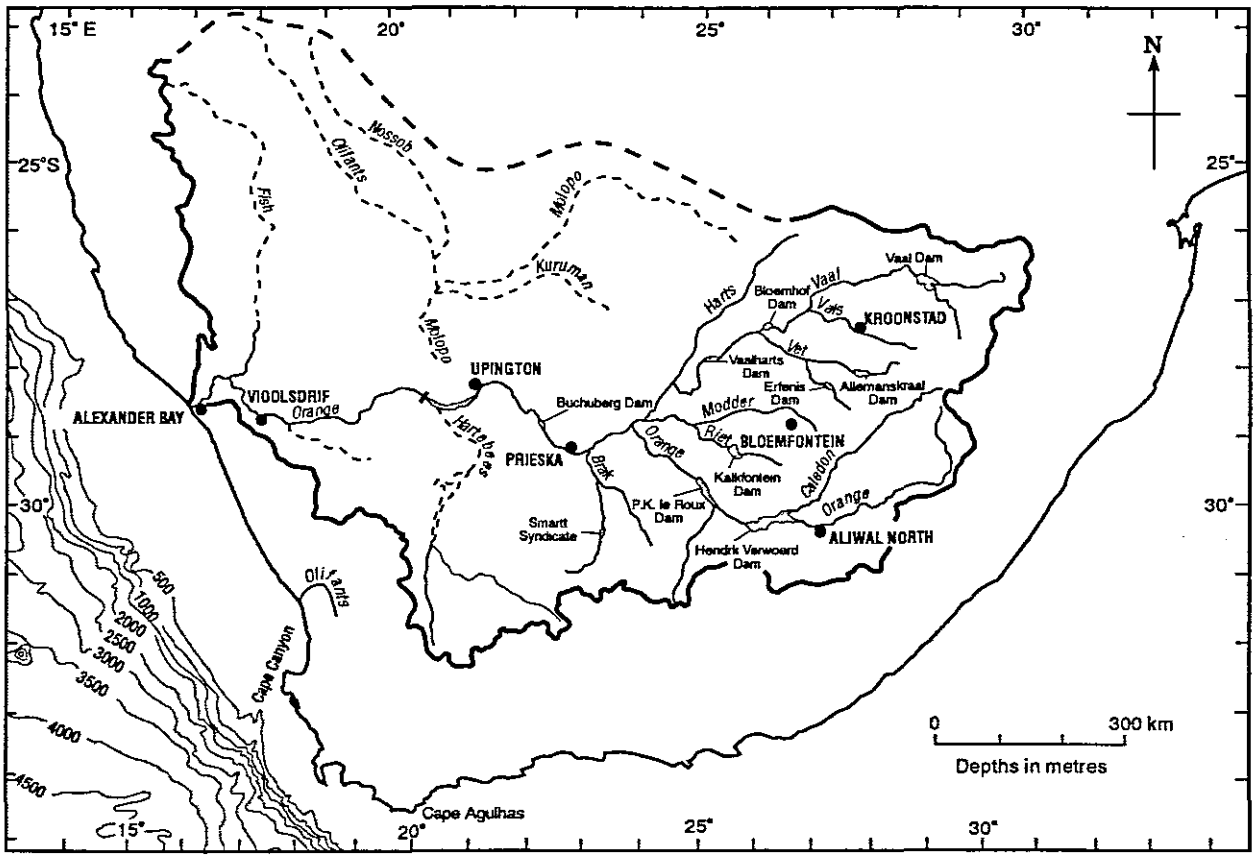

Figure 2.2 Orange River Catchment (after Bremner *et al.*, 1990).

Rain-Forming Mechanism

During summer, the Indian Ocean anticyclone lies well to the east of South Africa and this permits maritime air to penetrate beyond the Drakensberg. This results in the formation of orographic rain which precipitates over the headwaters of the Vaal and the Upper Orange River (Figure 2.2). If the Indian Ocean anticyclone maintains a stable westward position beside the east coast in summer, the rain-bearing winds cannot reach the interior and hence droughts result.

The high pressure-belt is found at the surface over both oceans and the continent in winter, leading to dry conditions inland. However, equatorward shifting of the westerlies brings the southwestern and southern coast into the path of the storm track of the Southern Ocean's westerlies. De Villiers and Sóhnge (1959) state that this cyclonic winter rain is precipitated orographically on the Western Cape mountains and on the Great Escarpment as far north as the Orange River, where it falls as a gentle drizzle.

As the Inter-Tropical Convergence shifts polewards with the sun in summer, tropical convectional rain moves polewards. This mechanism is responsible for bringing rain to the catchment of the north-bank tributaries of the Orange River and to the intermittent rivers of Namibia draining into the Namib Desert (De Villiers and Sóhnge, 1959). These authors note the erosional effect of a rare summer thunderstorm as far south as Vioolsdrif on the Lower Orange River (Figure 2.2).

2.3 OCEANOGRAPHY OF THE BENGUELA ECOSYSTEM

The Benguela Ecosystem is one of the four major eastern-boundary current regions of the world, namely, the California, Peru, Canary and Benguela Current Systems. The Benguela Ecosystem is found on the western continental margin of southern Africa. This region is characterised by cold, nutrient-rich upwelling water that supports an abundant biota.

A brief review of the water properties and current systems is presented in this section to provide background for understanding the composition and distribution of sediments in subsequent chapters. An analysis of storm-wave conditions is presented in an attempt to understand the textural distribution of uncosolidated sediments on the continental shelf.

2.3.1 Currents

2.3.1.1 Upwelling

There is a broad region of upwelling off the West Coast associated with the Benguela Current. Upwelling is defined by Jury (1981) as a compensating current for offshore transport of surface waters by long offshore wind stress (Ekman transport). This compensating current brings cold nutrient-rich subsurface water to the ocean surface and enhances productivity in the euphotic zone (O'Brien, 1983; Naidu and Malmgren, 1995). The combined effect of both the frictional stress of the Southeast Trade Wind on the sea surface, and the effect of the Earth's rotation (Coriolis Force), causes the

surface waters to move northwestwards away from the coast (i.e. causes offshore deflection). This deflection is accompanied by vertical movement (upwelling) of oxygen-depleted bottom water from depths of 200 to 500m as a compensatory mechanism. This northward and westward flow of surface currents (Figure 2.3) off the West Coast allows this deeper, cool (8°-16°C), low-salinity (34.6-35.0‰) water to well up to the surface with little or no loss of its characteristic water properties (Embley and Morley, 1980) and this creates a nutrient-rich zone with high biotic productivity. Upwelling to the surface depends on the strength of the coastal winds.

Although upwelling occurs along the entire coast (Figure 2.1), its intensity varies in time and space. It varies mainly as a function of the seasonality of the wind regime, but also due to modification of the latter by the coastal topography and thermal regime, whilst shelf bathymetry influences the movement of upwelling water across it (Shannon, 1985; Pether, 1994).

The most marked seasonal variation in the upwelling is in the south of the Olifants River, where the modulation of the South Atlantic Anticyclone Circulation by the westerlies is greatest, and hence suppresses upwelling-favourable winds in winter (Shannon, 1985). Farther north, upwelling is persistent throughout the year with a minimum in autumn and a maximum in spring. Upwelling occurs more frequently and intensely from the Orange River northward to Lúderitz (Figure 2.1), where wind speeds are highest than elsewhere along the coast (Schulze, 1965).

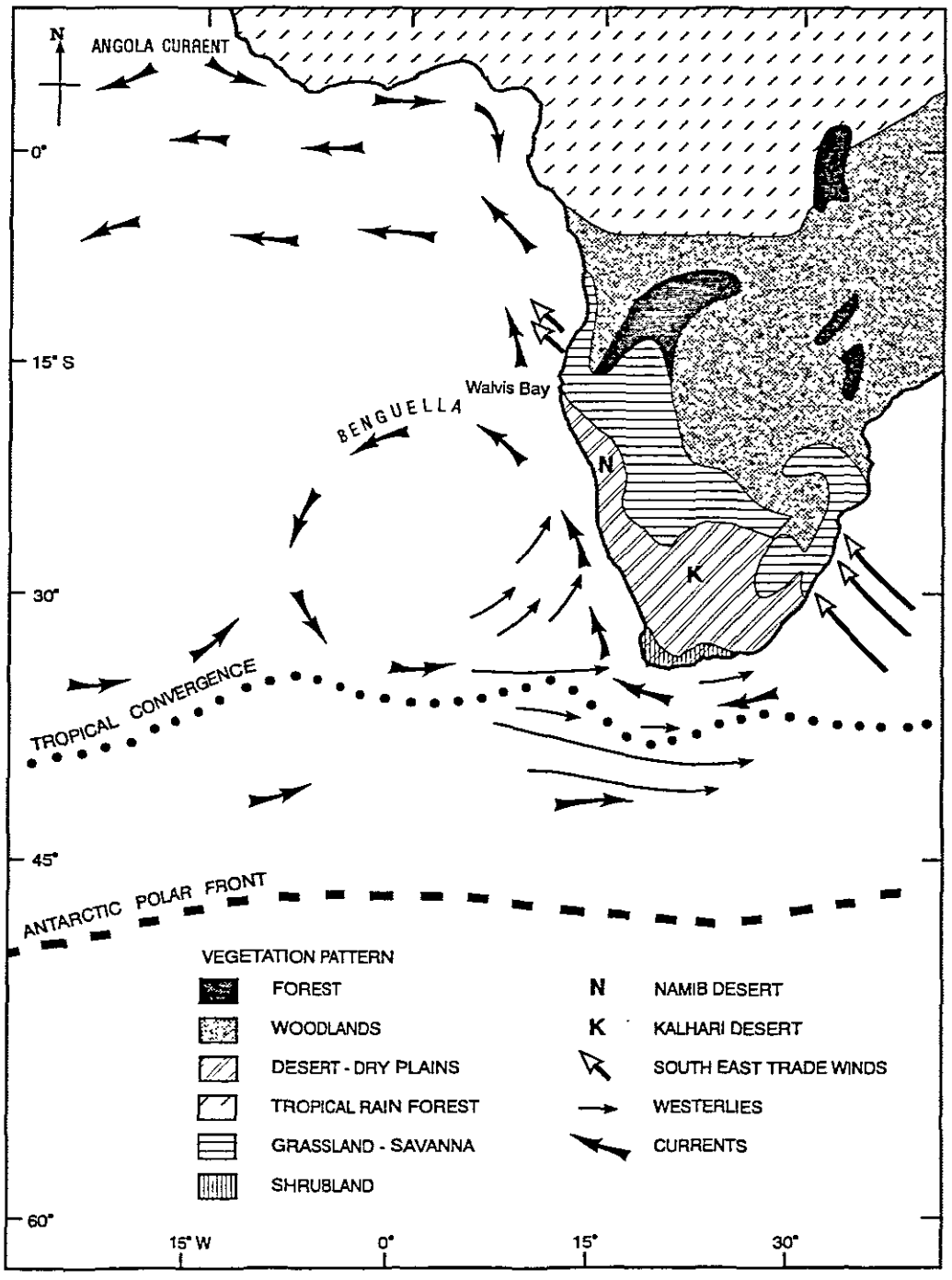

Figure 2.3 Surface currents, wind patterns and climatic zones of Southern Africa. Vegetation patterns basically reflect rainfall patterns (after Embley and Morley, 1980).

The study area lies in the Namaqua Upwelling Zone. Off Namaqualand, the Namaqua upwelling cell (Cell c) is present for about 60% of the time (Shannon, 1985) (Figure 2.1).

2.3.1.2 Poleward Undercurrent

Hart and Currie (1960), De Decker (1970) and Nelson (1989) have identified a very weak southward-flowing countercurrent underneath the Benguela Current, which is often referred to as the poleward undercurrent or the Benguela Undercurrent. This poleward undercurrent, which is found along the inner shelf, compensates for water removed from the 200 to 500 m level by perennial upwelling (Hart and Currie, 1960; Nelson, 1989). Evidence of the existence of the poleward undercurrent is provided by the advection of low-oxygen water as far south as the Orange River from Angola (Nelson, 1989). The average speed of this poleward undercurrent is about 5km/day and the shallowestisobath at which it has an effect varies but it can be generally regarded as being below 100m (Nelson, *Pers. comm.* 1997).

2.3.1.3 Benguela and Angola Currents

The northward-moving Benguela Current encounters the southward-moving Angola Current near the Kunene River mouth (Figure 2.1). Unlike the Benguela Current, the Angola Current is nutrient-poor, warm, saline and oxygen-deficient. The interaction between these two currents periodically results in mass mortalities of plankton and fish in the Walvis Bay region (Copenhagen, 1953) (Figure 2.1).

The distinction between the Benguela Current and the South Atlantic Trade Wind Drift around the Anticyclone can be drawn off Cape Town. This Drift lies over the shelf break, west of the Benguela Front (Birch *et al.*, 1976). There is intermittent development of south-setting surface currents close to the coast and these are ascribed to the Angola Current, north of Walvis Bay. South of Lüderitz, these currents are ascribed to northwesterly winter gales (Birch *et al.*, 1976). The persistence of the poleward undercurrent is also evident over the inner shelf. The poleward undercurrent affects the southward dispersal of suspended material (mud), which is deposited mainly in a long, coast-parallel mud-belt extending from the Orange Prodelta to St Helena Bay (Rogers, 1977; Birch *et al.* 1986; and Rogers and Bremner, 1991). This mudbelt is the focus of this study.

Rogers (1977), Bremner *et al* (1990) and Rogers and Bremner (1991) describe, in detail the influence of the wave and current regime in the fate of sediment delivered to the sea by the Orange River. These authors note that the sharp textural change in sediments north and south of the Orange River mouth is ascribed to waves and coastal currents. Rogers (1977) proposed that this textural change indicates that most of the terrigenous sand and gravel issuing from the Orange River is transported by northward-moving littoral drift, whereas the south-southeasterly moving poleward undercurrent transports terrigenous mud in suspension southward off the Orange River. This undercurrent is responsible for the extensive terrigenous mudbelt that continues southward for about 500 km along the inner shelf to St Helena Bay (Rogers 1977, Birch *et al.*, 1986; Bremner *et al.*, 1990; Rogers and Bremner 1991).

2.3.2 Productivity

The whole West Coast falls under the influence of the Benguela Current which is a cold watermass of extremely high productivity (Pollock and Beyers, 1981).

Andrews (1974) states that periodic calms during the summer months and reversals in wind direction in the equinoxes, cause marked variations in the nutrient content of the water. The resulting abundant nutrients in the upwelled waters make these waters the most productive in the world (Birch *et al.*, 1976). In spite of upwelling being most intense off the Bogenfels-Lúderitz region, where wind speeds are highest, productivity is highest towards Walvis Bay viz. 3.8 grams/m^3 (Steeman-Nielsen and Jensen, 1957 from Bremner, 1977). The high input of organic matter to the bottom sediments and its bacterial and chemical decomposition deplete the bottom water of oxygen and lead to anaerobic conditions, off Walvis Bay (Figure 2.1).

2.4 Oxygen, Salinity and Water Temperature

Oxygen levels, salinity and water temperatures affect the preservation of organic matter and hence are of vital importance in understanding the distribution of bottom sediments on the continental margin. A full account of these factors is presented in Rogers (1977). A cursory review of these factors will be presented in this section which is derived chiefly from Rogers (1977). Figure 2.4 summarises oxygen, salinity and temperature distributions off Orange River during periods of pronounced and reduced upwelling.

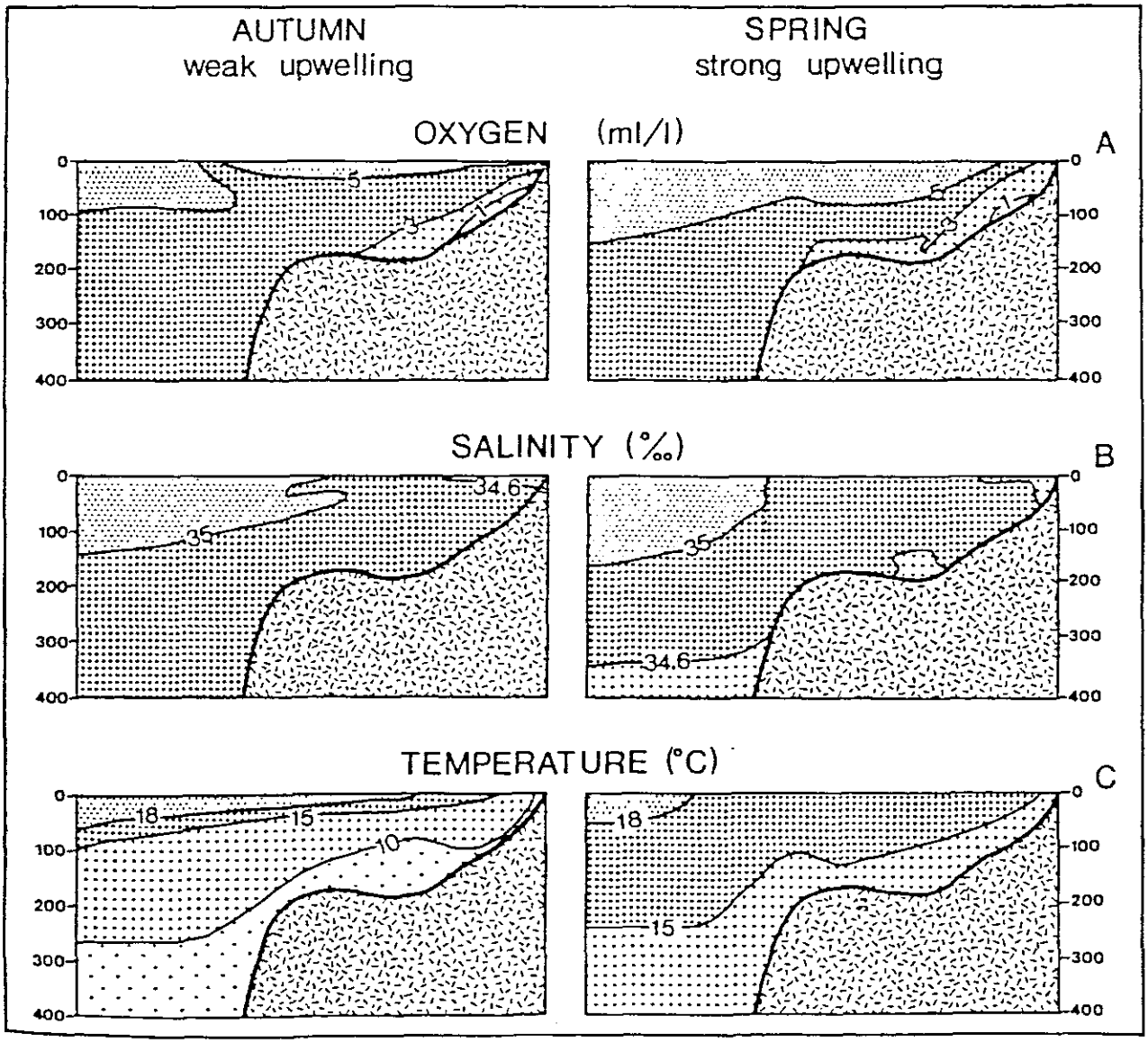

Figure 2.4 - Non-conservative properties of the continental-shelf water off the Orange River (modified from Rogers, 1977, from De Decker, 1987)

2.4.1 Oxygen

There is a seasonal fluctuation of interface between the oxygen-rich Benguela Current and the oxygen-deficient Angola Current with significant consequences for both marine organisms and biogenic sediments.

The formation of the 50 m-thick oxygen-minimum layer off the Congo River is attributed to three causes: 1) oxidation of dead plankton and their excreta (organic matter) while sinking through the water column; 2) respiration of oxygen by living plankton; and 3) chemical and bacterial decomposition of organic-rich biogenic sediments.

Oxygen is replenished mainly from the atmosphere at the air-sea interface in the mixed-surface layer. Phytoplankton also produces oxygen via photosynthesis. However, because plankton-rich water is less transparent to the light required for photosynthesis, this mode of oxygen is inhibited. In addition, thermocline stability helps to conserve the oxygen-poor water within it by hindering vertical mixing (Rogers 1977).

When upwelling ceases to replenish oxygen and calm conditions inhibit mixing in the surface layer, continuing oxidation of sinking organic detritus, respiration of plankton and decomposition of organic-rich sediments lead to upward expansion of the bottom layer of oxygen-poor water. When this oxygen-deficient layer reaches the surface, mass mortalities of plankton, nekton and birdlife result (Birch 1975, Birch *et al.* 1976; Rogers 1977). Rogers (1977) notes that this additional influx of organic detritus

accelerates the consumption of oxygen until anaerobic conditions occur, particularly in the interstitial waters of the sediments. Under such conditions, organic matter is not oxidized and accumulates on the sea floor (Rogers, 1977). Formation of pyrite and gypsum under similar conditions during Neogene is proposed by Siesser and Rogers (1976).

The poleward undercurrent has a greater influence north of the Orange River. This is evident from the fact that oxygen-deficient water is more extensive off Sylvia Hill than Orange River.

2.4.2 Temperature

Water with temperatures ranging from as low as 8°C during upwelling to about 16°C during quiescent (or downwelling periods) extends along the coast and up to 225 km offshore in winter and spring, and hence temperature gradients are correspondingly less pronounced (Pollock and Beyers, 1981; De Decker, 1987). This occurs when north-westerly winds push warm offshore surface waters towards the coast and suppress the upwelling of cold water. In summer and autumn, temperatures are higher and therefore temperature gradients are greater due to solar heating of surface water. Offshore, the coldest water (< 10°C) is found below 100m in spring (Bailey, 1979).

2.4.3 Salinity

Bailey (1979) notes the complexity of both salinity and temperatures above 200m water depth. He points out that salinity and temperature depend largely on:

1) whether an incursion of "oceanic water" has taken place; 2) whether upwelling has recently taken place, in which case "coastal water" will exist; 3) or whether quiescent conditions exist.

Like temperature and oxygen concentrations, salinity varies with seasonality. The seasonal variation of innershelf region salinity follows that of temperature, being lowest at about 34.90% (-100m) during the spring upwelling period (Figure 2.4). Low salinities occur near the Orange River mouth. These are localised effects caused by dilution of the sea water with river water, particularly after summer rains. The influence of the Orange River input is clearly indicated by the low-salinity tongue extending offshore (Hart and Currie, 1960). This low salinity is also found under weak upwelling conditions (De Decker, 1987).

2.5 Offshore Geology

This section gives a brief description of the salient features of sedimentation along the inner shelf off Namaqualand in order to give a better perspective to the ensuing description of sediment in the study area.

The bedrock of the inner shelf along the Namaqualand Coast is composed of Late Precambrian basement. This Precambrian basement continues between 2 and 10 km offshore onto which lap the shallow seaward-dipping Upper Cretaceous sediments of the middle shelf which dip seawards at a shallow angle (De Decker, 1987; Woodborne, 1991) 100 to 110m isobaths (Rogers, 1977). The Upper Cretaceous

rocks are the oldest marine deposits offshore covering the Precambrian basement Rocks (De Decker, 1987).

Regional studies by O'Shea (1971), Birch (1975), Birch *et al.* (1976), Rogers (1977), Birch *et al.*, (1986), De Decker (1987), Bremner *et al.*, (1990), Rogers and Bremner, (1991) and Woodborne (1991) indicate the presence of a prominent continuous wedge-like body of acoustically transparent mud, which lies south of the Orange Delta. This is a Holocene deposit of mud introduced onto the shelf by the Orange River and carried to the south by the poleward-flowing undercurrent. This deposit is about 25m thick along the inshore edge where it lies against the steep seaward slope of the inner-shelf bedrock and across the inner-shelf-middle shelf boundary in water depths between 60 and 90m (De Decker, 1987).

Another sediment body which averages 6m in thickness and consists of silty sand and shells, with occasional gravels near the base of the sequence, is present north of the delta and lies inshore of a series of bedrock ridges just seaward of the surf zone (De Decker, 1987).

2.6 Bathymetry

A detailed description of the bathymetry and surficial cover of the western continental shelf is presented in a trilogy of theses (Birch, 1975; Rogers, 1977; Bremner, 1977). Dingle *et al* (1987) comprehensively summarise the bathymetry of both the Southeast Atlantic and the South West Indian oceans in two charts at a scale of 1 : 3 200 000.

The most recent detailed bathymetry is presented by Woodborne (1991), however, this only covers a portion of the study area (i.e. between Kleinsee and Port Nolloth).

A general description of the morphology of the inner shelf is presented in this section. The aim is to give perspective to the more anomalous nature of the inner shelf in the study area.

(Birch *et al.* (1976) and Rogers (1977) have defined the inner shelf as a region along the coast underlain by pre-Mesozoic rocks. In contrast, De Decker (1987) prefers to define the inner shelf as the region between the coast and the shoreward edge of a terrigenous mudbelt that is continuous for most of the west coast. Rogers (1977) and Birch *et al.* (1991) term this the Orange River mudbelt. Where the mudbelt is absent, De Decker (1987) uses the 50m isobath as the boundary. His argument is that the inner-shelf slope (i.e. bedrock forming the relatively steep seaward slope of the inner shelf) generally dips beneath unconsolidated sediments at this depth.

In this study, the inner shelf is considered as the region along the coast underlain by pre-Mesozoic basement. De Decker (1987) states that the major part of the inner shelf is at a depth of 20-40m with a gradient of less than 0.5^0. Woodborne (1991) calls this low-grading region the "inner-shelf platform". Beyond this region, the "inner-shelf slope" grades down more steeply beneath the mudbelt (Figure 2.5).

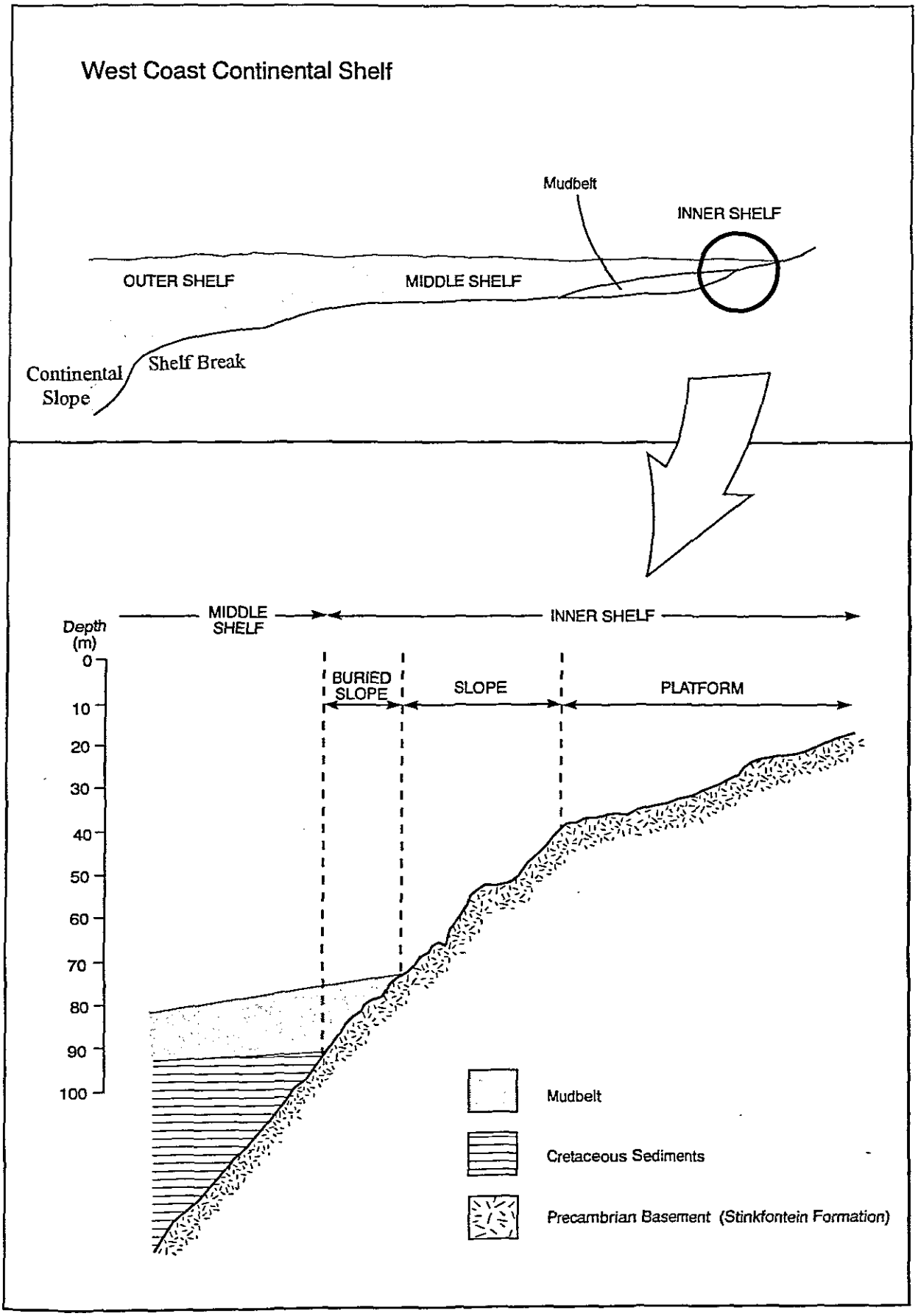

Figure 2.5 Bathymetric nomenclature for the West Coast continental shelf (from Woodborne, 1991).

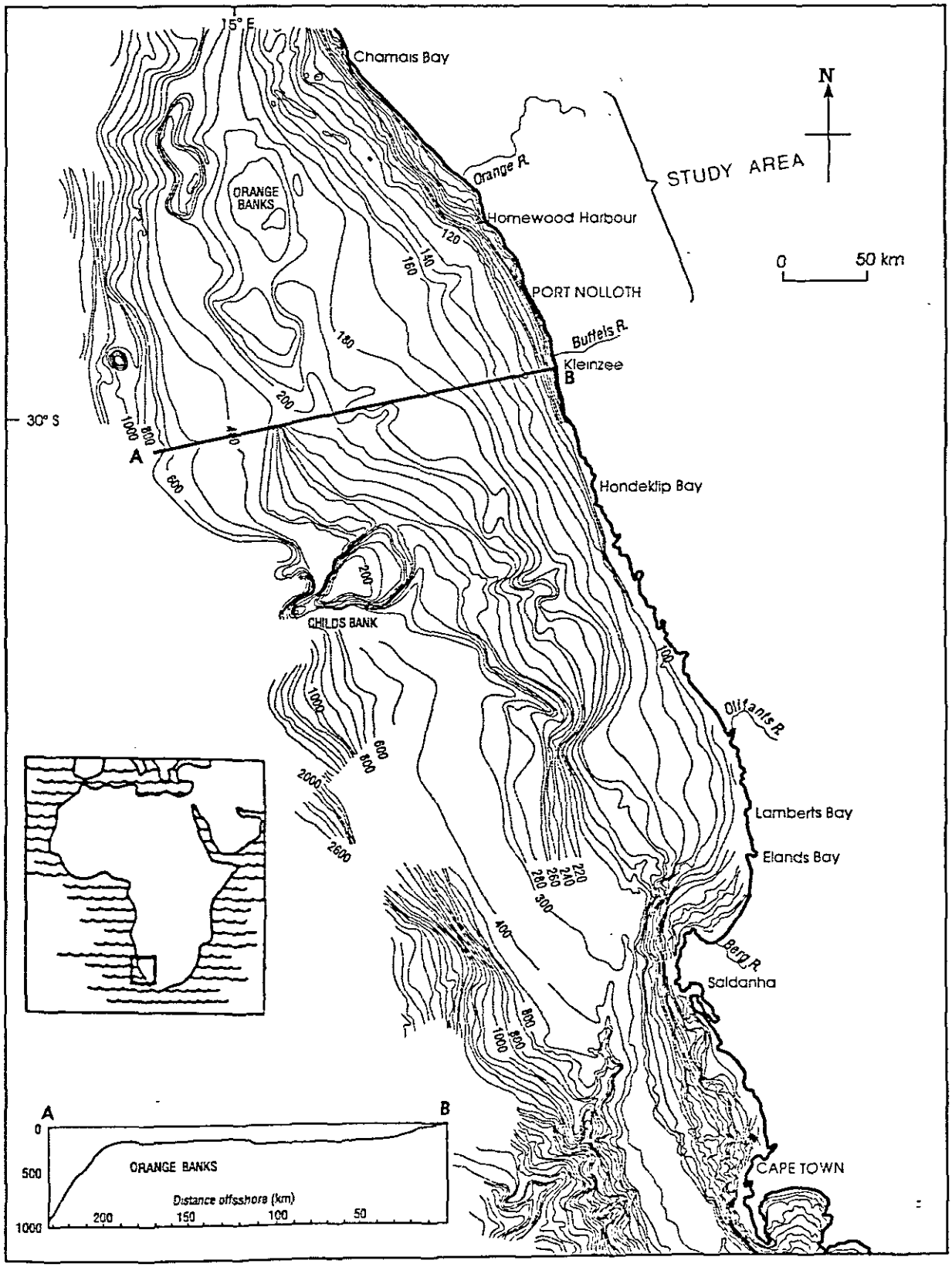

Figure 2.6 Bathymetry of the west coast margin (from Dingle *et al.*, 1976, adapted after Woodbourne 1991) and location of the study area.

The middle shelf lies seaward of the inner shelf. The boundary between the inner and middle shelves occurs at a depth of about 110m and can be identified by a distinct wave-cut terrace.

The middle shelf grades into the outer shelf, whose outer boundary is the shelf break. Below the shelf break lies the continental slope (Birch *et al.*, 1976). Bathymetric nomenclature used for the west coast continental shelf is shown in Figure 2.5. Although these terms are not rigorously defined in this study, they do, however facilitate description.

The western continental shelf can be divided into three parts viz. the Orange Shelf (between Hondeklip Bay ($30^0$30'S) and Chamais Bay (26^0S), The Walvis Shelf (north of Lúderitz (27^0S)) and a transitional section off Chamais Bay, where the shelf is at its narrowest (Birch *et al.*, 1976; Rogers, 1977). The thrust of this section will be the Orange Shelf since the study area is within this shelf.

The Orange Shelf bulges seaward (up to 180km wide, where the Cretaceous submarine delta has developed (Dingle and Hendey, 1984)) off the mouth of the Orange River with a shelf break at 200m north of the Orange River, but it deepens to about 500m southward, where a distinct inner shelf break also occurs at 200m (Birch *et al.*, 1976).

The outer shelf is at about 160m depth on the Orange Banks, (Figure 2.6) whereas the middle shelf is as deep as 190m (Bremner, 1977; Rogers, 1977). Between the Orange

and the Buffels Rivers, the inner shelf is mostly covered by sediments of the Orange Delta (Dingle, 1973a). Firm sediment is found on the sandy delta front, whereas soft sediment is found on the muddy Prodelta farther seaward, as well as its narrow extension to the south (Rogers and Bremner, 1991).

The study area is on the inner shelf off the Orange River and extends along the coast southwards to just north the of the Buffels River. Figure 2.6 depicts the bathymetry of the west-coast continental margin.

2.7 Onshore Topography (Rivers)

The rivers are major sources of terrigenous input into the oceans. This input is directly influenced by climatic factors, which control rainfall and the extent of the rivers' catchment areas. A brief summary of rivers draining into the study area is presented in this section.

Three major rivers are on the West Coast viz. the Orange, Buffels and Olifants Rivers. The first two rivers are in the vicinity of the study area.

The Orange River, which has already been discussed in detail in the preceding section, is the major perennial river which flows in the vicinity of the study area. It has a vast catchment area and drains the summer-rainfall region to the east. The Orange River contributes about 93% of the total sediment input on the west coast (Dingle *et al.*, 1987).

The episodic Buffels River is considered to be the second major river in the vicinity of the study area. It is an intermittent river which flows in times of exceptionally heavy rain in the arid west coast region (Rogers, 1977). The Buffels River has a catchment area of 9 375 km^2 and discharges an average annual sediment load of less than 50 $tons/km^2$ (Heydorn and Tinley, 1980). This river floods occasionally and Woodborne (1991) reports the most recent pre-1991 flooding event as being in May 1986.

Because of the modern interglacial aridity onshore, other ephemeral Namaqualand rivers rarely, if ever flow. They, thus, effectively, provide no sediment input to the South Atlantic Ocean.

To summarize, this chapter outlines climate (terrestrial and oceanographic) and physiography (hydrology and geology) of the study area (Namaqualand mudbelt) within the wider context of the southern African region. Chapter Three presents methods and techniques for data collection and analyses.

CHAPTER THREE

DATA COLLECTION AND METHODS

3.1 Introduction

The aim of this chapter is to provide details of the various approaches, methods and techniques used in this study. Where deem necessary, a justification for the choice of approach, method or technique will be given.

3.2 Fieldwork

3.2.1 Sampling Strategy and Procedures

Ten grab samples of surficial sediment and seven large-volume gravity cores, up to 6m in length, were retrieved from the Orange Prodelta southwards the inner-shelf terrigenous mudbelt between the Orange and Buffels Rivers, off the Namaqualand coast (Figure 1.2) in May, 1994 during a cruise of the South African Navy's Hydrographic Research Vessel, *SAS Protea* (Dingle, 1994; Meadows *et al.*, 1997). The sampling strategy was to obtain cores and surface grab samples of mudbelt sediment extending as far back through the Late Quaternary as possible, the idea being that cores from the outer, seaward, margin of the mudbelt, where sedimentation rates are presumed to be lower, would enable the chronological record to be extended further back in time, while Cores from the landward margin would provide a higher-

resolution record covering a shorter time period (Dingle, 1994; Meadows *et al.*, 1997). Samples were taken well below the influence of wave-induced currents, wave-base for a 10-second wave being 78m as shown in equation below:

$$L_o = 1.56\ T^2\ (m)$$

$$L_o = 1.56x100\ (m)$$

$$= 156m$$

$$\text{Wave-base} = L_o/2 = 78m$$

Where L_o = deepwater wavelength, T is wave period in seconds (Boggs, 1995).

Table 3.1 provides precise geographical locations of samples extracted, water depth at sampling localities and the lengths of each core. The depth of cores H6 and H7 is comparable with the wave-base for 10-second swell, while other cores are at depths less than the wave-base of 12-second swell. According to Professor F. Shillington (Pers. comm.), the wavelength of will certainly have an impact on the sedimentation processes. The 12-second swell will relatively disturb sedimentation processes more that the 10-second swell.

3.2.2 Data Collection

Ten Surface samples were obtained with a Shipek rotation grab sediment sampler, and the cores were taken with the aid of a 7m-long, 300mm-diameter gravity corer manufactured specifically for the task (Dingle, 1994). The extracted cores were cut onboard into 1m lengths and each length was split into two halves. One half was kept as an archive section while the other half was designated as the working half. The archive section of each 1m length was scraped perpendicular to the core-length, with a broad knife, to reveal undisturbed sediment structures, described, photographed in

resolution record covering a shorter time period (Dingle, 1994; Meadows *et al.*, 1997). Samples were taken well below the influence of wave-induced currents, wave-base for a 10-second wave being 78m as shown in equation below:

$$L_o = 1.56\,T^2\,(m)$$

$$L_o = 1.56x100\,(m)$$

$$= 156m$$

$$\text{Wave-base} = L_o/2 = 78m$$

Where L_o = deepwater wavelength, T is wave period in seconds (Boggs, 1995).

Table 3.1 provides precise geographical locations of samples extracted, water depth at sampling localities and the lengths of each core. The depth of cores H6 and H7 is comparable with the wave-base for 10-second swell, while other cores are at depths less than the wave-base of 12-second swell. According to Professor F. Shillington (Pers. comm.), the wavelength of will certainly have an impact on the sedimentation processes. The 12-second swell will relatively disturb sedimentation processes more that the 10-second swell.

3.2.2 Data Collection

Ten Surface samples were obtained with a Shipek rotation grab sediment sampler, and the cores were taken with the aid of a 7m-long, 300mm-diameter gravity corer manufactured specifically for the task (Dingle, 1994). The extracted cores were cut onboard into 1m lengths and each length was split into two halves. One half was kept as an archive section while the other half was designated as the working half. The archive section of each 1m length was scraped perpendicular to the core-length, with a broad knife, to reveal undisturbed sediment structures, described, photographed in

Table 3.1 - Geographical co-ordinates of sampling locations showing depth at sites and length of cores extracted (from Meadows *et al.*, 1997)

Site	Core	Grab	Latitude °S	Longitude °E	Water depth (m)	Core length (m)
H1		↑	28°52.67′	16°20.75′	117	
H1	↓		28°52.59′	16°20.71′	117	0.60
H2		↑	28°52.53′	16°21.29′	116	
H2	↓		28°52.53′	16°21.30′	115	6.03
H3		↑	28°51.22′	16°21.88′	103	
H3	↓		28°51.27′	16°21.87′	104	5.76
H4		↑	29°03.43′	16°35.07′	115	
H4	↓		29°03.38′	16°35.15′	115	5.40
H5		↑a	29°00.24′	16°35.67′	119	
H5		↑b	28°57.18′	16°28.24′	119	
H5		↑c	28°54.25′	16°25.51′	113	
H5	↓		28°57.26′	16°28.72′	118	2.52
H6		↑	29°16.10′	16°50.71′	78	
H6	↓		29°16.03′	16°50.38′	78	5.90
H7		↑	29°42.16′	17°00.71′		
H7	↓		29°42.12′	17°00.69′	80	5.65

Notes: ↓ indicates coring site. ↑ indicates grab sampling site.

colour (Appendix A) and then stored in custom-built wooden crates. Appendix B summarises core-lithology descriptions based on the preliminary shipboard observations made by Dr. J. Rogers and supplemented by Dr. R. V. Dingle's observations from the colour photographs, taken by Dr. Rogers onboard.

3.2.3 Sediment Sampling

The working halves of the cores were sub-sampled onboard at 5cm intervals using a specially manufactured, 1m-long, stainless-steel core-divider. Two sets of subsamples were obtained: 200 ml was immediately stored frozen in air-tight plastic jars for subsequent work on volatile organic complexes, and the rest (~600 ml) was stored in air-tight plastic jars at ambient temperatures until they were subsampled for a wide range of physical (this study and Gray, 1996) and chemical analyses in the laboratory by G. W. Bailey of South African Sea Fisheries Research Institute.

3.3 Laboratory Procedures

3.3.1 Grain-Size Analyses

A complete flowchart of the analytical laboratory procedures performed on the sediment is shown in Figure 3.1. A detailed discussion of these procedures is given in Appendix C. The proportions of gravel, sand, silt and clay were determined by the author on dialyzed, salt-free subsamples by wet sieving with a 63μm screen to separate the coarse and fine fractions. A 2 mm screen was used to sieve the dried coarse fraction to separate gravel and sand. The wet fine fraction was analysed by the

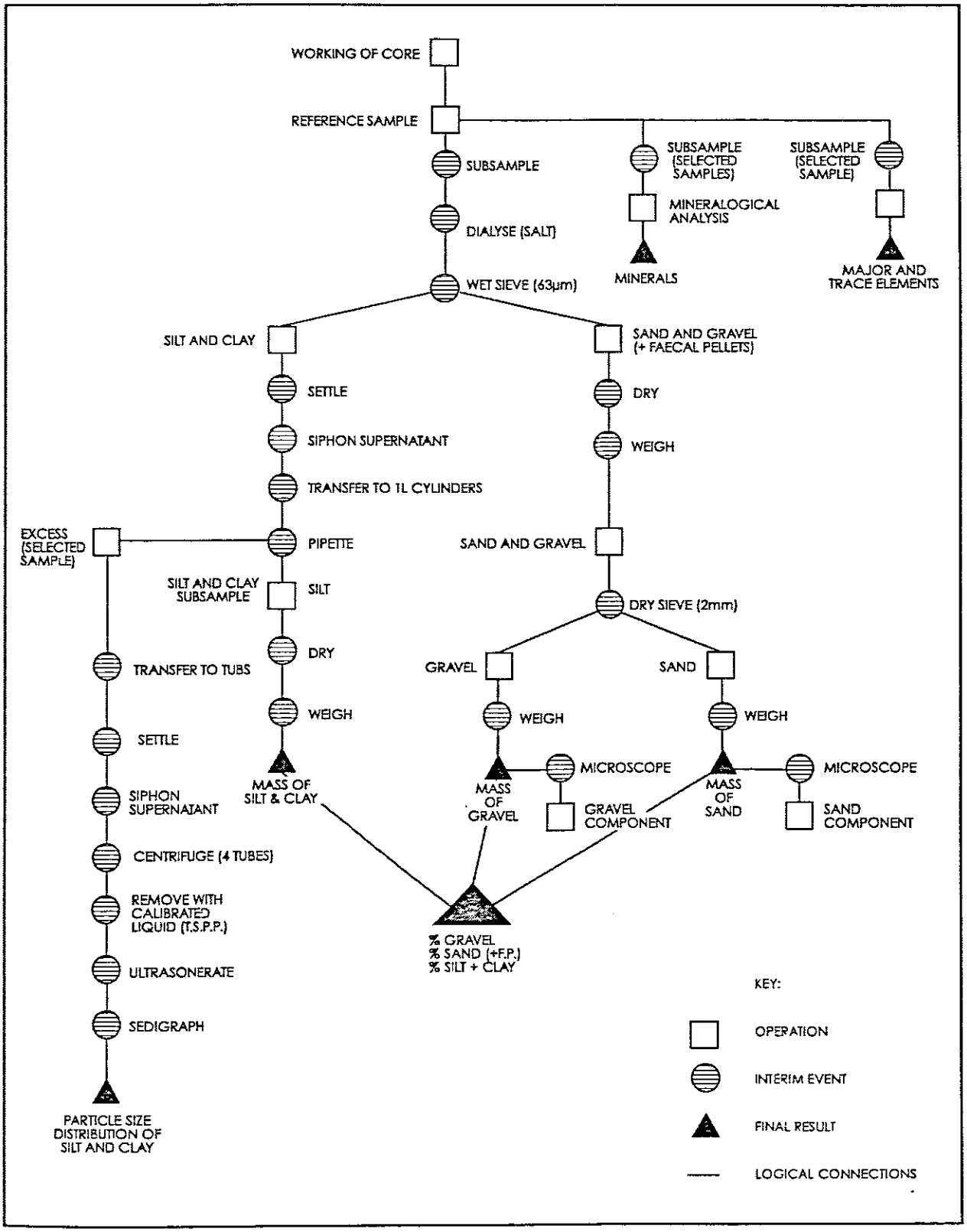

Figure 3.1 Flow chart of analytical laboratory procedures

author with an Andreasen Pipette (Anonymous, 1967) and a computerized Sedigraph 5000D to determine the proportions of silt and clay on selected subsamples.

3.3.2 Radiocarbon Dating of Core Samples

Twenty-four of the core and grab samples, were radiocarbon dated to reveal chronostratigraphy of the cores (Meadows *et al.* 1997). The ages were determined on the organic carbon. The organic content of the sediment was thought to be generally low (Rogers, 1977; Rogers and Bremner, 1991), and hence the samples were submitted untreated for age-dating by ACCELERATED MASS SPECTROMETRY (AMS) radiocarbon-dating, rather than conventional radiocarbon dating, at the National Ocean Sciences AMS Facility (NOSAMS) at the Woods Hole Oceanographic Institute, in Massachusetts, U.S.A.

3.3.3 Sediment Composition

The composition of the coarse-fraction (gravel and sand) was investigated by the author by examination under a binocular microscope. Coarse-fraction components were identified and their abundance estimated semi-quantitatively using the method of Ingram (1965). This method determines the size distribution, shape and roundness of the terrigenous fraction by binocular-microscope examination of subsamples of the coarse-fraction placed on a comparison-sampling tray. The terms **dominant** (> 50%), **subordinate** (5- 50%), **minor** (<5-1%) and **trace** (<1%) are used to describe the relative abundance of these components, terrigenous, authigenic and biogenic.

- **Unscaled Radiographs (positives) showing laminated muds from sections of (cores H2 and H3) and homogeneous muds (core H7) respectively.**

PLATE 1

3.3.4 X-ray Examinations of cores (Radiography)

The archived half of each core was X-rayed for the author at the South African Museum and X-ray negatives were developed into radiograph positives (Plate 1). These X-radiographs simplify the determination of sedimentary properties and facilitate the interpretation of changes in the depositional environment by revealing sedimentary structures (Axelsson, 1983). X-radiographic techniques employ absorption of x-rays, which is dependent upon the wavelength of the radiation, the density and thickness of sample, and the atomic number of the absorbing material. This means that inhomogeneities in the sediments will cause variable darkening of the x-ray film, and then the qualitative information given by the radiographic image may be quantified by densitometric evaluation (Axelsson, 1983). X-radiographs from three cores are presented and discussed in this thesis as being typical of the sequences observed.

3.3.5 Scanning Electron Microscopy

Selected specimens of coarse-fraction components were hand-picked by the author with the aid of a binocular microscope, gold-plated and examined at high magnifications using the JEOL JSM-5200 Scanning Electron Microscope (SEM) at the South African Museum, under the supervision of Ms Linda Bissett. Large shells were photographed for the author by Mr C. Mellem using a Pentax 30T camera.

3.3.6 X-Ray Diffraction Analysis

A total of 120 samples was subsampled at 10cm-intervals (1-6 m) in cores H2 and H7. These subsamples were analysed for clay mineral composition for the author by Dr. C.

Buhmann of the Institute for Soil, Climate and Water, in Pretoria. These subsamples were analysed on a Philips X-ray Diffractometer operated at 45 kV and 50 mA, at a scanning rate of 1° 2θ min^{-1}, using a Co target and graphite monochromator. Diffractograms were recorded from 2-35° θ.

The ground samples were dispersed by ultrasonic agitation and the clay (< 2μm) fractions were separated by centrifugation. Clay fractions were then saturated with $MgCl_2$ or KCl solutions, by shaking them in solution for one hour. The solution was then allowed to stand overnight to equilibrate. They were then freed of excess salt by repeated washings. Orientation of the clay was achieved by the suction through method (Gibbs, 1965, in Buhmann, 1994). Expansion tests were performed by solvation with ethylene glycol (vapour at 60°C for 24 hours) (Novich and Martin, 1983, in Buhmann, 1994). Potassium-saturated samples were analysed in the air dried state as well as after heating to 300°C and 550°C.

3.3.7 X-Ray Fluorescence Analysis

A total of twenty-three samples from both cores H2 and H7 were submitted to the department of Geological Sciences at the University of Cape Town for geochemical (element) analyses. These samples were chosen in such a way as to best represent various sedimentary units identified. The samples were analysed for ten major elements together with H_2O and Loss on Ignition (LOI) (which consists of CO_2, organic matter and water), and eighteen trace elements.

Nine major elements Fe, Mn, Ti, Ca, K, P, Si, Al and Mg were determined semi-quantitatively using fusion disks prepared according to the method of Norrish and

Hutton (1969 in Willis, 1996). The disks were analysed on a Phillips PW1480 wavelength dispersive XRF spectrometer with a dual target Mo/Sc x-ray tube. Iron, Mn, and Ti were measured with the tube at 100 kV, 25 mA. The other elements were determined with the tube at 40 kV and 65 mA. Peak only measurements were made on the elements Fe through Mg. Sodium was determined using powder briquettes, the tube at 40 kV and 65 mA, with backgrounds measured at -2.00 and +2.00° 2θ from the peak position.

Eighteen trace elements were determined on powder briquettes in a series of a analytical runs using a number of different X-ray tubes. Figure 3.2 is a sample preparation and analytical flowchart. Full details of these procedures are given in Appendix F.

In summary, this chapter provides details of the various approaches, methods and techniques used in this study. Chapter Four presents radiocarbon dates results.

CHAPTER FOUR

CHRONOLOGY -TIME SCALE

4.1 Introduction

For more than 40 years radiocarbon dating has proved a valuable tool in Late Quaternary studies. It has been used to study the chronology of soil and sediment development (Wang *et al.*, 1996). By providing numerical age control on stratigraphy, radiocarbon dating affords determination of the timing (time-scale) of erosional and depositional events and makes possible the calculation of the rate and magnitude of environmental, geomorphic (Martin and Johnson, 1995) and sedimentological change. While these radiocarbon dates or ages afford generally reliable chronometric control (Haas *et al.*, 1986), their significance is sometimes a perplexing problem (Perrin *et al.*, 1964; Gilet-Blein *et al.*, 1980; Geyh *et al.*, 1983; Scharpenseel and Becker-Heidmann, 1991). Radiocarbon dating of ancient soils and sediments is generally complicated by "contamination" with recently introduced organic matter (carbon) (Gilet-Blein *et al.*, 1980; Martin and Johnson, 1995; Mclachlan, 1995; Wang *et al.*, 1996). One reason being that, more than often, the organic matter comes from different sources and has different ages (Geyh *et al.*, 1983; Martin and Johnson, 1995). Sometimes, the problem arises from the fact that organic matter may be winnowed and subsequently redeposited.

4.2 Results

This chapter is based on data derived mainly from Meadows *et al.*, (1997), and presents the initial chronology and time-scale of the cores, which were obtained through radiocarbon dating of 24 of the core and grab samples, from the various identified sedimentary units. These chronology and time-scale upcore are discussed together with their associated problems in Chapter Seven.

The results of the samples analysed at the National Ocean Sciences AMS Facility (NOSAMS) at the Woods Hole Oceanographic Institute are presented in Table 4.1 and are summarized in Figure 4.1. Because of the low organic content of the sediments, the untreated samples were submitted for age-dating by AMS radiocarbon analysis, rather than by conventional radiocarbon dating (Meadows *et al.*, 1997).

While there are some significant problems, such as the absence of a consistent sequence of ages (Core H2 in particular) (Figure 4.1), these radiocarbon dates confirm the Holocene age of at least the top 6m of mudbelt sediments at all sampled localities. The youngest age of 570±35 years before present (BP) is derived from near the surface of Core H2, which is near the Orange River mouth (Table 4.1). The other young ages come from the tops of Cores H5 (795±40BP) and H7 (880±25BP). The oldest radiocarbon age is derived from near the base of Core H4, which is transitional in position between the Orange River mouth and the Namaqualand zones of the mudbelt (Meadows *et al.*, 1997). This is dated at 9790±45BP (Table 4.1). The only other early Holocene date comes from Core H5, which reveals an age of 7890±55BP at around 2.5m sediment depth.

Table 4.1 - AMS radiocarbon dates on 24 core and grab samples from the Namaqualand mudbelt. Material dated in each case is the organic carbon fraction. Dates courtesy of the Woods Hole Oceanographic Institution, Massachusetts (From Meadows *et al.*, 1997).

Site	Depth (cm)	Lab. No.	AMS date	$\delta^{13}C\%$
H2	5-10	8877	570±35	-19.11
H2	13-15	8876	1500±45	-16.75
H2	337-342	8875	1350±40	-17.70
H2	472-477	8874	1630±40	-16.93
H2	492-497	8873	1290±40	-17.76
H2	557-562	8872	1030±35	-19.25
H2	592-597	8871	990±40	-18.72
H5	5-10	8881	795±40	-18.63
H5	32-37	8880	1130±50	-18.01
H5	222-227	8879	2950±30	-19.90
H5	242-247	8878	7890±55	-19.56
H4	5-8	8885	950±30	-18.63
H4	95-100	8884	6540±35	-20.07
H4	295-300	8883	8850±50	-19.99
H4	505-510	8882	9750±45	-20.07
H6	25-30	8889	1250±30	-18.48
H6	85-90	8888	1120±35	-19.14
H6	105-110	8887	1280±35	-19.00
H6	615-620	8886	3340±30	-19.36
H7	10-15	8894	880±25	-20.67
H7	40-45	8893	1170±25	-19.75
H7	180-185	8892	2220±40	-19.93
H7	345-350	8891	3020±30	-19.82
H7	595-600	8890	3290±35	-19.89

Note: Prefix H indicates sample taken in May 1994 *SAS Protea* cruise.

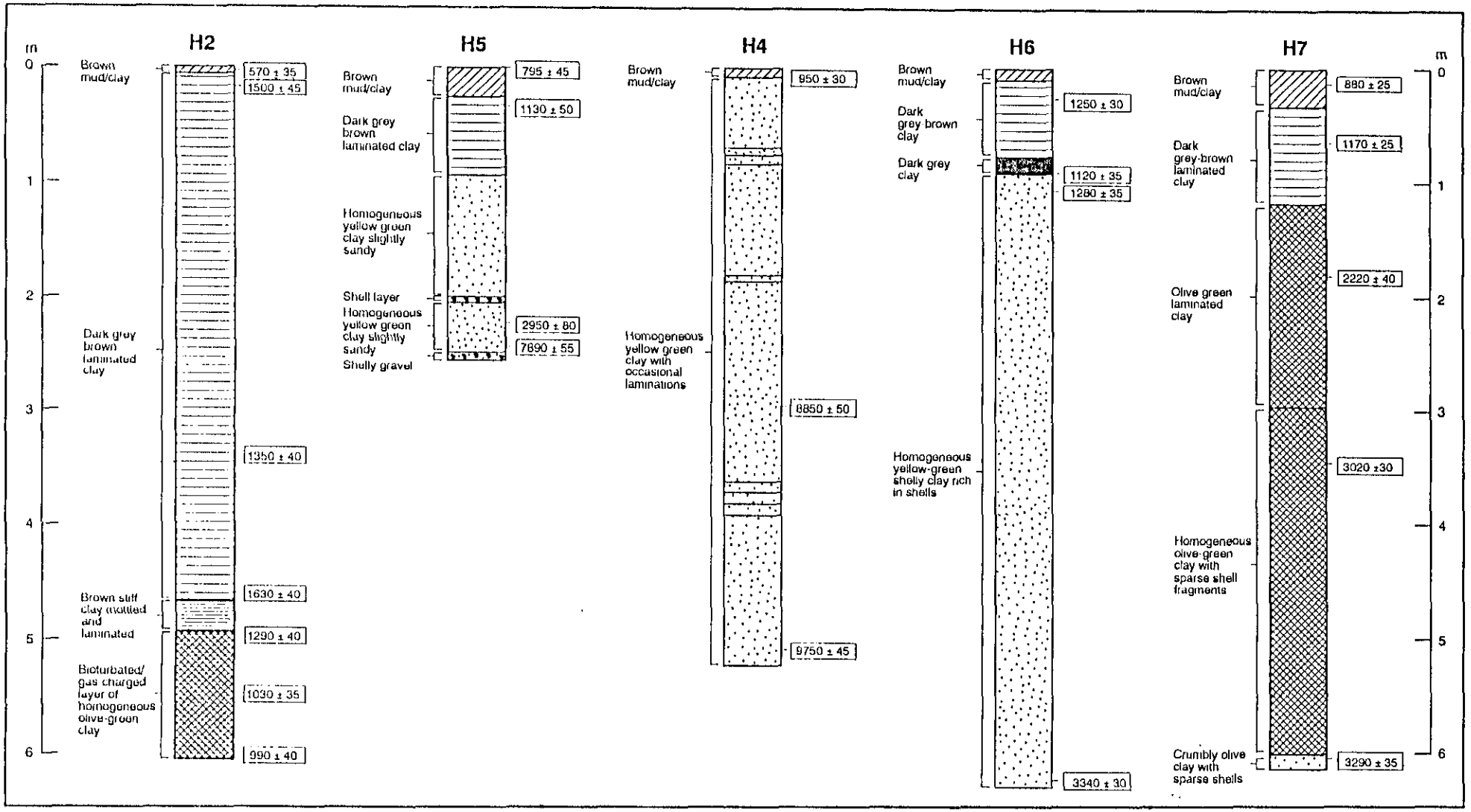

Figure 4.1 The lithology and carbon dates of the gravity cores (from Meadows *et al.*, 1997).

In summary, this chapter which is based on Meadows et al. (1997)'s work , presents radiocarbon dating of the Orange-Buffels mudbelt. It confirms the assumed Holocene-age of this area. Chapter Five presents sedimentological results.

CHAPTER FIVE

SEDIMENTOLOGY

5.1 Introduction

A detailed examination of the particle size distribution and composition of shelf sediments is a prerequisite to an understanding of sedimentary processes as they operate in the present and as have operated in the past, and it also serve as a powerful tool in the study of the geological record. To be more specific, biogenic components of the sediments, particularly foraminifera (both planktonic and benthic) are widely employed in stratigraphy and marine geology for age-dating and palaeoenvironmental interpretation (Muerdter and Kennett, 1984; McMillan, 1987; McMillan, 1993; Li and McGowran, 1994; Almogi-Labin *et al.*, 1995; Chang and Yoon, 1995; Li and McGowran, 1995; Li *et al.*, 1995; Vilela, 1995; Li *et al.*, 1996a; Li *et al.*, 1996).

The main focus of this chapter is therefore: (1) to examine particle size distribution and composition of shelf sediments and (2) to determine various sedimentary properties which are found in the surficial terrigenous sediments of the Orange Shelf. This is achieved through textural and compositional analyses, and radiographic techniques.

CHAPTER FIVE

SEDIMENTOLOGY

5.1 Introduction

A detailed examination of the particle size distribution and composition of shelf sediments is a prerequisite to an understanding of sedimentary processes as they operate in the present and as have operated in the past, and it also serve as a powerful tool in the study of the geological record. To be more specific, biogenic components of the sediments, particularly foraminifera (both planktonic and benthic) are widely employed in stratigraphy and marine geology for age-dating and palaeoenvironmental interpretation (Muerdter and Kennett, 1984; McMillan, 1987; McMillan, 1993; Li and McGowran, 1994; Almogi-Labin *et al.,* 1995; Chang and Yoon, 1995; Li and McGowran, 1995; Li *et al.,* 1995; Vilela, 1995; Li *et al.,* 1996a; Li *et al.,* 1996).

The main focus of this chapter is therefore: (1) to examine particle size distribution and composition of shelf sediments and (2) to determine various sedimentary properties which are found in the surficial terrigenous sediments of the Orange Shelf. This is achieved through textural and compositional analyses, and radiographic techniques.

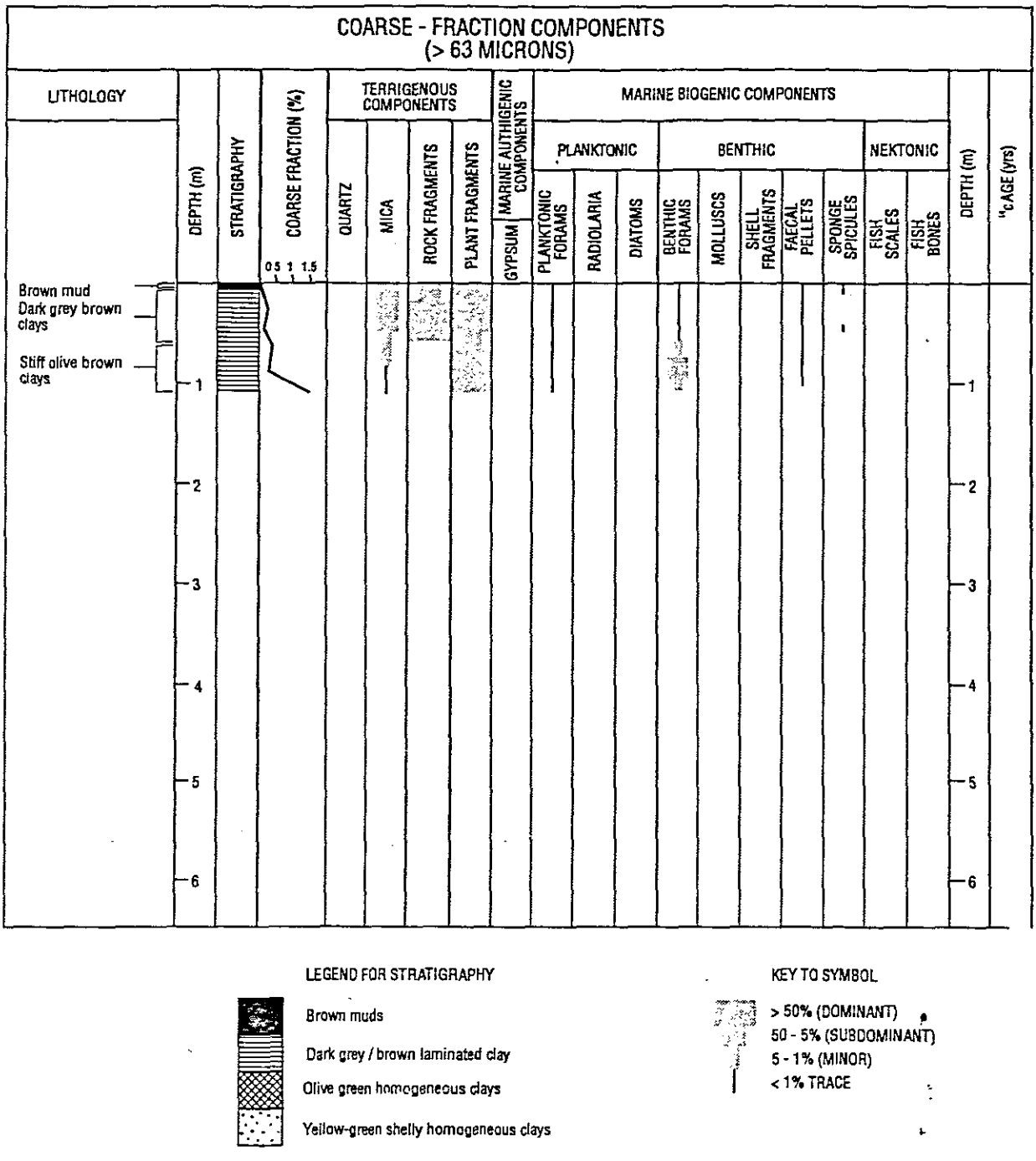

Figure 5.1 Graphic Log Illustrations of Core H1

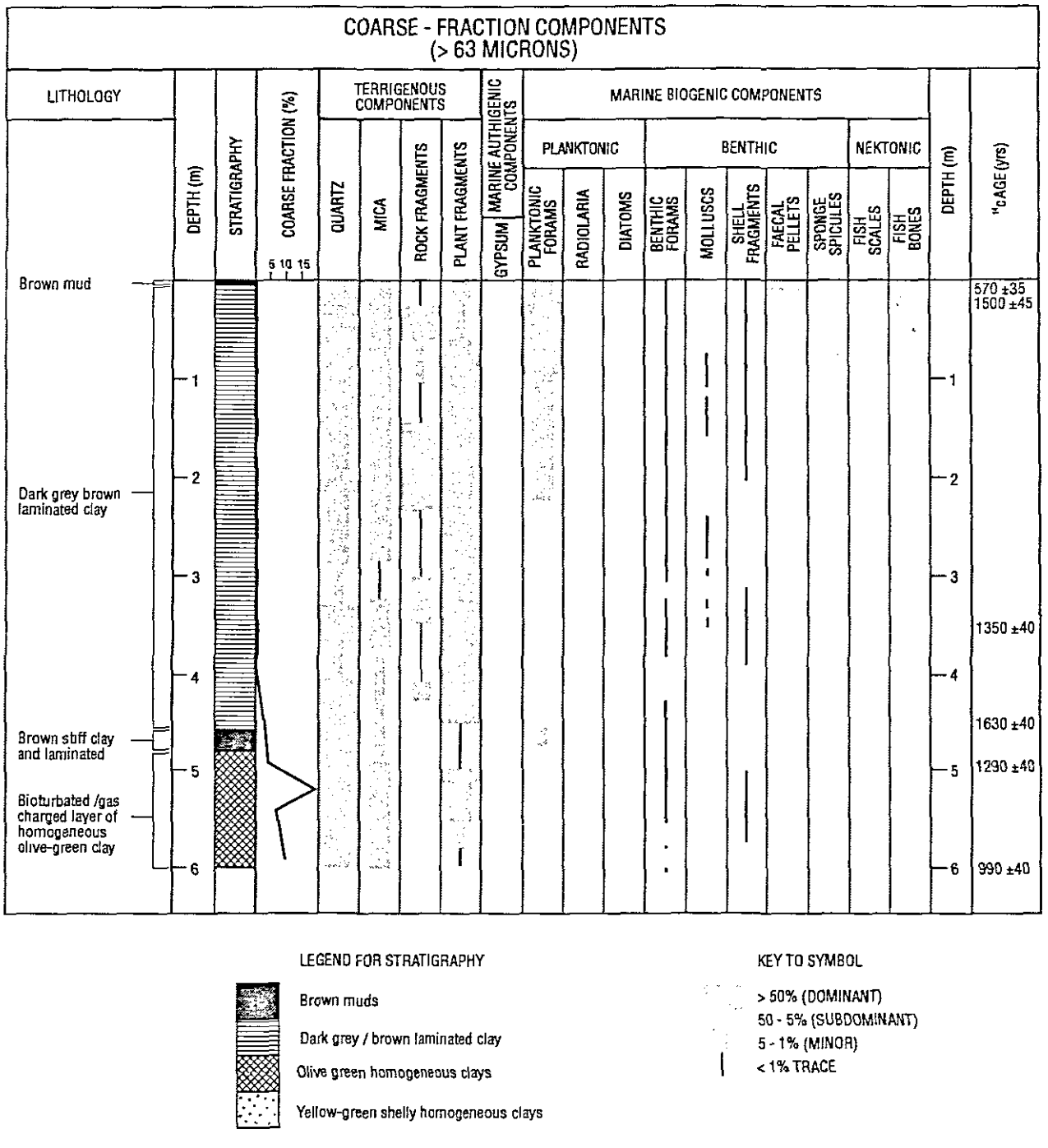

Figure 5.2 Graphic Log Illustrations of Core H2

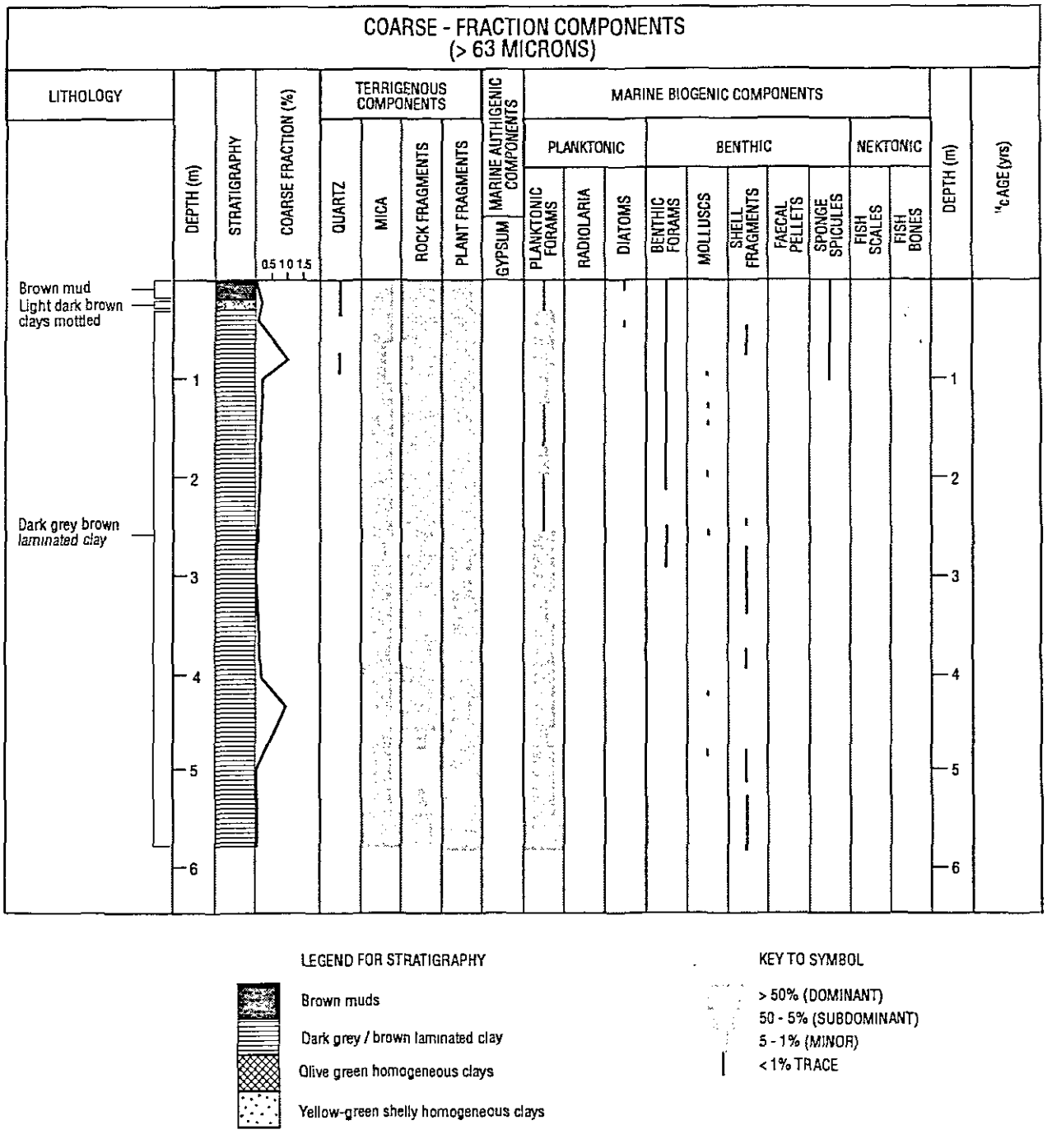

Figure 5.3 Graphic Log Illustrations of Core H3

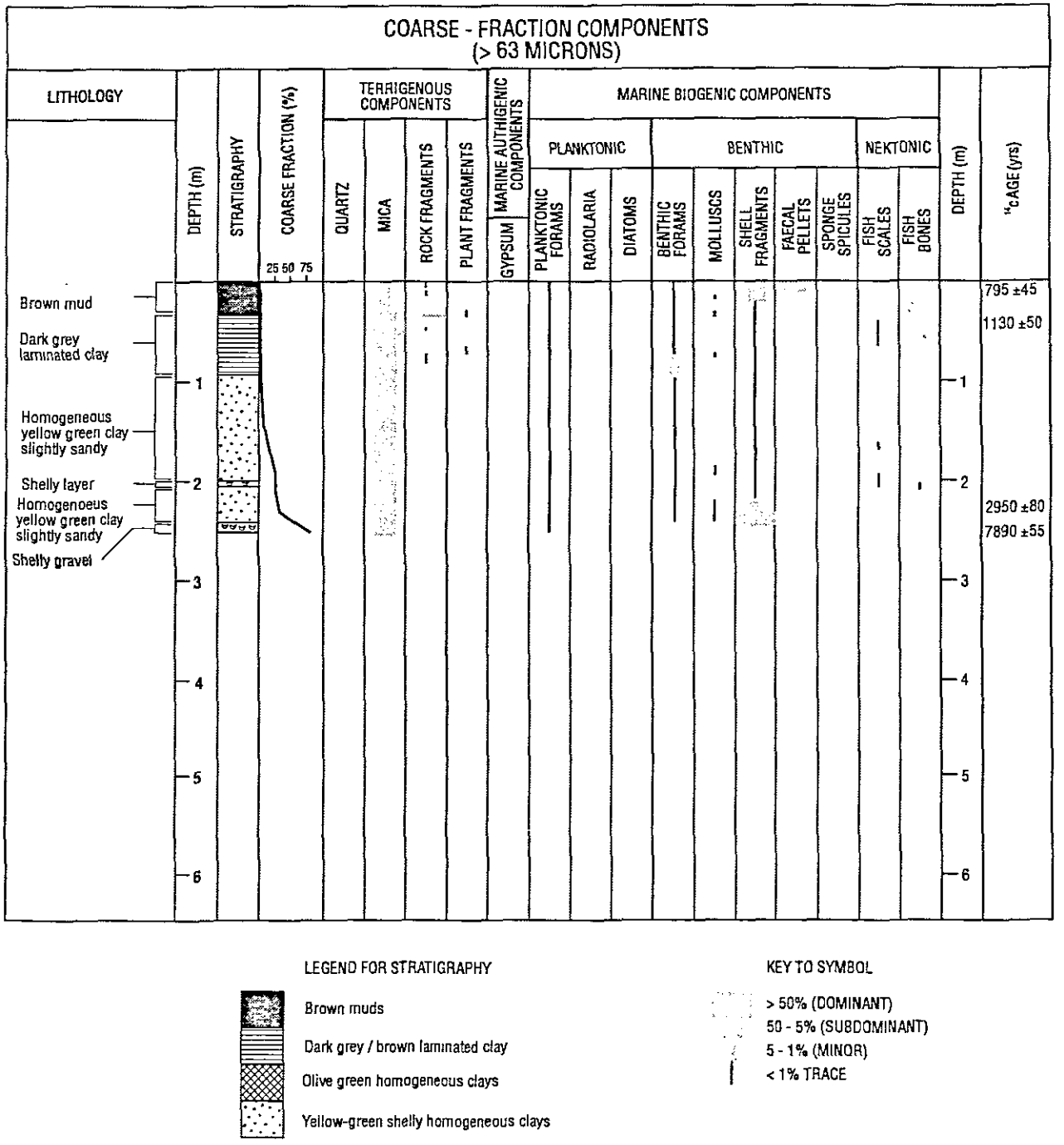

Figure 5.4 Graphic Log Illustrations of Core H5

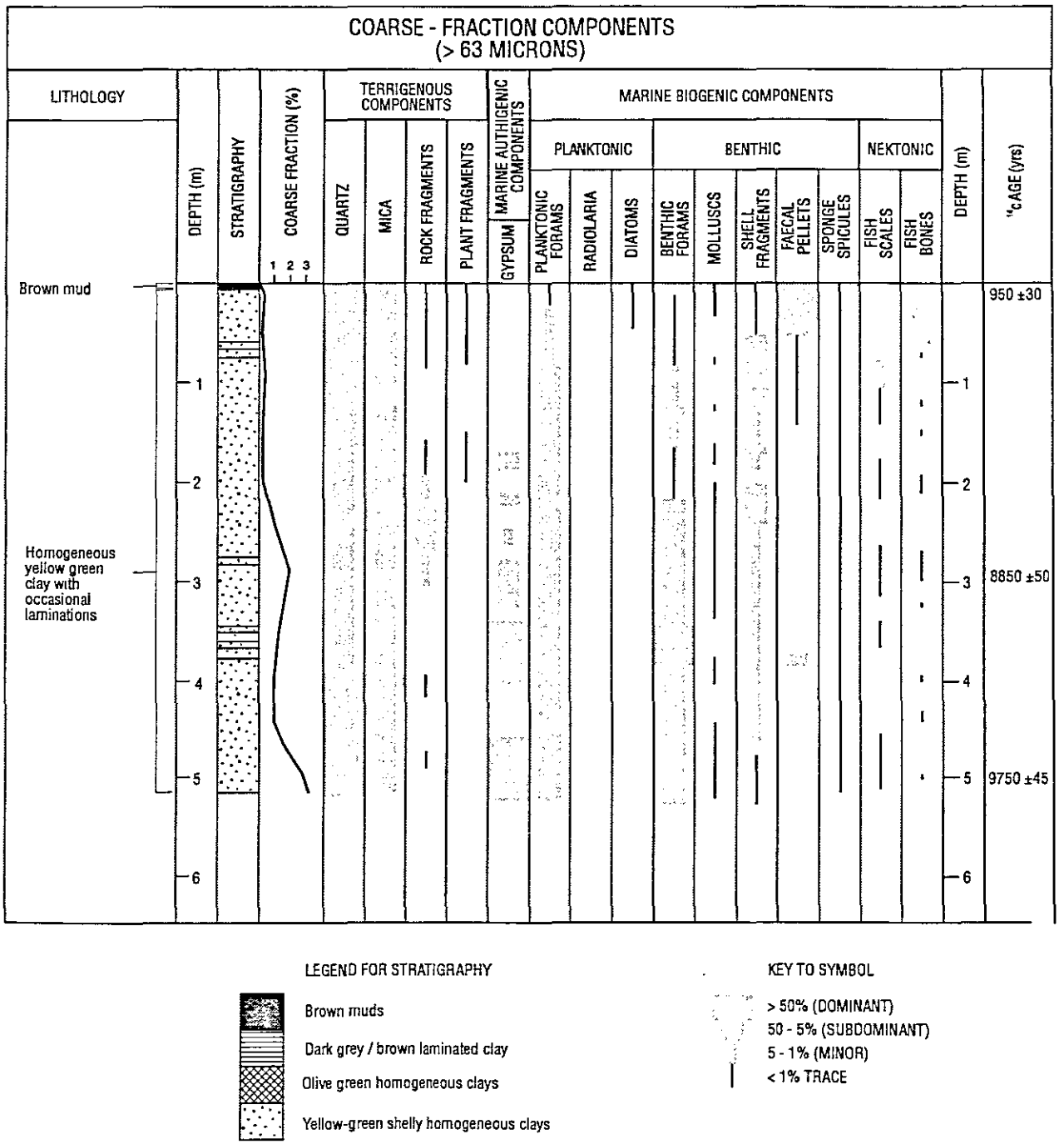

Figure 5.5 Graphic Log Illustrations of Core H4

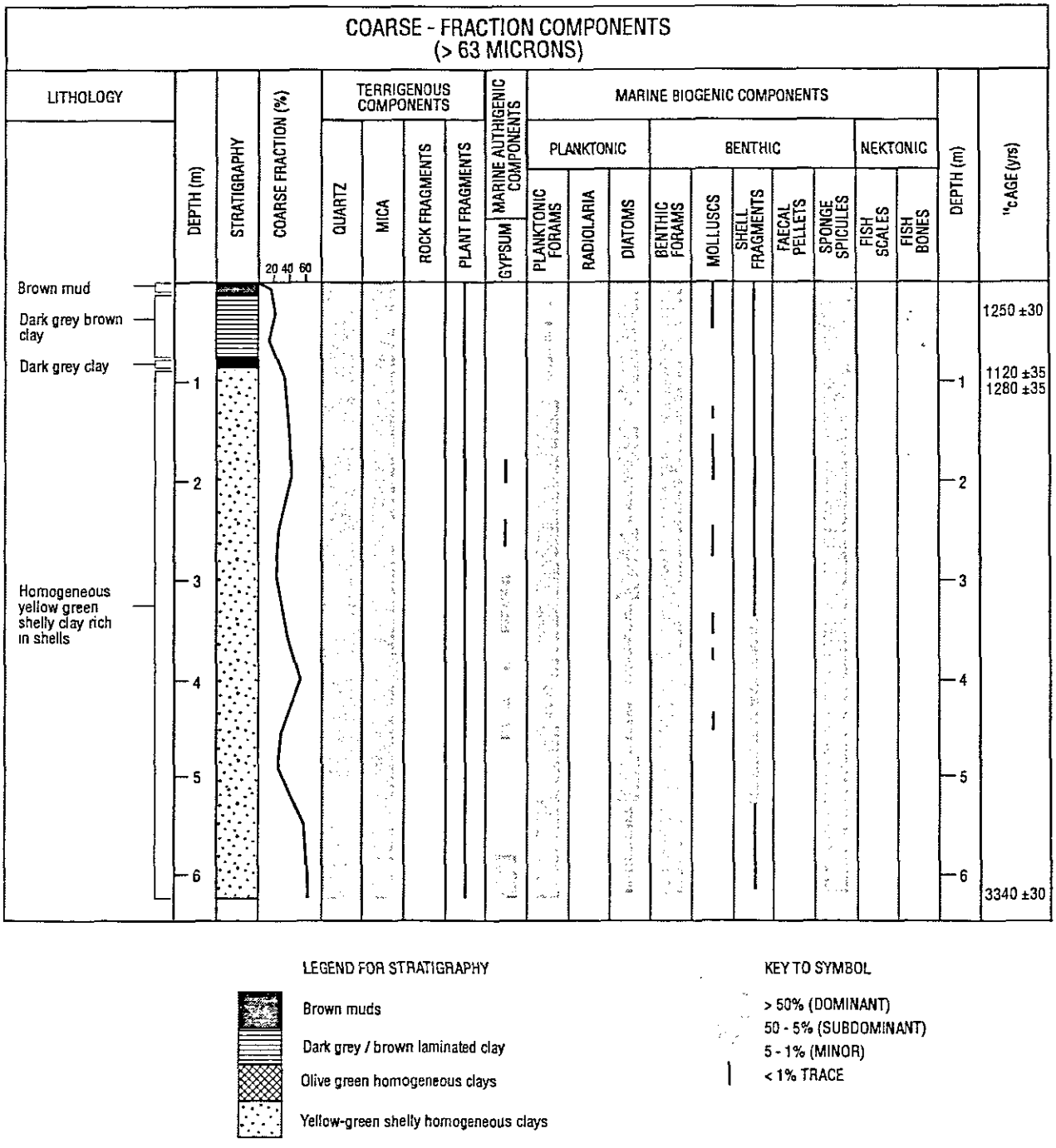

Figure 5.6 Graphic Log Illustrations of Core H6

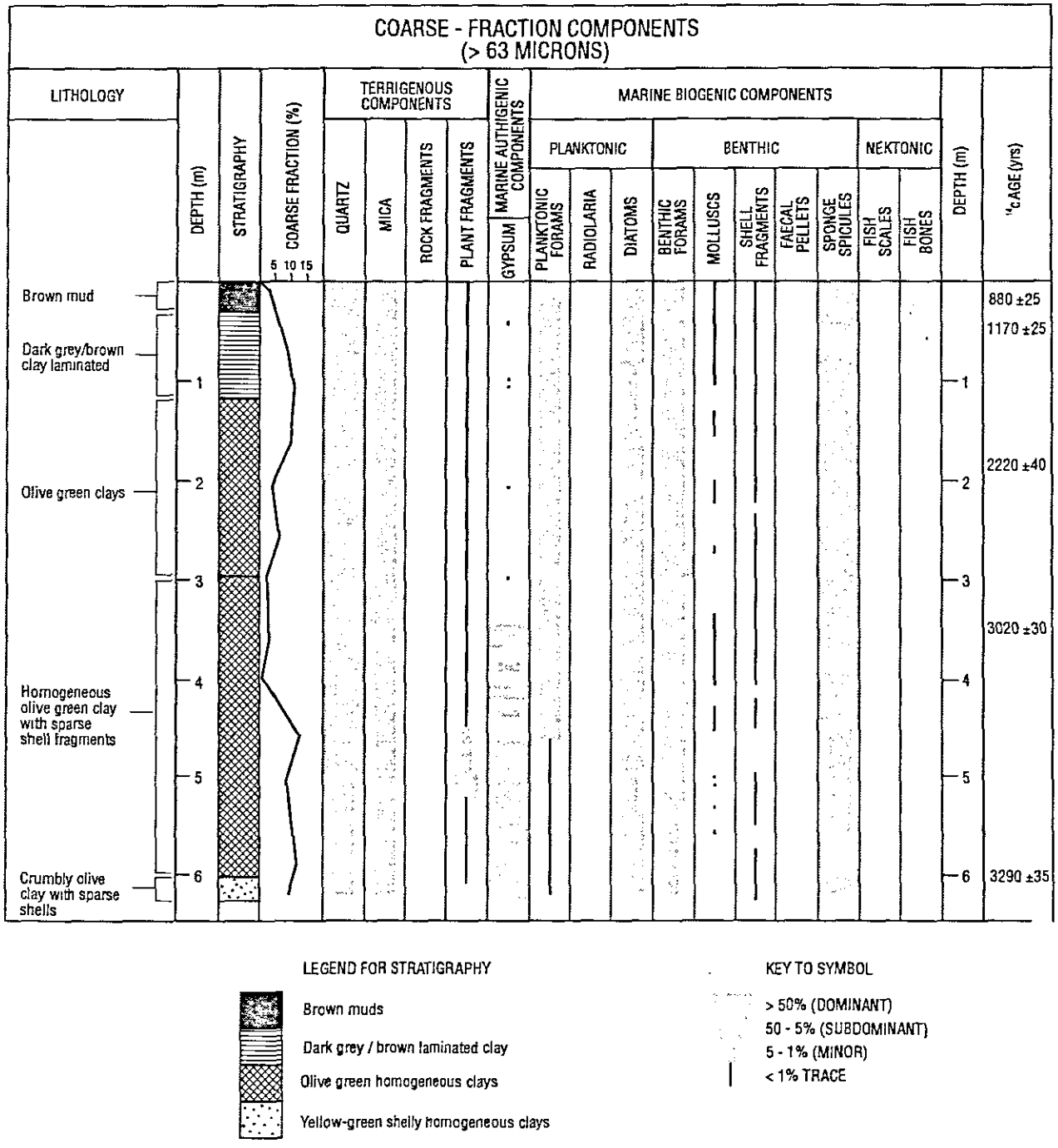

Figure 5.7 Graphic Log Illustrations of Core H7

5.3 Sediment Texture

(a) Cores H1, H2, and H3 (Prodeltaic muds)

Sediments from these three cores from the Orange Prodelta are grouped together in this section, because there was no significant difference between their texture and composition. On average, sediments from these cores consist of about 99 % mud (i.e. silt-plus-clay, which is defined as sediment finer than 63 μm (>4 phi) (Gary *et al.*, 1977 in Faas, 1991) and is subdivided into silt and clay, where silt is in the size range 63μm-2μm (4 phi-9 phi), after Udden-Wentworth size classification scheme, and clay is defined as sediment finer that 2μm (>9 phi)), about 1% sand whereas gravel content is negligible (Appendices G1, G2 and G3 respectively). However, Core H2 reveals a decrease in sand content up the core to about 4m below sediment surface (Figure 5.9). Sand content decreases from about 10% (of the total sediment content) at the base (6m) to almost 0 % at about 4m. Conversely, the mud content increases upcore so that the core, in general, fines upwards. In general, sand is present below a depth of 1m in all these cores (Figures 5.1 to 5.3). A selected number of 48 samples (due to Sedigraph failure to work properly) from Core H2 has been wet-sieved using a 63 μm sieve to separate mud (silt plus clay) from the coarse fraction (gravel plus sand). The mud fractions were analysed using a computerized Sedigraph 5000D to determine the proportions of silt and clay (Figure 5.9B, Figure 5.15). The mud-fractions are polymodal (Figure 5.15), major modes generally in the fine-silt to very fine-silt range (16μm-8μm). The Silt content (63-2μm) of the mud-fraction varies between 20 and 40%, and therefore, is clay-dominant (<2μm). On this basis,

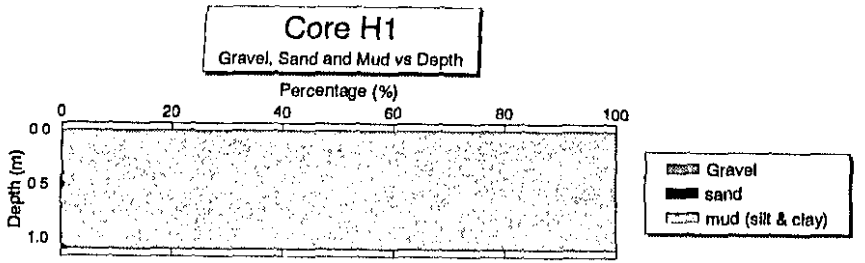

Figure 5.8 - Proportions of gravel, sand and mud (silt and clay) upcore H1 (Orange Prodelta)

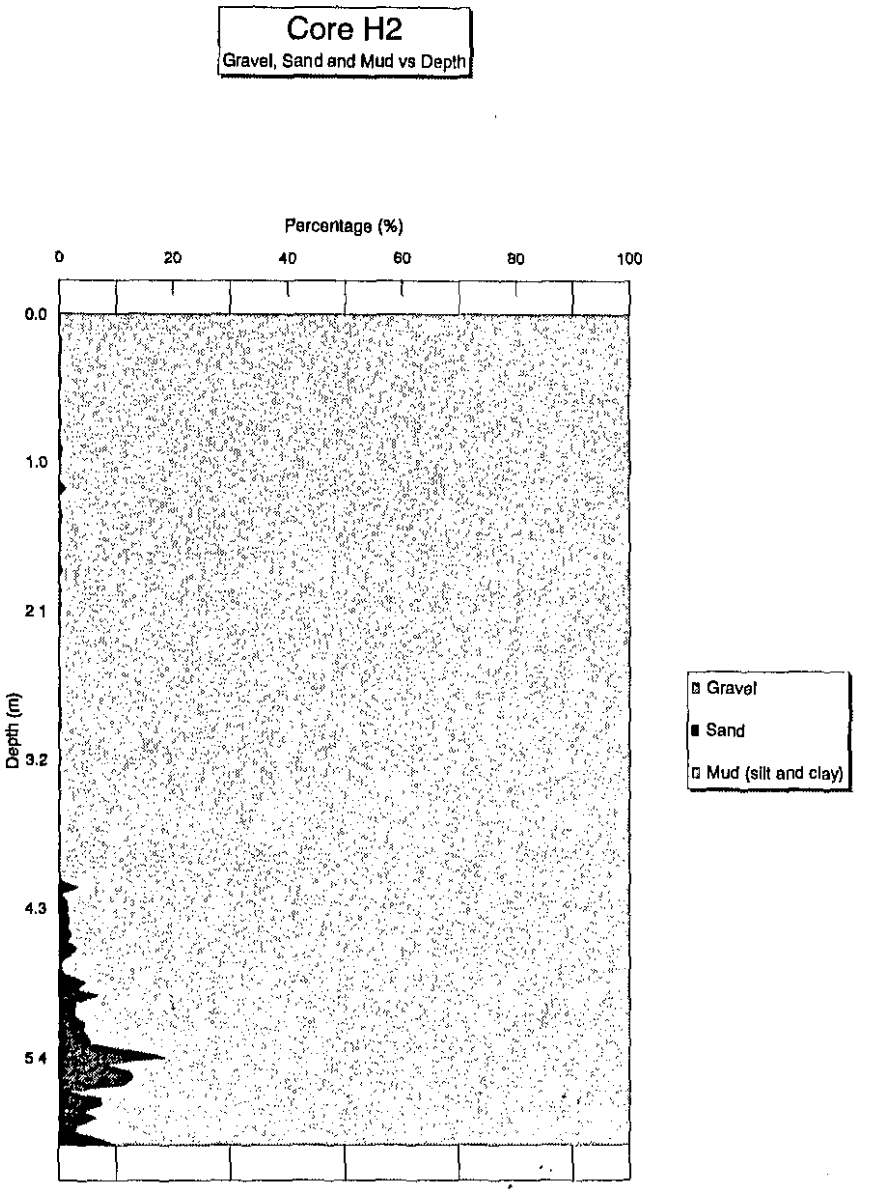

Figure 5.9 (A) - Proportions of gravel, sand and mud (silt and clay) upcore H2 (Orange Prodelta).

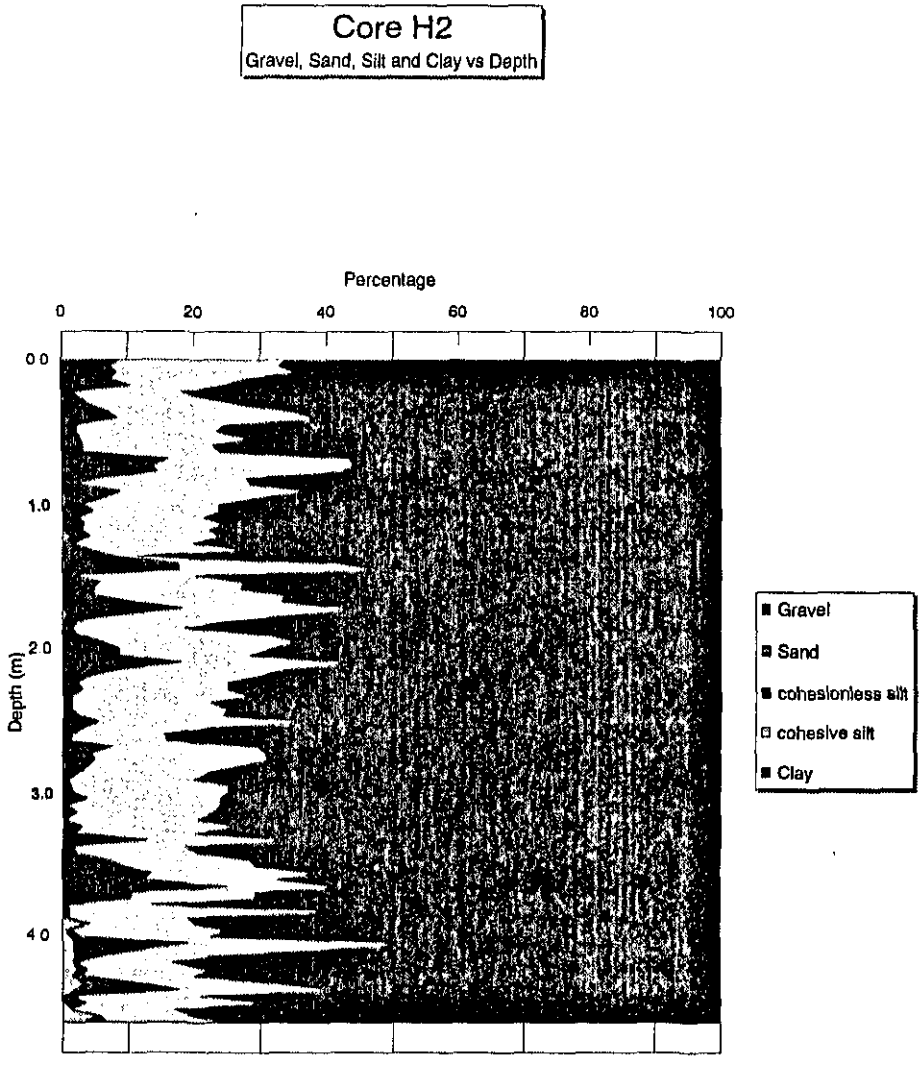

Figure 5.9 (B) - Proportions of gravel, sand, silt and clay upcore H2 (Orange Prodelta).

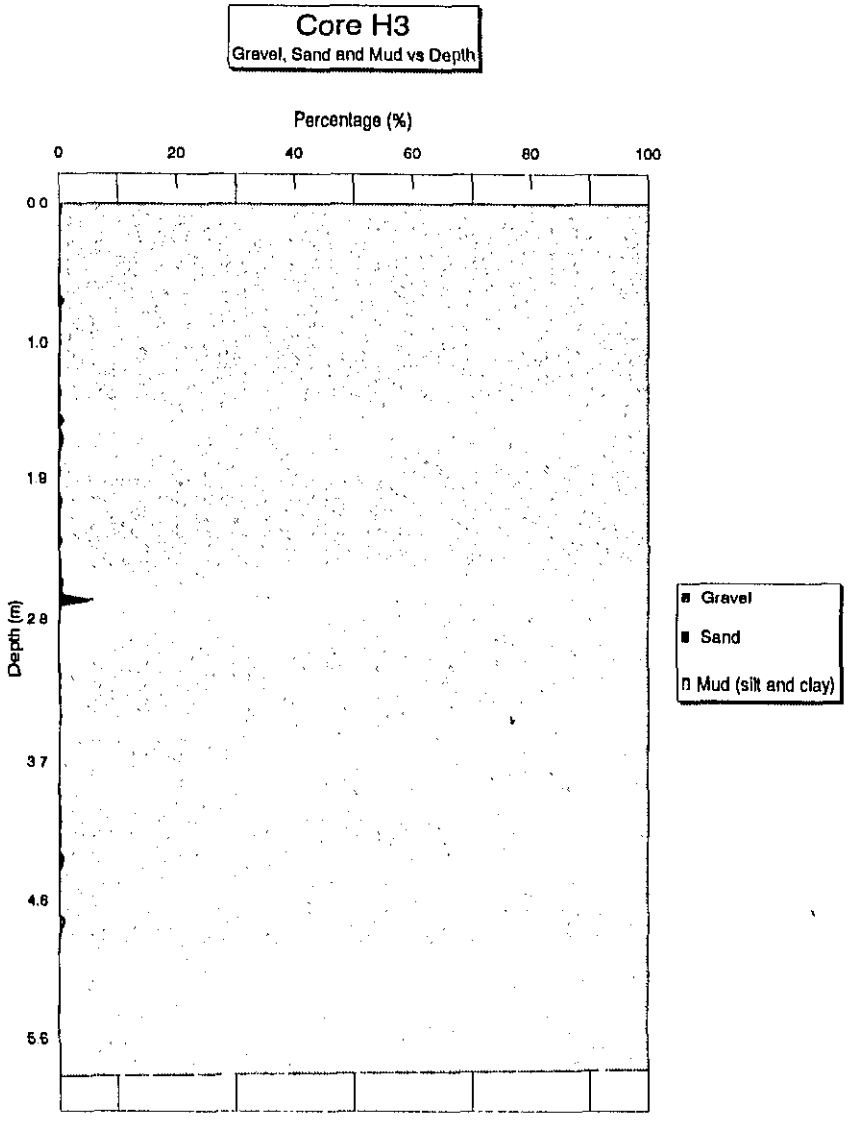

Figure 5.10 - Proportions of gravel, sand and mud (silt and clay) upcore H3 (Orange Prodelta)

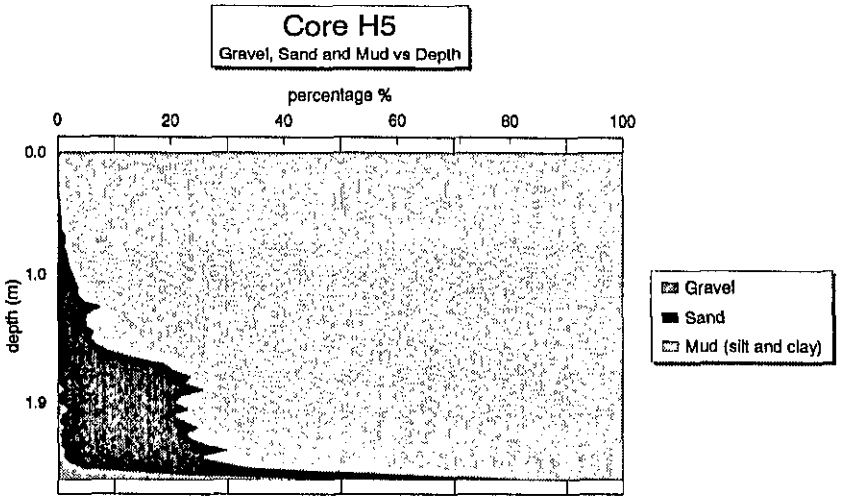

Figure 5.11 - Proportions of gravel, sand and mud (silt and clay) upcore H5 (West Wreck Point)

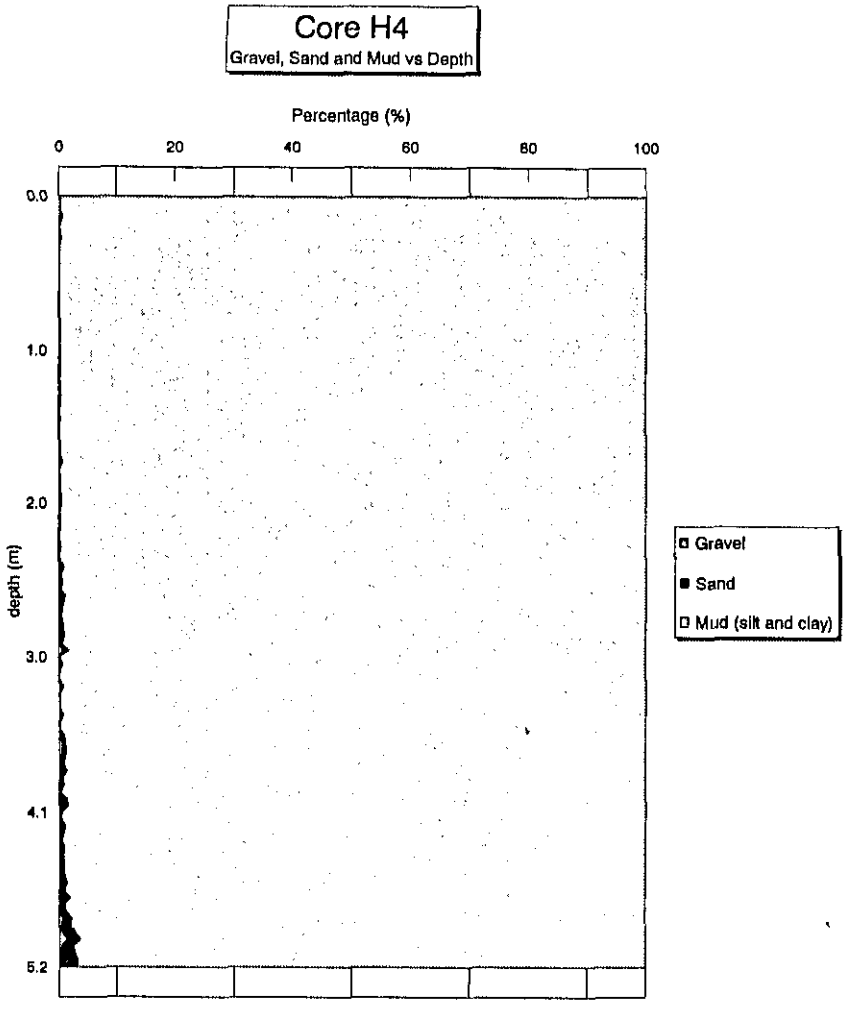

Figure 5.12 - Proportions of gravel, sand and mud (silt and clay) upcore H4 (South Wreck Point)

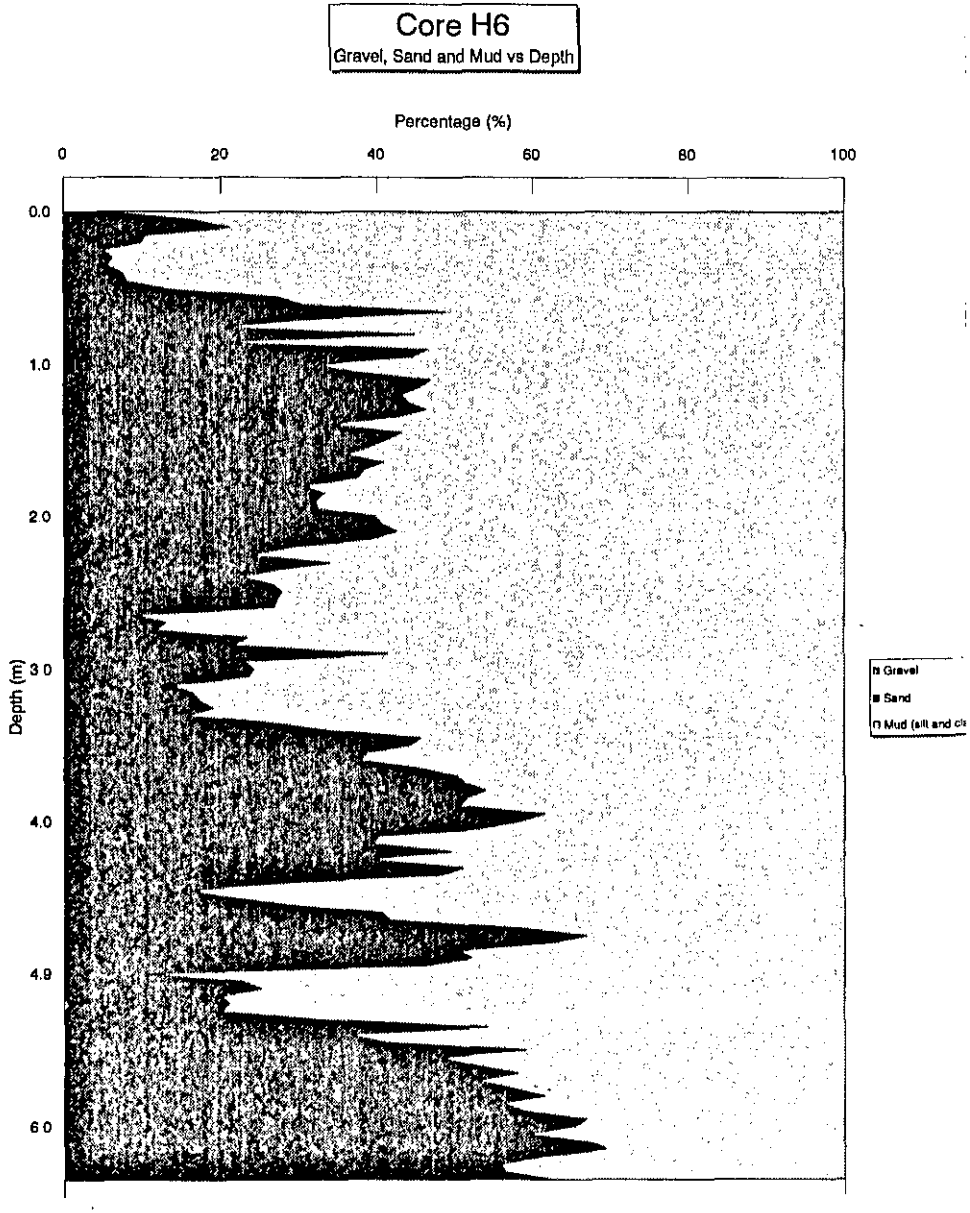

Figure 5.13 - Proportions of gravel, sand and mud (silt and clay) upcore H6 (off Port Nolloth).

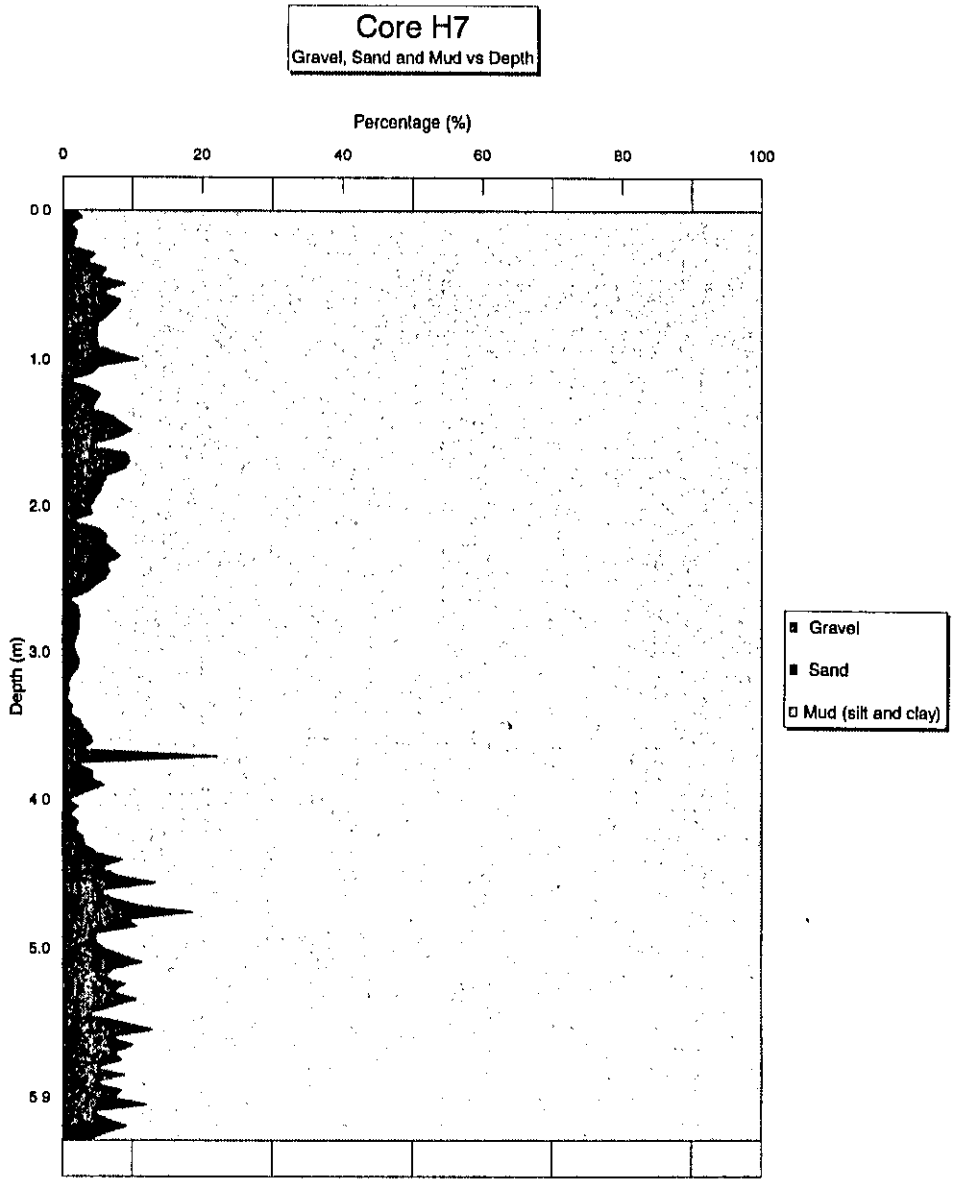

Figure 5.14 (A) - Proportions of gravel, sand and mud (silt and clay) upcore H7 (off Kleinsee).

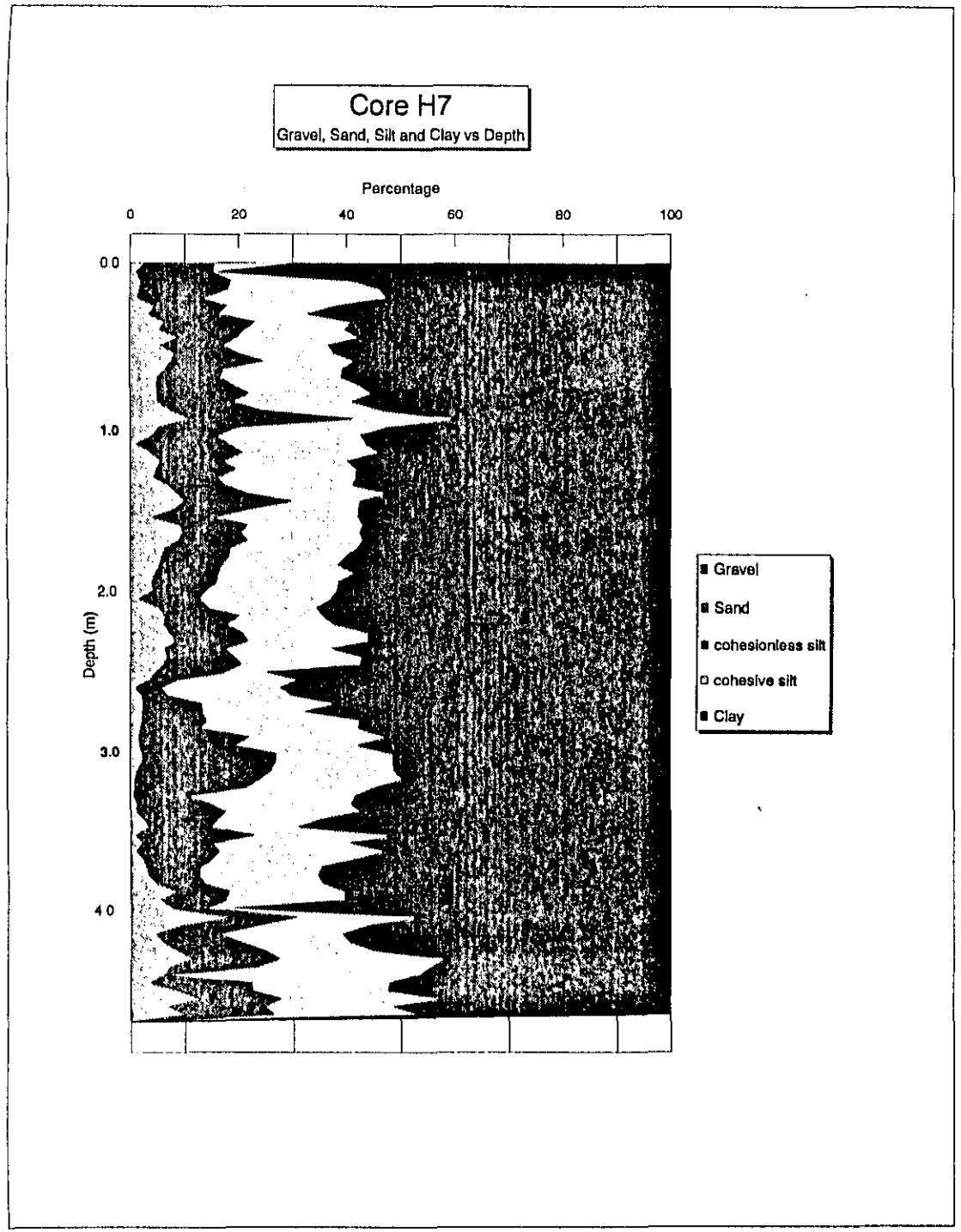

Figure 5.14 (B) - Proportions of gravel, sand, silt and clay upcore H7 (off Kleinsee).

igure 5.15 - 100 % cumulative option of selected samples from core H2 (particle size analysis using sedigraph).

real cumulative
frequency curve
probability curve

Depth (cm) I.D. No.

0 H2.G1

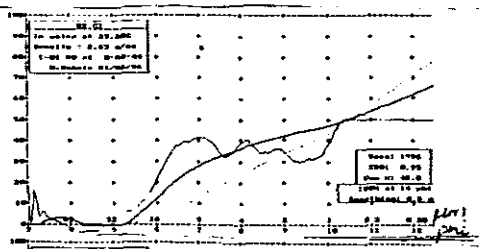

13.5 H2.7.2

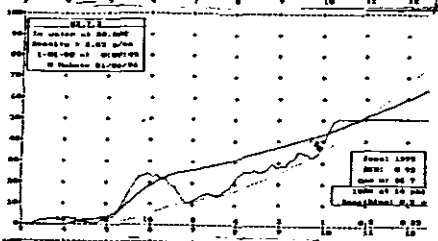

22.5 H2.6.12

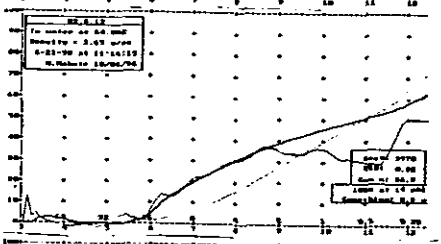

31.5 H2.6.10

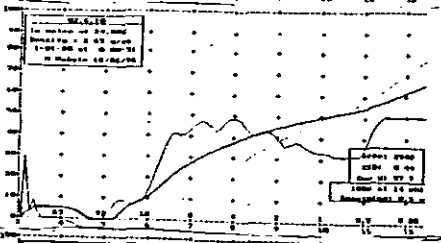

40.5 H2.6.8

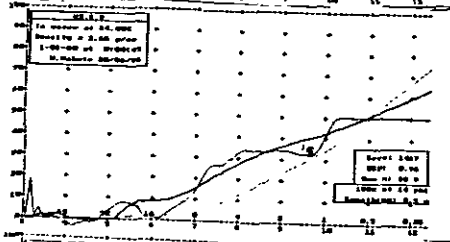

58.5 H2.6.4

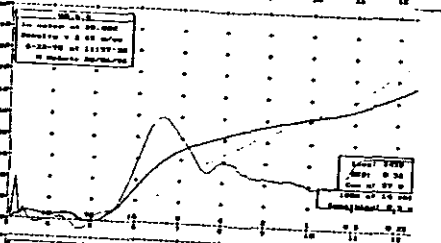

68.5 H2.6.2

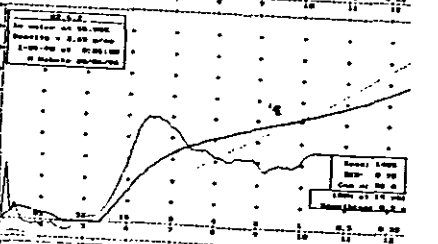

77 H2.5.20

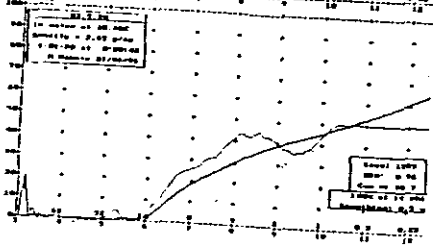

87 H2.5.18

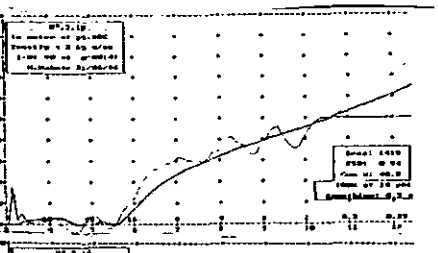

97 H2.5.16

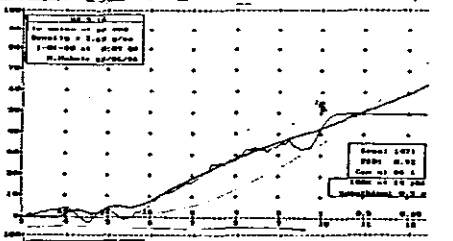

107 H2.5.14

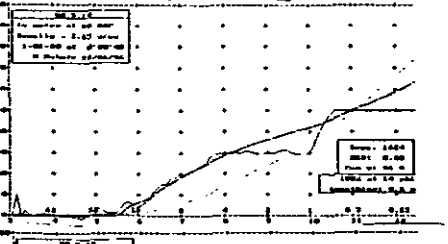

117 H2.5.12

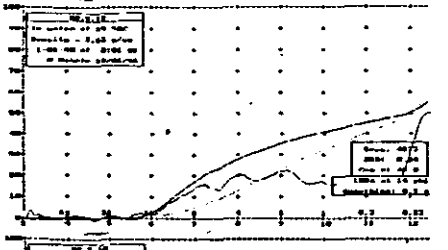

127 H2.5.10

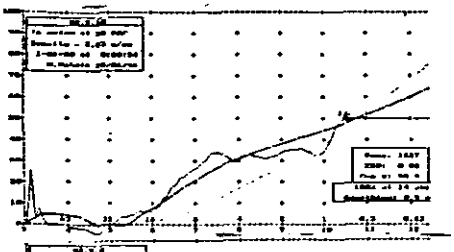

137 H2.5.8

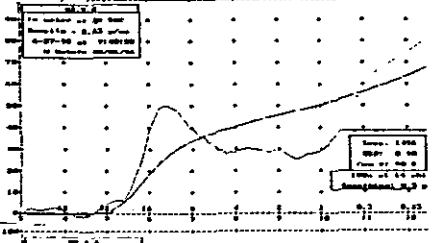

147 H2.5.6

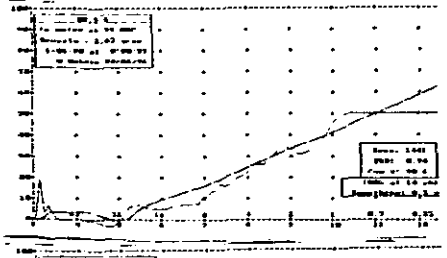

157 H2.5.4

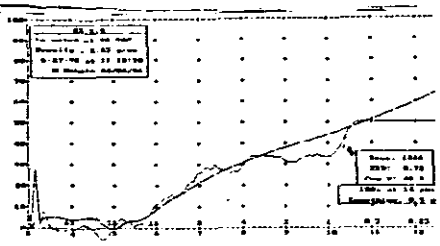

Depth (cm) I.D. No.

167 H2.5.2

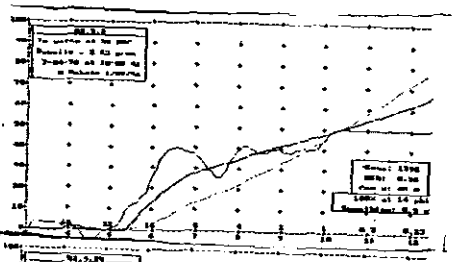

257 H2.4.4

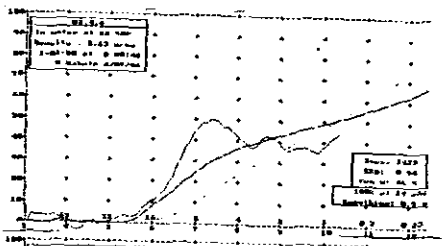

177 H2.4.20

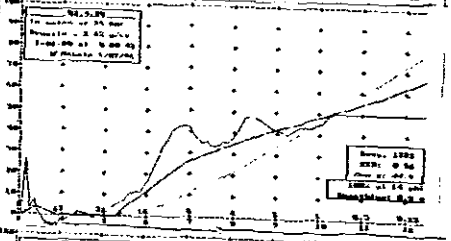

267 H2.4.2

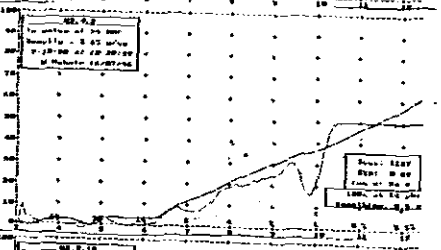

187 H2.4.18

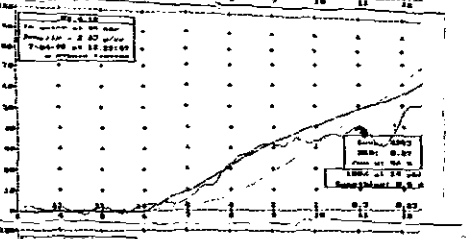

287 H2.3.18

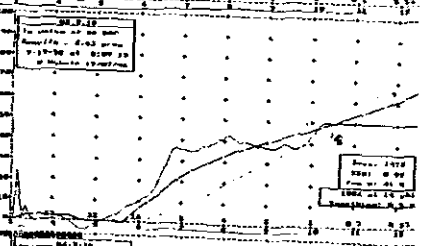

197 H2.4.16

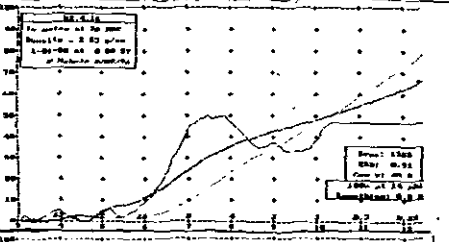

297 H2.3.16

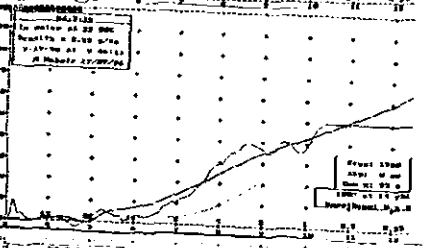

207 H2.4.14

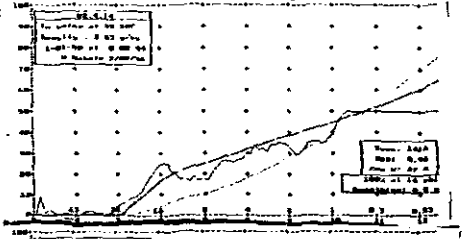

307 H2.3.14

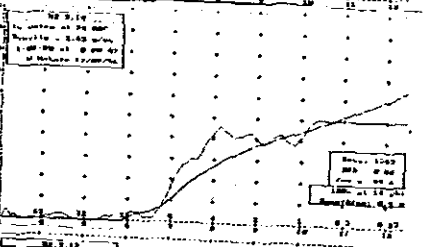

217 H2.4.12

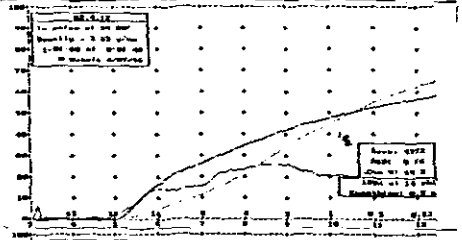

317 H2.3.12

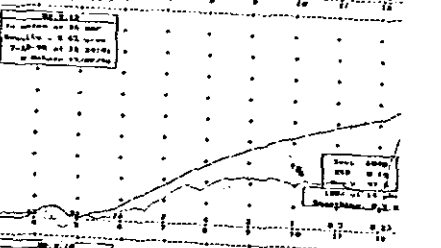

227 H2.4.10

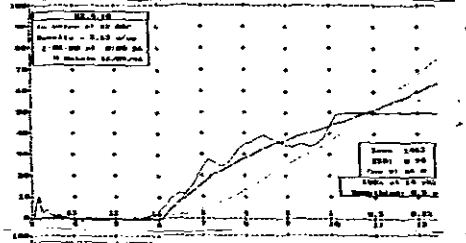

327 H2.3.10

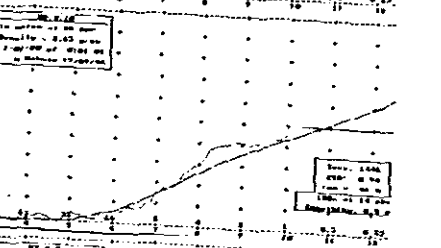

237 H2.4.8

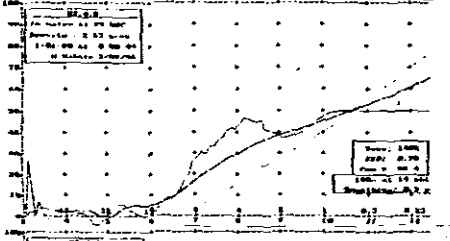

337 H2.3.8

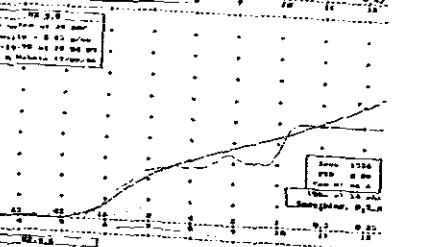

247 H2.4.6

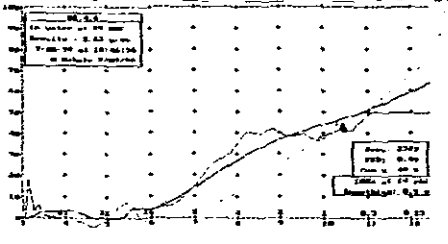

347 H2.3.6

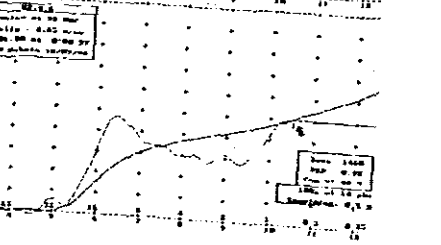

th(cm) ID.No.

357 H2.3.4

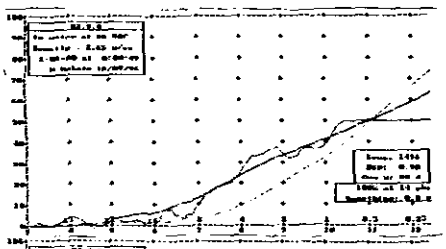

367 H2.3.2

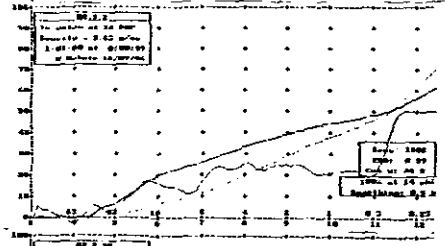

377 H2.2.20

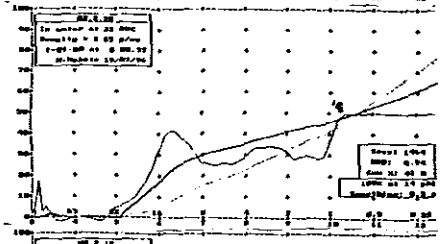

387 H2.2.18

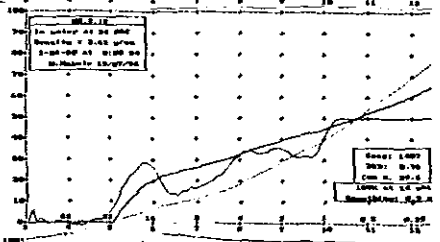

402 H2.2.16

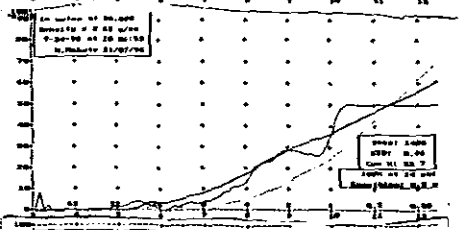

412 H2.2.13

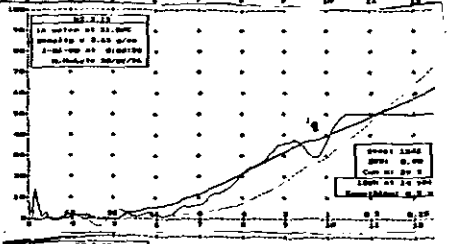

417 H2.2.12

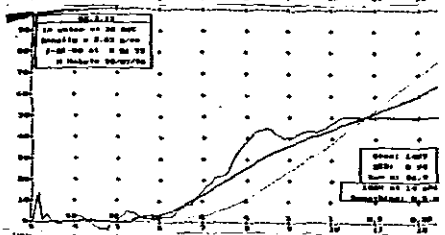

427 H2.2.10

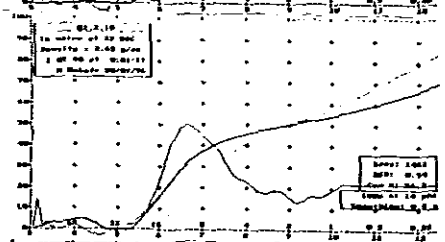

437 H2.2.8

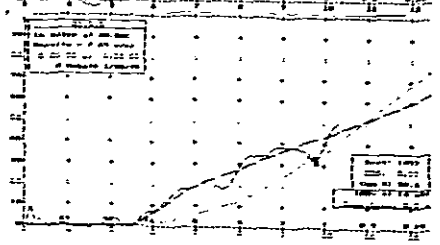

447 H2.2.6

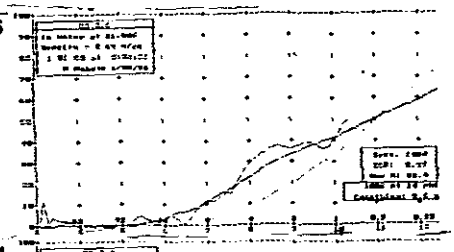

457 H2.2.4

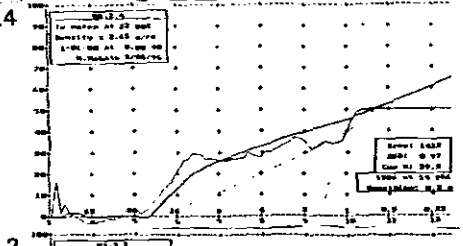

467 H2.2.2

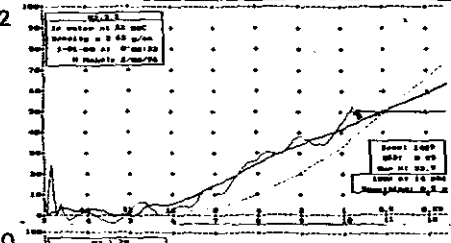

477 H2.1.20

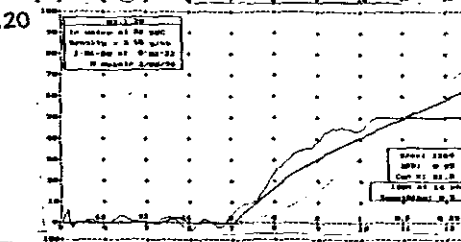

487 H2.1.18

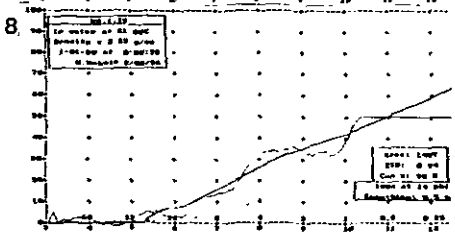

igure 5.16 - 100 % cumulative option of selected samples from core H7 (particle size analysis using sedigraph).

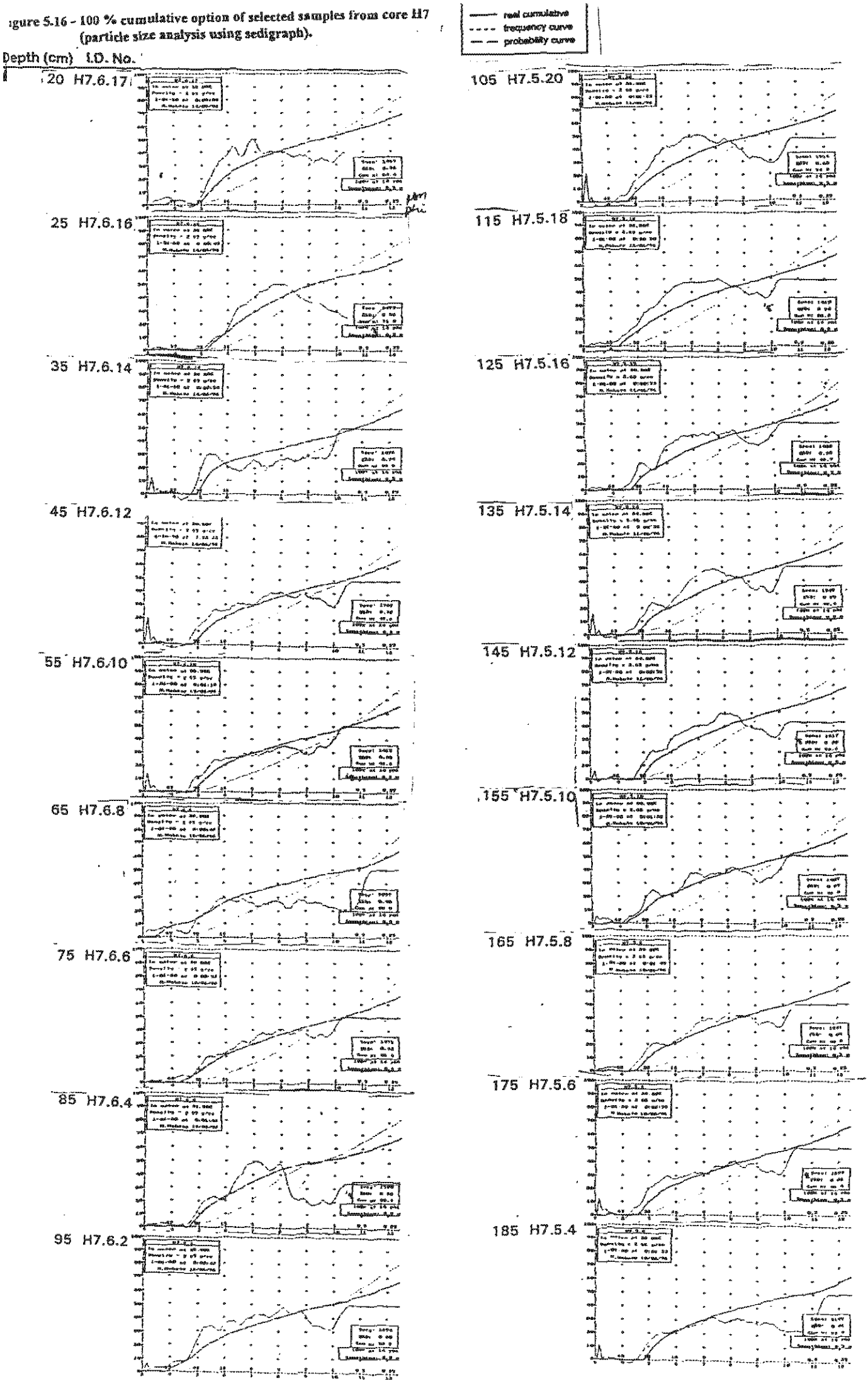

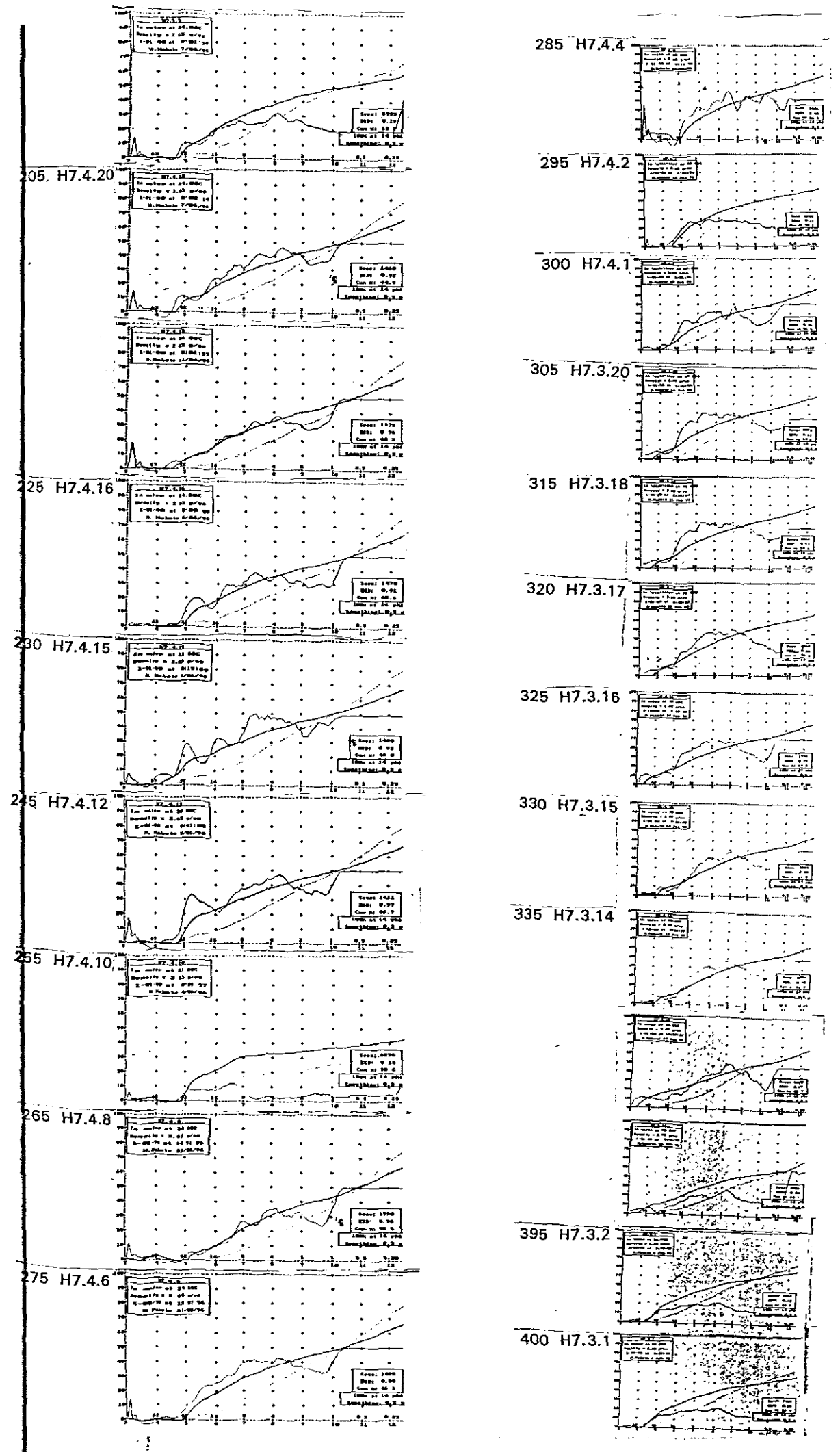
205 H7.4.20
225 H7.4.16
230 H7.4.15
245 H7.4.12
255 H7.4.10
265 H7.4.8
275 H7.4.6
285 H7.4.4
295 H7.4.2
300 H7.4.1
305 H7.3.20
315 H7.3.18
320 H7.3.17
325 H7.3.16
330 H7.3.15
335 H7.3.14
395 H7.3.2
400 H7.3.1

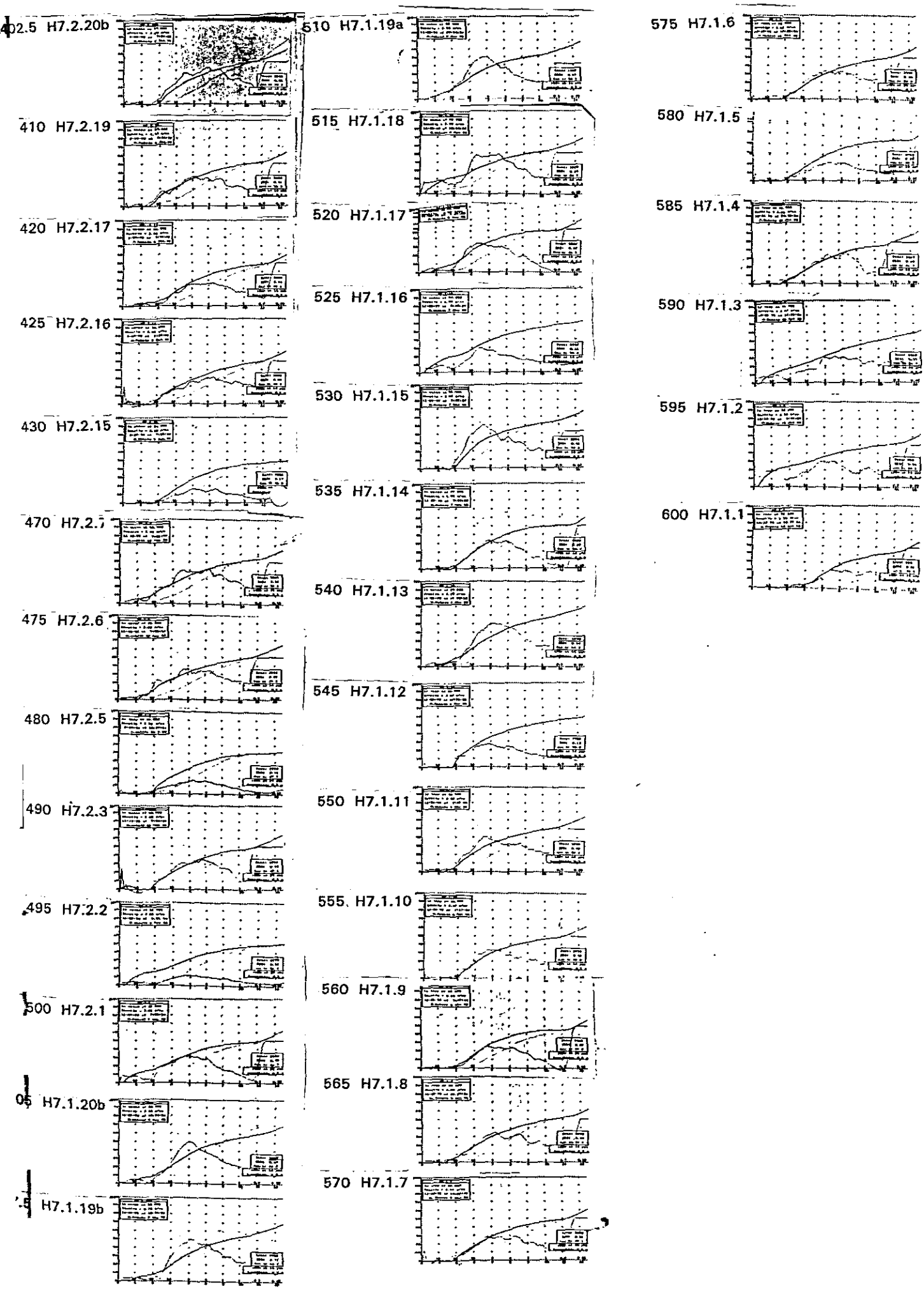
402.5 H7.2.20b
410 H7.2.19
420 H7.2.17
425 H7.2.16
430 H7.2.15
470 H7.2.7
475 H7.2.6
480 H7.2.5
490 H7.2.3
495 H7.2.2
500 H7.2.1
05 H7.1.20b
H7.1.19b
510 H7.1.19a
515 H7.1.18
520 H7.1.17
525 H7.1.16
530 H7.1.15
535 H7.1.14
540 H7.1.13
545 H7.1.12
550 H7.1.11
555 H7.1.10
560 H7.1.9
565 H7.1.8
570 H7.1.7
575 H7.1.6
580 H7.1.5
585 H7.1.4
590 H7.1.3
595 H7.1.2
600 H7.1.1

therefore, the sediments (Cores H1, H2 and H3) are classified as slightly silty clays (Figure 5.17a). Figures 5.8, 5.9A, B, and 5.10 depict textural variations against depth in Cores H1, H2 and H3 respectively (from the Orange Prodelta). Average sorting (a measure of the degree of uniformity in the deposit produced by current action during grain transport and deposition) (Leeder, 1982, Pg. 39) coefficient of the core H2 (Prodelta) samples is 2.28, and is verbally described as very poorly sorted (Folk, 1974, in Leeder, 1982). However, because these sediments are polymodal, sorting becomes statistically very unreliable parameter.

(b) Core H5 (West of Wreck Point)

Because Core H5 lies in a distal part of the Orange Delta, south of the Orange River mouth, its texture and composition are described before those of Core H4, which is located farther south (Figure 1.2). On average, mud contributes about 89 % of the entire core, whereas sand and gravel constitute about 10 % and 2 % respectively. These sediments are generally classified as slightly gravelly sandy mud (Figure 5.17b; Appendix G4). Both sand and gravel decrease markedly upcore and therefore the concomitant fining-upward trend is more distinct than in Core H2 (Figure 5.11). Sand decreases from about 30 % at the base of the core to almost 0 % at the sediment surface (Figure 5.12), whereas gravel decreases from about 50 % at the base of the core to 0 % at about 1.3 m below sediment surface.

(c) Core H4 (South Wreck Point)

The texture of the sediment in Core H4 (south Wreck Point) Figure 1.2) is almost the same as that of Core H2 (Orange Prodelta). On average, mud constitutes 99 % of the

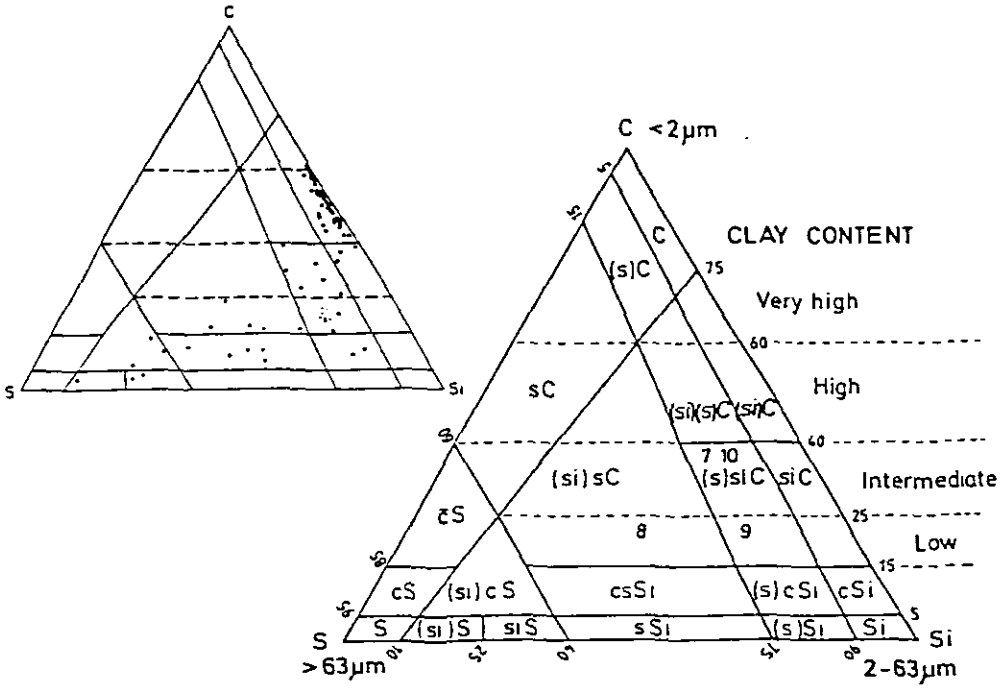

ABBREVIATIONS

S	sand	s	sandy	(s)	slightly sandy (sand >0.063 mm)
Si	*silt*	*si*	*silty*	(si)	slightly silty (silt >0.002 mm)
C	clay	c	clayey	(c)	slightly clayey (3-5% clay, not shown)
c̄	very clayey				

Optional modifiers:

-vh very high clay content
-h high clay content
-i intermediate clay content
-l low clay content

/s/ very slightly sandy (>line connecting 2 and 5% sand, not shown)
/si/ very slightly silty (>line connecting 5 and 15% silt, not shown)
/c/ very slightly clayey (1-3% clay, not shown)

Classification scheme for sand-silt-clay sediments (Stevens 1984). Optional modifiers for clay content (and relative plasticity) are shown to the right. The adjectives are used in order of increasing stress, that is (s) before si, and when equal in stress, in order of increasing grain size, e.g. (si)sCi-i. A plot of 61 analyzed samples from this study is also given.

A - Classification scheme for sand-silt-clay sediments (from Stevens, 1991).

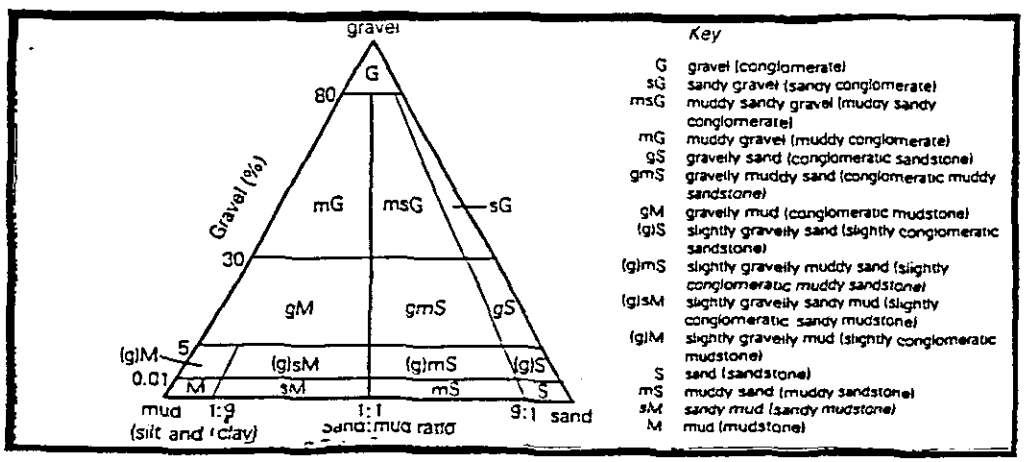

B - Wards Ternary Classification System (From Lindholm, 1981)

Figure 5.17 - Classification System for Sediments

North
(Orange Prodelta)

South
(off Kleinsee)

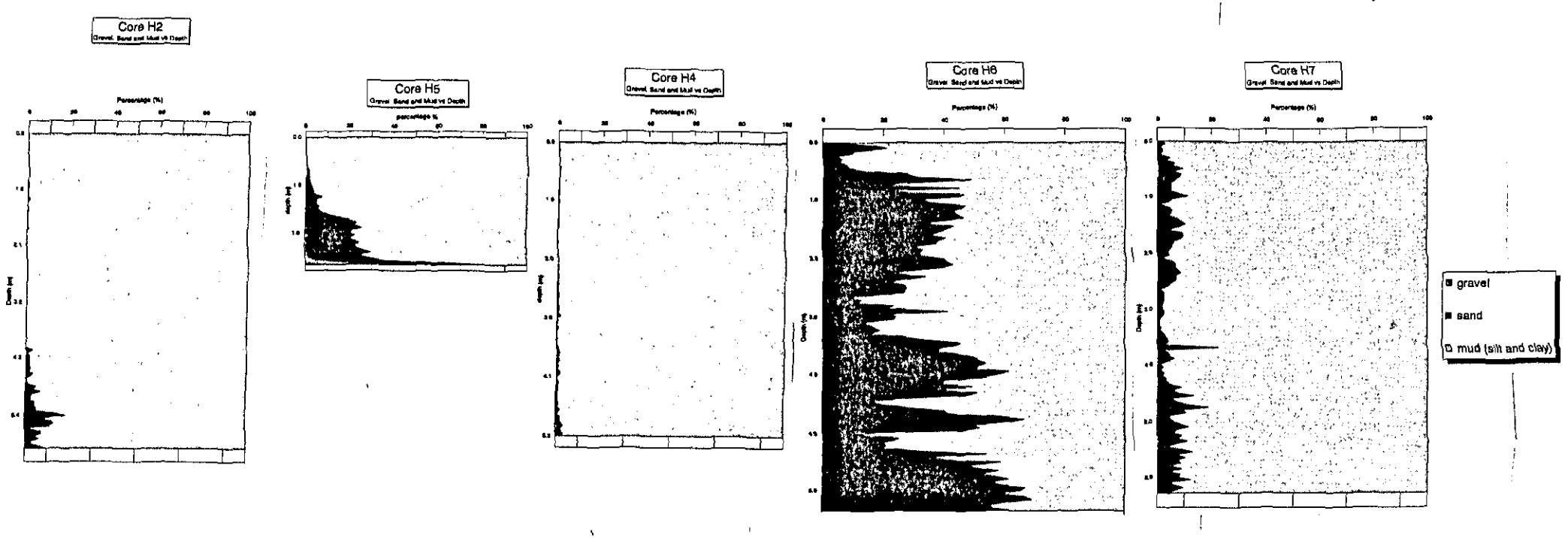

Figure 5.18 - Sediments from Namaqualand Mudbelt showing fining upcore sequence from north to south

sediment, whereas sand contributes about 1%. Gravel is negligible (Appendix G5). This is generally classified as mud (Figure 5.17b). Like Cores H2 and H5, Core H4 sand content decreases upcore and therefore the core again fines upward (Figure 5.11). Sand content decreases from about 3 % at the base of the core to almost 0 % above 1m of the core (Figure 5.11).

(d) Core H6 (Port Nolloth)

In Core H6 which is located off Port Nolloth (Figure 1.2), there is markedly high sand content relative to the rest of the cores. Mud values range between 33-96% whereas sand values range between 4-67%. However, on average, these sediments consist of 63% mud and about 37% sand and gravel content is negligible (Appendix G6). These sediments are generally classified as sandy mud (Figure 5.17b). Sand content decreases upcore, from about 70 % at the base of the core to about 20 % at the sediment surface, and therefore the concomitant fining-up trend is still evident. The first one metre from the base of the core is dominantly clayey sand (sand is dominant over mud) whereas the rest is sandy clay (clay dominant over sand). It was not possible to determine the proportions of silt and clay due to the failure of Sedigraph to function properly.

(e) Core H7 (off Kleinsee)

On average, Core H7 consists of 93.6% mud, whereas sand contributes an average of just 6.4%. Gravel content is negligible (Appendix G7 (i)). Generally, there seems to be no increase or decrease in sand content upcore except at about 3.7m below sediment surface, where sand constitutes about 22% (Figure 5.14A). As was the case

with Core H2, a selected number of 72 samples has been wet-sieved and analysed using the computerized Sedigraph to determine proportions of silt and clay (Figure 5.14A and Figure 5.15) and this reveals that the mud-fractions are polymodal; major modes generally lie between very fine-silt and clay (8-2μm), relatively finer than those of Core H2 (medium to fine silt) (Figure 5.16). Silt content of the mud varies between 11-47% (Figure 5.14B; Appendix G7 (ii)) and therefore is clay-dominant. On the basis of this, therefore, these sediments are defined as silty clays (Figure 5.17a). The average sorting coefficient of southern samples (Core H7), is 2.73, and are verbally described as poorly sorted. This sorting coefficient is once again statistically unreliable because the sediments are polymodal.

5.4 Sediment Composition (Coarse-Fraction)

Coarse-fractions from all the cores have been examined under a binocular microscope, revealing that the coarse fraction may be divided into terrigenous, authigenic and biogenic components as follows: *terrigenous components*: quartz, mica rock fragments and plant fragments; *biogenic components*: Foraminifera (benthic and planktonic), mollusca and shell fragments, sponge spicules, diatoms, and faecal pellets; *authigenic components:* gypsum. Authigenic gypsum is discussed in detail in chapter Six. The rest of these components are described in turn below.

5.4.1 Terrigenous Components

Quartz is the most prominent component of the coarse fractions in Cores H2, H4, H5, H6 and H7 (Figs 5.2, 5.5, 5.4, 5.6, and 5.7 respectively). It occurs in a wide range of

sizes, shapes and colour. Its size ranges from <63 μm to individual grains as coarse as 5mm (fine pebbles) or more in diameter. The dominant size varies between very fine to fine sand (63 to 250 μm), with sub-ordinate to minor quantities of medium to coarse sand (250 μm to 1mm). In general, the shapes are sub-angular to sub-rounded (Plate 2a) with traces of very rounded polished grains. The colour of these quartz grains ranges from colourless, pink, yellowish and reddish, with colourless grains being the most common. Most of this quartz have frosted surface. Quartz is generally absent in Cores H1 and H3 (Orange Prodelta) (Figures 5.1 and 5.3 respectively).

In general, mica occurs in subordinate to minor quantities in all cores, constituted by light to dark brown flakes with some signs of abrasion on their edges. Flake size ranges from <63 μm to 5 mm (Plate 2b).

Although rock fragments are generally present in the Orange Prodelta (Cores H1, H2, and H3) in dominant to subordinate quantities, they are only present in minor to trace quantities in Cores H4 and H5 (off Namaqualand) and they are completely absent in cores H6 and H7 (off Kleinsee) (Figures 5.1-5.7). The abundance of these fragments in the Prodeltaic sediments of H2 appears to increase upcore. A large number of the fragments have a greenish tinge colour and are sub-angular to sub-rounded in shape (Plate 3a).

Plant fragments are present in the form of plant fibres. They occur mainly in the Orange Prodelta in Cores H1, H2 and H3 and dominate the sand-fractions in these cores (Figures 5.1-5.3). The plant fragments are only found in trace amounts in cores

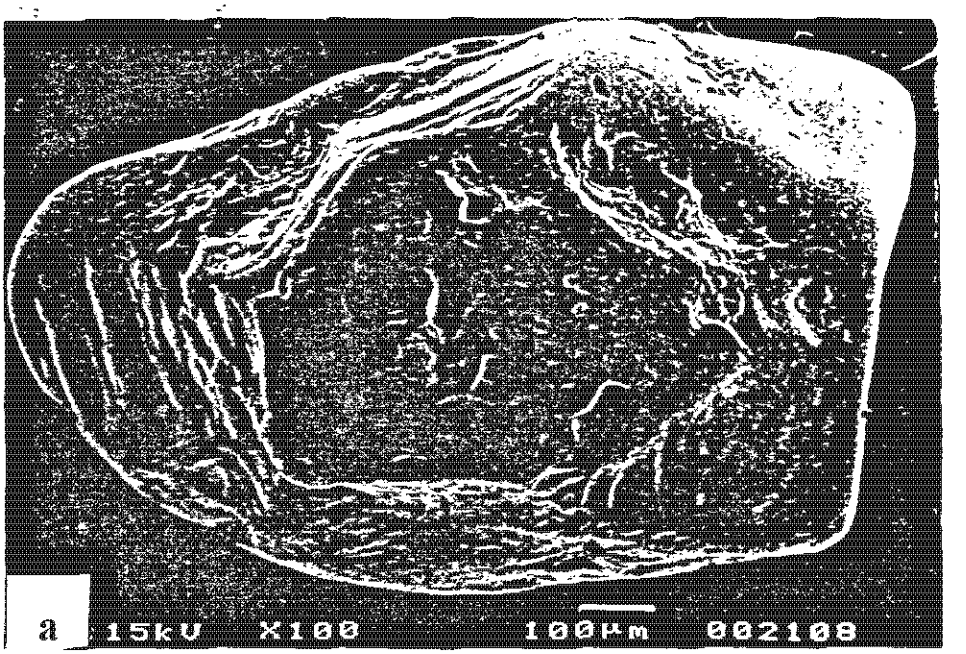

- Sub-rounded quartz grain from core 2 at 537 cm from the top (1.15 mm, very coarse sand)

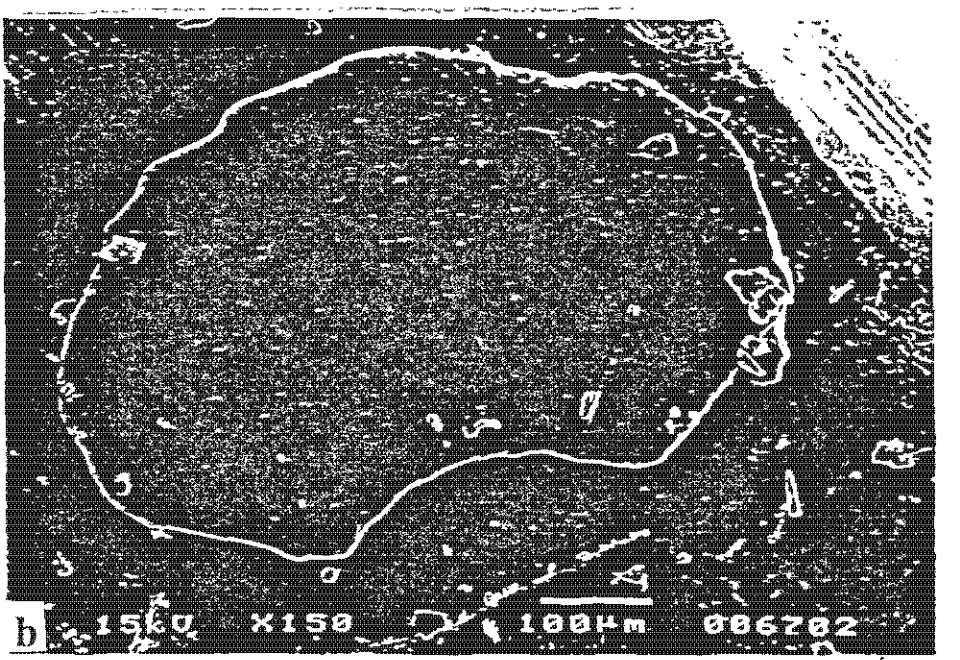

- Mica flake from core H6 at 75 cm from the sediment surface (667 µm, coarse sand)

PLATE 2

H4, H5, H6 and H7 (Figures 5.4-5.7), farther south. These plant fragments are light to dark brown in colour.

5.4.2 Authigenic Components

Authigenic components in the form of gypsum crystals are present in the samples. The identification of this mineral was confirmed by Dr. Frank Eckardt of Oxford University by X-ray Diffraction.. The gypsum crystals are only found in Cores H4, H6 and H7 (far south of Orange Delta). Gypsum occurs as clear colourless crystals in the fine to medium sand-fraction and occasionally in gravel size as intergrown crystals (sometimes as large as 2mm) (Plates 3b, 4a-b). They occur in dominant to trace quantities (Figures 5.4-5.7), and their abundance decreases upcore, since they are found mainly below a depth of 1.6m. A detailed discussion of the origin of these crystals can be found in Chapter Seven. No gypsum crystals are found in Cores H1, H2, H3 and H5, north of Cores H4, H6 and H7.

5.4.3 Biogenic Components

The biogenic components of the sediments are grouped into plankton, benthos and nekton in this study. The biogenic component of the sediment is constituted mostly of foraminifera (benthic and planktonic), diatoms and sponge spicules. Mollusca, radiolaria, shell fragments and fish debris are present in trace quantities. Planktonic and benthic foraminifera were identified by Dr. I. K. McMillan, while shells and their fragments were identified by Mr. J. Pether, both of De Beers Marine.

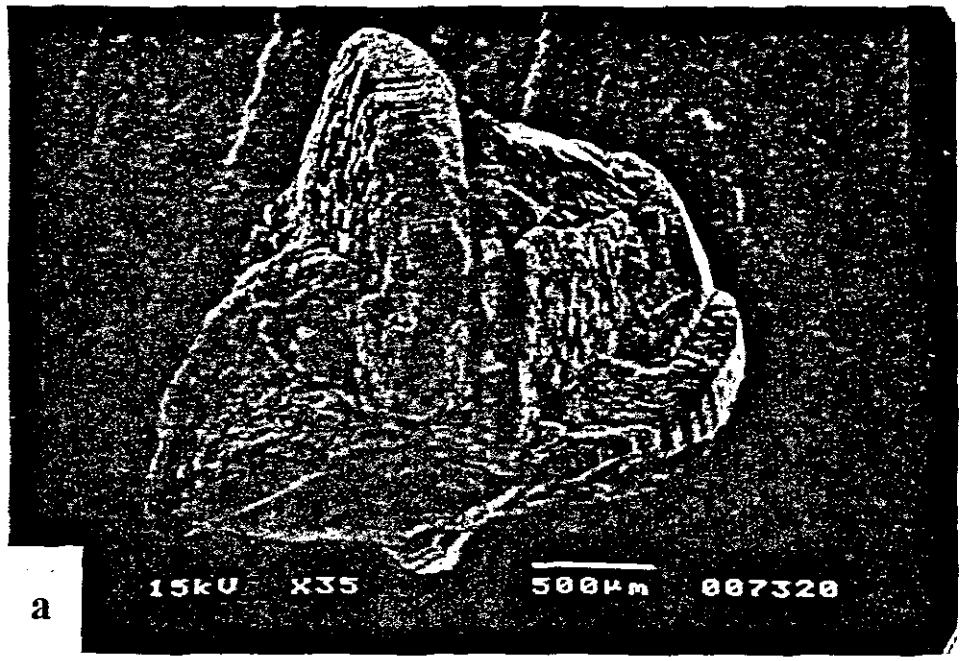

a

- Intergrown gypsum crystal from core 7 at 305 cm from the sediment surface

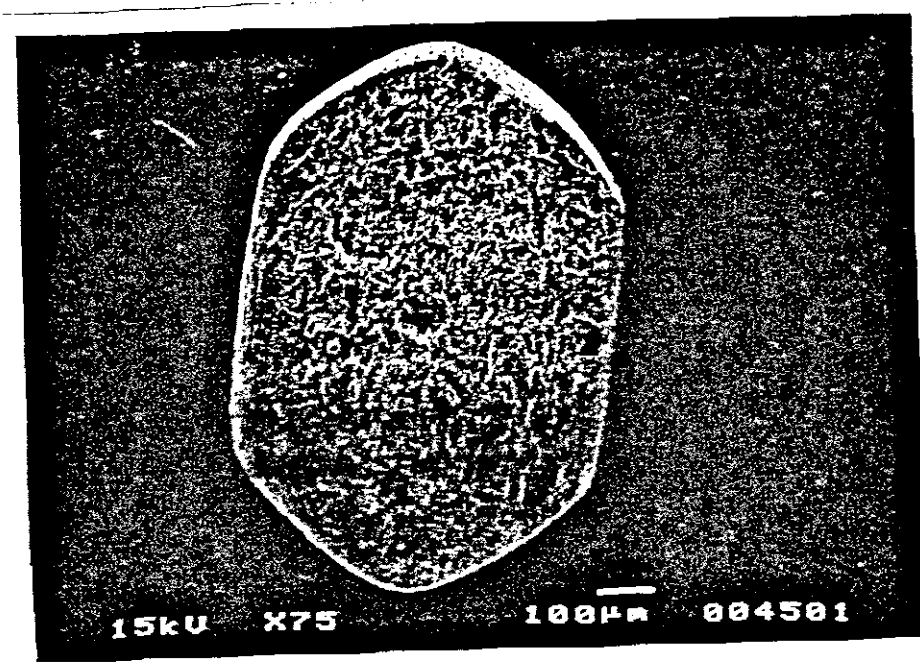

b

- Euhedral gypsum crystal from core 4 at 305 from the sediment surface. -

PLATE 4

5.4.3.1 Plankton

(a) Planktonic Foraminifera

Planktonic foraminifera occur in subordinate to trace quantities in all cores (i.e. Cores H1, H2, H3, H4, H5, H6 and H7, Figures 5.1-5.7), however, they generally occur in subordinate quantities. Among species that are identified are left-coiling *Neogloboquadrina pachyderma* (Ehrenberg) (Plate 5a-d), *Globorotalia inflata* (d'Orbigny) (Plate 6a) and *Globigerina quinqueloba* Natland (Plate 7a-b).

(b) Diatoms

Diatom frustules are generally made up of random network of tetrahedrally bound silicon atoms with nonstructural water (approximately 10%) (Calvert, 1966, 1974, in Bremner, 1977). Their wall microstructures consist of a sponge-like mass which gives the frustules an extremely high porosity (Lewin, 1961, in Bremner, 1977). Diatoms are generally restricted to the Namaqualand-shelf (Cores H6 and H7) (Figures 5.6-5.7). In general, they are present in subordinate quantities. Some of these siliceous frustules of centric diatoms are large, up to 1mm in diameter (Plate 8a), although no attempt was made to classify them taxonomically.

(c) Radiolaria

Radiolarians are almost absent throughout the study area (Figures 5.2-5.7). Where present, they occur occasionally in trace quantities. Plates 9a-d show radiolarians observed in these cores. As was the case with diatoms, no attempt was made to classify them taxonomically, but Robson, (1981; 1983) also illustrated the radiolarian in both Plates 9a-b, as *Hymeniastrum euclides* Haeckel. Plate 9a, is an example of

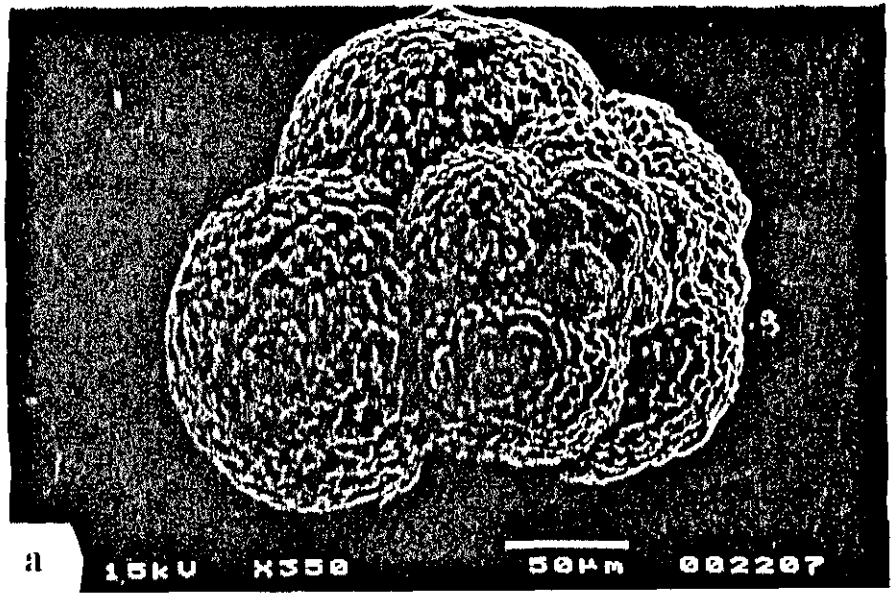
a
15kV X350 50µm 002207

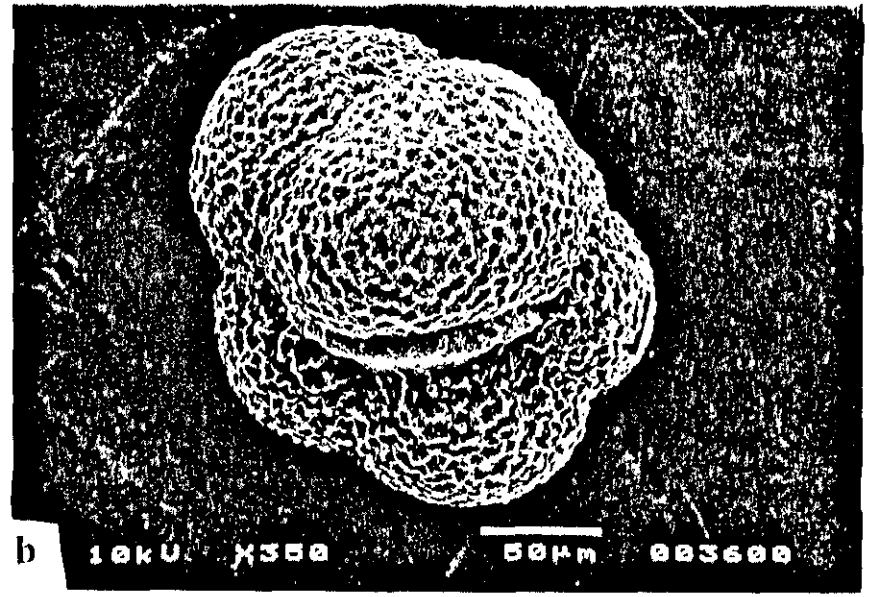
b
10kV X350 50µm 003600

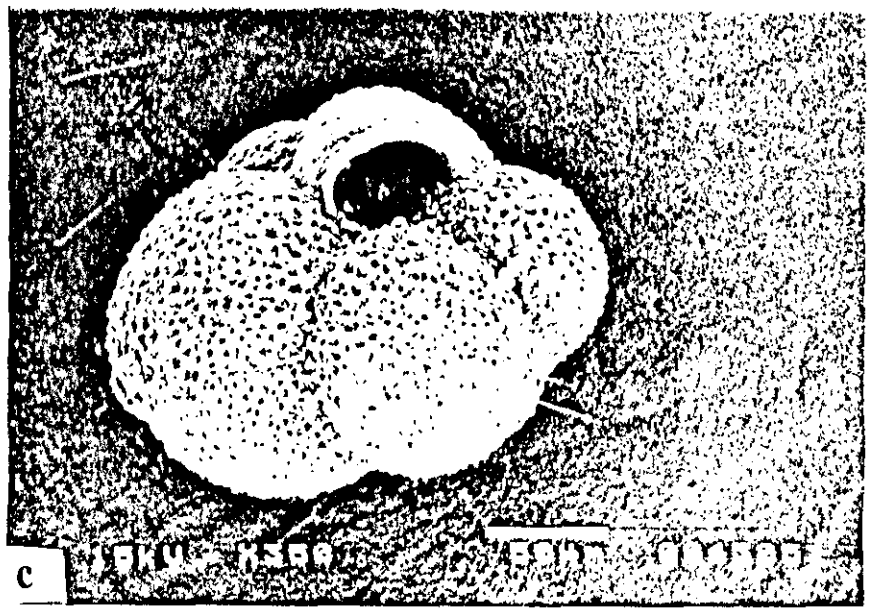
c

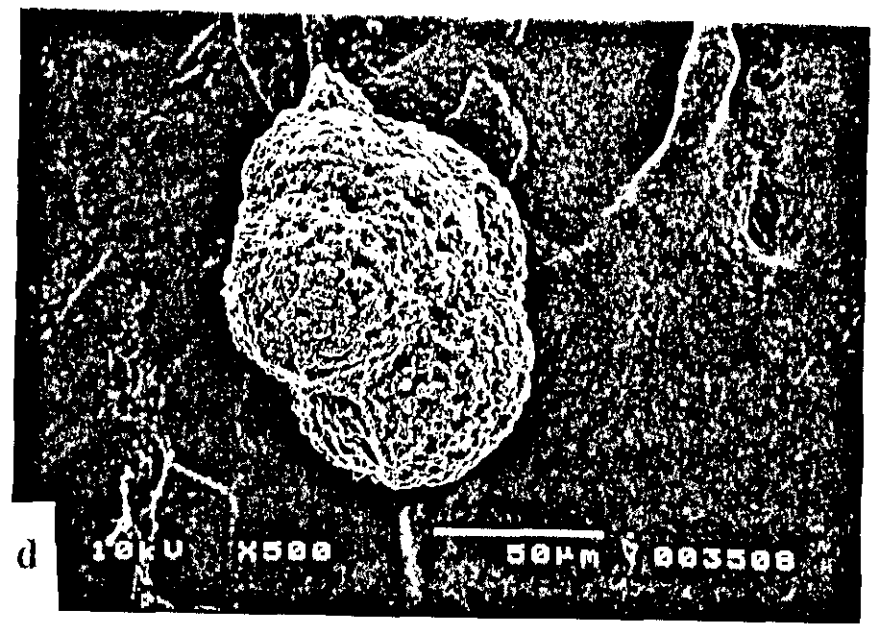
d
10kV X500 50µm 003500

PLATE 5

a

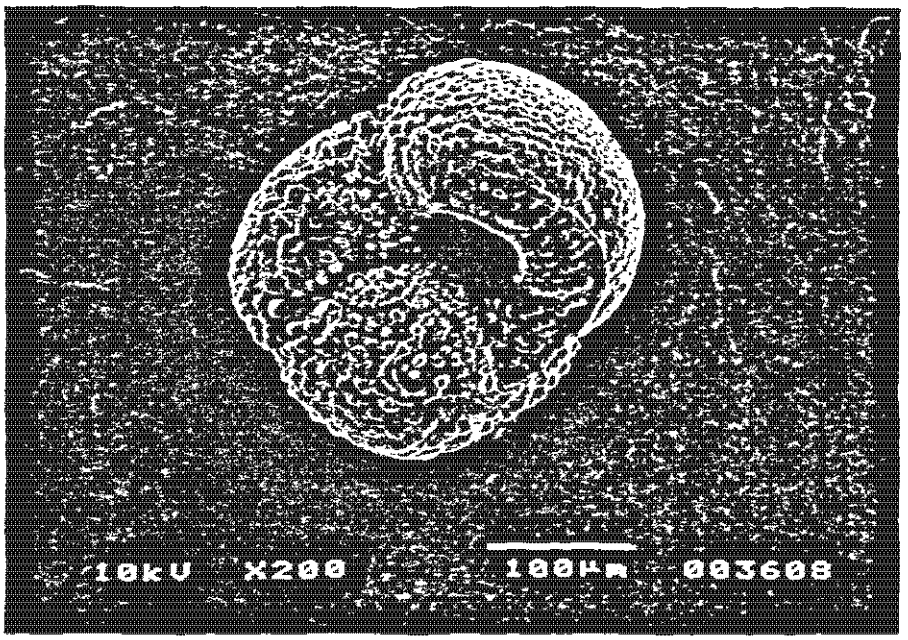

b

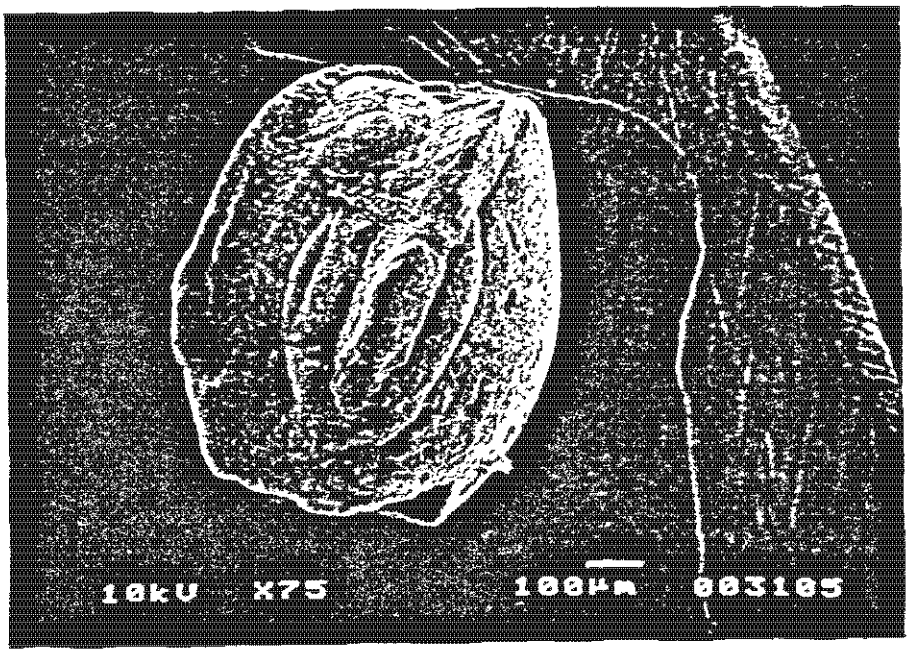

PLATE 6

a

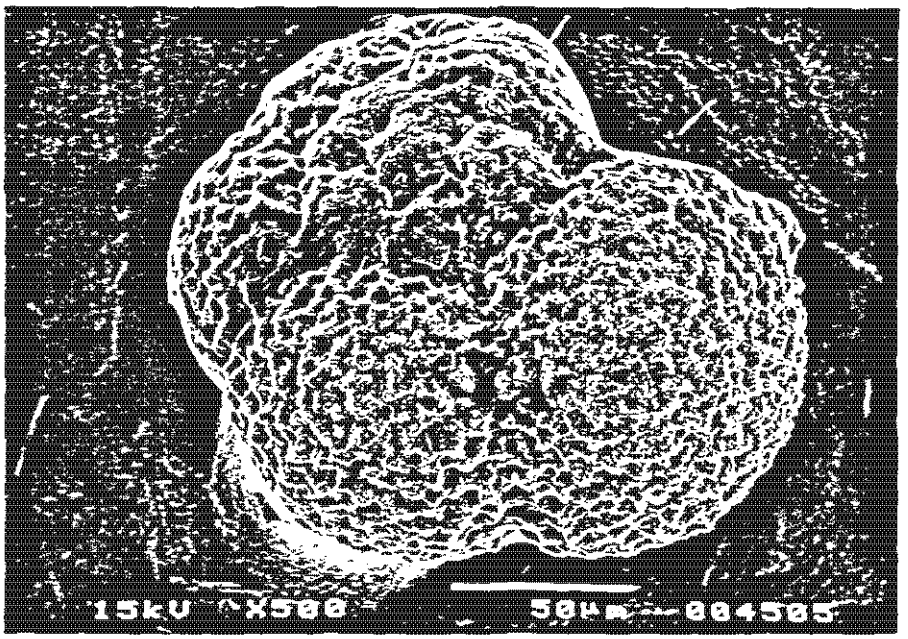

b

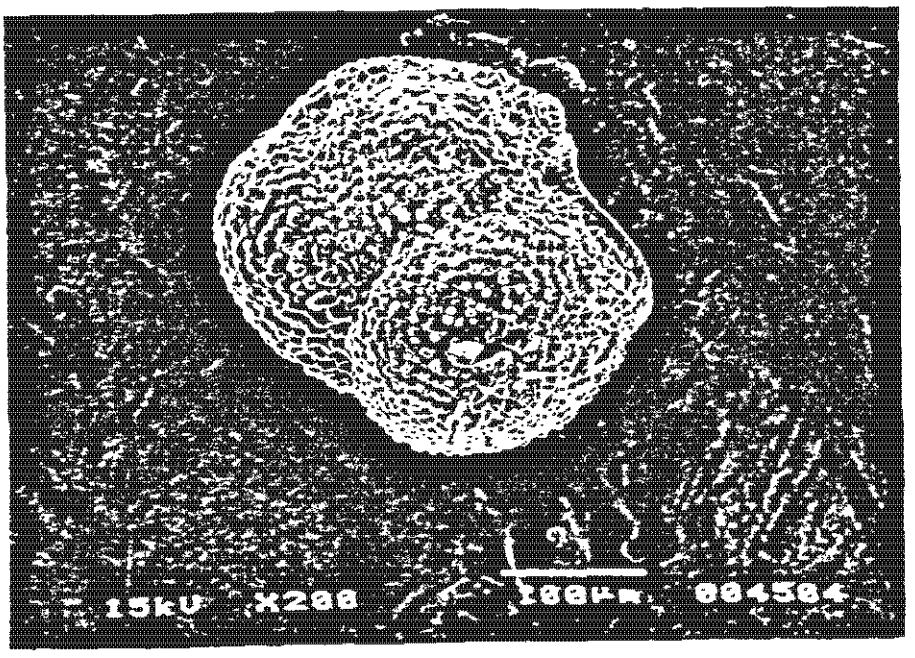

PLATE 7

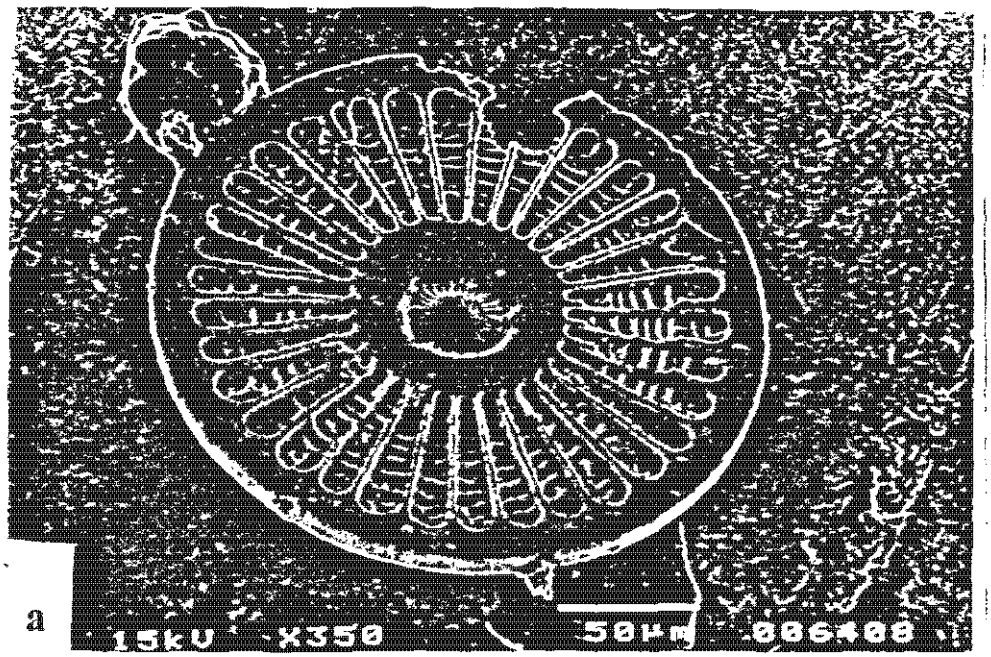

a

PLATE 8

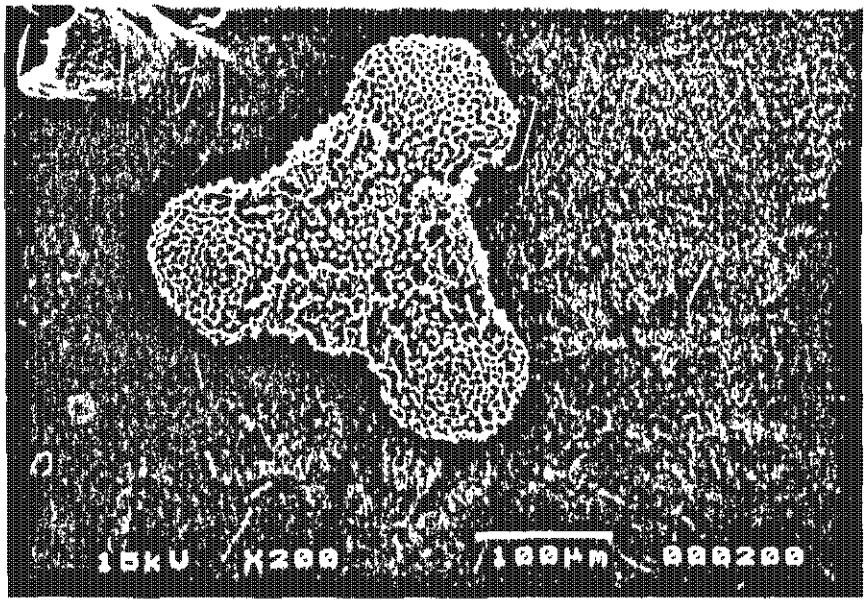
15kV X200 100µm 000200

a

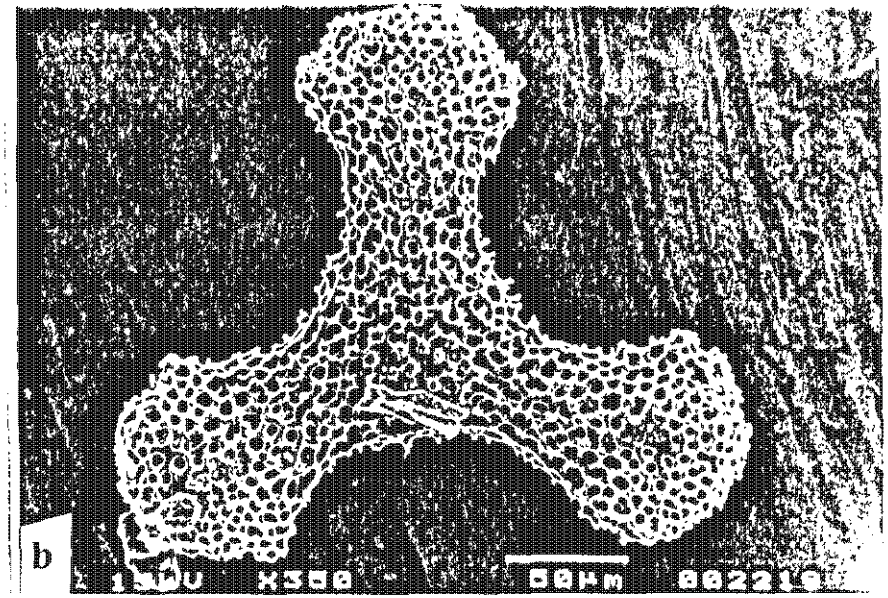
X500 50µm

b

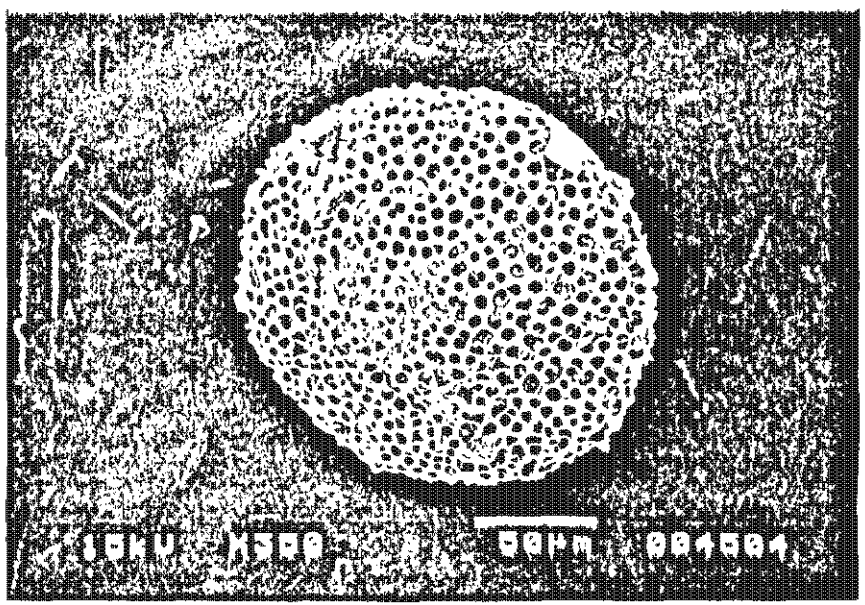
10kV X500 50µm 001001

c

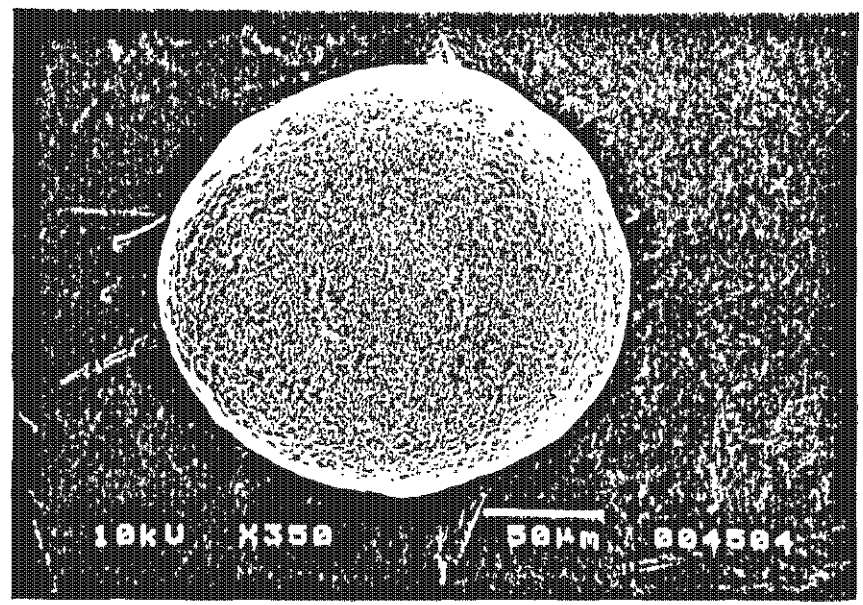
10kV X500 50µm 001001

d

PLATE 9

secondary growth on a specimen of the same species (Robson, 1981; 1983). Plate 9c is identified as *Spongotrocus venustum* (Bailey) (Robson, 1981; 1983) while Plate 9d is unidentified.

5.4.3.2 Benthos

(a) Benthic foraminifera

Benthic foraminifera are found only in trace quantities in Cores H1, H2 and H3 in the Orange Prodelta. They are less common than planktonic foraminifera in these cores, i.e. the Benthic/planktonic ratio (B/P) in these cores is <1.

Quinqueloculina sp. (Plate 6b), *Cassidulina laevigata* d'Orbigny (Plates 10a-d), *Bulimina exilis* Brady (Plates 11a-b), *Bulimina aculeata* d'Orbigny (Plates 12-a-d), *Ammonia japonica* (Hada) (Plates 13a-d) and *Nonion boueanus* (d'Orbigny) or *Pseudononion chiliensis* (Cushman and Kellett) (Plate 14a) and *Nonionella turgida* (Williamson) (Plates 15a-c) are the most common species in these cores, from the Orange Prodelta.

Southward from the Orange River mouth, both the abundance and diversity of benthic foraminifera increase. In general, benthic foraminifera are present in subordinate quantities and less often dominate sand-fraction components in Cores H4, H5, H6 and H7 (Figures 5.4-5.7). Common species in these cores are *Cassidulina laevigata* (Plates 10a-d), *Bulimina exilis* (Plates 11a-b), *Bulimina aculeata* (Plates 12a-d), *Ammonia japonica* (Plates 13a-d), *Stainforthia fusiformis* (Williamson) (Plates 16a-c), *Nonionella turgida* (Plates 15a-c), *Brizalina pseudopunctata* (Hoglund) (Plate 17a), *Elphidium macellum* (Fichtel and Moll) (Plate 18a), *Elphidium advenum* (Cushman)

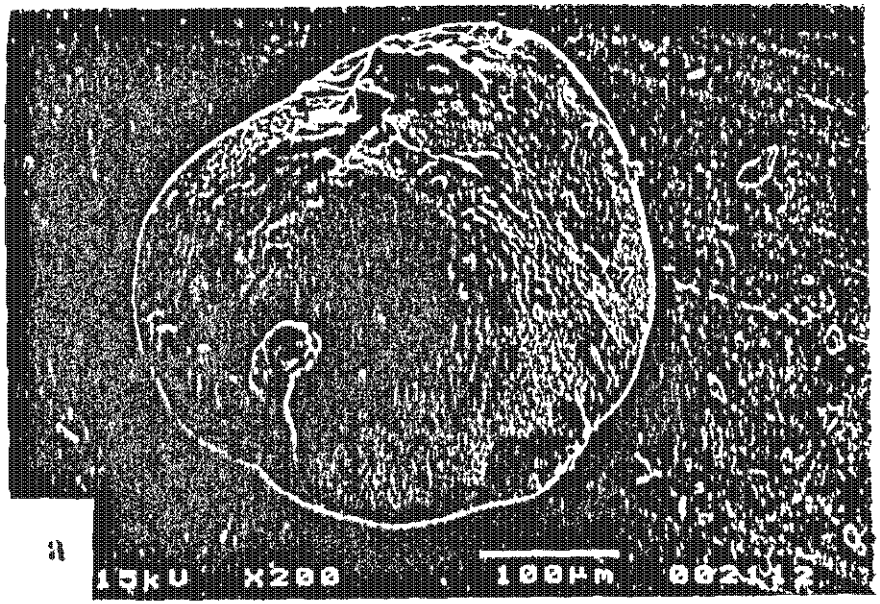
a
15kV X200 100µm 002112

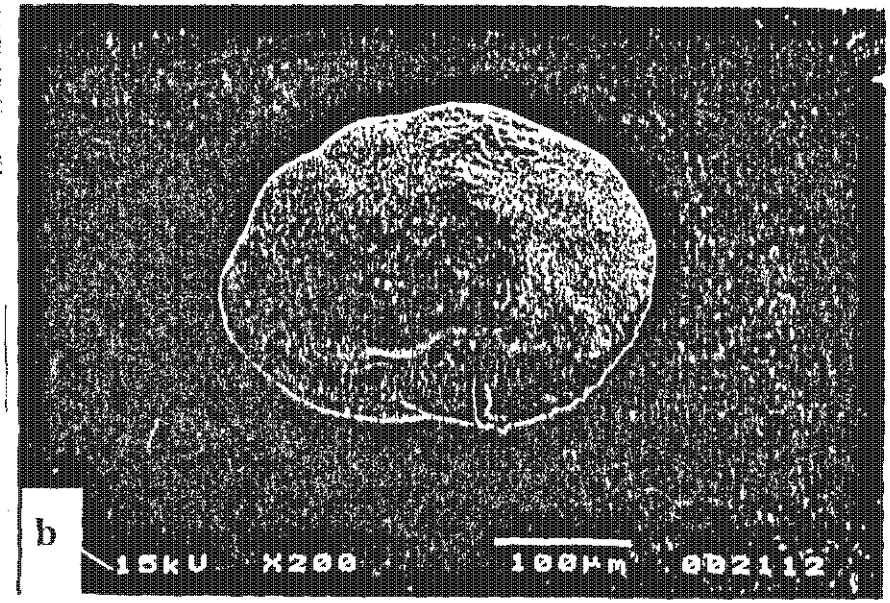
b
15kV X200 100µm 002112

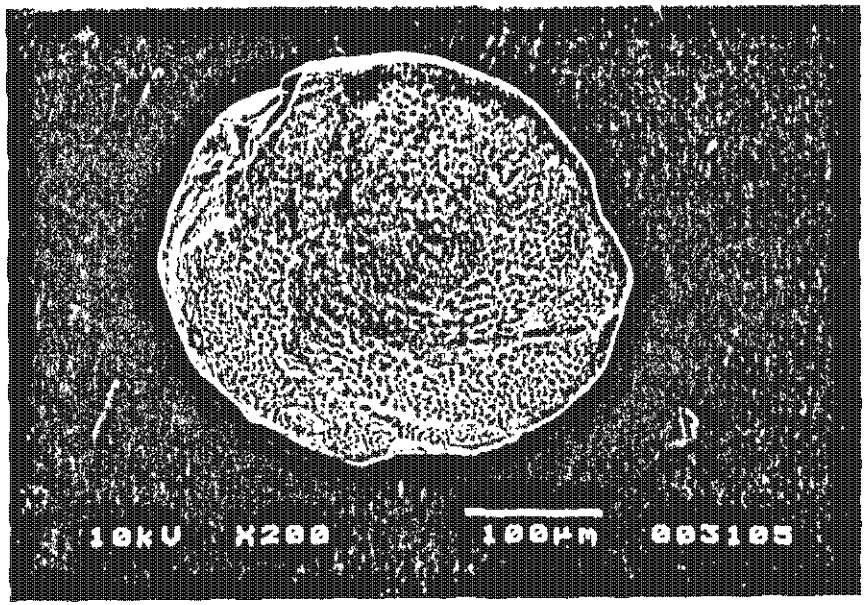
c
10kV X200 100µm 003105

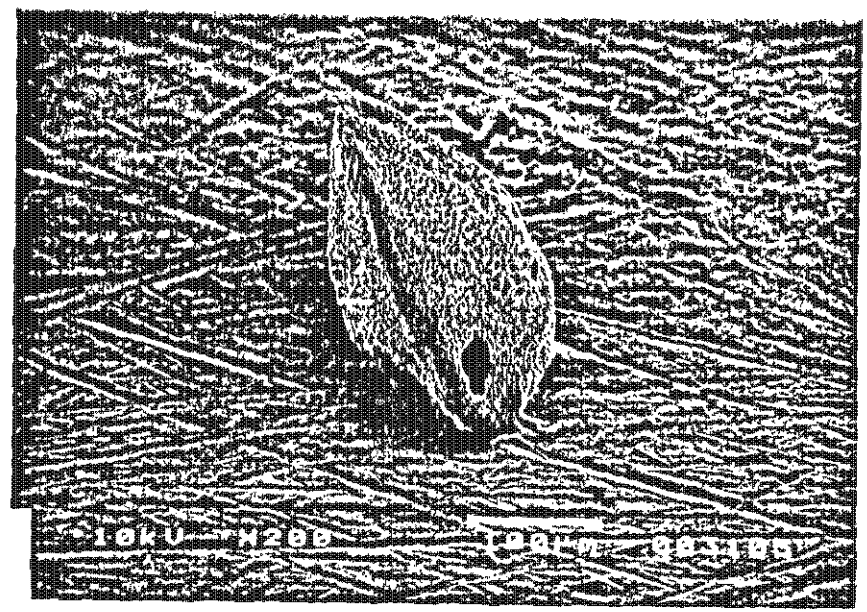
d
10kV X200

PLATE 10

a

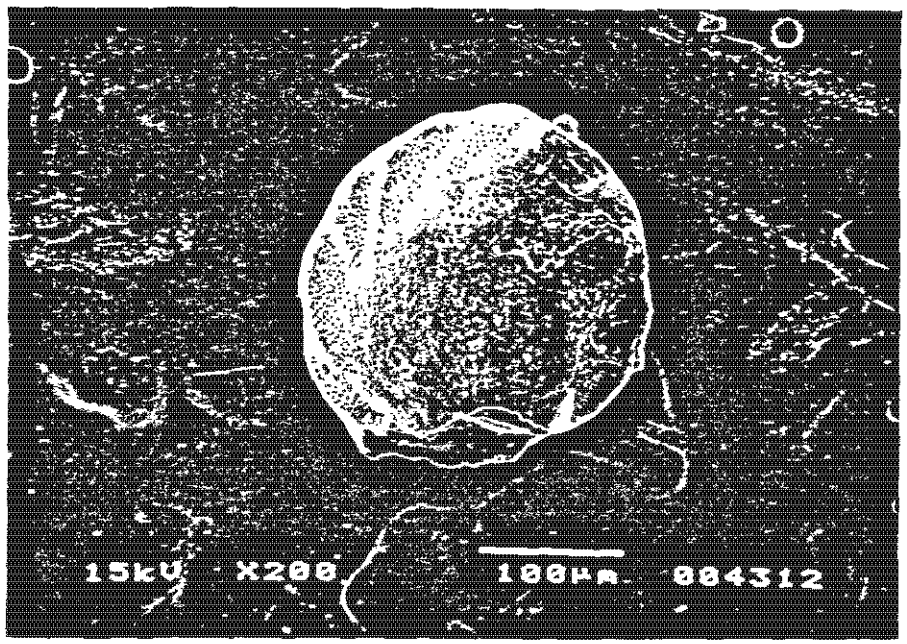

b

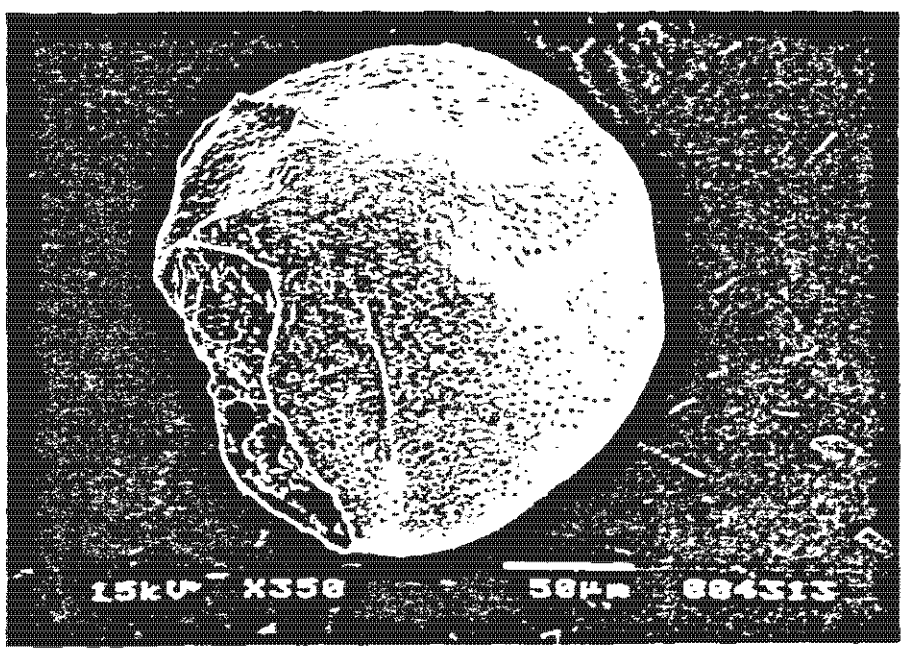

PLATE 11

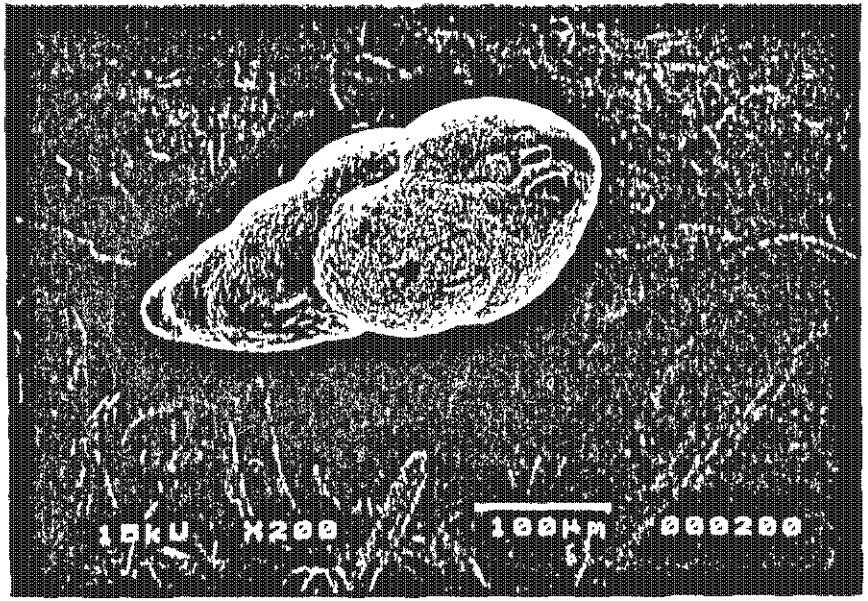

a

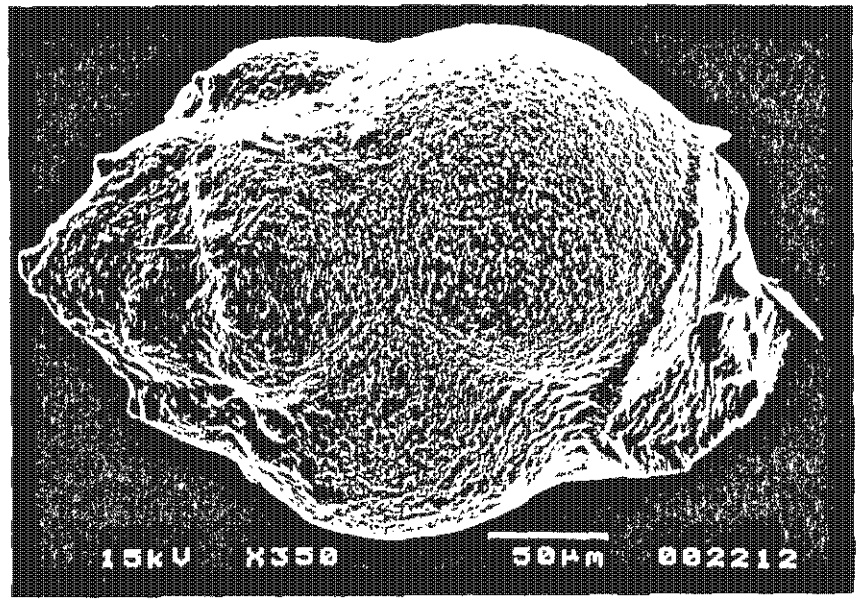

b

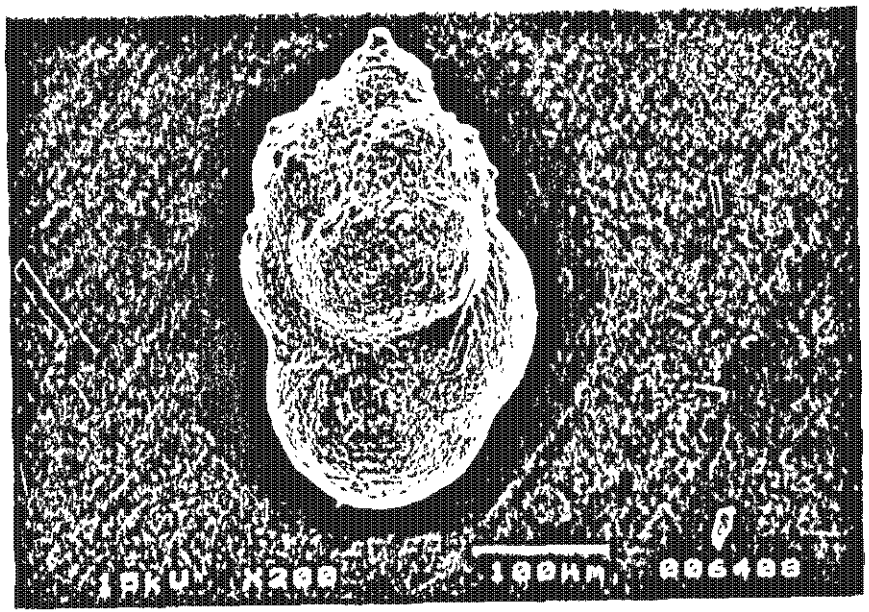

c

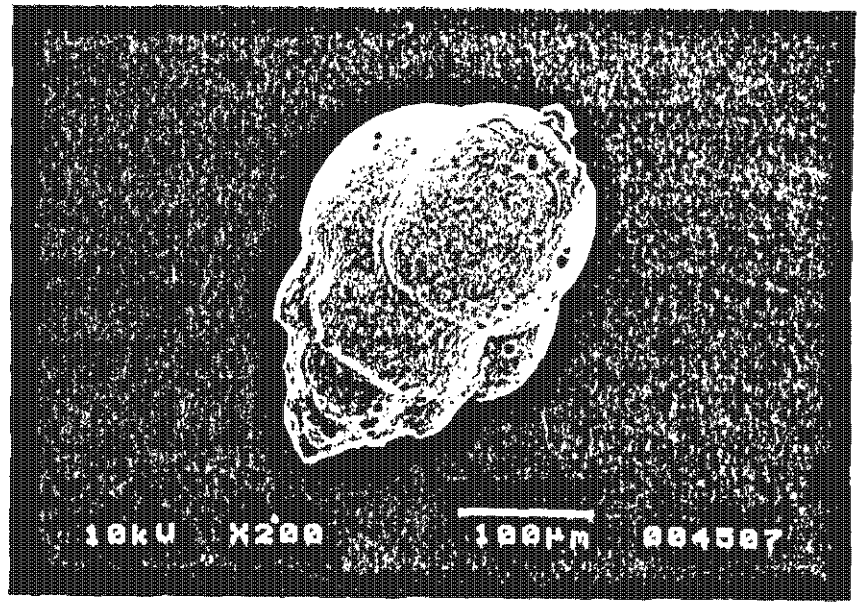

d

PLATE 12

a

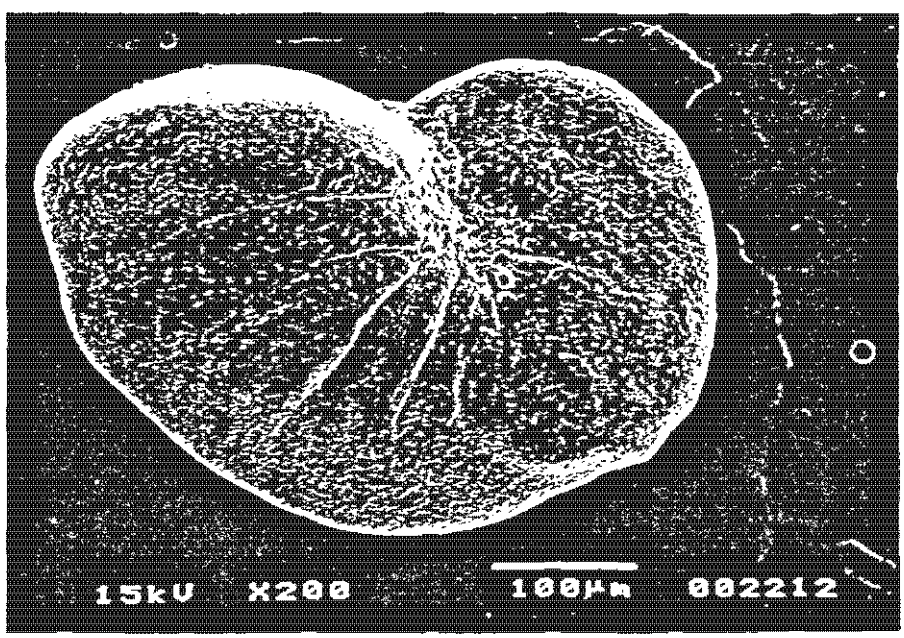

PLATE 14

a

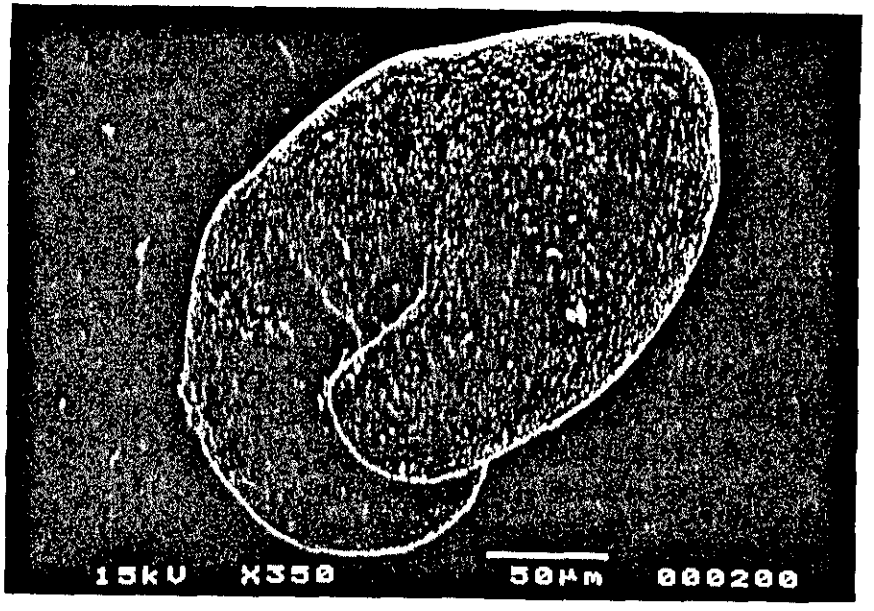
15kV X350 50µm 000200

b

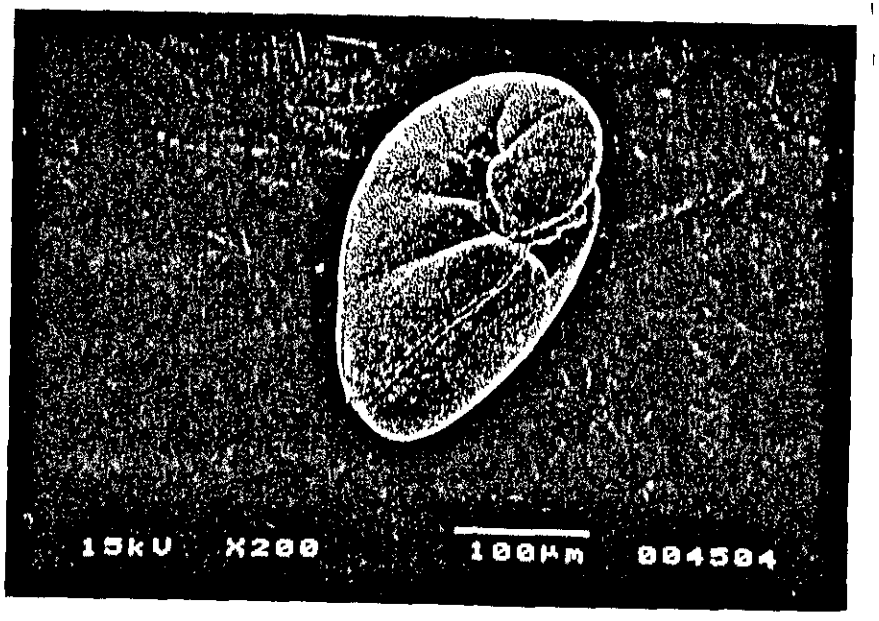
15kV X200 100µm 004504

c

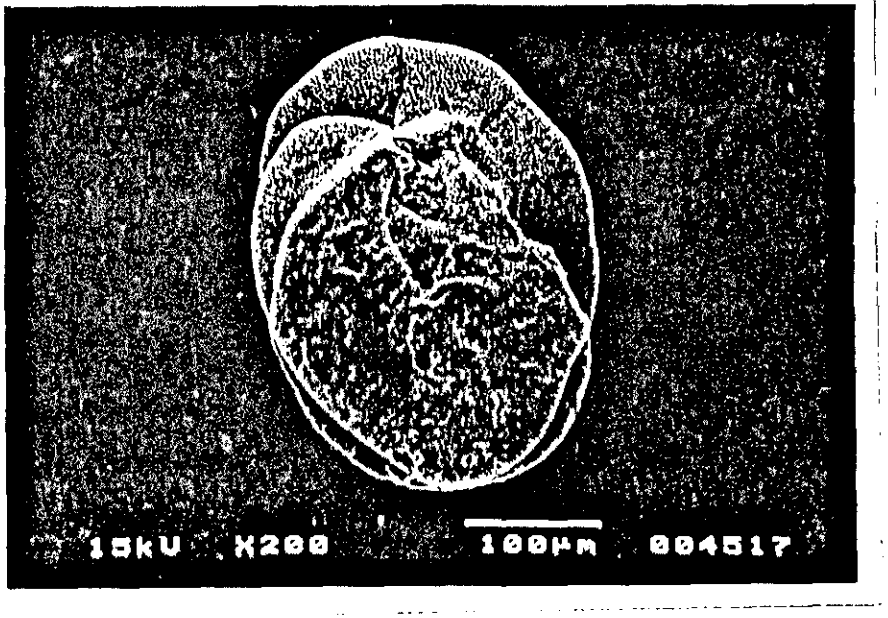
15kV X200 100µm 004517

PLATE 15

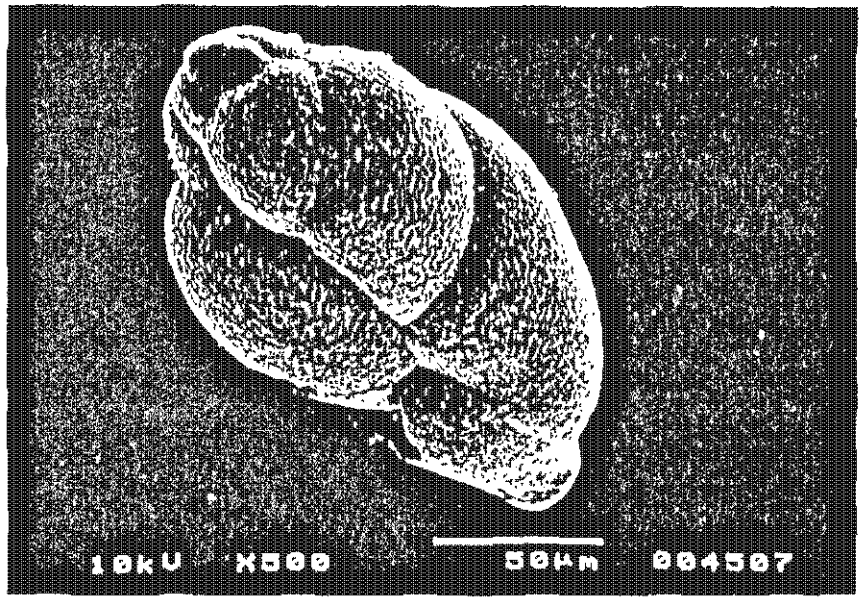
10kV X500 50µm 004507

a

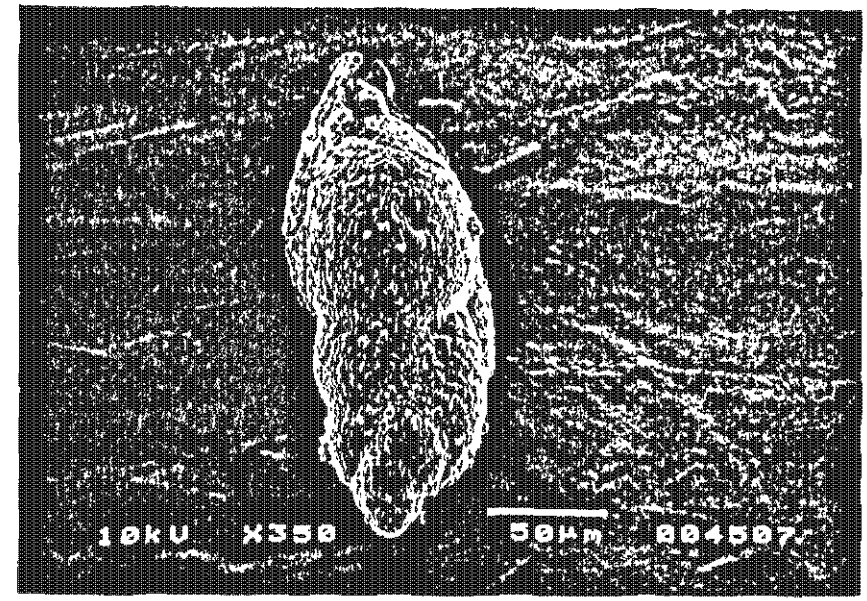
10kV X350 50µm 004507

b

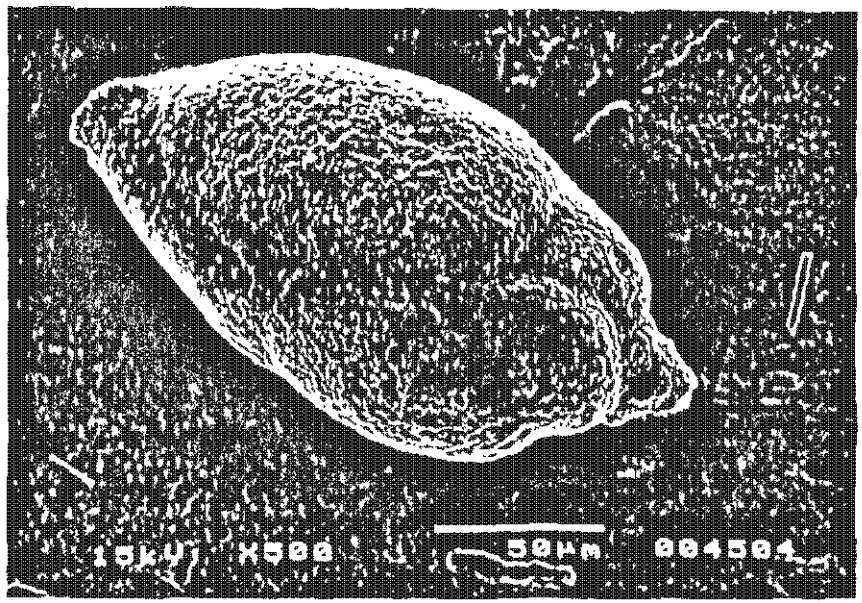
15kV X500 50µm 004504

c

PLATE 16

a

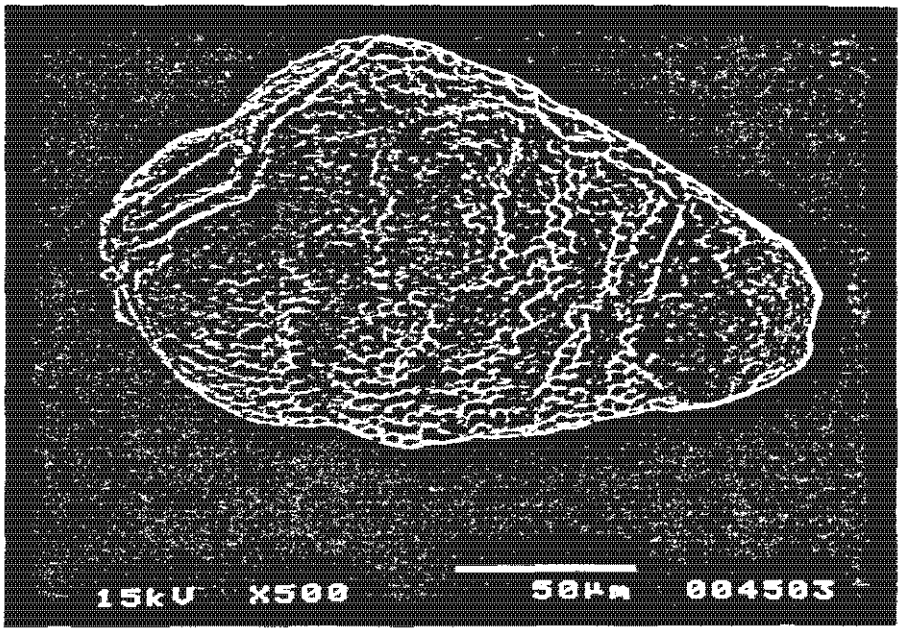

PLATE 17

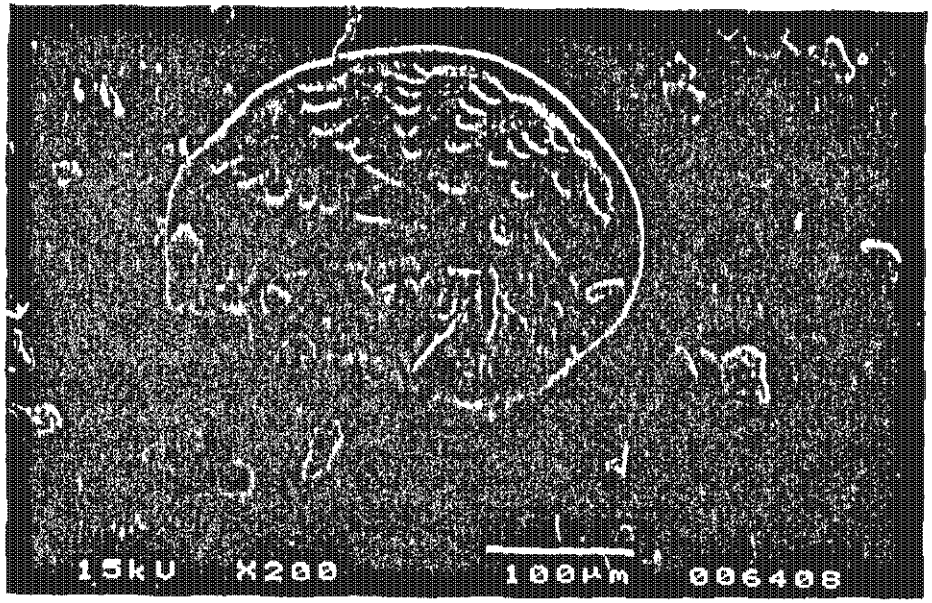
15kV X200 100µm 006408

b

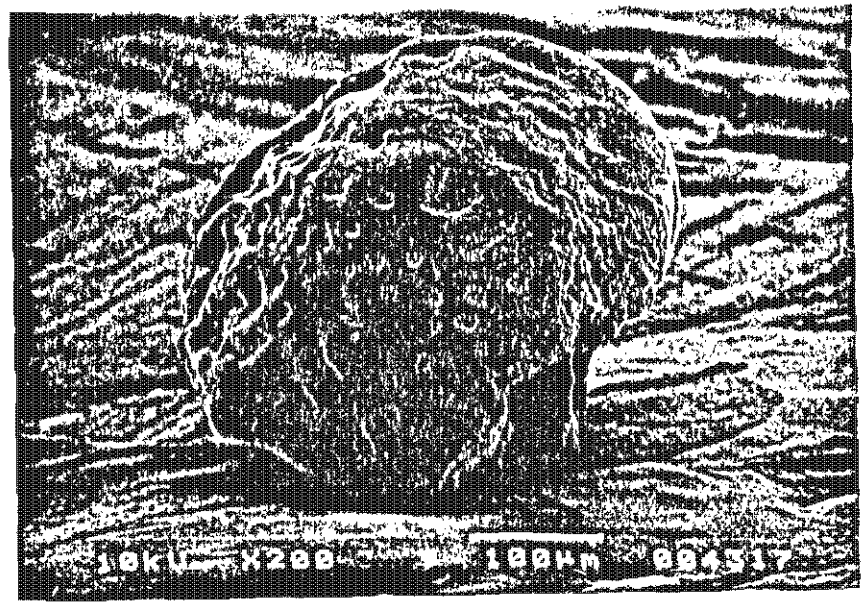
15kV X200 100µm 006417

c

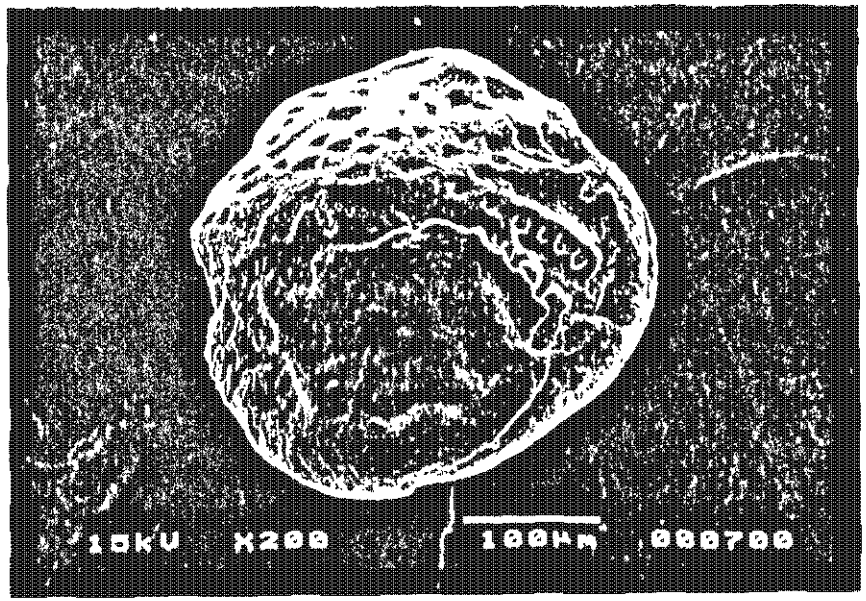
15kV X200 100µm 000700

d

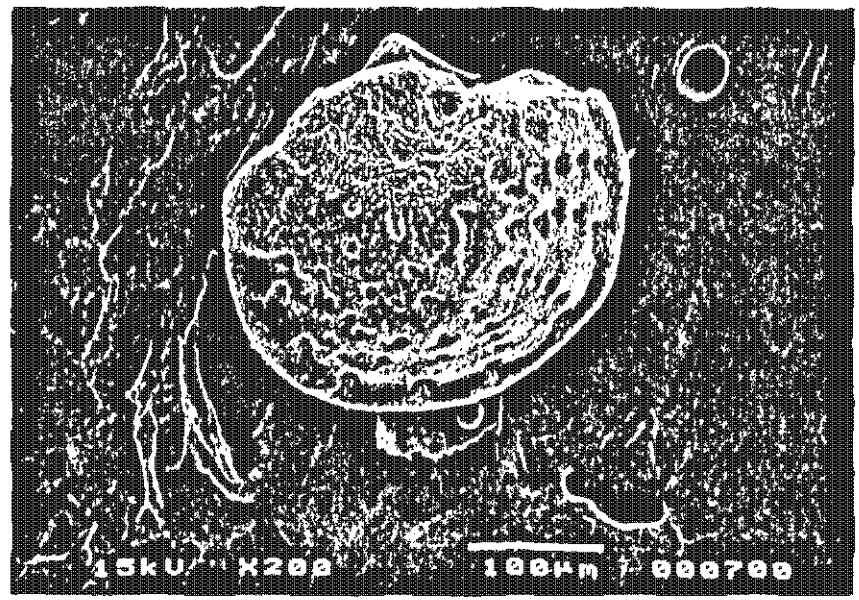
15kV X200 100µm 000700

PLATE 18

Plates 18b-d), *Lobatula lobatula* (Walker and Jacob) (Plates 19a-d), *Lagena semilineata* Wright var. (Plate 20a), *Oolina sp.* McMillan (Plates 20b-c), *Elphidium cf. alvarezianum* (Plate 20d), *Discammina compressa* Goes (Plate 21a) and Bu*liminella elegantissima* (d'Orbigny) (not on plate).

(b) Sponge spicules

No sponge spicules were observed in Cores H1 and H2, on the Orange Prodelta. Sponge spicules are found only in trace quantities in Cores H3 and H4. Their abundance increases southwards away from the Orange River mouth. They are present in dominant to subordinate quantities in Cores H6 and H7, which are the most southerly cores in the study area. Sponge spicules are composed of silica and resemble delicate glass rods (Plate 22a). Although their diameter is estimated as less than 63 μm, they are longer than 63 μm, and hence found in sand-fraction.

(c) Shell and shell fragments

Mollusc (gastropods) shells and their fragments are the chief components of shell and shell fragments. Other shell fragments include bivalves. In general, shell fragments are present only in trace quantities in all cores except Core H1 on the Orange Prodelta, where no shells fragments are observed, and core H5 where these shell fragments dominate gravel and sand fractions at the bottom of the core (Figures 5.1-5.7). Unbroken gastropod shells are observed in Cores H4, H5, H6 and H7, but are most frequently found in Core H4. Unbroken gastropod shells are exclusive to Cores H4 and H5 and are the chief component of the gravel fraction. The most common species of gastropods identified in these sediments are *Burnupena limbosa* (Lamark, 1822)

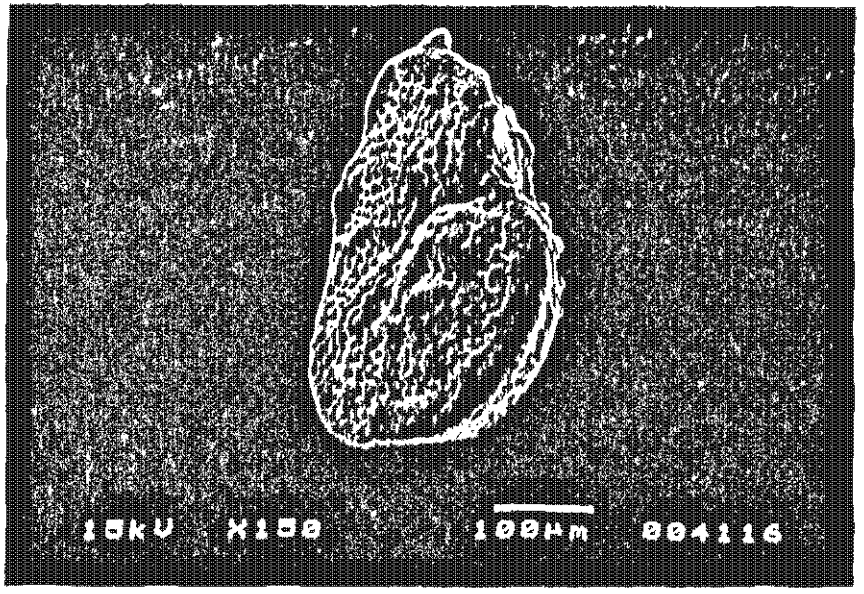

a

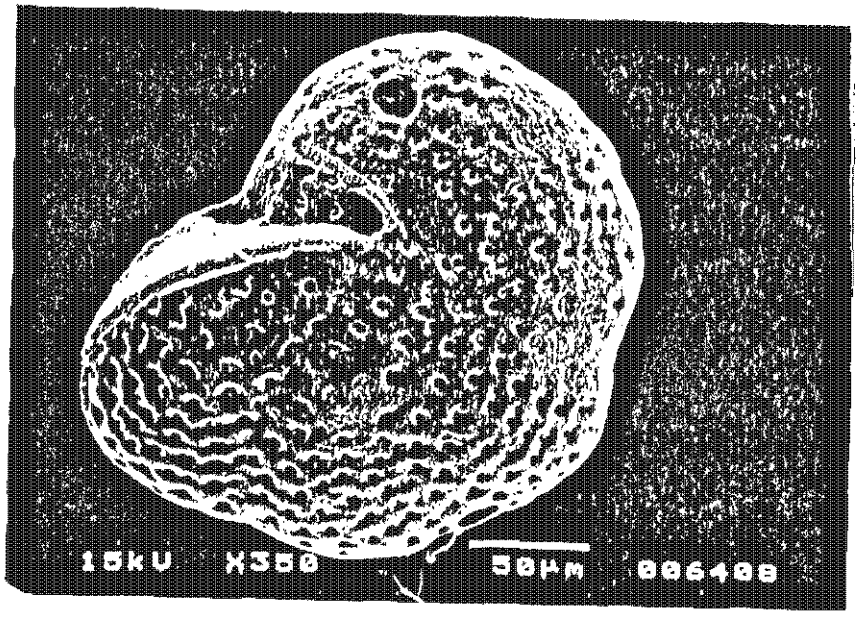

b

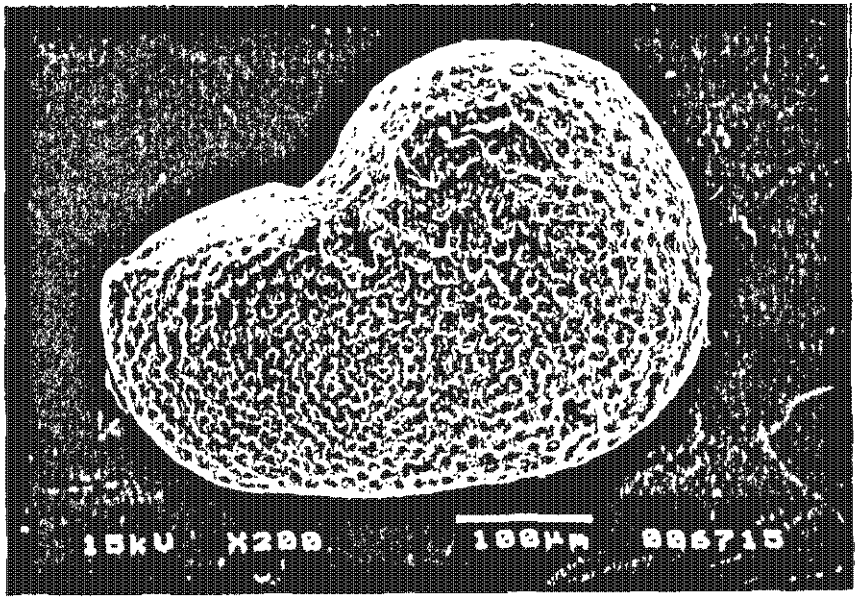

c

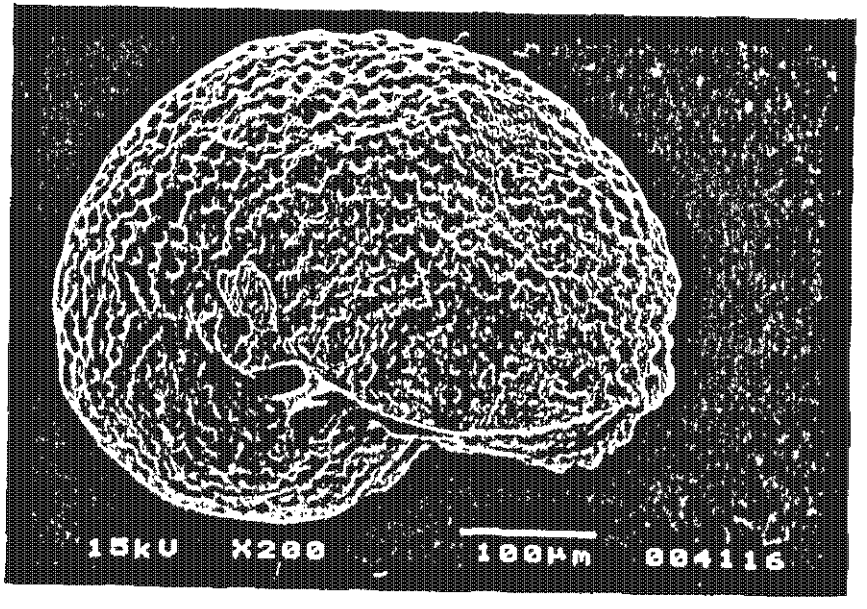

d

PLATE 19

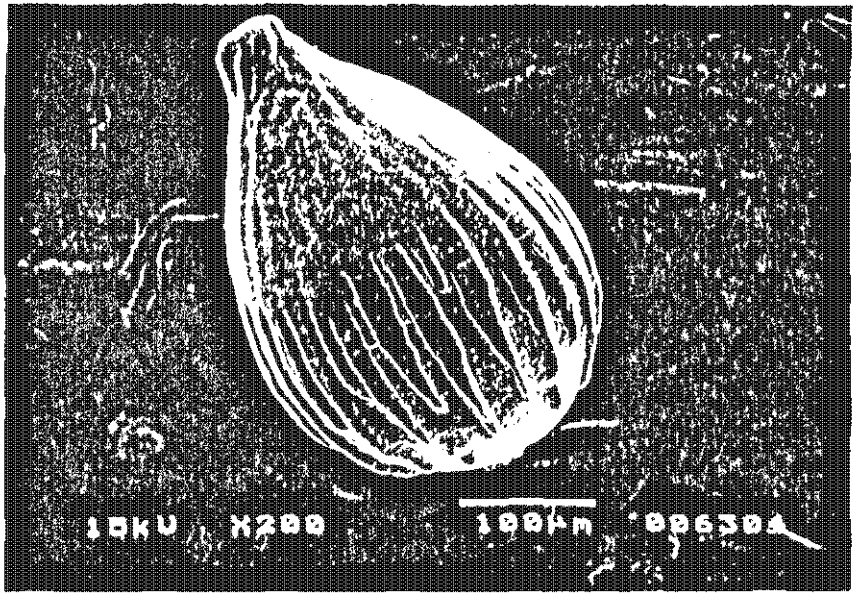

a

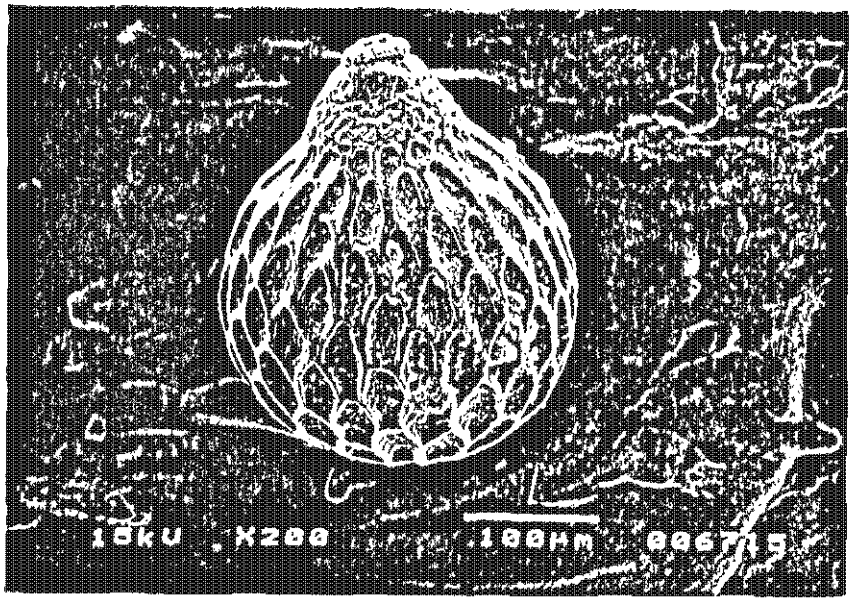

b

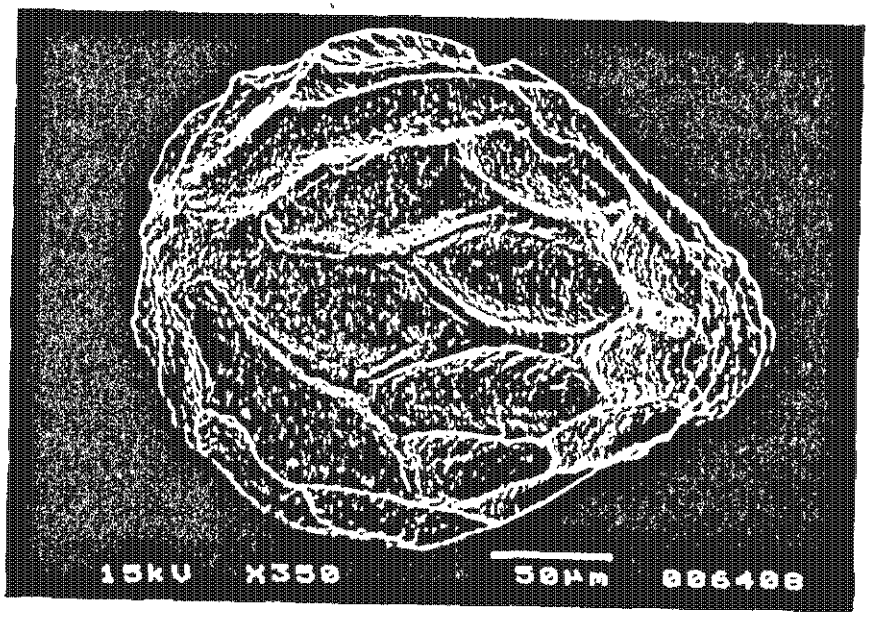

c

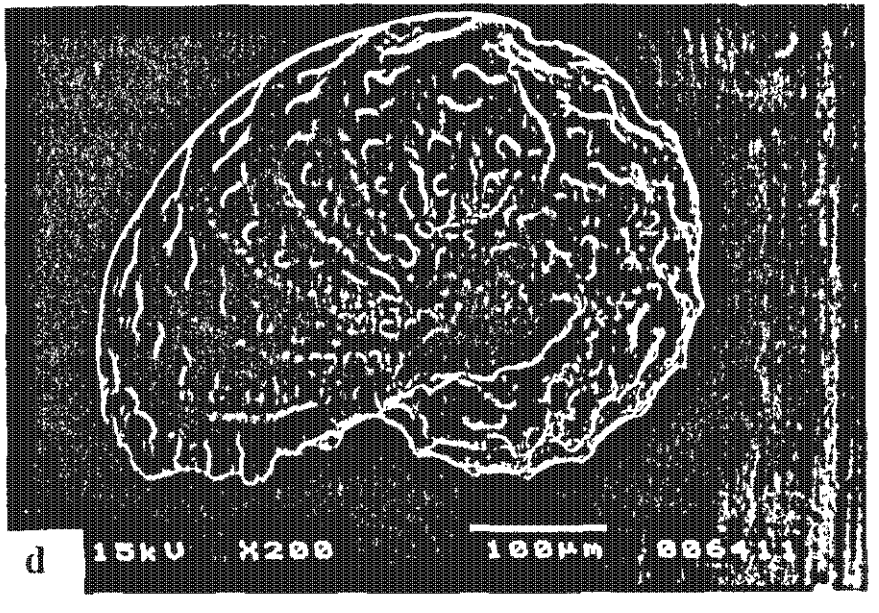

d

PLATE 20

a

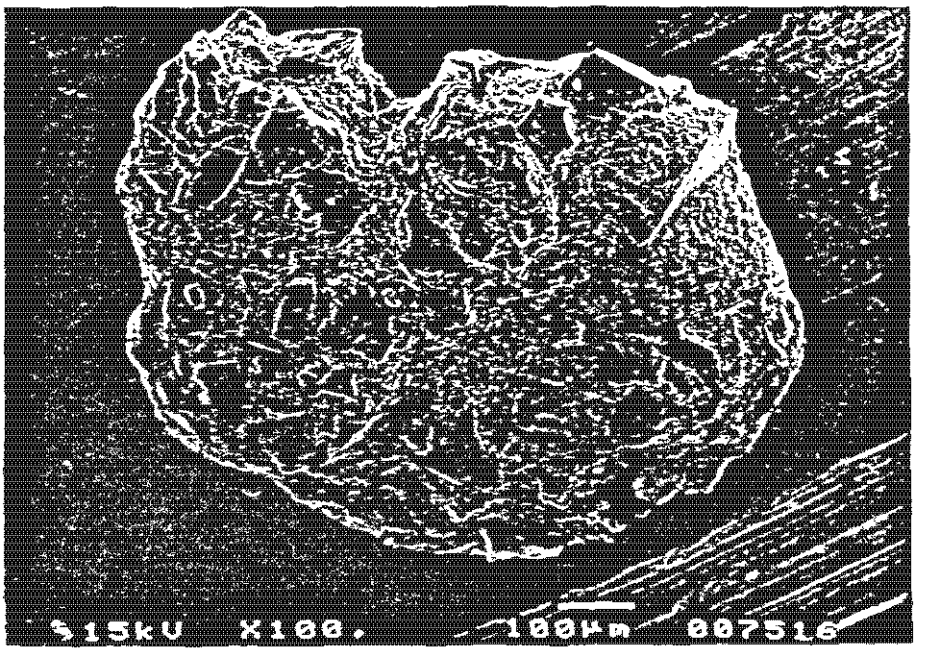

PLATE 21

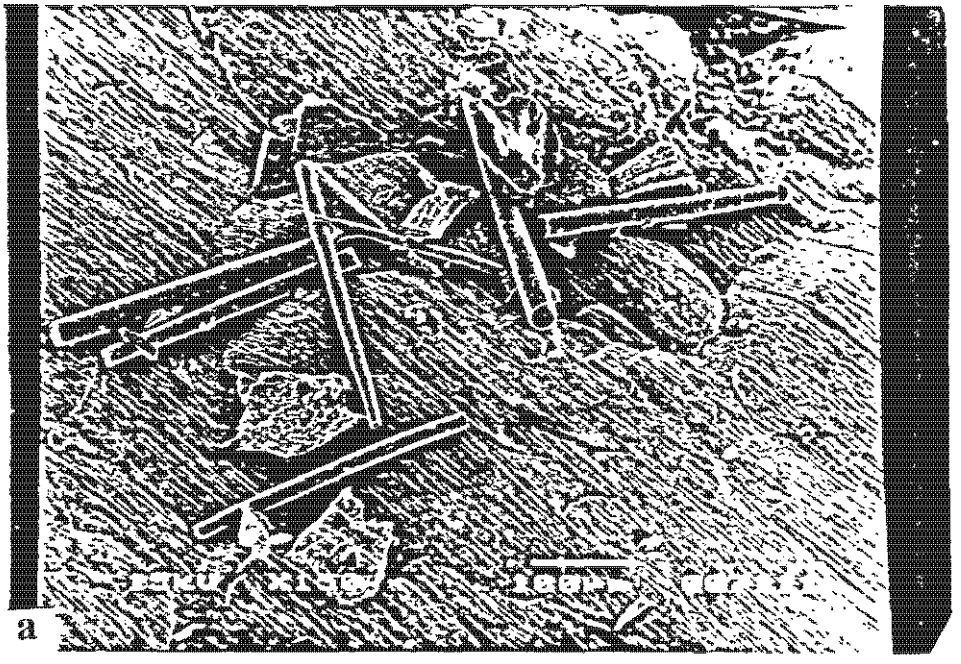

a

PLATE 22

(Plate 23a), *Nassarius vinctus* (Marrat, 1877) (Plate 23b), *Volutocorbis lutosa* Koch, 1948 (Plates 24a-b) and *Comitas saldanhae* (Barnard, 1958) (25a). These shells are usually not corroded and "fresh" looking. The most common bivalve is *Tellina analogica* Sowerby, 1904 (Plate 25b).

(d) Ostracods

Ostracods are generally found occasionally in trace amounts and hence no detailed work was attempted on them. However, where present, they have either smooth exterior or an ornament of some nature (Plate 26a).

(e) Faecal Pellets

Although they are absent or present only in trace quantities in Cores H1, H3, H6 and H7, benthic faecal pellets are abundant in Cores H2, H4 and H5 (Figures 5.1-5.7). They are found as ovoid particles, medium to coarse sand (500 to 250 μm) in size (Plate 26b). Their occurrence in Cores H2, H4 and H5 varies from dominant to subordinate, although they are most abundant near the surface of the cores, particularly in the upper 30cm.

5.4.3.3 Nekton

(a) Fish Debris

Fish remains are almost exclusive to Core H4 (Figures 5.1-5.7). These fish remains consist of scales, fish otolith (Plate 27a), crab claw (Plate 27b), fish tooth (Plate 27c), vertebra (Plate 28a) and a jaw (Plate 28b).

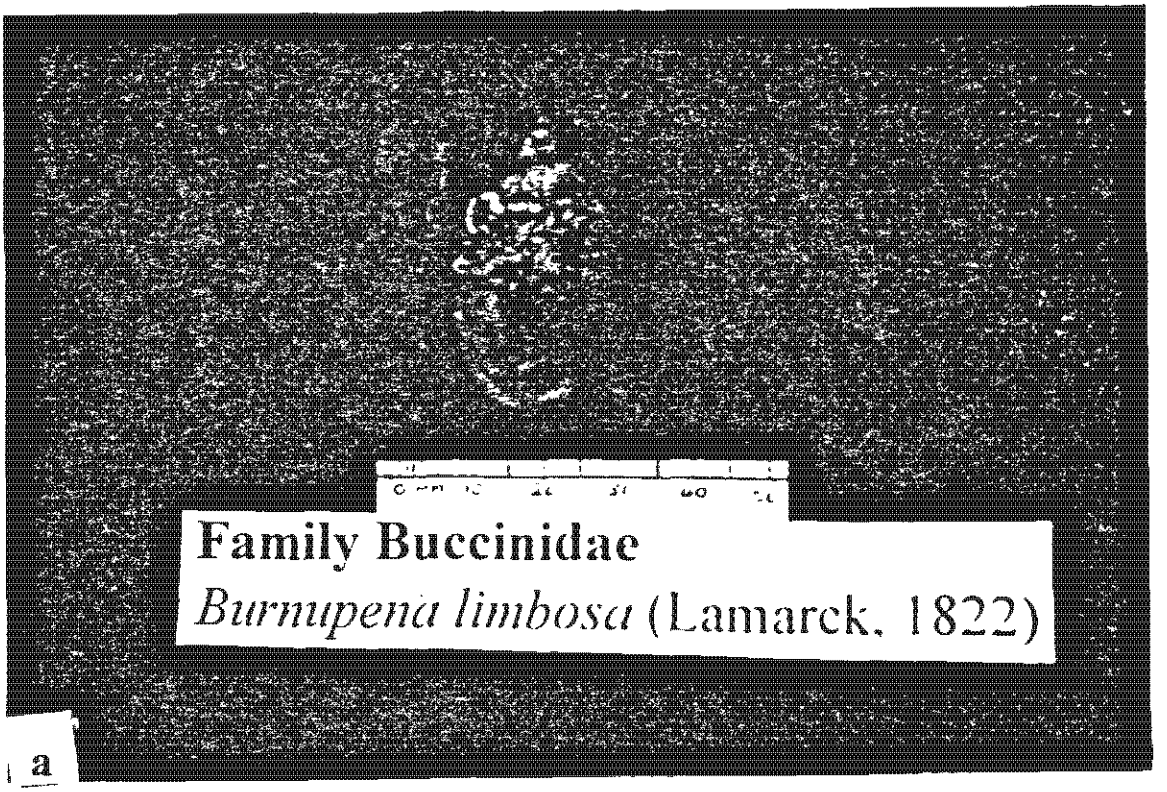

Family Buccinidae
Burnupena limbosa (Lamarck, 1822)

a

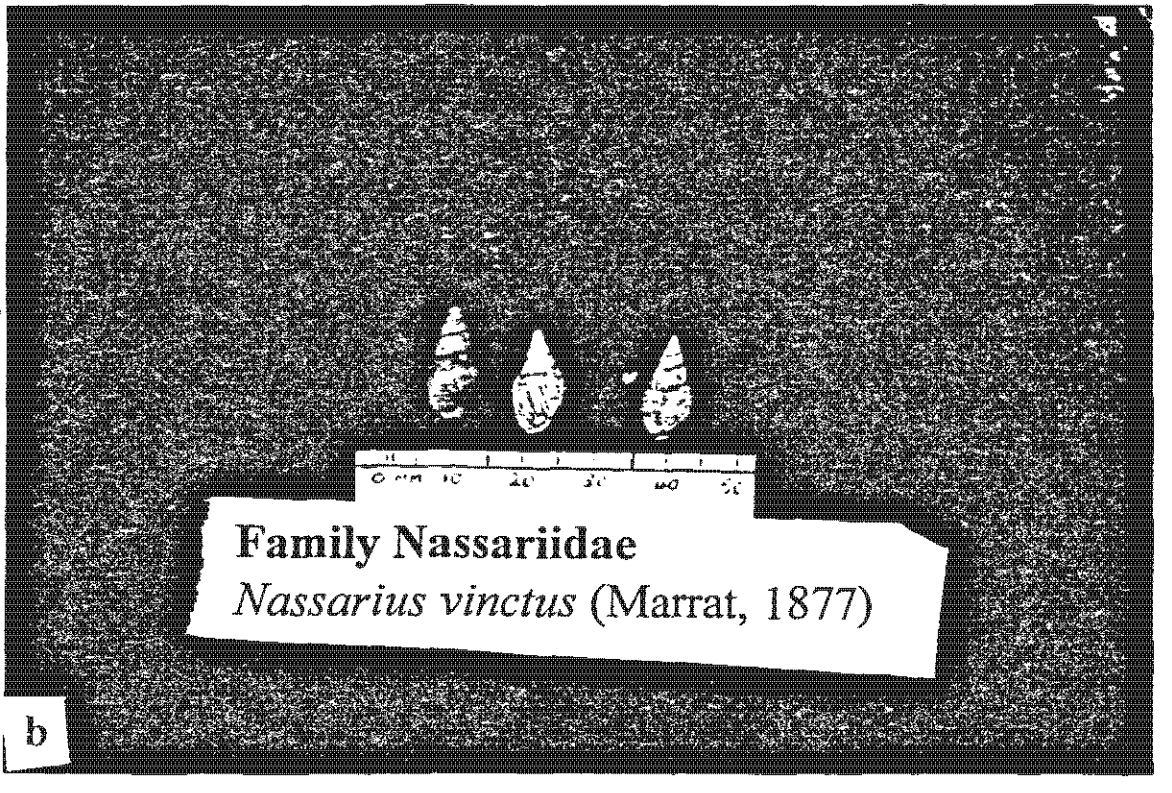

Family Nassariidae
Nassarius vinctus (Marrat, 1877)

b

PLATE 23

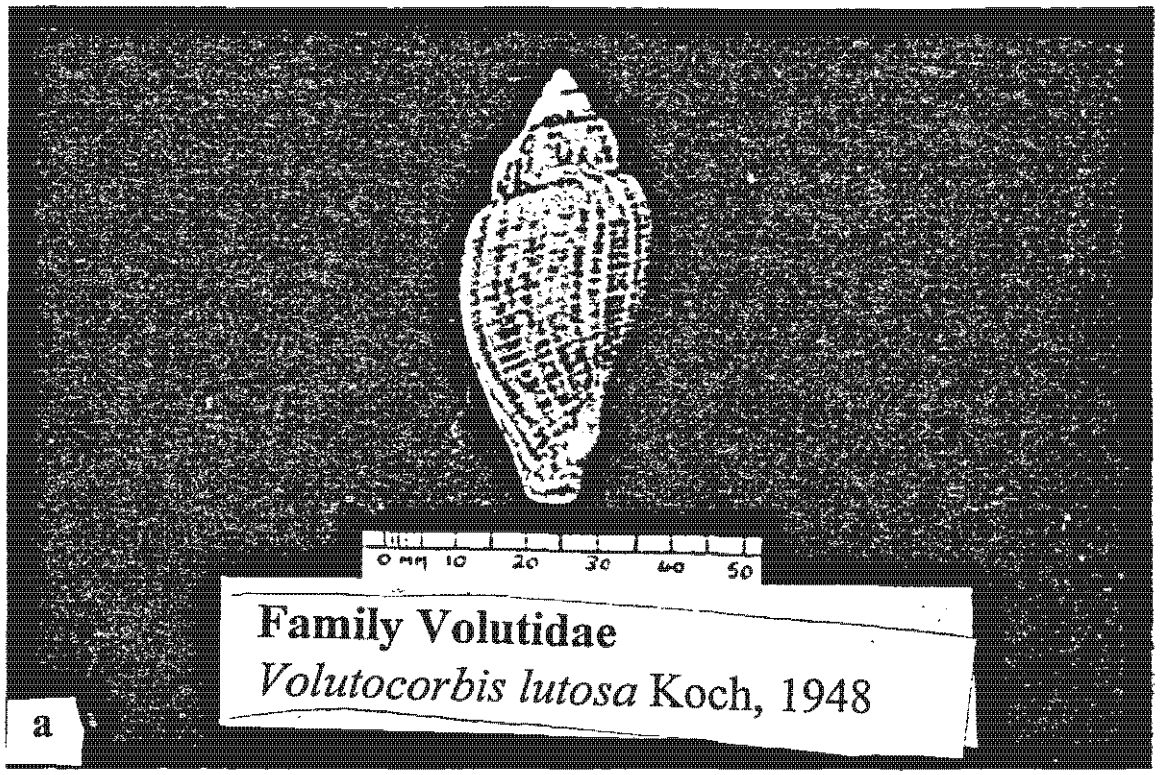
0 mm 10 20 30 40 50
Family Volutidae
Volutocorbis lutosa Koch, 1948
a

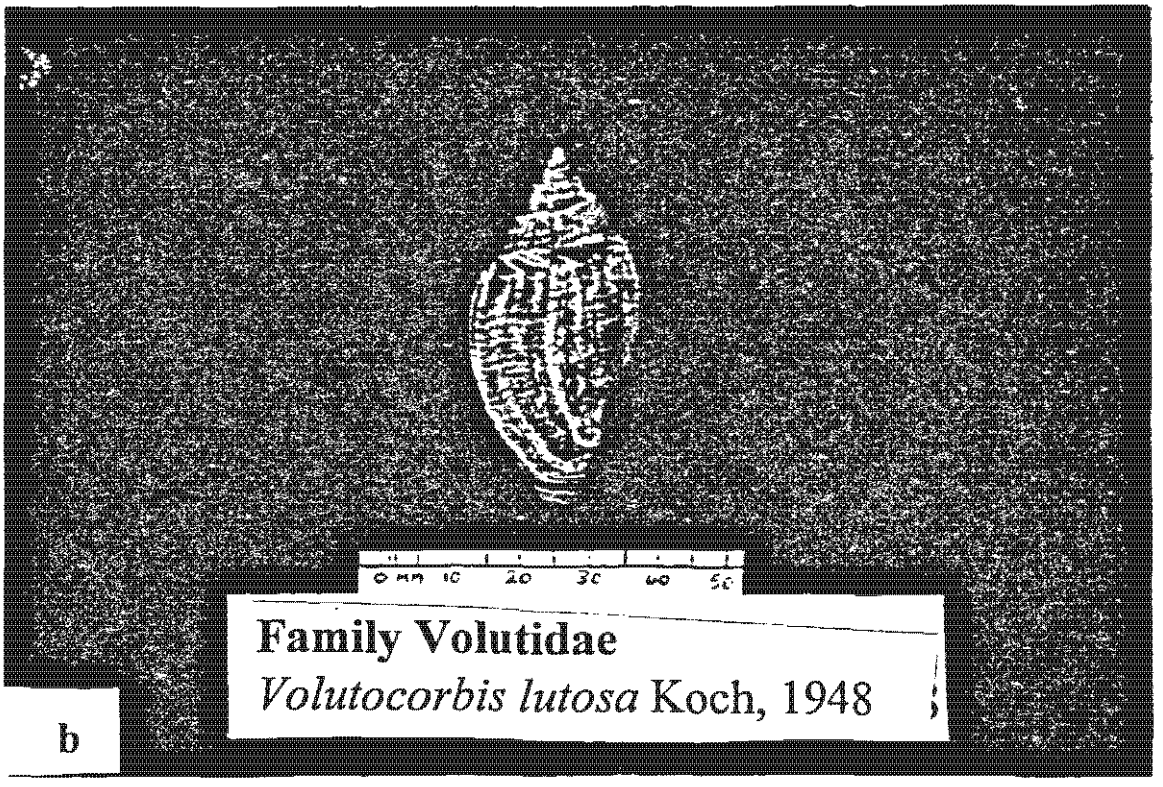
0 mm 10 20 30 40 50
Family Volutidae
Volutocorbis lutosa Koch, 1948
b

PLATE 24

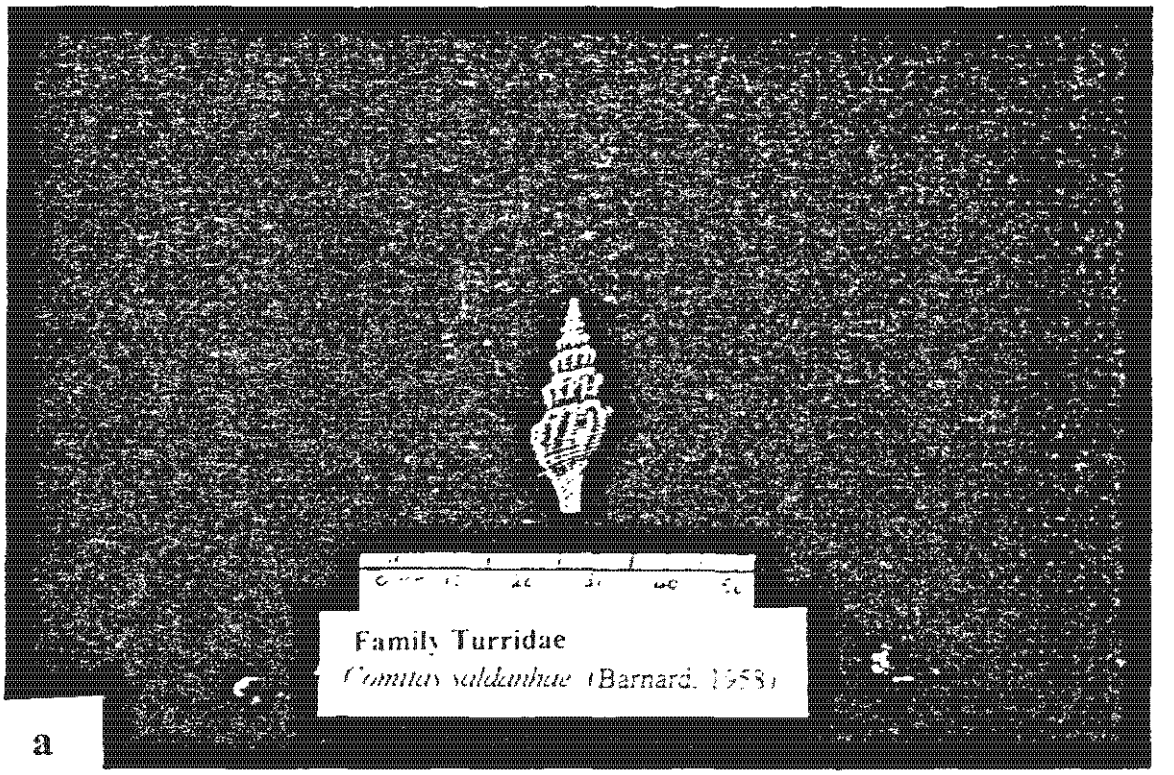
Family Turridae
Comitas saldanhae (Barnard, 1958)

a

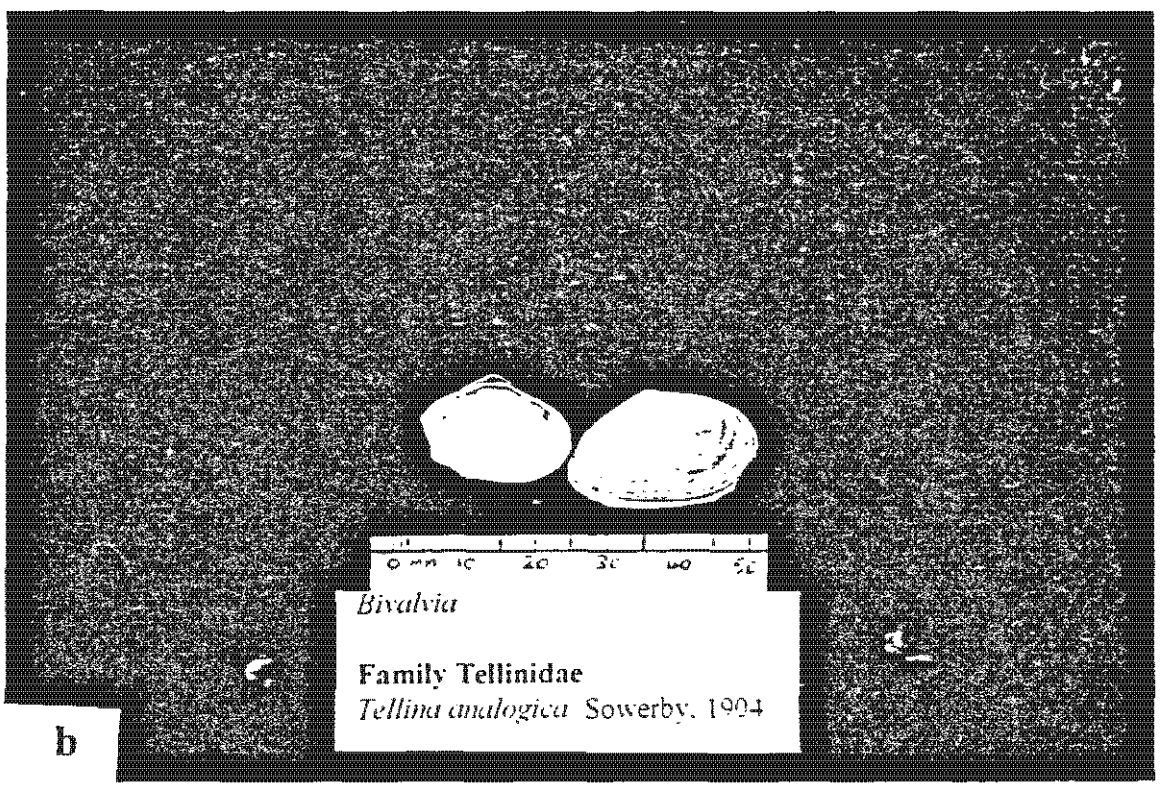
Bivalvia
Family Tellinidae
Tellina analogica Sowerby, 1904

b

PLATE 25

a

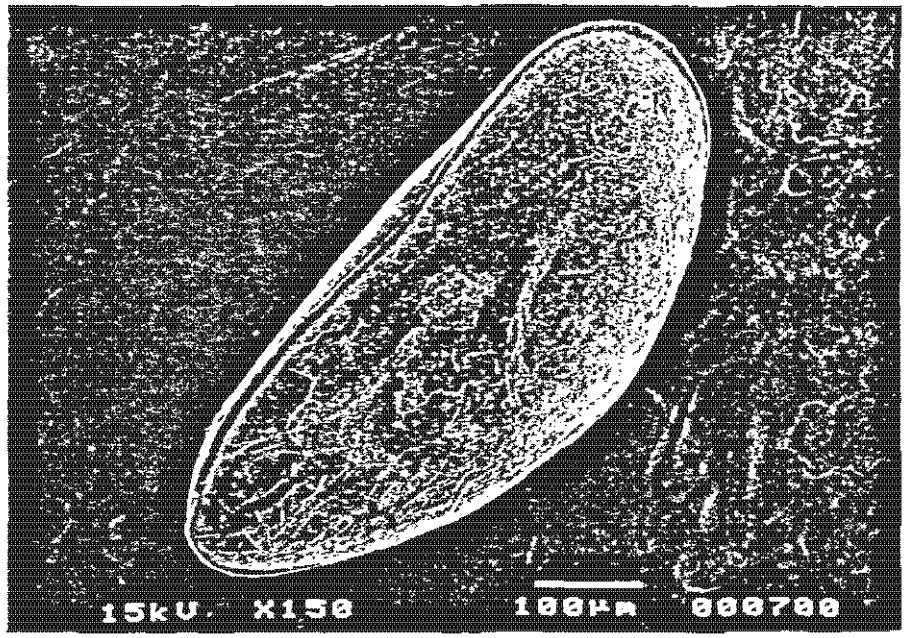

b

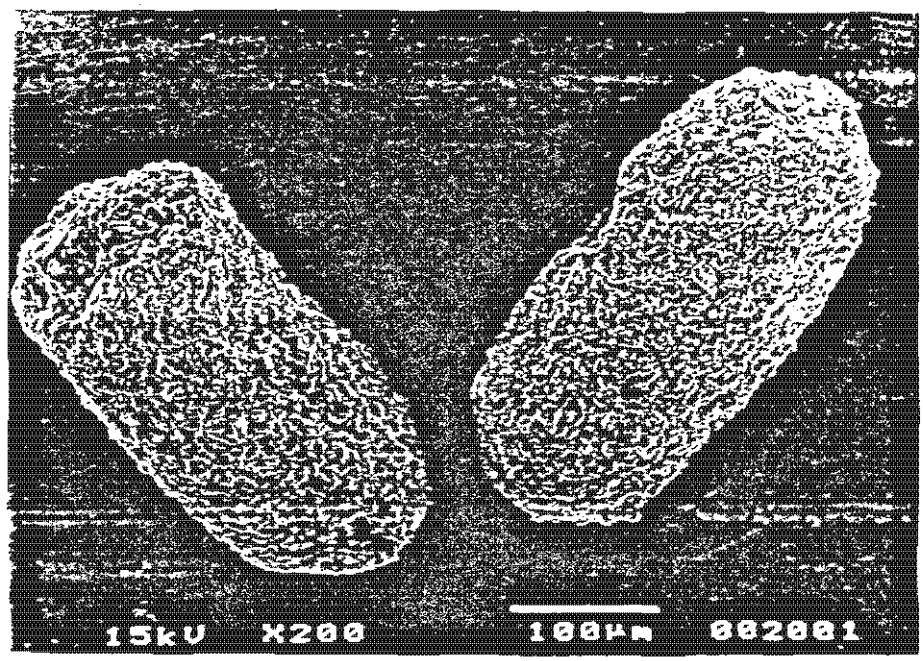

PLATE 26

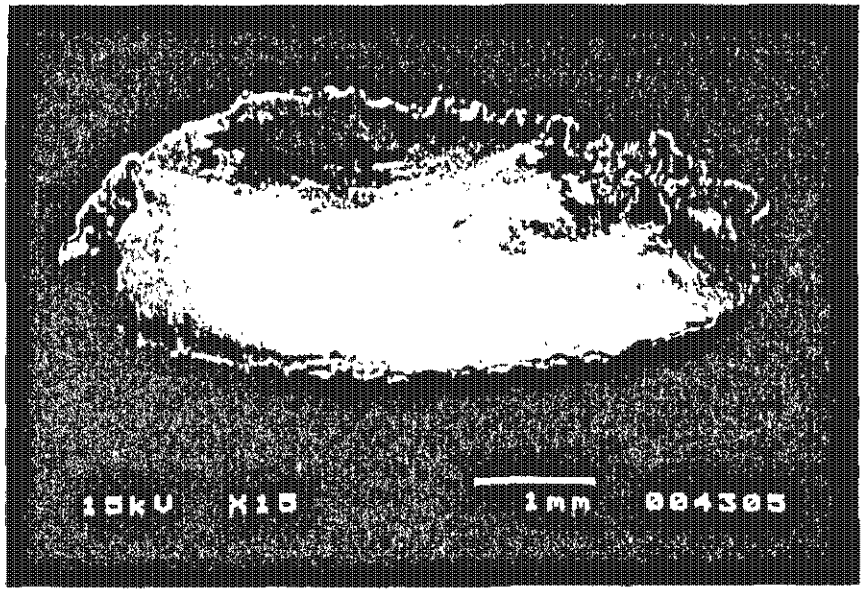

a

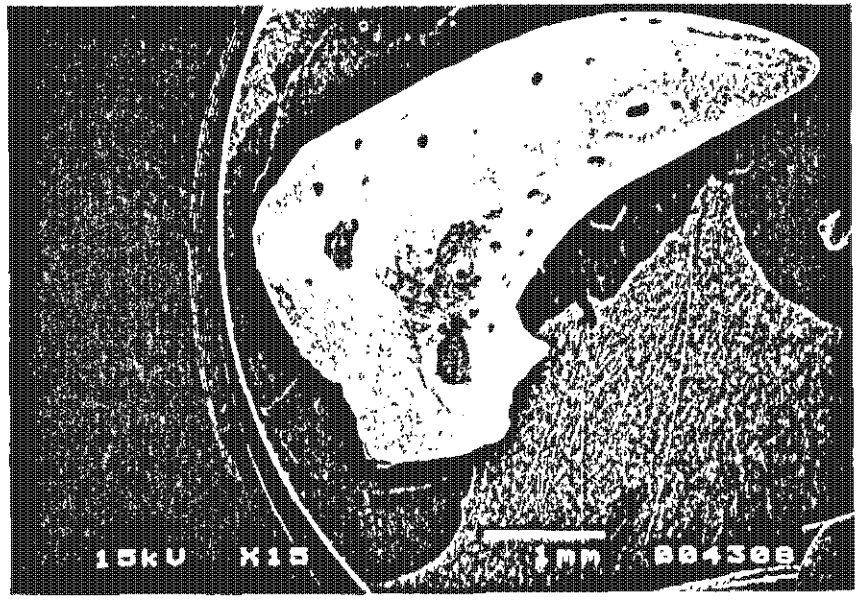

b

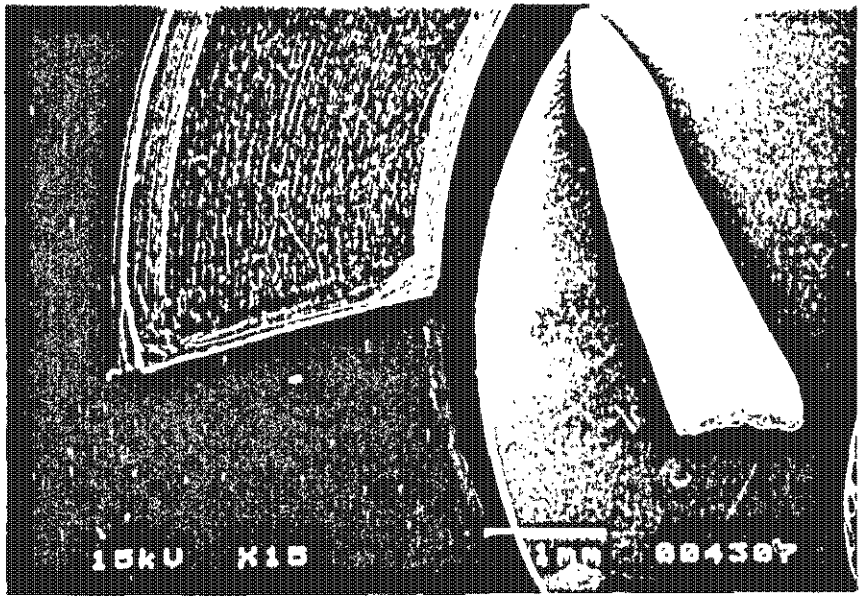

c

PLATE 27

a

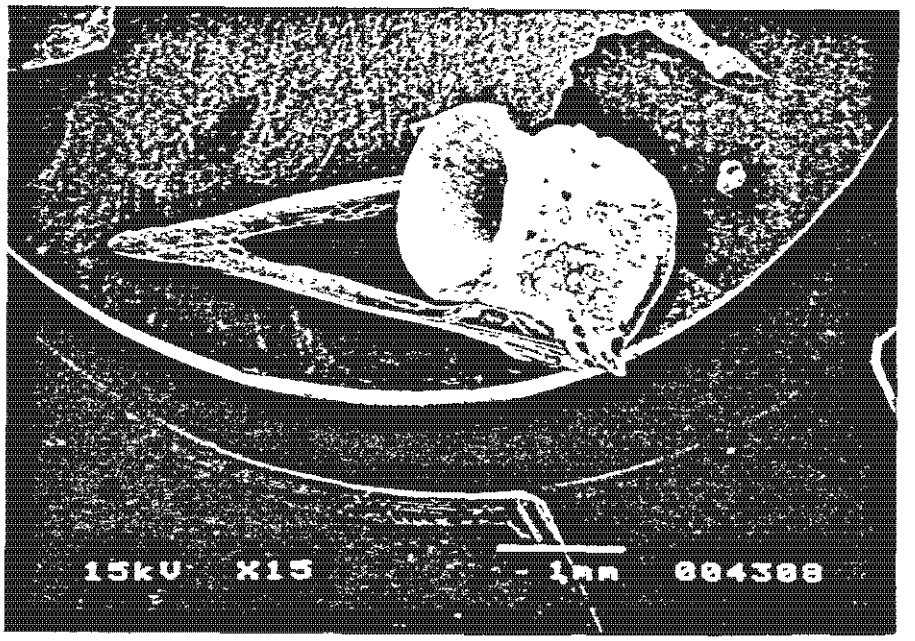

b

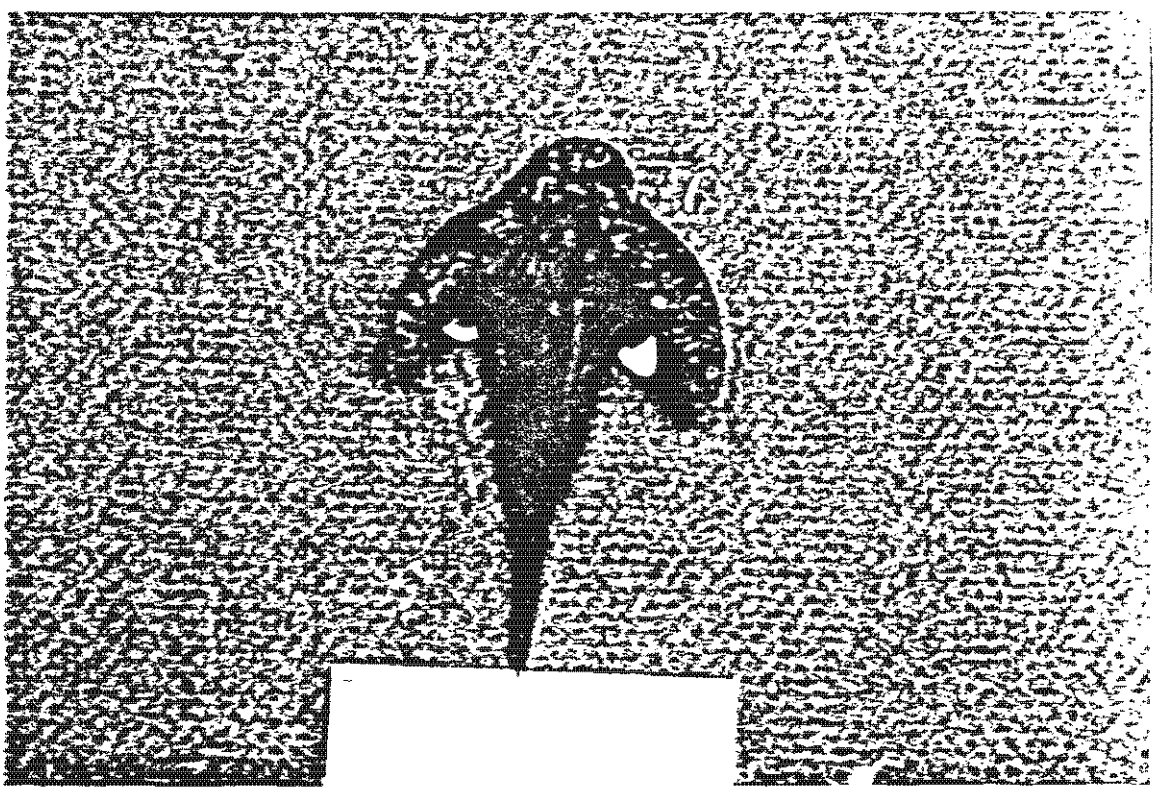

PLATE 28

In summary, this chapter presents sedimentological and biogenic results. Particle size distribution and composition of shelf sediments are examined and, various sedimentary properties which are found in the surficial terrigenous sediments of the Orange Shelf are determined in this chapter. Chapter Six presents mineralogical and geochemistry results.

CHAPTER SIX

MINERALOGY AND GEOCHEMISTRY

6.1 Introduction

Clay minerals are major products of weathering processes and major components of most sedimentary rocks, and hence the clay mineralogy of the sediments is determined mainly by the weathering conditions in the source area (Brownlow, 1996) and is a product of essentially three factors which are: (1) the nature of the detritus, (2) the environment of deposition and (3) the metamorphic history (Jeans, 1986, in Buhmann, 1994) . Therefore because the character of clay minerals is largely dependent on the geology and climate of the source area (Birch, 1975) and the environment of deposition, geochemical and mineralogical aspects of sediments are closely linked. Brownlow (1996) notes that knowledge of the major and trace elements content of rocks allows plausible speculations on their origin and history. A comprehensive investigation of mineralogical and geochemistry of continental margin sediments may provide valuable information regarding the origin of these sediments and paleoclimate of the source area and conditions at the environment of deposition.

The results of a mineralogical analysis of the <2μm sediment size fraction and geochemical investigations on the whole rock are presented in this chapter. The results are reported in two sections according to geographic location. Sixty samples

from Core H2 form the first group and are referred to as Orange Prodelta clay minerals. The second group of sixty samples is from Core H7 and are referred to as the inner shelf clay minerals off Namaqualand. Distribution of gypsum is reported and its origin in marine sediments is discussed. Finally, these two groups of clay minerals are compared to each other and then compared with major and trace elements determined from selected samples in the same groups. It is hoped that these results will aid in the identification of provenance areas and their dispersal patterns. These results may also help to determine the influence which onland variations exert on the adjacent sediment (Birch, 1975).

It must be noted that clay minerals mentioned in this work (e.g. smectite, mica, vermiculite etc.) are mineral group names, and no attempt was made to identify the actual mineral species (e.g. muscovite mica or montmorillonite within the smectite group). Analytical methods used to determine these minerals and elements are described in chapter Two.

6.2 Mineralogy

Eight clay minerals were identified in both Orange Prodelta (Core H2) and the inner shelf off Namaqualand (Core H7, off Kleinsee), viz. smectite, vermiculite, chlorite, mica, kaolinite, quartz, plagioclase and alkali feldspars. A complete listing of clay mineral proportions is given in Appendices D and E. Figure 6.1 and 6.2 are visual representations of these clay minerals upcore. The terms, detrital, secondary,

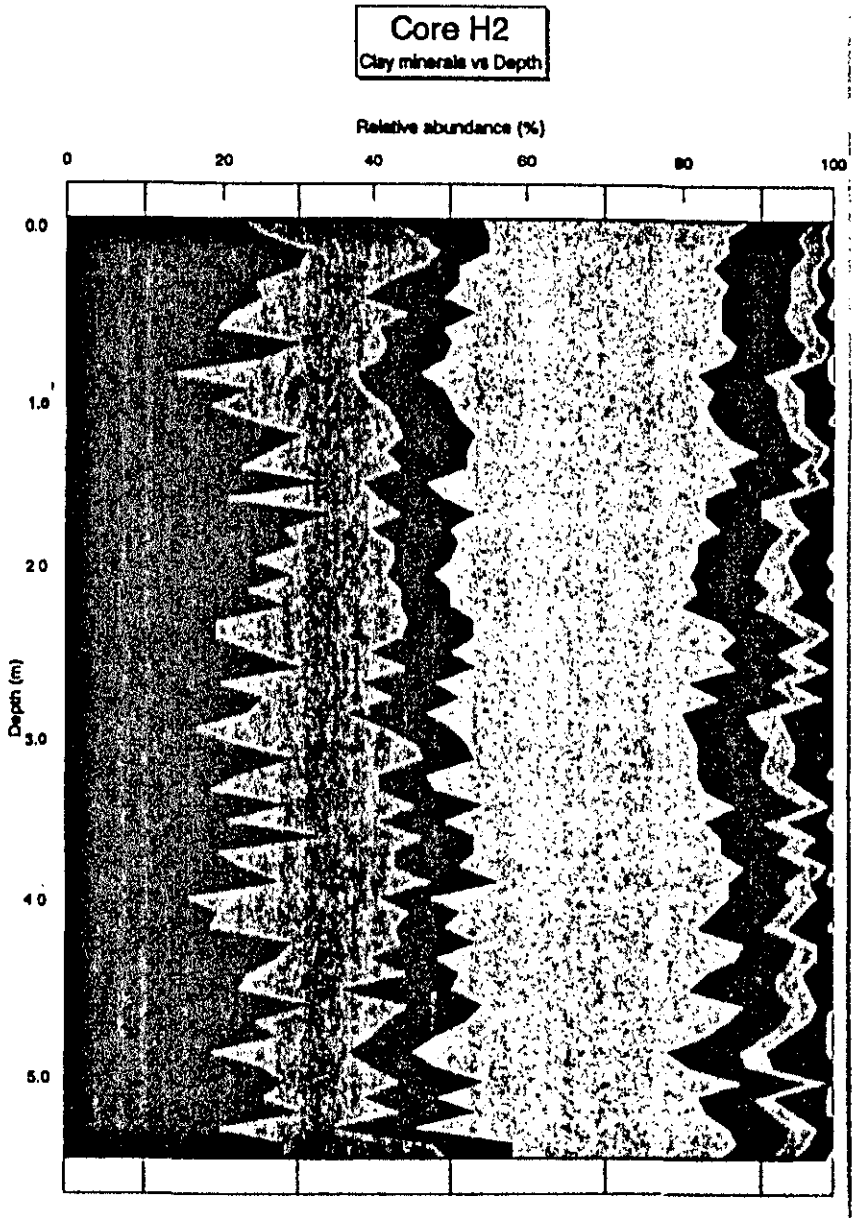

Figure 6.1 - Visual representation of clay minerals upcore in H2 (Orange Prodelta)

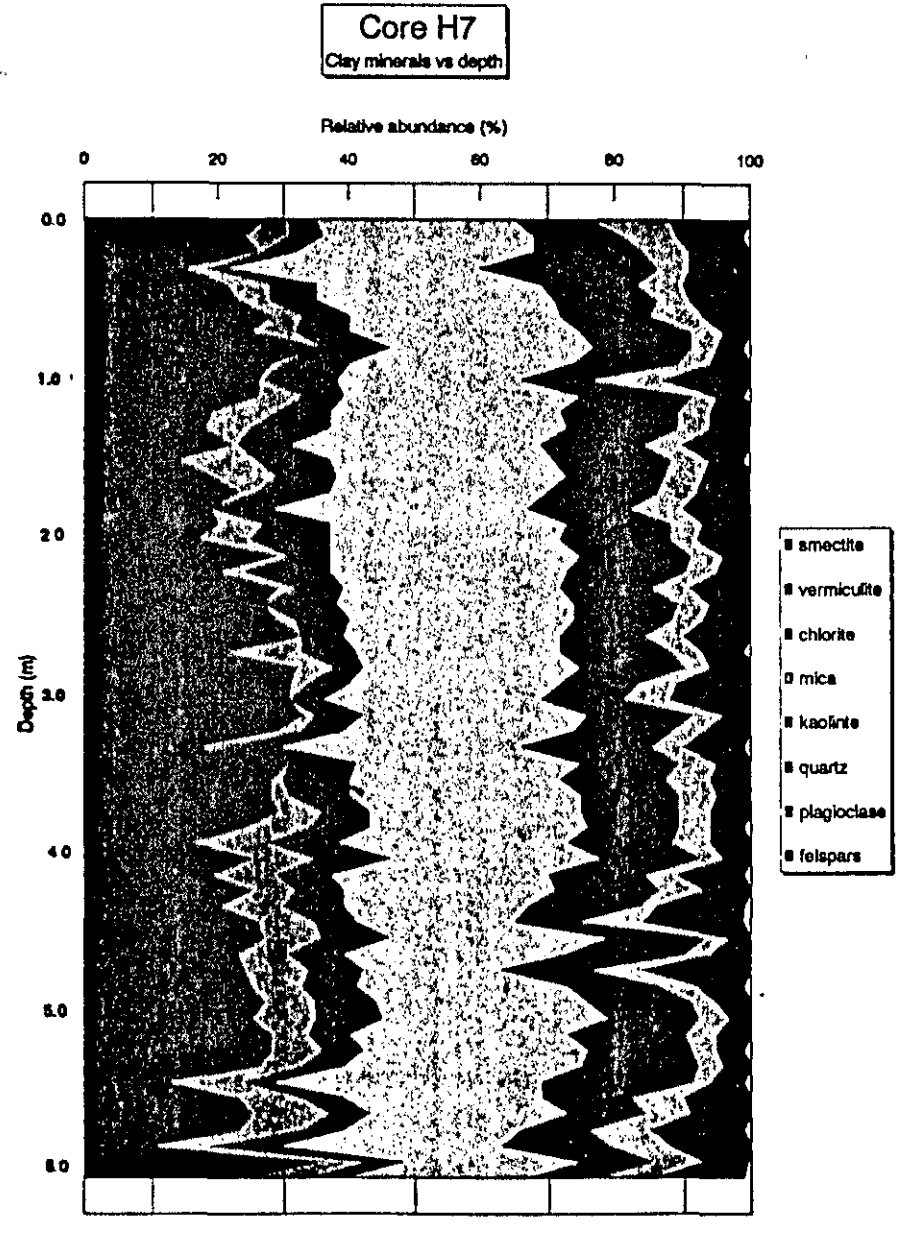

Figure 6.2 - Visual representation of clay minerals upcore in H7 (off Kleinsee)

precipitated and authigenic minerals are used in this study. Therefore their definitions are given below so as to avoid ambiguity.

Detrital minerals are those minerals which survived during weathering and transportation (Boggs, 1995). Secondary minerals refer to new minerals formed during weathering and transportation. Precipitated minerals are those minerals formed directly from solution, chemically or biologically, and authigenic minerals are formed in sediments during and after deposition (Leeder, 1982).

Mica (probably illite species) is the most dominant clay mineral in both the Orange Prodelta (Core H2) and the inner shelf, off Kleinsee (Core H7). The concentrations of this mineral (which will be referred to as illite in sections to follow in order to facilitate comparison of this work with other works done in the region) range between 27 and 41% in the Orange Prodelta (Core H2), and 21 and 41% in the inner shelf (Core H7). Its average concentration in both locations is about 33% (appendices D and E).

Smectite (most probably montmorillonite species) is subordinate to mica in both locations. Its concentrations range between 13 and 34% in the Orange Prodelta (Core H2) and 10 and 36% in the inner shelf, off Kleinsee (Core H7). The average concentration of smectite (to be referred to as montmorillonite) in both is about 24% (appendices D and E).

Vermiculite is the third most abundant clay mineral in the Orange Prodelta (Core H2). Its concentrations vary between 6 and 26%, and its average concentration is about

18%. On the other hand, vermiculite appears to be subordinate to kaolinite, chlorite and plagioclase clay minerals in the inner shelf off Kleinsee (Core H7). Its concentrations range between 0 and 12% and its average concentration is 6%, the value well below those of kaolinite, chlorite and plagioclase, which are about 15%, 8% and 7 %, respectively Appendices D and E).

Kaolinite and chlorite minerals are present in almost equal quantities in the Orange Prodelta (Core H2) (Appendix D). Their average concentration is about 8%. Chlorite mineral concentrations range between 4 and 14% in the Orange Prodelta (Core H2), whereas kaolinite concentrations range between 6 and 11% in the inner shelf (Core H7). Kaolinite is the third most abundant clay mineral in the inner shelf off Kleinsee (Core H7), with its concentrations varying between 9 and 26% (Appendix E). Its average concentration is about 14%. This average concentration of kaolinite (14%) is interesting when compared to the much lower average concentration (8%) in the Orange Prodelta.

Quartz is subordinate to kaolinite and chlorite in the Orange Prodelta (Core H2) but dominant over plagioclase (Appendix D) . Its values range from 3 to 5% and its average concentration is about 4%. On the other hand, plagioclase and vermiculite clays are dominant over quartz in the inner shelf off Kleinsee (Core H7) (Appendix E). Plagioclase and vermiculite clays average 7% and 6%, respectively. Their values range from between 3 to 16% and 0 to 12% respectively.

Alkali feldspars are present in trace quantities in both locations. Average values in both Orange Prodelta and the inner shelf are less than 1%.

Large, unbroken tabular euhedral gypsum crystals (Plates 3b, 4a-b) are found on the inner shelf in Cores H4, H6, and H7. There are no gypsum crystals found on the Orange Prodelta (Cores H2 and H3). The gypsum crystals occur as clear, colourless crystals of fine to medium size and occasionally in gravel size as intergrown crystals. They occur in dominant to trace quantities and abundance decreases upcore. They are found mainly at the bottom of the cores, generally more than 1.6m below the sediment surface.

6.3 Geochemistry

Silicon (Si) is the most dominant element in both Cores H2 (Prodelta) and H7 (off Kleinsee) (Table 6.1). Its concentrations range between 28.76 and 48.84% in the Orange Prodelta (Core H2), whereas its average concentration is 43.09% (Table 6.1). The Si concentrations in Core H7 vary between 31.97 and 41.47%, and its average concentration is 37.86% (Table 6.1).

Titanium (Ti) is generally present in trace quantities in both Cores H2 and H7. Its concentration ranges between 0.77 and 0.85%, and its average concentration is 0.82 in Core H2. Titanium concentration in core H7 ranges between 0.56 and 0.87%, while its average concentration is 0.76%.

Table 6.1'MAJOR ELEMENTS

(CORE H2)

Sample No.	SiO2	TIO2	Al2O3	FE2O3	MNO	MGO	CAO	NA2O	K20	P2O5	S	H2O	LOI	TOTAL
H2.71B	46.03	0.69	16.45	7.65	0.059	2.24	0.8	1.85	2.67	0.15	0.21	7.97	10.76	97.53
H2.3.14	47.23	0.68	16.22	7.88	0.049	2.56	1.2	1.11	2.75	0.17	0.21	5.34	12.05	97.45
H2.G2	47.73	0.66	14.62	6.92	0.039	2.52	1.78	2.61	2.64	0.18	0.24	7.5	11.11	98.55
H2.3.7	47.68	0.63	16.39	7.34	0.048	2.38	1.43	1.9	3.04	0.15	0.19	7.02	10.16	98.36
H2.1.16	48.91	0.64	15.88	7.31	0.042	2.42	1.57	1.4	2.95	0.14	0.21	6.39	10.17	98.03
H2.1.20	47.16	0.64	16.24	7.46	0.043	2.34	0.92	3.43	2.95	0.14	0.22	9.06	9.41	100.01
H2.5.1	47.99	0.7	16.14	7.25	0.044	2.21	1.24	1.22	2.69	0.15	0.18	6.54	10.66	97.01
H2.4.14	49.1	0.68	15.27	7.16	0.046	2.13	1.43	3.39	2.56	0.15	0.25	7.18	10.14	99.48
H2CC2	49.67	0.68	13.87	7.05	0.04	2.54	1.92	1.2	2.43	0.21	0.62	5.16	10.3	95.69
H2.1.3	47.47	0.66	14.02	6.97	0.042	2.66	3.54	1.25	2.55	0.18	0.61	5.81	12.34	98.1
AVERAGE	**47.90**	**0.67**	**15.51**	**7.30**	**0.05**	**2.40**	**1.58**	**1.94**	**2.72**	**0.16**	**0.29**	**6.80**	**10.71**	**98.02**

(CORE H7)

Sample No.	SiO2	TIO2	Al2O3	FE2O3	MNO	MGO	CAO	NA2O	K20	P2O5	S	H2O	LOI	TOTAL
H7.5.4	41.4	0.56	11.81	6.05	0.036	2.5	5.27	1.15	2.39	0.18	1.69	8.08	16.04	97.16
H7.1.1	44.12	0.62	12.53	6.49	0.037	2.71	4.26	1.2	2.39	0.2	1.62	5.12	16.58	97.87
H7. 6.18	45.71	0.68	14.07	6.41	0.035	2.38	2.11	2.72	2.91	0.15	1.27	7.05	12.89	98.38
H7.6.12	43.92	0.61	12.91	6.05	0.034	2.37	3.59	5.06	2.68	0.16	1.52	8.09	14.3	101.3
H7.1.2	43.11	0.6	12.21	6.3	0.036	2.63	4.23	2.95	2.34	0.19	1.48	6.91	16.26	99.25
H7.5.18	43.32	0.61	12.56	6.15	0.035	2.62	4.2	3.91	2.56	0.19	1.34	6.76	15.9	100.15
H7.2.18	42.13	0.61	12.39	6.33	0.035	2.72	4.8	5.41	2.45	0.19	1.52	5.8	17.42	101.81
H7.1.18	43.44	0.64	12.59	6.28	0.037	2.54	2.99	4.3	2.5	0.18	1.49	10.14	12.91	100.04
H7.G2	44.44	0.57	12.62	5.79	0.032	2.36	3.09	3.42	2.53	0.23	1.06	8.65	14.12	98.91
H7.3.11	41.26	0.57	11.81	5.97	0.034	2.8	6.57	1.04	2.2	0.22	1.46	5.65	17.66	97.24
H7.4.18	42.81	0.58	12.32	6.16	0.033	2.68	5.1	2	2.5	0.19	1.49	6.27	14.66	96.79
H7.6.14	44.95	0.61	13.6	6.5	0.036	2.41	2.95	2.51	2.74	0.16	1.37	6.7	13.82	98.35
H7.3.11B	40.47	0.55	11.59	5.85	0.033	2.74	6.42	1.06	2.14	0.22	1.37	8.08	16.04	96.56
AVERAGE	**43.16**	**0.60**	**12.54**	**6.18**	**0.03**	**2.57**	**4.28**	**2.83**	**2.49**	**0.19**	**1.44**	**7.18**	**15.28**	**98.75**

Aluminium (Al) is the second most abundant element in both cores. It is subordinate to Silicon. Its concentrations vary between 16.61 and 20.47% in Core H2 (Orange Prodelta), and its average concentration is 18.99%. The concentrations of Aluminium in Core H7 (inner shelf, off Kleinsee) vary between 11.76 and 17.84%. Its average concentration is 15.83%.

Manganese (Mn) is also present in trace quantities in both Cores H2 and H7. Manganese concentrations range between 0.06% and 0.07%, but its average concentration is 0.06% in Core H2. Manganese concentrations in Core H7 vary between 0.03 and 0.05%. Its average concentration is 0.046%.

Magnesium (Mg) concentrations vary between 2.61 and 3.28%, and its average concentration is 2.94% in Core H2. The concentrations of Mg range between 2.5% and 3.72%, whereas its average concentration is 3.25% in Core H7.

The concentrations of Calcium (Ca) vary between 1 and 4.36% in Core H2 (Orange Prodelta), while its average concentration is 1.94% (Table 6.1). The concentrations of Ca range between 2.68 and 8.72% (Core H7) (the inner shell, off Kleinsee), and its average concentration is 5.33, well above that of Core H2.

Potassium (K) is present in both Cores H2 and H7 in low concentrations. The potassium concentrations in Core H2 vary between 2.91 and 3.7%, and its average concentration is 3.34%. Its concentrations in Core H7 range between 2.17 and 3.69%, and its average concentration is 3.14%, slightly less than that of Core H2.

Phosphorus (P) is also present in trace quantities in both Cores H2 and H7. Its concentrations vary between 0.17 and 0.25% in Core H2, while its average concentration is 0.2%. The Phosphorus concentrations in Core H7 vary between 0.18 and 0.3%, and its average concentration is 0.23%, almost the same as in Core H2.

Mineralogical and geochemical results are presented in this chapter. Chapter Seven provides a general discussion of all findings of this research and their implications.

CHAPTER SEVEN

DISCUSSION

7.1 Introduction

The aim of this chapter is to provide a general overview of the findings of the research and to review and discuss implications of the results presented in Chapters Four, Five and Six.

7.2 Chronology

The radiocarbon-dates chronology reveals some interesting observations, which deserve closer scrutiny. Ten of the 24 dates fall within the narrow temporal range of 1000 to 1700 BP, and these dates are associated with the strongly laminated facies. The material comprising the laminated clays appears to be consistent with their deposition within a narrow time range of just a few hundred years; alternatively, the sediments contain organic material which has a relatively uniform radiocarbon signal (Meadows *et al.*, 1997).

Although the temporal sequence in most of the cores (e.g.. Core H7), is indicative of sediments deposited in a logical chronosequence, other cores (H2 in particular) reveal an absence of consistency in a chronological pattern; in fact, the pattern could even be described as random (Meadows *et al.*, 1997). Meadows *et al.* (1997) identified two types of inconsistency. Firstly, the surface or near-surface sediments, which were

expected to yield very recent or even contemporary ages, are considerably older and, secondly the dates are not always compliant with the Principle of Superposition that deeper layers are older than younger overlying layers. Each of these problems is discussed below.

Meadows *et al.* (1997) note with concern that the absence of modern or contemporary ages in presumed surface is unexpected. The dates at the "surface" are as follows: H2: 570±35BP, H5: 795±40BP, and H4: 950±30BP. This anomaly may be explained through several hypotheses which are examined in turn. The presence of old "surfaces" (over 570 years old) may be attributed to over-penetration by the corer. In her Master of Science research at the University of Natal, McLachlan (1995) found cores in the innershelf, off Walvis Bay, having tops over 1000 years old and argued that over-penetration of the entire corer beyond the sediment-water interface could have occurred, because of the fluid nature of the mud at the sediment-water interface and the weight of the core, even when empty. Alternatively, the modern material may not have been sampled at all, due to the failure of the sampling techniques to capture it, but Meadows *et al* (1997) rule out these possibilities on the grounds that the Van Veen grab sampler which was used to obtain surface dates at H2 and H5, is generally regarded as a highly effective means of obtaining submarine surface sediment material. Nevertheless, this method could also be a problem in highly fluid interface situation.

Another possible explanation could be that modern material has either failed to be deposited, or has settled out but been transported elsewhere by bottom currents

thereafter. This hypothesis is supported by Birch *et al* (1986) (in Meadows *et al.,* 1997) through their sediment-budget studies which indicate that accumulations of offshore material in the region fall short of sediment supply estimations by a considerable margin. This is further supported by a suggestion that deceleration of shelf-subsidence during the Quaternary could result in sediment being washed across the shelf, into deeper water (Meadows *et al.,* 1997). In addition, this hypothesis is also favoured by high turbidity of the mudbelt sediment-sea interface (Rogers, 1977, in Meadows *et al.,* 1997). However, this hypothesis needs to be properly substantiated.

Another possible explanation might be "contamination" of older sediments by modern material through bioturbation following sedimentation. This possibility is however ruled out by the presence of strongly developed laminations, particularly in the Orange River section cores (Mabote *et al.* 1997; Meadows *et al.,* 1997).

A fourth possibility may be incorporation of older carbon into the sediments, either from a marine or a terrestrial source. Meadows *et al.,* (1997) note that this possibility has some merit, especially because marine carbon is often several hundred years older (in the marine context) than its terrestrial counterpart, and some of the samples may contain more marine- than terrestrial-carbon. Moreover, these authors suggest that different carbon fractions could yield different carbon ages by having distinctive radiocarbon age offsets, and this, coupled with the fact that bulk samples were submitted for dating, may account for some of the anomalies. This possibility is once again ruled out on the grounds that age calculation was done on organic carbon only,

as carbonates were effectively removed by acid hydrolysis. Another possible explanation is that of erosion of older sediment from elsewhere in the catchment and subsequent redeposition at the core site. It is argued that if prior to the burial of the soil or sediment, old organic matter derived from the surrounding landscape is mixed with younger organic matter of the soil or sediment, an anomolously old age can result (Geyh *et al.*, 1983; Martin and Johnson, 1995; McLachlan, 1995; Meadows *et al.*, 1997). This is the most reasonable deduction, particularly in the Orange catchment, where (according to Meadows *et al.*, 1997) "..at least some of the transported sediments may contain organic material several thousands of years old, for example if it originated in the upper parts of the catchment characterised by organic soils (e.g. Maluti Mountain peat deposits)". Furthermore, these authors state that much of the material eroded by the Orange River during flood events appears to be derived from former flood deposits in the river banks and they argue that this material may well contain organic matter which is not older than the age of the flood itself.

The chronological inconsistency of ages in some of the cores may well also be attributed to some or all of the above-mentioned processes. Meadows *et al* (1997) point to bioturbation and the incorporation of older and/or younger marine-derived carbon as definite potential causes of the dating anomalies which, in the most extreme case (Core H2) results in the sediments at the base of the core being apparently younger than those just a few centimetres from its surface (Table 4.1). However, presence of well laminated muds and absence of traces of burrowing fauna (Mabote *et al.*, 1997) pose very important questions on his contention.

Another possible explanation could be that sediments are or were subjected to post-depositional reworking, that is old sediment might have mixed with new sediment during mass slides of the prodelta which are common, in the Mississippi for example (Meadows, Pers. comm.). This might have led to old carbon being mixed with new carbon. In addition to this, Meadows *et al* (1997) state that some of the surface deposits, and even some of those at depth, are relatively unconsolidated and this could render them susceptible to movement through slumping and folding which would certainly overturn the stratigraphy. However, Dr. J. Rogers (pers comm.) thinks the chances of such an incident occurring are very slim.

Although the radiocarbon dates have obviously enabled us to confirm the Holocene age of mudbelt, a need for a more appropriate and reliable means of establishing a chronology cannot be overemphasized. A reliable method will obviously provide significant information regarding sediment erosion and accumulation rates in the past, thus helping in the elucidation of the Late Quaternary erosional history of southern Africa. To mention but a few potential techniques to help in this regard are a) radionuclide techniques involving the measurement of Caesium-137 and Lead-210 which are commonly employed to throw light on soil-erosion and sedimentation rates in the recent past, b) AMS radiocarbon dating of organisms which are known to occur at the sediment-marine interface, such as benthic foraminifera. Radiocarbon dates of foraminifera would provide us with the age of the burial of the sediment and thus accurately reflect timing of the terrestrial erosion and offshore sediment event (Meadows *et al.,* 1997), c) pollen is also identified as a useful stratigraphic marker,

especially because the date of introduction to the southern Africa of most exotic species is known to within a few years (Gray, 1996; Meadows *et al.*, 1997).

7.3 Sedimentology

(a) Stratigraphy

Orange Prodelta

A critical analysis of one or combination of lithostratigraphy, chronostratigraphy, coarse-fraction components and geochemistry (mineralogy and major elements) offers exciting opportunities for reconstruction of sedimentary history in the Namaqualand offshore mudbelt. Some of the information accruing from such analyses are discussed below.

The two most common and dominant lithofacies in these fine-grained deposits (Figures 5.1-5.7; Plate 1), are lamination-dominated muds and homogeneous muds. Primary sedimentary structures (horizontal laminae) are present particularly in the Orange Prodelta Cores H2 and H3 and they decrease in abundance southward from the Orange River mouth, where muddy sediment is increasingly homogeneous. No or, only indistinct, laminations are observed in Cores H4, H6 and H7 (Namaqualand inner shelf) (Figures 5.5, 5.6 and 5.7 respectively).

Some interesting features of these lithofacies deserve closer scrutiny. Figure 7.1 shows a relationship between lithostratigraphy and chronostratigraphy. This Figure reveals that the laminations are synchronous between different cores. The radiocarbon

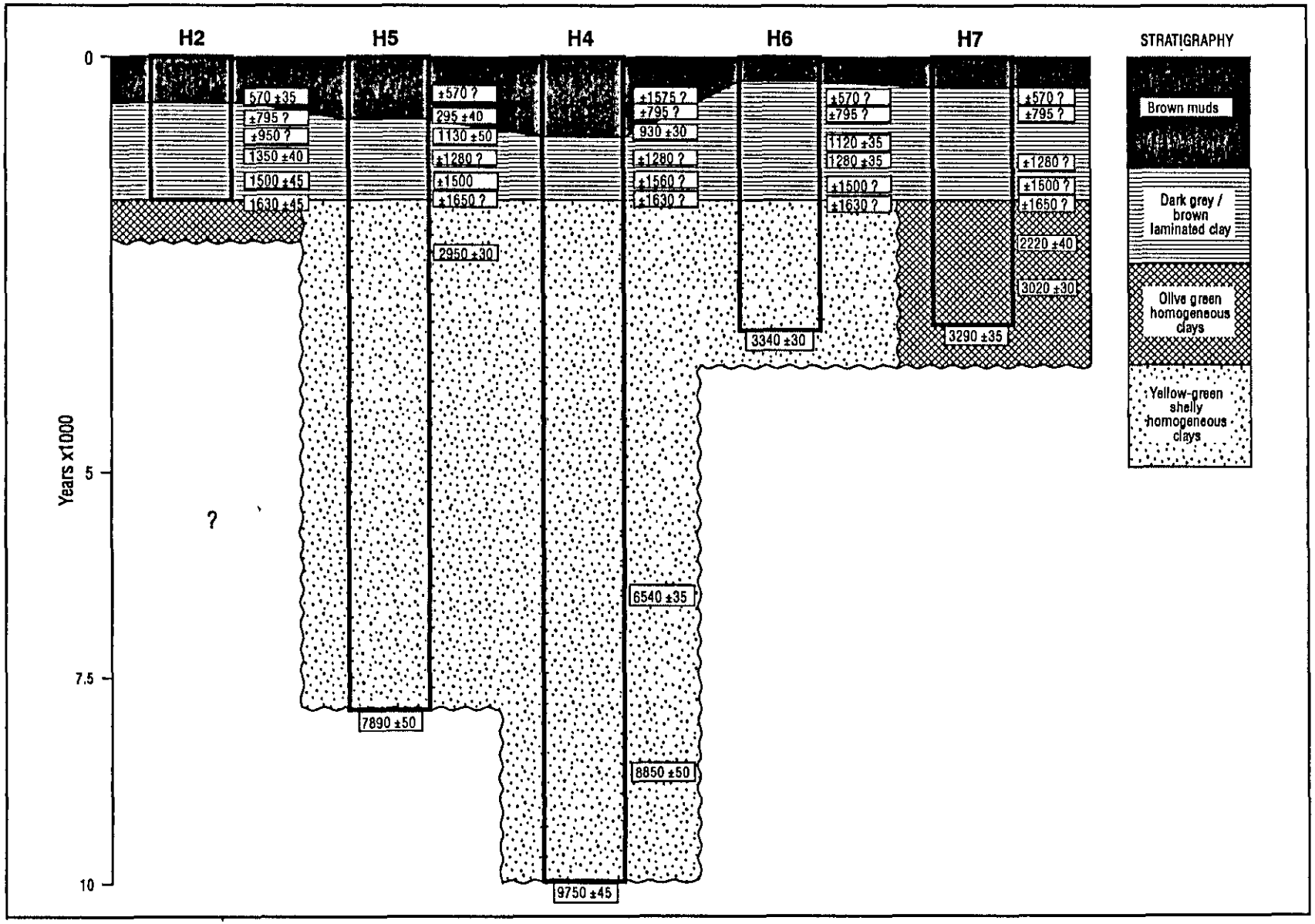

Figure 7.1 A relationship between lithostratigraphy and chromostratigraphy.

ages of laminated muds fall within the narrow range of 1000 to 1700 BP (Figures 4.1 and 7.1) (Meadows *et al,* 1997). While these laminations seem to occur in greater abundance closer to the Orange River mouth (Cores H1, H2 and H3), Radiocarbon dates indicate that their succession correlates with those other laminations in other cores (they all fall within a narrow range of 1000 to 1700 BP).

Although only about 1m core was retrieved from Site H1, the Holocene mudbelt at Site H1 is about 4.5m thick (Dingle, 1994). The whole of the sedimentary record at this site looks more similar to the lower part of the record at Site H3 (Figures 5.1 and 5.3). This is further indicated by the lithology of these cores where dark laminated muds overlie the homogeneous muds (Figure 4.1 and Appendix B). This observations suggest that the dark laminated clays overlie, as well as pass laterally downslope into the homogeneous olive-brown clays. Dingle (1994) illustrates these observations by model A in Figure 7.2 and suggests that this model may help to explain the observed stratigraphy. However, since there is no unequivocal cored evidence as to the thickness of the lower olive-brown clays at Site 1, one possibility may be that this layer is thin, and it is underlain by further dark clays (Dingle, 1994). Because of this, model B (Figure 7.2) is therefore proposed as a better way of expressing stratigraphy where the dark clays are essentially prograding seawards.

Moreover, the upper, soft brown muds are also present at Site H5 and overlie a thin (68cm) sequence of greyish laminated clays. The latter looks more akin to the dark laminated clays that charaterise Sites H1-3. The radiocarbon dates indicate that this succession at Site 5 correlates with that at Sites H1-3. The radiocarbon ages of

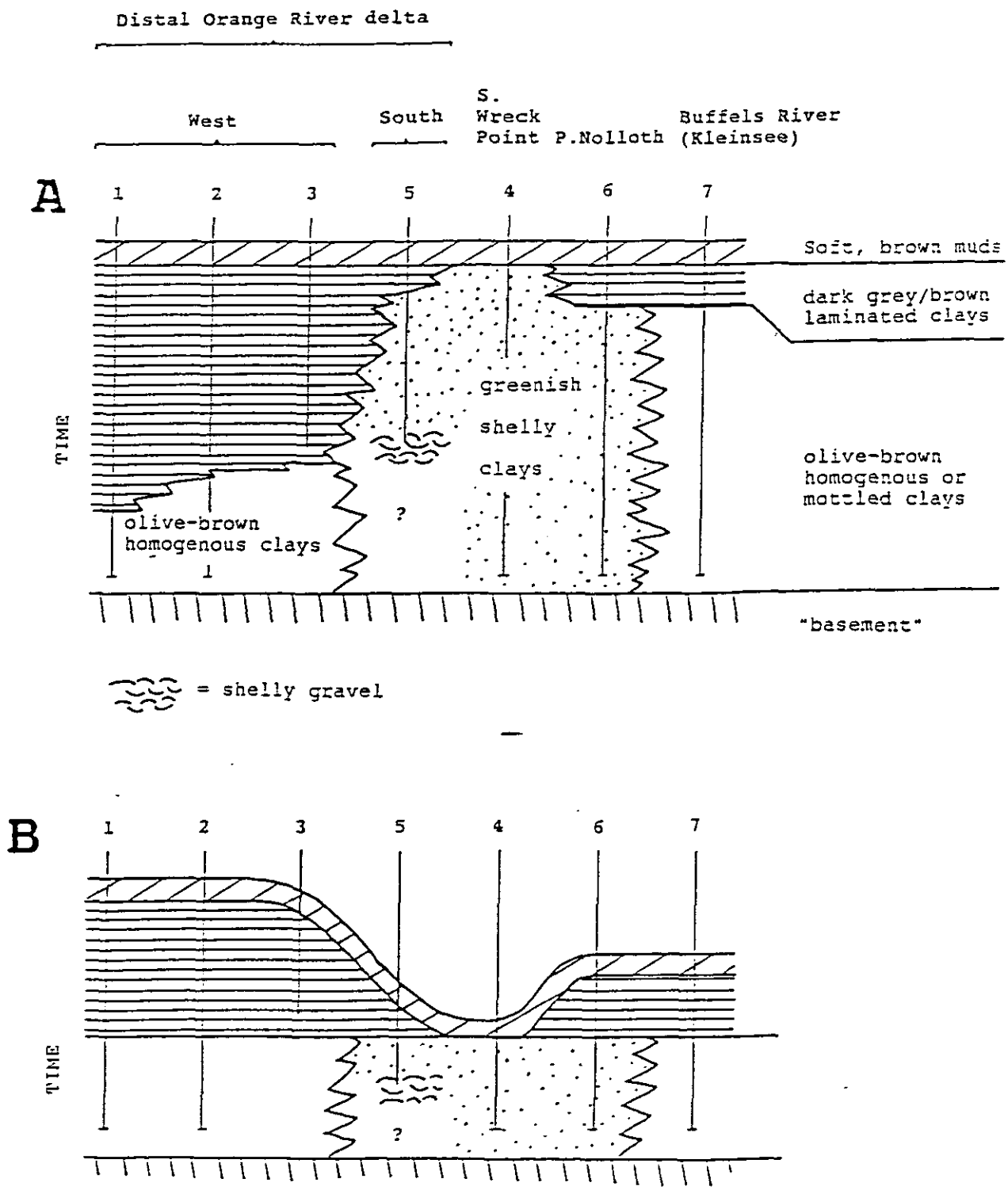

Figure 7.2 - Lithostratigraphy relationship between Orange Shelf Sediments (Dingle, 1994)

greyish laminated clays from Site H2 (representing Orange Prodelta) and H5 fall within a narrow range of 1000 to 1700BP. These ages suggest that these laminated clays are consistent with their deposition within a narrow time range of just a few hundred years (Meadows *et al.*, 1997). If extrapolated further, these radiocarbon dates suggest that these greyish laminated clays are derived primarily from the Orange River and are essentially overstepping (seaward prograding)(Figure 7.2, model B) as suggested by Dingle (1994).

Site 4 (Core H4) lies south of Wreck Point and it was originally chosen to illustrate the succession in a most-distal part position where any terrigenous influx from the Orange River would have been primarily by shore-parallel poleward undercurrent movement (Dingle, 1994). The sequence at this site does not show evidence of an upper grey or well laminated clays. Instead, a surface layer of soft brown mud resting directly above 5m of yellowish green clays with occasional shells is encountered (Figures 4.1 and 5.4). However, these yellow green clays appear to have some feint laminations although their colour variations are very subtle (Dingle, 1994). These observations indicate that the dark laminated clays of the Orange Prodelta do not extend south of a position somewhere between Sites 5 and 4. These observations seem to negate the earlier inferences (e.g. Rogers, 1977; Dingle *et al.*, 1987; Rogers and Bremner, 1991) that the Namaqualand mudbelt is primarily derived from the Orange River.

Namaqualand Inner Shelf

The Namaqualand Inner Shelf is represented by Sites 6 (H6) and 7 (H7). A three-fold sequence is observed at Site 6:

- A thin, upper soft brown mud
- A composite median unit of dark greyish clays
- A thick, lower yellowish-green clays with occasional shelly horizon (Figure 4.1).

While shelly clays may be correlated with similar horizons at Sites 5 and 4, the appearance of an upper, grey laminated sequence suggests that this material is derived from the ephemeral rivers of southern Namaqualand (Dingle, 1994). This is further supported by a succession at Site 7, where soft, brown muds overlie a composite unit (158cm) of greyish green clays that are variously laminated or homogenous (Figure 4.1). These clays overlie homogeneous olive-green clays with sparse shell fragments (Figure 4.1).

These greyish laminated clays at Sites 6 and 7 look akin and all fall within a narrow range of 1170-1250BP (Figure 4.1 and Table 4.1). These clays could represent discrete terrigenous units derived from local ephemeral Namaqualand rivers (Dingle, 1994). This is logical since these sites are only about 50km apart, and there is no evidence at present, to suggest that the grey, laminated sequences are continuous.

On the basis of preliminary stratigraphic analysis, Dingle (1994) suggested two possible alternatives for sedimentary development in the study area which are:-

1) an early period of deposition dominated by marine conditions (represented by homogeneous yellowish-green clay with shells at Sites H5, H4 and H6, and olive-green clay at Site 7) off the coast, but with significant terrigenous input in the north and south (Sites 1-3, and 7) (homogeneous texture of the clays indicates well oxygenated sea-floor and upper-sediment conditions) (Dingle, 1994) and

2) a major climatic, or catchment area-related change occurred, which resulted in the progressive spread of dark laminated terrigenous dominated clays over the entire study are, except Site H4.

In the light of radiocarbon dates, coarse-fraction components and mineralogical analyses (to be discussed in the sections to follow), alternative 1 offers the best explanation for sedimentary history of the Namaqualand mudbelt. Of particular interest in the coarse-fraction components is their relative abundance at Sites H1, H2 and H3 where terrigenous components constitute the dominant fraction. This clearly indicates the terrestrial influence of the Orange River at these Sites (Orange Prodelta) (Figures 5.1-5.3). On the other hand, marine-biogenic components are the dominant fractions at Sites H6 and H7 (Figures 5.6-5.7). This clearly indicates marine influence at these sites (inner shelf).

It is also interesting to note the presence of a thin layer of muds overlying the entire study area (Figures 4.1 and 7.1). Although it is tempting to equate this to the 1988 Orange River flood layer (Dingle, 1994), the radiocarbon dates of these layer do not support this contention. However, this is probably due to the problems associated with the radiocarbon dating of these sediments which are discussed in section 7.2.

Could these laminations be a relatively undisturbed signatures of major floods or increased rates of soil erosion due to anthropogenic activities?. They are presumably a periodicity of some sort.

Why is there limited bioturbation at sites H2 and H3 on the Orange Prodelta?

The preservation of primary sedimentary structures is governed by the ratio between the rate of biological mixing (bioturbation) and the rate of sediment accumulation (Leithold, 1989; Nittrouer and Sternberg, 1981; Nittrouer *et al.*, 1984). Nittrouer *et al.* (1984) indicate that, where this ratio is small, primary sedimentary structures are preserved, but where the ratio is large, biological mixing is effective and the stratification is bioturbated (homogenized) by benthic macrofauna before it is preserved.

The presence or absence of a rich benthic macrofauna is governed by many factors, amongst which are sedimentation rates and oxygen levels of bottom water. An environment with high sedimentation rates is less favourable for benthic communities than an environment with low sedimentation rates. On the other hand, an environment with low concentrations of oxygen in the bottom water is expected to be less favourable to benthic communities than one with high oxygen concentrations. Dingle and Nelson (1993) found aerobic bottom water (1.5-2 ml/l oxygen) and Bailey (pers. comm., 1996) recorded >2ml/l oxygen on the Orange Prodelta (Sites H2 and H3). At these high oxygen concentrations, one would expect bioturbation to be effective. Radiographic examination of these two cores (H2 and H3) (Plate 1) however, reveals that the sediment has in fact *not* been reworked by benthic

macrofauna (e.g. by polychaete worms) since the preservation of primary laminations indicates a sparse or absent benthic population (Leithold, 1989; Lesueur and Tastet, 1994). Therefore, laminated Orange Prodelta muds are probably protected from bioturbation by high sedimentation rates, rather than by low oxygen levels in the bottom water. Meadows *et al.* (1997) calculate a sedimentation rate of 3.70 mm yr^{-1} at these two Sites (Cores H2 and H3) which is double the sedimentation rate of 1.82 mm yr^{-1} at site H7 near Kleinsee, where there are no laminations. Figure 7.1 reveals that the material comprising the laminated clays is consistent with their deposition within a narrow time range of just a few hundred years (Meadows *et al.*, 1997). Homogeneous clays are more prominent in the off Namaqualand shelf Cores (H4, H5, H6 and H7) farther south, which are either bioturbated and have lost their laminations or may be more marine than terrigenous and were never laminated in the first place.

Bioturbation (biological sedimentary structures) consists of the traces of the activity of an animal (e.g. burrows) (Lesueur and Tastet, 1994). Because very few organisms were present in the sampled sediment, associating organisms with bioturbation is difficult in the Namaqualand-shelf cores (Cores H4, H5, H6 and H7). This difficulty prompted the use of radiographs, which aids the detection of sedimentary structures and facilitates the interpretation of changes in the depositional environment (Axelsson, 1983). Careful examination of radiographs does not reveal any distinct burrows. These observations therefore suggest that the homogenous clays more prominent in the Namaqualand shelf were never laminated in the first place. This is a further evidence that these Namaqualand sediments are more marine than terrigenous.

(b) Texture

Mud (i.e. silt and clay), is on average, the dominant fraction, well above 90% of sediment in all the cores. This is part of the mud which is carried south of the Orange River mouth by a postulated weak poleward undercurrent to form an extensive belt of terrigenous mud on the innershelf, whereas sand and gravel are swept to the north of the Orange River mouth (Rogers, 1977; Dingle *et al.*, 1987; Rogers and Bremner, 1991). Although not all mud samples in the study area were analysed for silt and clay proportions, intensive size analysis of mud fractions from Cores H2 and H7 show distinct trends (Figures 5.15 and 5.16 respectively). Size analyses from both cores show that terrigenous sediments in the Orange River mudbelt are polymodal (Figures 5.15 and 5.16). Major modes in samples from Core H2 are generally in the medium-silt to fine-silt range, whereas Core H7 samples have their major modes in the very fine silt to coarse clay range. These results reveal a fining of sediments in a poleward direction. This poleward fining of sediments suggests that mainly medium silt to fine silt is deposited over a small area on the Orange Prodelta and that south of the Orange Delta (e.g. Core H7), the sediment is mainly fine-silt to clay. This observation links well with the observations of Verfaille (1987) who pioneered Sedigraph analyses of grab samples in the study area. He found coarser material near the Orange River mouth and finer material south of the Orange Delta at around 29° 50'S. These results confirm that the sediments (Prodelta sediments) are part of mud which is carried south of the Orange Delta by a postulated weak, poleward undercurrent to form an extensive belt of terrigenous mud. This undercurrent is not competent to transport medium to fine silt as far south as Core H7, off Kleinsee. The sources of muds at Site H7 are regarded as local ephemeral Namaqualand rivers. The polymodal sediments

from Cores H2 (Prodelta) and H7 (far south, off Kleinsee) suggest that there has been mixing with sediment of a different type. These results indicate that, whereas the Orange River is a major source of these muds in the mudbelt, it is an undeniable fact that additional inputs of silt and clay into mudbelt occur during adiabatic bergwind events (Figure 7.3) (Bremner, 1977; Shannon and Anderson, 1982; Whitaker, 1984).

There is fining-upward sequences in Cores H2. H4, H5 H6, and H7 (Figure 5.18). This fining-up trend is generally indicative of shoreward transgression of the sea (rising sea-level) (Boggs, 1995). As sea-level rises (shoreward transgression), finer grained deeper water deposits migrate landward and are deposited over shallower water deposits (Boggs, 1995) and hence the fining-upward sequence results. This sequence may suggest rising sea-level during Holocene (Mabote *et al.*, 1997).

What is the source of the sand?

A detailed seismic survey conducted by Birch *et. al.* (1991) showed that an inner-shelf sediment wedge consists of seaward-thinning sand units that form what is termed a "middle-inner-shelf sediment wedge" (Figure 7.4). This sediment wedge is in turn overlain by a thin deposit (1-8m) of Holocene mud. According to this model, the sediment on the inner-shelf platform forms a separate "inner-shelf-platform sand sheet" (Figure 7.4). Though this generalized model was based on observations from the southern end of the mudbelt off the Olifants River mouth, high-resolution seismic profiles from Woodborne's 1991 study revealed that the sand sheet on the inner-shelf platform extends across the inner-shelf slope, and continues seaward beneath the landward edge of the Orange River mudbelt. This observation shows that the "inner-

shelf platform sand sheet" and the "middle-inner-shelf sediment wedge" (Figure 7.4) are sometimes continuous (Woodborne, 1991). From his study, Woodborne (1991) concluded that much of the sediment wedge at the base of the inner-shelf slope is composed of sand. On the basis of this, it is therefore suggested in this study that the sand which seems to decrease upcore in Cores H2, H4, H5, H6 and H7, is part of this middle-inner shelf sediment wedge. This upward decrease of sand is not observed in other cores, the reason being that the middle-inner-shelf sediment wedge is sometimes not continuous (Woodborne, 1991). In fact, this upcore decrease of sand is not observed in Cores H1 and H3, which are both located on the Orange Prodelta. This observation links well with the observations of De Decker (1987), who was not able to locate the change from sand to mud on the inner shelf off the Orange River. This basal sand is considered to be from Quaternary coastal dunes that were eroded and partly redistributed in the littoral zone during the Flandrian transgression (Tankard and Rogers, 1978). This source is discussed in detail in the following section.

Gravelly shells are found to be dominant at the base of Core H5, immediately south of Orange Prodelta (Figure 5.4). These shells are dominated by the gastropods *Nassarius vinctus* (Marrat, 1877) (Plate 23b), *Volutocorbis lutosa*, Koch, 1948 (Plates 24a-b) and *Comitas saldanhae* (Barnard, 1958) (Plate 25a) and the bivalve *Tellina analogica*, Sowerby, 1904 (Plate 25b), which are all shallow-marine taxa (John Pether, Pers. comm.). These gastropods must have been killed during the lowering of sea level to about -130m during the last glacial period. The lowering of sea-level would cause mortality in the benthic macromollusc assemblage resulting in the gravelly (shell) basal unit in the light olive brown Quaternary sediments (Figure 5.5). The

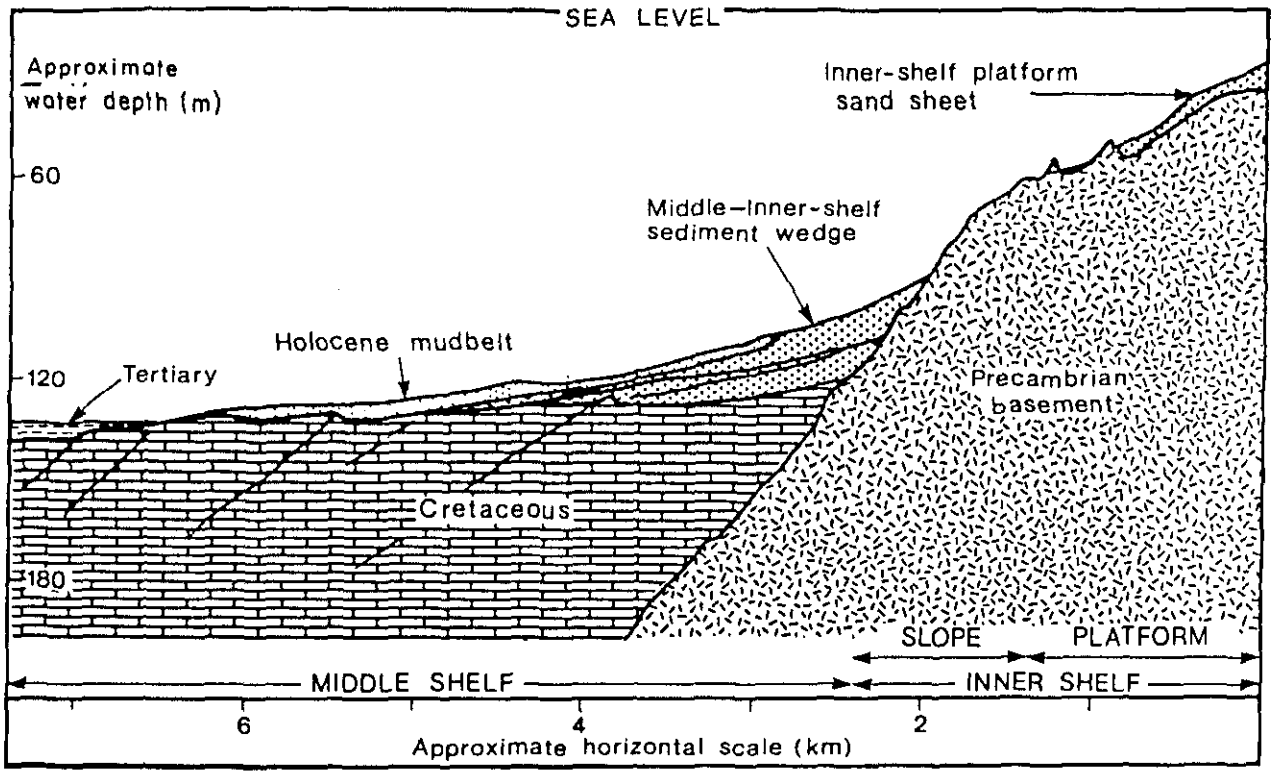

Figure 7.4 - Generalized morphology of sediment on the inner and middle shelves off the west coast (from Woodborne, 1991).

radiocarbon date of the sediment immediately above this shelly layer indicates that it was deposited at about 8000 years BP. This implies that this shelly layer found below it is older that than 8000 years. These observations suggest fluctuations in sea levels during Holocene.

(c) Terrigenous components

Quartz sand appears to become more abundant southward from the Orange River mouth, and it is most dominant in the Namaqualand-shelf Cores (H4, H5, H6 and H7). The source of these quartz grains is considered to be from Quaternary coastal dunes that were eroded and partly redistributed in the littoral zone during the Flandrian transgression (Woodborne, 1991). Figure 7.5 is a LANDSAT satellite image showing an extensive vegetated palaeodune field immediately north of the Buffels River. This dune field terminates 15km north of Port Nolloth (Woodborne, 1991) and on the basis of morphology, correlates well with the Late Pleistocene paleodunes lying immediately north of the Swartlintjies River, which lies 65km south of the Buffels River (Tankard and Rogers, 1978; Woodborne, 1991). Rogers (1977) and Tankard and Rogers (1978) suggest that the palaeodunes off the Buffels River probably formed contemporaneously with the Swartlintjies dune field during the last glacial period, 18000 BP.

Migration of the climatic belts towards the equator during the last glacial period, caused an increase in the intensity of atmospheric circulation, and northward expansion of the winter-rainfall region over Southern Africa (Tankard and Rogers, 1978; Woodborne, 1991). Tankard and Rogers (1978) note that lowering of sea level

to -130m, coupled with the increased winter precipitation, resulted in the rejuvenation of Namaqualand rivers. Woodborne (1991) suggests that the Buffels River (Figure 1.2) may have occupied a more southerly course across the shelf, entering the sea approximately 10-15 km south of its present position. It is suggested that, a wave-dominated delta, similar to the present-day Orange River delta, probably developed at the Buffels River mouth (Woodborne, 1991). This would have formed a large northward-tapering deposit of sediment at the base of the present inner-shelf slope as sediment was transported northwards away from the river mouth by wave-generated littoral currents. Perhaps these currents are the ones responsible for the abundance of quartzose fine sand in the cores as far north as off Wreck Point (Core H5, Figure 1.2). Tankard and Rogers (1978) and Woodborne (1991) suggest that sand carried onto beaches was then blown inland by strong prevailing southerly winds, thereby forming the palaeodunes north of the Buffels River (Figure 7.5). Woodborne states that dune sands blanketing the exposed innershelf were eroded and reworked during Flandrian transgression, as sea level rose rapidly from -130 m to reach its present level about 6500 BP. Increasing coastal aridity accompanied by rising sea level resulted in a steadily decreasing supply of fluvial sediment, and dune erosion then became the dominant source of sediment on the inner shelf (Rogers, 1977; Tankard and Rogers, 1978). However, the rapid rise in sea level during the Holocene prevented complete reworking and erosion of the pre-Flandrian dune sands, thereby leaving the northward-tapering blanket of sand on the inner-shelf platform and slope (Woodborne, 1991) between Kleinsee and Wreck Point. The dominance of well- to sub-rounded, quartzose fine sands in the sediment samples between the Buffels River mouth (Core H7, off Kleinsee) and Wreck Point (Core H5) supports this argument. Their texture

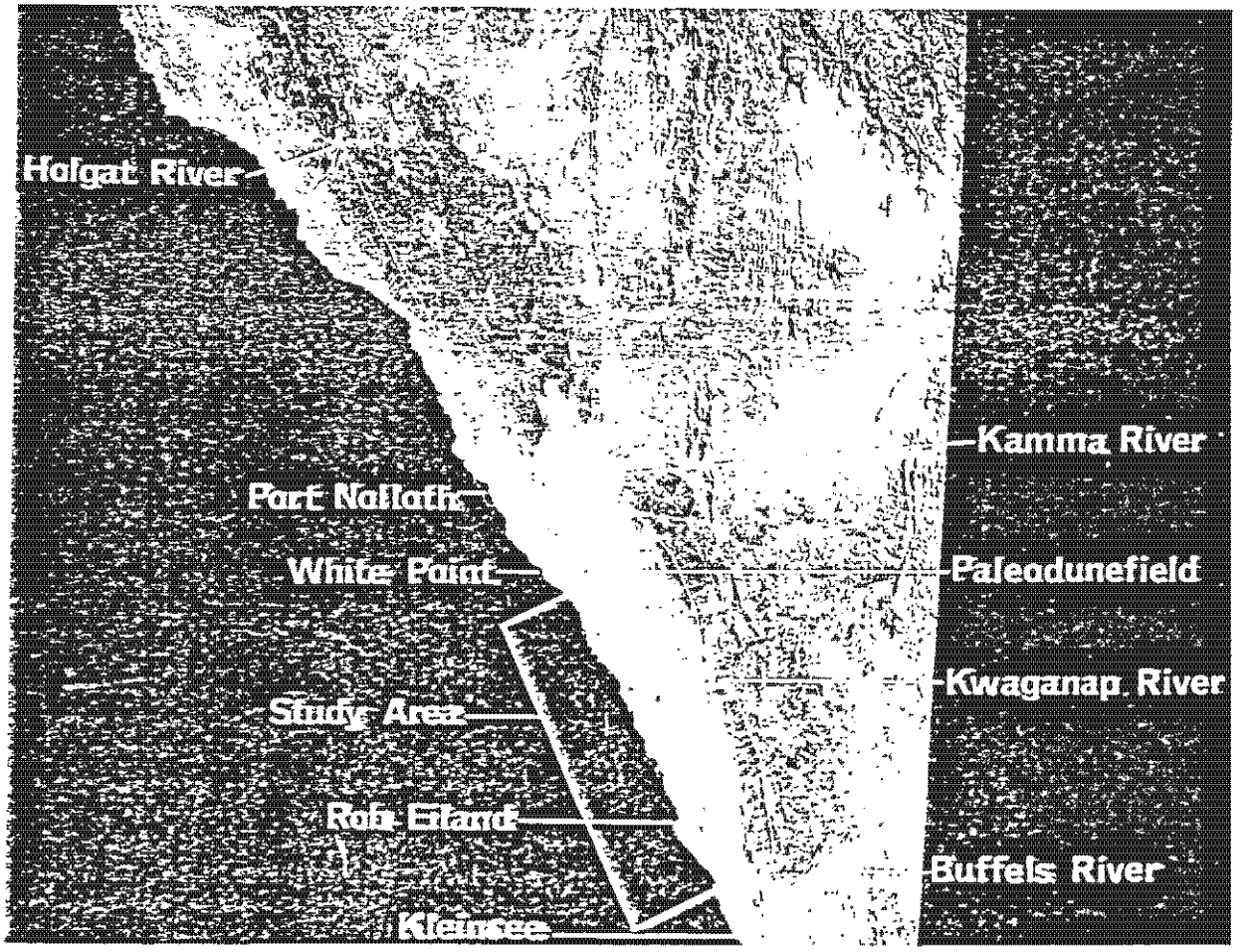

Figure 7.5 - Landsat -3 satellite image of northeastern Namaqualand showing a pre-Flandrian palaeodune field extending north from the Buffels River (From Woodborne, 1991).

(well- to subrounded) fine sands) points to the aeolian source of these sediments. This observation tallies with Woodborne's (1991) observations. The fact that there is almost no quartz found in the Orange Prodelta (Cores H1 and H3) clearly supports Meadows *et al.*, (1997) conclusion that mudbelt sediments are not all derived from terrigenous inputs by the Orange River and those in the southern part of the sampled area, i.e. offshore Namaqualand may well receive significant inputs from alternative sources.

Mica occurs in subordinate to minor quantities throughout the study area. It is present in almost equal quantities from the Orange River mouth to the far south off Kleinsee. The occurrence of these mica flakes is related to the semi-arid climate of onshore Namaqualand. Mica is entrained by adiabatic Berg winds moving offshore from the interior (Figure 7.3) (Shannon and Anderson, 1982; Whitaker, 1984).

Rock fragments dominate coarse fraction components off the Orange River and their abundance decrease southward away from the influence of the river mouth (Figures 5.1-5.7). No attempt has been made to identify these rock fragments in order to trace their origin. However, the fact that rock fragments abundance drops off rapidly south of the Orange River mouth, clearly indicates that these rock fragments are brought to the shelf by the Orange River, and hence their distribution closely reflects the composition of the local onland geology.

Plant fragments are dominant off the Orange River but also decrease southwards, i.e., their distribution is similar to that of rock fragments. This observation reveals that the

Orange River supplies to the Atlantic Ocean much sediment with both rock fragments and plant fragments, which are mostly deposited on the river's Prodelta. This distribution clearly indicates terrestrial influence of Orange River in the Orange Prodelta.

(d) Biogenic Sediments

Planktonic and Benthic Foraminifera

In general, foraminifera are present in trace to minor quantities in Cores H1, H2 and H3 on the Orange Prodelta (Figure 1.2). These lower quantities are attributed to high influx and sedimentation accumulation rate of terrigenous sediments, which would dilute the foraminifera. This observation tallies with De Decker's (1987) observations in this area.

Most of the foraminifera observed in the study area are known to be Holocene in age (McMillan, pers. comm.). These species include left-coiling *Neogloboquadrina pachyderma, Globorotalia inflata, Quinqueloculina* sp. and *Bulimina aculeata.*

Elphidium advenum, Elphidium macellum, Elphidium cf. alvarezianum and *Ammonia japonica* can occur in shallow marine environments. There is something distinctive about their tests which helps to determine their age. Deeper-water species (Holocene), are the ones found well-preserved or muddy infilled, or acid-corroded, or pyrite-infilled, whereas shallow-water species (latest Pleistocene) are the ones with thick-walled, polished, abraded and tumbled or broken (McMillan, *Pers. Comm.*). The age of these species is therefore regarded as being Pleistocene (Chapman, 1907, in McMillan, 1987). The presence of these shallow-water microfauna is partly explained by glacial-period lowering of sea level to -130 m during the Late Pleistocene (Rogers

and Bremner, 1991). Another explanation could be that these species had been reworked from bedrock. This is supported by the presence of *Elphidium cf. alvarezianum* especially in Cores H6 and H7. *Elphidium cf. alvarezianum* is generally believed to be Late Pleistocene in age (McMillan, pers. comm.). In contrast, McMillan (1987) argues that the age of *Ammonia japonica* probably also includes Holocene, and hence finds it more proper to consider *Ammonia japonica* as indeterminable late Quaternary.

The species composition of the assemblages of planktonic foraminifera found in the study area are dominated by polar taxa such as left-coiling *Neogloboquadrina pachyderma*. *Globorotalia inflata* is the only indigenous species of the transitional faunal zone that exists between sub-polar and sub-tropical waters (McLachlan, 1995). Its presence in the study area suggests the existence of either the Benguela Nino or increased input of Agulhas Current water to the Southern Benguela region (Figure 7.6). The Benguela Nino is described as an episodic incursion of warm water from the Angolan region onto the Namibian shelf, which penetrates farther south than normal, and develops into a major, persistent warm event (Shannon *et al.*, 1986; Siegrfried *et al.*, 1990). The enhanced poleward flow and warm coastal waters in years of Benguela Ninos allow (or displace) species from warmer areas (Northern Namibia) so that they extend their ranges poleward (to the south) (Siegrfried *et al.*, 1990; Crawford *et al.*, 1990; Giraudeau, 1993).

Similarly, substantial volumes of water from Agulhas Current may intrude the Southern Benguela region, and penetrate as far north as Luderitz (Siegrfried *et al.*, 1990).

These two scenarios may generate an environment favourable for *Globorotalia inflata*. However, further research is required to confirm this hypothesis, as other factors such as altered wind stress and warming of surface waters due to global warming will obviously affect the distribution of marine biota in the open-shelf environment.

The distribution of benthic foraminifera *Stainforthia fusiformis, Nonionella turgida,* and *Discammina compressa* in the study area seems to be controlled by certain environmental conditions. These species are associated with low oxygen levels (MacMillan, pers. comm.). These species are common in Cores H5, H4, H6 and H7, all of which are relatively closer to the Namaqua upwelling cell. Upwelling increases nutrient content of the water at these sites and this results in enhanced biological activity. Aerobic bacteria decomposes dead plankton tissues and consume most of oxygen found in these sediments in the process. This enhanced biological activity effectively causes anaerobic conditions in the bottom sediments (De Decker, 1970). The resulting low oxygen levels at these sites make them favourable for these species. This argument is once more supported by the presence of left-coiling *Neogloboquadrina pachyderma,* which is identified as an indicator of the cold upwelled water over the inner-middle shelf (Herbert, 1984; Herbert *et. al.,* 1989). In addition to this, of particular interest is the presence of the agglutinated benthic foraminifer, *Discammina compressa*, in these cores which, are relatively rich in quartzose sand. This is possibly due to the fact that the agglutinated benthic foraminifera require detrital grains with which to construct a shell (Birch, 1975).

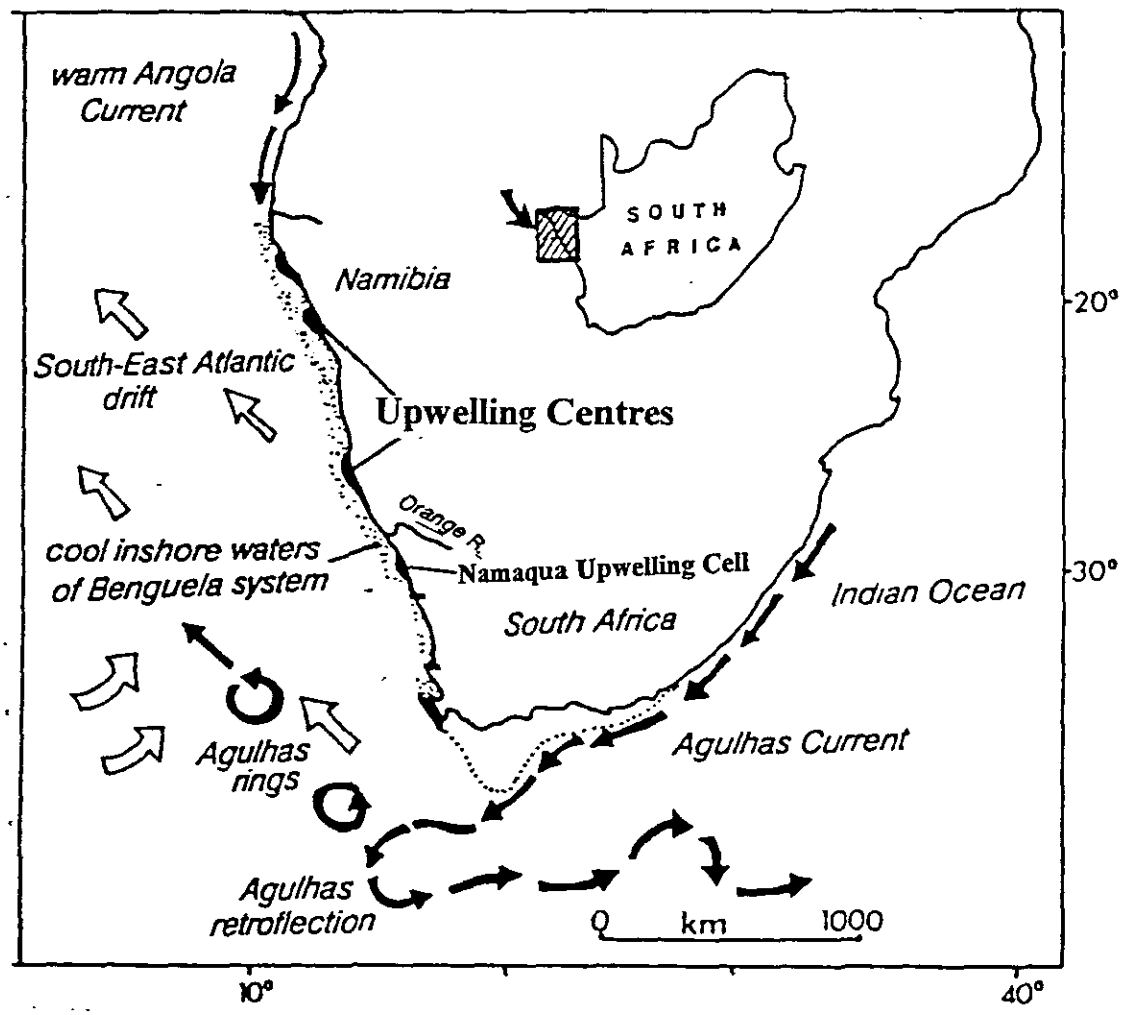

Figure 7.5 - Map showing some aspects of the physical oceanography around southern Africa. Warm water enters the southeast Atlantic via the shedding of "rings" of "eddies" from the Agulhas current as it retroflects southwest of the Agulhas Bank. (After Cohen *et al.*, 1992)

Shells and shell fragments

Burnupena limbosa, Volutocorbis lutosa, Comitas saldanhae and *Tellina analogica* are the most dominant shells in the cores. *Volutocorbis lutosa, Comitas saldanhae* and *Tellina analogica* are expected to be present in the study area because they inhabit fine-grained sediments on the lower inner shelf and middle shelf. They would have lived on it from its inception to the present (Pether, *Pers.comm.*).

Burnupena limbosa inhabits the shoreface and would expect to find this in shoreface-beach sediments (Pether, pers. comm.). However, *Burnupena limbosa* may be carried seawards during storms and deposited in proximal tempesites. Most examples of *Burnupena limbosa* show evidence of residence in shelly gravel in the shoreface (e.g. abrasion or/and boring and/or encrustation), for example, *Burnupena limbosa* on Plate 23a has encrustations. Where present, these shells are found at the base of the cores (Figure 5.4, and Figure 4.1 (Core H5)).

Diatoms and fish debris

In general, siliceous frustules of centric diatoms are restricted to Cores H6 and H7, off Namaqualand whereas fish debris are found mainly in Cores H4 and H5, farther north, closer to the Orange Delta. Diatoms characterise upwelling regimes (Calvert and Price, 1983). Their high specific growth rate, in particular, which provides them with a competitive advantage where nutrient supplies are variable and pulsed, makes diatoms well suited to upwelling environments (Calvert and Price, 1983). Therefore, the presence of diatoms in Cores H6 and H7 suggests that upwelling, generated by the prevailing offshore summer winds is probably intense, and the increased nutrient content in this region results in enhanced biological activity and anaerobic bottom

sediments (De Decker, 1970; Birch, 1975). Diatoms are almost absent in Cores H1, H2 and H3 on the Orange Prodelta. This is probably so because upwelling is less intense and more spasmodic off the Orange River mouth. Moreover, the relatively higher oxygen content of the faster-moving waters at these sites (due to river inflow) favours more rapid oxidation and dispersal of the fine organic matter (Birch, 1975). The increased oxygen content helps in the oxidation of organic matter and hence less nutrients (organic matter) become available for diatoms. The reduced food supply for diatoms results in few diatoms inhabiting this area. Also, diatoms species which inhabit the Cape waters are smaller and softer and therefore more susceptible to oxidation and fragmentation than are the more robust Phytoplankton occurring off South Namibia. It is likely that most of these diatoms are subjected to oxidation and fragmentation, and those few observed in this region are those which have survived or avoided these processes.

Fish debris is occasionally encountered in the form of vertebrae, jawbones, teeth and scales in cores H4, and H5, off Namaqualand. The presence of fish debris in these cores is indicative of high productivity during Holocene. The presence of fish debris may also be associated with organic-rich sediments (Birch, 1975) and low sedimentation rates. The absence of fish debris in the Orange Prodelta (Cores H1, H2 and H3) may be explained in terms of rapid sedimentation rates at this area. These high sedimentation rates may have caused this area unfavourable for fishes.

Radiolaria

The study area is almost barren of radiolaria. Where present, they occur occasionally in trace quantities. They are present only in Core H2, just off the Orange River mouth and none were observed in Core H7 off Kleinsee. Because of their small numbers, no palaeoenvironmental parameters could be deduced from their distribution.

Sponge spicules

Sponge spicules increase southwards from the Orange River mouth. They dominate the sand-fraction components in Cores H6 and H7 (Figures 5.1-5.7). Sponge spicules indicate the presence of filter-feeding animals (epifauna). Sponge spicules are absent or present in trace quantities near the river mouth (Cores H1, H2, H3, H4 and H5). Filter-feeding fauna probably avoid this region due to high sedimentation rates near the river mouth, which make it unfavourable for filter-feeding animals to inhabit. In fact, Meadows *et al.*(1997) reported a sedimentation rate of 3.70 mm yr^{-1} at H2 and H3 sites on the Orange Prodelta, which is double the sedimentation rate of 1.82 mm yr^{-1} at site H7, near Kleinsee. On the other hand, these sponge spicules could have some relationship to low salinity. However, this needs to be investigated.

Polychaete Worm Faecal Pellets

Benthic faecal pellets are found mainly in Cores H2, H4, and H5 as ovoid, sub-rounded particles. They are most abundant towards the top of the cores. These benthic faecal pellets seem to be confined to cores found between areas of high oxygen concentrations and high sedimentation rates (Cores H1 and H3 on the Orange

Prodelta) and low oxygen concentrations and low sedimentation rates (Cores H6 and H7, near Kleinsee). These faecal pellets are produced by burrowing animals such as polychaete worms (Birch, 1975). The distribution of benthic faecal pellets suggests that although these burrowing animals require oxygen for their metabolic processes, they are excluded from the Orange River mouth (where oxygen levels are apparently highest) by high sedimentation rates. Similarly, although sedimentation rates are low and favourable for establishment of burrowing animals at Sites H6 and H7, low oxygen levels seem to be the inhibiting factor and hence make these sites less favourable for the establishment of burrowing animals.

The selective accumulation of ovoid faecal pellets at the sediment surface is characteristic of a 'conveyer-belt feeder' such as *Heteromatus filiformis* (Rhoads, 1974; Cadee, 1979; Bromley, 1990). Cadee (1979) and Bromley (1990) note that this polychaete worm derives all its food from sediment ingested in the layer 10 to 30cm below the surface and deposits its faecal pellets at the surface.

In general, marine biogenic sediments are more dominant further south of the Orange River (Namaqualand inner shelf, Cores H4, H6, and H7) (Figures 5.5, 5.6 and 5.7). This also another indication that sediments are mostly of marine origin in the Namaqualand inner shelf whereas prodeltaic sediments are mostly terrestrially derived.

7.4 Mineralogy and Geochemistry

It is important to note factors responsible for distribution of clay minerals on the continental margin before any conclusions could be made. Bremner (1977) notes that relative abundance of clay minerals in marine sediments depends primarily on the composition of source rock in the adjacent hinterland, and on the nature of the prevailing climate in the region. The distribution of clay minerals on the continental shelves depend on the transporting medium in the hinterland (aeolian or fluviatile), current systems operative on the shelf, and on the flocculation rates of the different clay minerals in sea water (Biscaye, 1965; Bremner, 1977). The contribution made by each of these factors will be discussed below.

(a) Sources and Distribution of Clay Minerals

Mica (probably illite species as established by Rogers, 1977, in the same region, hence the term illite will be used interchangeably with mica where convenient) is the most dominant clay mineral present in all marine sediments found in the study area. This is mainly because of the high concentration of mica in many rock types from the more arid regions in the western-catchment of the Orange River, and owing to its relative resistance to chemical weathering (Biscaye, 1965; Bremner, 1977). Therefore mechanical disintegration of these rocks provide an ample source of mica. This mica is then entrained by adiabatic Berg winds moving offshore (Figure 7.3) from the interior (Shannon and Anderson, 1982; Whitaker, 1984). This high content of mica is in consistent with the semi-arid climate of onshore Namaqualand. In addition to this,

it is likely that mica is a dominant component of fine silt and clay in the Orange River and other rivers contributing to it (e.g. Caledon River) (Dr. Fey, *pers. comm.*, 1997; Mabote *et al.*, 1997). Fey (per. comm., 1997) suggested that this mica might also be emanating from the Upper Orange River catchment (Lesotho), where he expects many of the soils on sedimentary rocks to be micaceous.

Van der Merwe and Heysteck (1955) have shown that smectite-rich soils (montmorillonite being a dominant mineral) overlie weathered basalts in the Drakensberg mountains and on weathered dolerite in the High Veld within the catchment of the Upper Orange (Figure 2.2). Rogers (1977) has established that the Upper Orange catchment, underlain by sediments of the Karoo Supergroup, is the chief source of suspended sediment in the Orange River. Bremner *et al.*(1990) also have shown that smectite-rich soils (mainly montmorillonite) carried by Orange River are from the high-rainfall areas of the Upper Orange where the weathered basalts of the Drakensberg rim the eastern catchment. These terrigenous sediments of the Orange River are fractionated at the mouth where they encounter long-period Southern Ocean Southwesterly swell (Bremner *et al.*, 1990). Rogers (1977) has established that gravel and sand are swept to the north by strong wave-driven littoral drift whereas a postulated weak poleward undercurrent (Nelson, 1989) carries silt and clay to the south of the Orange River to form extensive belt of terrigenous mud. As a result of this poleward undercurrent, smectite-rich sediments are distributed throughout the mudbelt.

Vermiculite was found to be the third most abundant mineral in the Orange Prodelta, (being more abundant than kaolinite, chlorite and plagioclase) whereas vermiculite was found to be less abundant than these minerals in the inner shelf off Namaqualand. In their analyses of river samples, Rogers (1977); and Bremner *et al.* (1990) did not report presence of vermiculite in river samples from rivers draining into the Orange shelf (study area). Moreover, Bremner (1977) did not report presence of vermiculite in the river samples from Kunene River, north of study area. These observations suggest that vermiculite could not have originated in the hinterland and then delivered into the continental shelf by fluvial transport.

There are two types of vermiculite both of which occur in nature. These are dioctahedral and trioctahedral vermiculites (Brownlow, 1996). Dioctahedral vermiculite ($Al_2Si_4O_{10}(OH)_2.nH_2O$) originates from weathering of mica muscovite ($KAl_2(AlSi_3)O_{10}(OH)_2$ with concomitant fixation of Al^{3+} in the interlayer positions (Hathaway, 1955 in Bremner. 1977), whereas trioctahedral vermiculite ($Mg_3Si_4O_{10}(OH)_2.nH_20$ forms either from leaching of brucite layers in the trioctahedral chlorite lattices (Johnson, 1964, in Bremner, 1977), or else from the alteration of finely comminuted biotite flakes (Kazantzev, 1934; Bremner, 1977). Kazantzev (1934) notes that, finely comminuted biotite flakes, which are found in the Namib Sand Sea, are relatively easily transformed to trioctahedral vermiculite. This is transformed by replacement of K^+ by H^+, and Mg^{2+} replacing Fe^{2+} and Fe^{3+}.

Nicolayev and Senin (1972), Bremner (1977) and Bremner *et al* (1993) have reported the presence of trioctahedral vermiculite north of study area. Since no vermiculite has been reported to occur in the river samples, Bremner (1977) therefore postulated its mode of formation to be due to partial stripping of K from finely comminuted biotite

flakes in the arid hinterland, followed by diagenetic replacement of Fe by Mg in the marine environment.

On the basis of this information, it is proposed that vermiculite found in the study area must have originated in the arid hinterland north of study area by the above-mentioned mode of formation. Having been formed diagenetically north of study area, vermiculite is then transported southward by the poleward undercurrent, which exists along the whole shelf down to Cape Point (Nelson, 1990). This explanation may also account for relatively low concentrations of vermiculite in the inner shelf off Namaqualand (Core H7). As poleward undercurrent transports vermiculite from as far as offshore of Namib Sand Sea, it (vermiculite) flocculates on the way, and by the time it reaches the inner shelf, there are relatively low vermiculite concentrations remaining. Thus, its concentrations get lower southward. Its distribution clearly indicates terrestrial influence by Orange River (i.e. it is abundant in the prodelta where terrestrial input by the Orange River is at a maximum).

Kaolinite is the third most abundant clay mineral in the inner shelf off Namaqualand. It is subordinate to smectite. Birch (1977) has observed that rivers draining the Namaqualand metasediments contain clays rich in kaolinite, and a value exceeding 60% kaolinite was recorded in one of these rivers (Brak River). Likewise, Rogers (1977) recorded a value of kaolinite (plus chlorite) which was between 20-30% at the mouth of Buffels River (in the inner shelf region). This river drains the Namaqualand metasediments. The sum of kaolinite and chlorite recorded in this study ((in core H7) is 20-30%. These results tally with earlier analyses in this region (Rogers, 1977). It is

therefore proposed that kaolinite found in the inner shelf off Namaqualand is brought by rivers draining the Namaqualand metasediments. Kaolinite concentrations in the Orange Prodelta are relatively lower than in the inner shelf off Namaqualand. Two possibilities exist regarding the source of this clay mineral in the Orange Prodelta, viz.: (1) kaolinite brought to sea by rivers draining Namaqualand metasediments, is at times of high, southerly wind stress, carried equatorward by the surface layer of the Benguela current or, (2) kaolinite is fluvially introduced in the Orange Prodelta by Fish River (Figure 2.2) which drains some part of the arid hinterland (Namibia) (Bremner *et al.* (1990) observed kaolinite concentration in Fish River sediments to be relatively higher than kaolinite concentrations in sediments of other rivers draining into the Orange shelf) or (3) kaolinite might have been brought to the sea by Kunene River (north of study area). These clay minerals were then entrained by poleward-directed tongues of the Angola-Benguela Front, or poleward undercurrent, eventually settling south of Kunene River mouth, and at times as far as Orange Prodelta (Core H2). In the absence of further details, the source of kaolinite in the Orange Prodelta cannot be traced.

Chlorite, quartz, plagioclase and alkali feldspars occur in minor quantities in the study area and hence, little effort was made to trace their sources or origin.

Griffin *et al* (1968) (in Bremner, 1977) indicate that chlorite is classified as a typical high-latitude mineral and would therefore not be expected to occur off the coast of South West Africa. Its introduction to the marine environment is mainly through the medium of glacial rock flour (Bremner, 1977). Presence of quartz clearly points to the aeolian input by bergwinds, as it is the case with mica minerals. This is supported by

the fact that the abundance of quartz seems not to be affected by the increasing distance away from the river mouth.

(b) Gypsum Crystals and their Formation

As mentioned earlier, the study area lies within the Benguela Current region, which is dominated by the upwelling of cold nutrient-enriched waters. Siesser and Rogers (1976) model explaining the formation of marine authigenic gypsum in slope sediments off Luderitz (north of the study area) may be invoked to explain the presence of gypsum in the coarse-fraction off Namaqualand. These authors point out that decomposition, by aerobic bacteria, of dead plankton as it settles on the bottom, consumes oxygen. I postulate the same process to anaerobic conditions in terrigenous mud on the inner shelf.

Anaerobic bacteria thriving under such conditions reduce sulphate (SO_4), dissolved in sea water, initiating the formation of hydrogen sulphide (H_2S):

$$5H_2 + SO_4^{2-} \rightarrow H_2S + 4H_2O \qquad (1)$$

H_2S then reacts with iron cations in the interstitial water to form iron monosulphide (FeS):

$$H_2S + Fe^{2+} \rightarrow FeS + 2H^+ \qquad (2)$$

Oxidation of these sulphides releases dissolved SO_4 and causes a lowering of pH:

$$4FeS + 9O_2 + 6H_2O \rightarrow 4FeO(OH) + 4SO_4^{2-} + 8H^+ \quad (3)$$

It should be noted that a considerable amount of dissolved oxygen is removed from sea water during oxidation of hydrogen sulphide to sulphates (Rogers, 1977; Mabote *et al.*, 1997). Rogers (1977) notes that the "milky" sea water often observed in the sea in and around Walvis Bay (North of the study area) may be due to colloidal sulphur formed by the oxidation of hydrogen sulphide.

Planktonic calcareous microfossils then dissolve in these more acidic sea waters, releasing calcium and bicarbonate ions:

$$H^+ + CaCO_3 \rightarrow Ca^{2+} + HCO_3^- \quad (4)$$

The elevated levels of both calcium and sulphate then lead to supersaturation and finally precipitation of gypsum:

$$Ca^{2+} + SO_4^{2+} + 2H_2O \rightarrow CaSO_4.2H_2O \text{ (gypsum)} \quad (5)$$

These reactions are based on the models of Siesser and Rogers (1976), Briskin and Schreiber (1978) and Mabote *et al.* (1997).

Primary or secondary gypsum?

Gypsum occurs as large unbroken tabular euhedral crystals, indicating that the gypsum is not a product of reworking. If these gypsum crystals were reworked, then some of the crystals would show signs of breakage and thus cleaved and abraded particles would be evident (Briskin and Schreiber, 1978). There are no cleaved and abraded particles (Plates 3b, and 4a-b). Gypsum is also not an artifact of desiccation during storage and selective concentration of pore waters. If gypsum were an artifact, one would expect to find gypsum throughout the core (Briskin and Schreiber, 1978). Careful examination of the sediment in these cores shows that gypsum-bearing layers are restricted to the bottom of cores H4, H6 and H7 off Namaqualand (Figure 1.2), but not in the cores H2 and H3 on the Orange Prodelta. It is therefore concluded that the gypsum is neither reworked, nor the result of sampling and desiccation following sample recovery, but is rather developed *in situ* as an authigenic component of the marine sediments. It is therefore secondary, not primary.

(c) Geochemistry

The high concentrations of Silicon (Si) in both Cores H2 (Prodelta) and H7 (off Kleinsee) sediments, along with the composition and textural data (Chapter Five) indicate that most of the Si in the study area is present as quartz (but no exclusive) in a coarse fractions. The fact that quartz (SiO_2) is only present in minor quantities (~5%) as clay minerals, suggests that the presence of crystalline quartz is more prevalent in the fine sands in the study area. This is also supported by observations of the sand fractions from all cores under the binocular microscope (Figures 5.1-5.7, Chapter

Five). The Silicon is thought to be of terrigenous origin as suggested in section 6.4.1. Moreover, there has been no evidence found in this study or others in the region to suggest biogenic SiO_2 formation.

The presence of Titanium (Ti) is most likely explained by the mixing of clay minerals with amorphous or finely dispersed crystalline Titanium oxide (probably ilmenite and rutile) or Titanium dioxide hydrate released during weathering (Degens, 1965; Felhaber, 1984). In his study of Quaternary shelf sediments, off Tugela River in Natal, Felhaber (1984) detected the highest concentration of Ti (>1%) in the very fine nearshore sands, and suggested that this was due to their proximity to the river mouth which is the source of the heavy minerals in that area. The same argument goes for high concentrations of Ti in Core H2 (averaging 0.82%) which is near the Orange River mouth, relative to Core H7 sediments (averaging 0.76%). Nevetherless, the difference of Ti between these two cores is not that wide. This probably due to the contribution made by Buffels River (Figure 1.2) during its active periods.

Al, K, Fe and Mn

The areal distribution of Al, K, Fe and Mn on the mudbelt is very similar. They are most abundant in the Orange Prodelta (Core H2) region adjacent to the point of maximum terrestrial input which is the Orange River.

Felhaber (1984) notes that the fate of Aluminium (Al) is in the hydrolysates (clay minerals). Therefore the highest concentrations of Al (16.61-20.47%) in Core H2 (Prodelta) sediments, is undoubtedly a result of their high contents of clays relative to

Core H7 (off Kleinsee) sediments (11.76-17.84%). This is confirmed by textural analysis in Chapter Five. The Aluminium content is often considered the best representative of clay content dues to its immobility in the sedimentary environment (Felhaber, 1984). The Al is probably derived from subtropical chemical weathering of K-feldspars in the basement granite-gneisses north of the study area, and from kaolinitization of muscovite micas introduced from the Namib Desert by the prevailing winds as suggested earlier.

Potassium (K) is present and seems to vary slightly over the study area. It is slightly higher in Core H2 (Table 6.1). This K is predominantly located in the clay minerals, presumably mostly in illite or K-feldspars (Felhaber, 1984). Presence of K in the study area may be attributed to the abundance of mica in the hinterland.

Iron (Fe) is present in the form of Fe_2O_3. This is due to the generally oxidized nature of surficial marine sediments.

Presence of Manganese (Mn) in the mudbelt may be attributed to the Ecca sediments which are rich in Mn.

Calcium (Ca) is present in the study area in low quantities. Unlike those other elements discussed so far, it is least abundant in Core H2 (near the river mouth) and the highest concentrations of Ca are detected in Core H7 sediments (2.68-8.72%, averaging 5.33%). This is well above its concentration in Core H2 sediments (1-4.36%, averaging 1.94%) (Table 6.1). The areal distribution of Ca follows very closely that of foraminifera (Calcareous organisms) and authigenic gypsum in the total sediment (Chapter Five). The foraminifera and authigenic gypsum were found in

abundance south of the Orange River (Cores H4, H6 and H7), away from the river influence. This observations suggest that Ca-rich sediments are found south of the Orange Prodelta and decrease sharply northwards towards the Orange River (Core H2). This is probably due to the high influx of (Ca-poor) terrestrial sediments. In addition, these observations are evidence that the major proportion of Ca is present in the area as $CaCO_3$ of predominantly biogenic origin. This is because Ca enrichment south of the Orange Prodelta (Cores H4, H6 and H7) corresponds to increased carbonate deposition in the form of foraminifera, suggesting that calcium is being derived by breakdown of calcareous organisms. It is interesting to note absence of authigenic gypsum in Cores H1, H2 and H3 sediments. The formation of this mineral requires significant proportion of calcium to be available.

Magnesium (Mg) is present in both cores in almost equal quantities. The average concentration of Mg in Core H2 sediments is 2.94%, whereas in Core H7 sediments is 3.25%. The difference between the two is not that significant. The Mg concentrations in the study area could be due to an association of Mg with clays (it is usually present in chlorites and montmorillonites) (Felhaber, 1984).

Phosphorus (P) is present in trace quantities in both Cores H2 and H7 sediments. Its average concentration in both cores is about 0.2%. Its presence in the study area could be attributed to finely disseminated apatite, although it (apatite) was not identified in the X-ray diffractograms. Felhaber (1984) states that P may also

be supplied by plant material associated with the organic matter found in the muds.

Water (H_2O) is present in both Cores H2 and H7 sediments in almost equal concentrations (averaging about 7%). Felhaber (1984) found H_2O+ highly positively correlated with the clay mineral factor, and suggested that most, if not all, of water is located in the intersheet positions of the clay minerals or present in the octahedral layers as OH- ions.

In summary, this chapter discusses all the results obtained in this study, chapter Eight presents main conclusions of this study.

CHAPTER EIGHT

CONCLUSION

8.1 Introduction

This chapter aims at providing a general overview of the findings of this research. The broader aims of this research have been to contribute to the evidence for environmental change during the late Quaternary in southern Africa from the analysis of continental shelf sediments, and more specifically, to examine the feasibility of using Namaqualand mudbelts as a key to understanding late Quaternary environmental dynamics of both terrestrial and marine environment. In order to achieve these aims a number of objectives had to be realised which were:-

- To establish a detailed chronostratigraphy and test or confirm the Holocene age of the superficial deposits of the mudbelt,
- To establish a detailed lithostratigraphy of the superficial deposits of the mudbelt,
- To examine particle size distribution and composition of the mudbelt sediments,
- To determine and interpret various sedimentary properties which are found in the terrigenous sediments of the Orange Shelf,
- To relate these sedimentary properties to environmental changes, processes in the depositional environment and anthropogenic activities or influence,
- To see whether the muds found on both the Orange Prodelta and the inner shelf of Namaqualand are part of the same modern depositional event or whether they

represent different periods of deposition with possibly different mineralogical and geochemical compositions and,

- To investigate the origin of Orange Shelf sediments and where possible, palaeoclimate of the source area and conditions at the environment of deposition through mineralogical, geochemistry and biogenic analysis.

A review of the sedimentology and geochemistry of the area in conjunction with radiocarbon dates and information taken from other sources allows the reconstruction of environmental changes that took place during the late Quaternary.

8.2 Chronology

Despite of the obvious inconsistencies in the radiocarbon ages of some of the cores (H2 in particular), these radiocarbon dates confirm the Holocene age of the Namaqualand mudbelt deposits. Moreover, the ages suggest that laminations evident in the Namaqualand mudbelt sediments are recent terrestrially-derived sediments input. They have been deposited at least in the last 1700BP.

Although the radiocarbon dates have obviously enabled us to confirm the Holocene age of mudbelt, a need for a more appropriate and reliable means of establishing a chronology cannot be overemphasized. A reliable method will obviously provide significant information regarding sediment erosion and accumulation rates in the past, thus helping in the elucidation of the Late Quaternary erosional history of Southern Africa.

8.3 Sedimentology

Preservation of parallel laminations in the terrigenous muds on the Orange Prodelta suggests that there is high sediment accumulation rate and low biological mixing near the Orange River mouth (Orange Prodelta). The decrease of these laminations southward is mainly due to low sediment accumulation rate at these sites (Mabote *et al.*, 1997). Analyses of radiographs suggest that biological mixing is not effective in the study area.

A relationship between lithostratigraphy and chronostratigraphy indicates that the laminations are synchronous between different cores. The radiocarbon ages of laminated muds suggest that they were deposited in the last 1700BP. These laminations could be signatures of increased soil erosion due to anthropogenic activities.

The stratigraphic analyses combined with radiocarbon dates suggest that the dark laminated clays are derived primarily from the Orange River and are essentially overstepping (prograding seaward). Nevetherless, they do not extend south of a position somewhere between west (Site H5) and south of Wreck Point (Site H4) (Figures 1.2 and 4.1). These results therefore negate the earlier inferences (e.g. Rogers, 1977; Dingle *et al.*, 1987; Rogers and Bremner, 1991) that the Namaqualand mudbelt is primarily derived from the Orange River. This contention is further

supported by appearance of grey laminated sequence at Sites H6 and H7 which seems to be originating from ephemeral rivers of southern Namaqualand.

On the basis of chrono- and lithostratigraphic, coarse-fraction components and mineralogical analyses, the following sedimentary development on the Namaqualand Mudbelt is suggested:-

An early period of deposition dominated by marine conditions (represented by homogeneous yellowish-green clay with shells at Sites 5, 4 and 6, and olive-green clay at Site 7) off the coast, but with significant terrigenous input in the north and south (Sites 1-3, and 7).

Although not all mud samples in the study area were analysed for silt and clay proportions, intensive size analysis of mud fractions from Cores H2 and H7 show that terrigenous sediments on the Namaqualand Mudbelt are polymodal (Figures 5.15 and 5.16). Major modes in samples from Core H2 are generally in the medium silt to fine silt range, whereas Core H7 samples have their major modes in the very fine silt to coarse clay range. These results reveal a fining of sediments in a poleward direction. This poleward fining of sediments suggests that mainly medium-silt to fine-silt is deposited over a small area near the Orange River mouth and, that south of the river (e.g. Core H7), the sediment is mainly fine-silt to clay. The polymodal sediments from the study area are generally indicative of some mixing with sediment of a different type. This further suggests that the Orange River is not the only source of sediment deposited on the mudbelt, other sources such as bergwinds events make a significant contribution.

The fining-upward sequence in Cores H2, H5, H4, H6 and H7 is generally indicative of rising sea-level during the Holocene period.

Terrigenous components are dominant in the Orange Prodelta (H1, H2, and H3) whereas marine biogenic components are more abundant in the inner shelf (H4, H6 and H7). This observation indicates terrestrial influence of the perennial Orange River on the Orange Prodelta. The sediments near the river mouth are greatly diluted by terrestrially derived sediments. On the other hand, marine-biogenic components are comparatively higher in the inner shelf. This is apparently due to relatively low influx of terrigenous components and higher productivity at this region (H4, H6 and H7 are relatively closer to Namaqua Upwelling Cell (Figures 2.1 and 7.6). It is generally concluded that Namaqualand mudbelt sediments are more terrigenous near the Orange River mouth (Orange Delta) whereas south of Wreck Point (between Site H4), sediments are more marine. This further supports the contention that Namaqualand Mudbelt is not primarily derived from the Orange River.

Quartz appears to be more abundant southward from the Orange River mouth, and is its highest quantities are present in the Namaqualand shelf cores (Core H6, off Port Nolloth in particular). This quartz is considered to be from Quaternary coastal dunes that were eroded and partly redistributed in the littoral zone during the Flandrian transgression (Woodborne, 1991) (Figure 7.5). It appears as though Buffels River (Figure 1.2) had occupied a more southerly course across the shelf, entering the sea approximately 10-15km of its present position.

In addition, the occurrence of quartz and mica in the sediments is consistent with the semi-arid climate of onshore Namaqualand, where quartz and mica are entrained by adiabatic Berg winds (Shannon and Anderson, 1982; Whitaker, 1984) moving offshore from the micaceous metamorphic rocks of Namaqualand interior. Moreover, it is likely that mica is a dominant component of fine sand in the Orange River and other rivers contributing to it (e.g. Caledon River). It is suggested that this mica might also be emanating from the Upper Orange River catchment (including Lesotho), where many of the soils on sedimentary rocks are expected to be micaceous.

In General, terrigenous components are more abundant on the Orange Prodelta whereas marine-biogenic components (e.g. foraminifera, sponge spicules and diatoms) are more abundant South of Orange Delta (off Kleinsee). This distribution clearly reflects terrestrial influence of the Orange River on the Orange Prodelta. addition, the dominance of marine-biogenic sediments south of the Orange Delta suggests that the sediments at this site are more marine-influenced than those on the Orange Prodelta. The latter observation negates the earlier inferences that the Namaqualand mudbelt is primarily derived from the Orange River (Rogers, 1977; Dingle *et al.*, 1987; Rogers and Bremner, 1991).

8.4 Mineralogy and Geochemistry

(a) Mineralogy

The presence of mica as the major constituent of both clay minerals and coarse-fraction, and quartz (major constituent of coarse-fraction) in the study area supports

the classification of these sediments as terrigenous. However, the calcium-minerals (e.g. gypsum) and calcareous organisms (e.g. foraminifera) with their increasing concentration south of the Orange Prodelta, appear to be indicative of little deposition of terrigenous material occurring on the innershelf of Namaqualand (H4, H6 and H7).

(b) Geochemistry

The presence of silicon, aluminium, iron, titanium and manganese in high concentrations on the Orange River Prodelta (Core H2) closer to the Orange River mouth substantiates the classification of these sediments as terrigenous. Their abundance is comparatively lower on the innershelf (Core H7) where most of the sediments are dominantly of marine origin. Conversely, calcium concentrations are highest on the innershelf (Core H7) and decrease sharply northwards towards the Orange River. These high concentrations on the innershelf correspond to increased carbonate deposition in the form of foraminifera. This is generally indicative of calcium being derived from calcium carbonate of predominantly biogenic origin.

In conclusion, the review of sedimentological and geochemical information derived from the analyses of Namaqualand continental shelf sediments may be used as a key to understanding late Quaternary environmental dynamics of both terrestrial and marine environment. Such information can eventually contribute to the evidence for environmental change during the late Quaternary in the southern Africa.

In summary, the main conclusion of this research is that although the terrestrial influence of the Orange River is strongly presented by relatively high-coarse fraction

components at the Orange Prodelta (Sites H1, H2 and H3), the dominance of these coarse-fraction by marine-biogenic components at Sites H6 and H7 clearly indicates that the Namaqua part of the mudbelt has a strong marine influence and that it is not simply Orange River mud as previously indicated by Rogers, (1977) and Rogers and Bremner, (1991).

References

Almogi-Labin, A., Simon-Tov, R., Rosenfeld, A. and Debard, E. 1995: Occurrence and distribution of the foraminifera *Ammonia beccarri tepida* (Cushman) in water bodies, Recent and Quaternary, of the Dead Sea Rift, Israel. *Marine Micropaleontology,* 26, 153-159.

Andrews, P. B. 1974: Late Quaternary continental shelf sediments off Otago Peninsula, New Zealand. *New Zealand Journal of Geology and Geophisics* 16 (4): 793-830.

Anonymous, 1967: Methods of testing Soils for Civil Engineering purposes. *British Standards Institution,* London, BS 1377.

Axelsson, V. 1983: The use of X-ray radiographic methods in studying sedimentary properties and rates of sediment accumulation. *Hydrobiologia* 103, 65-69.

Bailey, G. W. 1979: *Physical and Chemical Aspects of the Benguela Current in the Luderitz Region.* Unpublished Msc thesis, Department of Oceanography, University of Cape Town. 224pp.

Beltagy, A. I., Chester, R. and Padgham, R. C. 1972: The particle-size distribution of quartz in some North Atlantic Deep-Sea sediments. *Marine Geology* 13; 297-310.

Birch, G. F. 1975: Sediments on the continental margin off the West Coast of South Africa. *Bulletin Geological Survey/University of Cape Town Marine Geoscience Unit* 6; 1-135.

Birch, G. F., Day, R. W. and Du Plessis, A. 1991: Nearshore Quaternary Sediments on the West Coast of Southern Africa. *Bulletin of the Geological Survey Unit* 101; 1-14.

Birch, G. F., Rogers J., Bremner, J. M. and Moir, G. 1976: Sedimentation controls on the continental margin of Southern Africa: *Proc. 1st Interdisciplinary conf. Marine and Freshwater Research, S. Afr. (Port Elizabeth),* Fiche 20A, S122, C1-C12.

Birch, G. F., Rogers, J. and Bremner, J. M. 1986: Texture and composition of surficial sediments of the continental margin of the republics of South Africa, Transkei and Ciskei. *Maps, Geological Survey of South Africa. Marine Geoscience Series* 3 (Sheets 1-4).

Biscaye, P. E., 1965: Mineralogy and sedimentation on Recent Deep-Sea clay in the Atlantic Ocean and adjacent seas and oceans. *Bulletin of the Geological Society of America*, 76, 803-832.

Boggs, S. Jr., 1995: *Principles of Sedimentology and Stratigraphy*. Merril Publishing.

Bremner, J. M., 1977: Sediments on the Continental Margin off South West Africa between latitudes 17° 25°S. PhD thesis, Geol. Dept. University of Cape Town, pp. 210.

Bremner, J. M., Rogers, J. and Willis J. P. 1990: Sedimentological aspects of the 1988 Orange River floods. *Transactions of the Royal Society of South Africa* 47: 247-294.

Bremner, J. M. and Willis, J. P. 1993: Mineralogy and geochemistry of the clay fraction of sediments from the Namibian continental margin and the adjacent hinterland. *Marine Geology,* 115: 85-116.

Briskin M. and Schreiber B. C. 1978: Authigenic gypsum in marine sediments. *Marine Geology,* 28, 37-49.

Bromley R. C., 1990: *Trace Fossils: Biology and Taphonomy*. Unwin Hyman, London.

Brownlow, A. H. 1996: *Geochemistry* 2n edition. Prentice Hall, New Jersey.

Buhmann, C. 1994: Parent material and Pedogenic Processes in South Africa. *Clay minerals* 29, 239-246.

Cadee, G. C. 1979: Sediment Reworking by the Polychaete *Heteromastus Filiformis* on a tidal flat in the Dutch Wadden Sea. *Netherlands Journal of Sea Research,* 13 (3/4) 441-456.

Calvert, S. E. 1966: Accumulation of diatomaceous silica in the sediments of the Gulf of California. *Geol. Soc. Am. Bull.*, 77, 569-596.

Calvert, S. E. 1974: Deposition and diagenesis of silica in marine sediments. In: Pelagic sediments on land and under the sea, Ed. K. J. Hsu and H. C. Jenkyns, *Spec. Publ. Inst. Assoc. Sed. No. 1,* Blackwell Scientific Publication Ltd., Oxford, 273-199.

Calvert, S. E. and Price N. B. 1983: Geochemistry of Namibian Shelf Sediments. In, Coastal Upwelling: Its Sediment Record. Part B: Sedimentary Recods of Ancient Coastal Upwelling. Edited by J. Thiede and E. Suess, New York, pp. 337-375.

Carrington, A. J. and Kensley, B. F. 1969: Pleistocene molluscs from the Namaqualand Coast. *Annals of the South African Museum* 52 (9), 189-223.

Chang, S-K. and Yoon, H. I. 1995: Foraminiferal assemblages from bottom sediments at Marian Cove, South Shetland Islands, West Antartica. *Marine Micropaleontology* 26, 223-232.

Chapman, F. 1907: Report on Pleistocene Microzoa from a boring in the bed of the Buffalo River, East London. *Records Albany Mus.* 2 (1), 6-17.

Cohen, A. L., Parkington, J. E., Brundrit, G. B. and Van de Merwe, N. J. 1992: A Holocene Climate Record in mollusc shells from the Southwest African coast. *Quaternary Research* 38, 379-385.

Copenhagen, W. J. 1953: The periodic mortality of fish in the Walvis region. A phenomenon within the Benguela Current. *Invest!. Rep. Div. Sea Fish. S. Afr.* 14, 1-35.

Crawford, R. J. M., Siegrfried, W. R., Shannon L. V., Villacastin-Herrero, C. A., Underhill, L. G., 1990: Environmental influences on Marine Biota off Southern Africa. *South African Journal of Science* 86, 330-339.

De Decker, A. H. B. 1970: Notes on an oxygen-depleted subsurface current off the west coast of South Africa. *Invest!. Rept. Div. Fish. S. Afr.* 84, 1-24.

De Decker, R. H. 1987: The geological setting of diamondiferous deposits on the inner shelf between the Orange River and Wreck Point, Namaqualand, *Bulletin of the Geological Survey, South Africa* 86, 1-99.

De Villiers, J. and Sohnge, P. G. 1959: Geology of the Richtersveld. *Memoir Geological Survey South Africa* 48, 1-295.

Diester-Haass, L. 1975: Sedimentation and climate in the Late Quaternary between Senegal and the Cape Verde Islands. *"Meteor" Forsch.-Ergenisse, Reihe C,* 20: 1-32.

Diester-Haass, L. 1976: Late Quaternary Climatic Variations in Northwest Africa Deduced from East Atlantic Sediment Cores. *Quaternary Research* 6, 299-314.

Dingle, R. V. 1973a: The geology of the continental shelf between Luderitz and Cape Town (southwest Africa), with special reference to Tertiary strata. *Journal of the Geological Society of London*, 129, 337-363.

Dingle, R. V. 1973b: Regional distribution and thickness of Post-Paleozoic sediments on the continental margin of Southern Africa. *Geological Magazine* 110 (3), 97-102.

Dingle, R. V. 1973c: Preliminary stratigraphic classification of the Cainozoic succession on the South African continental shelf. *Transactions of the Royal Society of South Africa* 40 (5), 367-372.

Dingle, R.V., 1994: *First Cruise of HODSA Programme, SAS Protea, 11-18 May 1994.* Unpublished report.

Dingle, R. V. and Hendey, Q. B. 1984: Late Mesozoic and Tertiary sediment supply to the Eastern Cape Basin (SE Atlantic) and palaeo-drainage systems in Southwestern Africa. *Marine Geology* 56, 13-26.

Dingle, R. V., Birch, G. F., Bremner, J. M., De Decker, R. H., Du Plessis, A., Engelbrecht, J. C., Fincham, M. J., Fitton, I., Flemming, B. W., Gentle, R. I., Goodlad, S. W., Martin, A. K., Mills, E. G., Moir, G. J., Parker, R. J., Robson, S. H., Rogers, J., Salmon, D. A., Siesser, W. G., Simpson, E. S. W., Summerhayes C. P., Westall F., Winter A. and Woodborne M. W. 1987: Deep Sea sedimentary environments around Southern Africa. *Annals of the South African Museum* 98 (1), 1-27.

Dingle, R. V., Moir, G. J., Bremner, J. M. and Rogers, J. 1976: Bathymetry of the continental shelf off the Republic of South Africa and S.W.A.: *Map. Mar. Geosci. Ser. Geol. Surv. S. Afr.*, 1.

Dingle, R. V. and Nelson G. 1993: Sea-bottom Temperature, Salinity and Dissolved Oxygen on the Continental Margin off South-Western Africa. *South African vJournal of Marine Science* 13, 33-49.

Einsele, G., Chough, S. K. and Shiki, T. 1996: Depositional events and their records -an introduction. *Sedimentary Geology* 104, 1-9.

Embley, R. W. and Morley, J. J. 1980: Quaternary sedimentation and palaeoenvironmental studies off Namibia (South-West Africa) *Marine Geology* 36, 183-204.

Faas, R. W. 1991: Rheological Boundaries of mud: Where are the limits? *Geo-Marine Letters* 11, 143-146

Felhaber, T. A. 1984: *The Geochemistry and Sedimentology of Quaternary Shelf Sediments off the Tugela River, Natal, South Africa*. Unpublished Msc Thesis, Department of Geological Sciences, University of Cape Town. 237 pp.

Folk, R. L. 1974*: Petrology of Sedimentary Rocks*. Austin, Tex.: Hemphills.

Gary, M., McAfee, R. Jr. and Wolf, C. L., 1977: *Glossary of Geology*. American Geological Institute, Washington D.C. 805pp.

Geyh, M. A., Roeschmann, G., Wijmstra, T. A. and Middeldorp, A. A. 1983: The Unreliability of 14C dates obtained from buried Sandy podzols. *Radiocarbon* 25, 409-416.

Gibbs, R. J. 1965: Error due to segregation in quantitative clay mineral X-ray diffraction mounting technique. *Am. Miner. 50, 741-751.*

Gilet-Blein, N., Marien, G. and Evin, J. 1980: Unreliability of ^{14}C dates from organic matter of soils. *Radiocarbon* 22, 919-929.

Giraudeau, J. 1993: Planktonic foraminiferal assemblages in surface sediments from the Southwest African continental margin. *Marine Geology*, 110, 47-62.

Gray, C. E. D. 1996: *A Preliminary Palynological Investigation of the Namaqualand Deltaic Mudbelt.* Unpublished Bsc (Hons), Department of Environmental and Geographical Science, University of Cape Town. 71pp.

Griffin, J. J., Windom, H. and Goldberg E. D., 1968: The distribution of clay minerals in the world ocean. *Deep-Sea Res.*, Vol. 15, 433-459.

Haas, H., Holliday, V. T., and Stuckenrath, R., 1986: Dating of Holocene with soluble and insoluble organic fractions at the Lubbock Lake archaeological site, Texas: An ideal case study. *Radiocarbon* 28, 473-585.

Hart, T. J. and Currie, R. I. 1960: The Benguela Current. *Discovery Report, University of Cambridge,* 31, 123-298.

Hathaway, J. C., 1955: Studies of some vermiculite-type clay minerals, clays and clay minerals. *Nat. Acad. Sci., Publ.* 395, 74-86.

Herbert, R. 1984: *Planktonic Foraminifera in the nearshore sediments on the continental shelf off S.W.A. Their distribution and Reflection of Oceanography.* Unpublished Bsc (Hons) project, Geology Department, University of Cape Town, 42pp.

Herbert, R. S., Shackleton, L. Y., Thackeray, J. F. and Rogers, J. 1989: Diatomaceous oozes off Walvis Bay: collaborative research on climatic change. *South African Journal of Science* 85, 295-296.

Heydorn, A. E. F. and Tinley, K. L. 1980: Synopsis of the Cape Coast. Natural features, dynamics, and utilization. in Estuaries of the Cape. Part 1: *Res. Rep. Nat. Res. Inst. Oceanol. S. Afr. C.S.I.R., Stellenbosch*, 380: 1-96.

Hoyt, J. H., Oostdam, B. L. and Smith, D. D. 1969: Offshore sediments and valleys of the Orange River (South and South West Africa). *Marine Geology,* 7: 69-84.

Hoyt, J. H., Smith, D. D. and Oostdam, B. L. 1965: Sediment distribution on the inner continental shelf, west coast of southern Africa. *Bulletin of the American Association of Petrology Geology,* 49: 344-345.

Ingram R. L. 1965: Facies maps based on the microscopic examination of modern sediments. *Journal of Sedimentary Petrology,* 35, 619-625.

Jeans, C. V. 1986: Features of Mineral diagenesis in hydrocarbon reservoirs: an introduction. *Clay Minerals* 21, 429-444.

Johnson, L. J., 1964: Occurrence of regularly interstratified chlorite-vermiculite in a weathering product of chlorite in a soil. *Am. Mineral.*, 49. 556-572.

Johnson, L. R. 1979: Mineralogical dispersal patterns of North Atlantic Deep-Sea sediments with particular reference to aeolian dusts. *Marine Geology,* 29: 335-345.

Jury, M. 1981: Coastal winds and upwelling. *Transactions of the Royal Society of South Africa,* 44 (3): 299-302.

Kamstra, F. 1985: Environmental features of the Southern Benguela with special reference to wind stress in Shannon L. V. (Ed.) *South African Ocean Colour and upwelling Experiment.* Sea Fisheries Research Institute, Cape Town, pp. 13-27.

Kazantzev, V. P., 1934: Structure of vermiculite. *Mem. Soc. Russe Mineral.*, 63, 464-480.

Krumbein, W. C. and Pettijohn, F. J. 1938: *Manual of Sedimentary Petrography*. New York, Appleton-Century-Crofts, 549pp.

Leeder, M. R. 1982: *Sedimentology, Process and Product*. Unwin Hyman, London.

Leithold E. 1989: Depositional processes on an ancient and modern muddy shelf, Northern California. *Sedimentology*, 36, 179-202.

Lesueur, P. and Tastet, J. P. 1994: Facies, internal structures and sequences of modern Gironde-derived muds on the Aquitaine inner shelf, France. *Marine Geology*, 120, 267-290.

Lever, L. and McCave, I. N. 1983: Eolian components in Cretaceous and Tertiary North Atlantic sediments. *Journal of Sedimentary Petrology*, 53: 811-832.

Lewin, J. C. 1961: The dissolution of silica from diatom walls. *Geochim. Cosmochin. Acta.*, 21, 182-198.

Li, Q. and McGowran, B. 1994: Evolutionary morphological changes in the new genus *Duoforisa*: Implication for classification and habit of the unilocular foraminifera. *Alcheringa*, 18, 121-134.

Li, Q. and McGowran, B. 1995: Comments on some Southern Australian foraminifera and description of the new genus *Parredicta*. *Trans. R. Soc. S. Aust.* 119 (3) 99-112.

Li, Q., McGowran, B. and Boergma, A. 1995: Early Palaeocene *Parvularugoglobigerina* and Late Eocene *Praetenuitella*: does evolutionary convergence imply similar habitat? *Journal of Micropalaeontology*, 14, 119-134.

Li, Q., McGowran, B., James, N. P., and Bone Y. 1996a: Foraminiferal biofacies on the Mid-latitude Lincoln Shelf, South Australia: Oceanographic and Sedimentological implications. *Marine Geology*, 129, 285-312.

Li, Q., McGowran, B., James, N. P., and Bone Y. and Cann, J. H. 1996b: Mixed foraminiferal Biofacies on the Mesotrophic Mid-Latitude Lacepede Shelf, South Australia. *Palaios*, 11, 176-191.

Lindholm, R. 1981: *A Practical Approach to Sedimentology*. Allen and Unwin (Inc) Boston.

Mabote M. E. 1994: *Rainfall Simulation Experiments and the Impact of Rainfall on Soil Erosion under Different Conditions in the Southern Cape*. Unpublished Bsc (Hons) Project, Department of Environmental and Geographical Sciences, University of Cape Town, 54pp.

Mabote, M. E., Rogers J. and Meadows M. E. 1997: Sedimentology of terrigenous mud from the Orange River delta and the inner shelf off Namaqualand, South Africa. *South African Geographical Journal,* 79 (2), 108-114.

Martin, C. W. and Johnson W. C. 1995: Variation in Radiocarbon Ages of Soil Organic Matter Fractions from Late Quaternary Buried Soils. *Quaternary Research*, 43, 232-237.

McLachlan, A. J., 1995: *Fish population Dynamics assessed using Sediment Box Cores from the Southern Eastern Atlantic Ocean*. Unpublished Msc thesis, University of Natal, 90pp.

McMillan, I. K. 1987: *Late Quaternary Foraminifera from the Southern part of offshore South West Africa/Namibia*. Unpublished Phd thesis, University College of Wales, Aberytwyth, 481pp.

McMillan, I. K. 1993: Foraminifer biostratigraphy, sequence stratigraphy and interpreted chronostratigraphy of marine Quaternary sedimentation on the South African Continental Shelf. *South African Journal of Science*, 89, 83-89.

Meadows, M. E. 1995: Marine Sedimentary Record of Terrestrial Ecosystem during the Holocene Denudation of Southern Africa. Unpublished manuscript. University of Cape Town.

Meadows, M. E. Dingle, R. V., Rogers, J. and Mills, E.G. 1997: Radiocarbon chronology of Namaqualand Mudbelt sediments: Problems and Prospects *South African Journal of Science*, 93, 321-327.

Muerdter, D. R. and Kennett, J. P. 1984: Late Quaternary planktonic foraminiferal biostratigraphy, Strait of Sicily, Mediterranean Sea. *Marine Micropaleontology*, 8, 339-350.

Murray, L. G. 1969: Exploration and sampling methods employed in the offshore diamond industry: *Proc. 9th. Commonw. Miner. Metall. Congr. London*, 71-124.

Murray, L. G., Hoynt, R. H., O'Shea, D. O'C., Foster, R. W. and Kleinjan, L. 1970: The geological environment of some diamond deposits off the coast of S.W.A. In: Delany, F. (Ed.). *The geology of the East Atlantic Continental Margin. Rep. Inst. Geol. Sci.* 70 (16): 119-141.

Naidu, P. D. and Malmgren, B.A. 1995: Do benthic foraminifer records represent a productivity index in a minimum zone areas? An evaluation from the Oman Margin, Arabian Sea. *Marine Micropaleontology* 26, 49-55.

Nelson, G. 1989: Poleward motion in the Benguela area. In: Neshyba S. J., Mooers Ch. N. K., Smith R. L., and Barber R. T.(Eds.) *Poleward Flows Along Eastern Ocean Boundaries*. Springer-Verlag, New York. pp. 110-130.

Nelson, G., 1990: Shelf and eastern boundary current patterns between Cape Point and Walvis Bay. Poster, Oceans, 90. 7th Natl. *Oceanogr. Conf.* (San Lameer, S. Afr., June 25-29, 1990).

Nelson, G. and Hutchings, L. 1983: The Benguela Upwelling area: *Progress in Oceanography,* 12: 333-356.

Nicolayev, I. V., and Senin, Yu. M., 1972: Changes in the facies of authigenous silicates in sediments of the West African Shelf. *Oceanology* 12 (3), 378-386.

Nittrouer C.A. and Sternberg R. W. 1984: The formation of sedimentary strata in an allochthonous shelf environment: the Washington continental shelf. *Marine Geology* 42, 201-232.

Nittrouer C.A., Demaster DJ and Mckee B.A. 1984: Fine scale stratigraphy in proximal and distal deposits of sediment dispersal system in the East China Sea. *Marine Geology,* 61, 13-24.

Norrish, K. and Hutton, J. T. 1969: An accurate X-ray spectrographic method for the analysis of a wide range of geological samples. *Geochim. Cosmochim. Acta* 33, 432-453.

Novich, K. and Martin, R. T. 1983: Solvation methods for expandable layers. *Clays Clay Miner.* 31, 235-238.

O'Brien, J. J. 1983: The physical environment in coastal upwelling regions. *Progress in Oceanography,* 12: 1-221.

O'Shea, D. O'C. 1971: *An Outline of the Inshore Submarine Geology of Southern S.W.A. and Namaqualand.* Unpublished Msc thesis, Department of Geological Sciences, University of Cape Town. 95pp.

Perrin, R. M. S., Willis, E. H. and Hodge, D. A. H. 1964: Dating of humus podzols by residual Radiocarbon activity. *Nature*, 202, 165-166.

Petersen N. D. 1983: *Vibrocore study of sediments on the inner and middle continental shelf between the Orange River and Chamais Bay - South West Africa.* Unpublished B.Sc. Honours project, University of Cape Town. 36pp.

Pether, J. 1983: *The Lithostratigraphy of HondeklipBaai - A Reconnaissance.* Bsc Hons Project, Department of Geological Sciences, University of Cape Town. 77pp.

Pether, J., 1994: *The Sedimentology, Paleontology and Stratigraphy of Coastal-Plain Deposits at Hondeklip Bay, Namaqualand, South Africa.* Unpublished Msc thesis, Department of Geological Sciences, University of Cape Town. 313pp.

Pokras, E. M. and Mix, A. C. 1985: Eolian evidence for spatial variability of Late Quaternary climates in Tropical Africa. *Quaternary Research,* 24: 134-149.

Pollock, D. E. and Beyers, C. J. 1981: Environment, distribution and growth rates of the west rock lobster *Jasus lalandii* (H. Milne Edwards). *Transactions of the Royal Society of South Africa,* 44 (3): 379-400.

Rhoads D. C., 1974: Organism-sediment relations on the muddy seafloor. *Annual Review of Marine Biology,* 12, 263-300.

Robson, S. 1981: *A study of the Radiolaria in the Surficial sediments on the northern part of the continental margin of Namibia*. Unpublished Bsc (Hons) project, Geology Department, University of Cape Town, 87pp.

Robson, S. 1983: The distribution of Recent Radiolaria in surficial sediments of the continental margin off northern Namibia. *Journal of Micropalaeontology* 2, 31-38.

Rogers, J. 1975: Sediment flow along the coastal zone of Namaqualand and the Southern Namib. *Technical Report Joint Geological Survey/University of Cape Town, 7*: 35-36.

Rogers, J. 1977: *Sedimentation on the Continental Margin off the Orange River and the Namib Desert*. Unpublished PhD thesis, Department of Geological Sciences, University of Cape Town.

Rogers, J. and Bremner, J. M. 1991: The Benguela Ecosystem. Part V11. Marine-Geological Aspects. *Oceanography and Marine Biology. An Annual Review*, 29: 1-85.

Scharpenseel, H. W. and Becker-Heidmann, P. 1991: 25 years of radiocarbon dating soils: a paradigm of erring and learning. *Radiocarbon* 33, 238.

Schulze, B. R. 1965: Climate of South Africa, Part 8. General Survey. *Weather Bureau, Department of Transport, South Africa*, WB 28: 1-330.

Shannon L. V. and Anderson F. P. 1982: Applications of Satellite Ocean colour imagery in the study of the Benguela Current System. *The South African Journal of Photogrammetry, Remote Sensing and Cartography*. 13, 153-169.

Shannon L. V., Boyd, A. J., Brundrit, G. B. and Taunton-Clark, J. 1986: On the existence of El Nino-type phenomenon in the Benguela System. *Journal of Marine Research*, 44, 495-520.

Shannon, L. V. 1985: The Benguela Ecosystem, Part 1. Evolution of the Benguela, physical features and processes: *Oceanography and Marine Biology. An Annual Review*, 23: 105-182.

Siegrfried, W. R., Crawford, R. J. M., Shannon, L. N., Pollock, D. E., Payne, A. I. L., and Krohn, R. G., 1990. Scenarios for global-warming induced change in the open-shelf environment and selected fisheries of the west coast of Southern Africa. *South Africa Journal of Science*, 86, 281-285.

Siesser, W. G. and Dingle, R. V. 1981: Tertiary sea-level movements around Southern Africa. *Journal of Geology,* 89: 83-96.

Siesser, W. G. and Rogers, J., 1976: Authigenic pyrite and gypsum in South West African Continental slope sediments. *Sedimentology,* 23: 567-577.

Steeman-Nielsen, E. and Jensen, E. A. 1957: Primary Oceanic Production. *Galathea Rep. Sci. Res. Dan. Deep-sea Exped. 1950-1952,* Vol. 1, 49-136.

Stevens, R. L. 1977: Triangle Plots and Textural Nomenclature for Muddy Sediments. *Geo-Marine Letters* 11 (3/4), 166-169.

Taljaard, J. J. and Schumann, T. G. W. 1940: Upper air temperatures and humidities at Walvis Bay, South West Africa. *Bulletin of the American Meteorological Society,* 21: 293-296.

Taljaard, J. J., Schmidt, W. and Van Loon, H. 1961: Frontal analysis in the application to the Southern Hemisphere: *Notos (Weather Bureau) South African Department of Transport,* 10: 25-58.

Tankard, A. J. and Rogers, J. 1978: Late Cenozoic palaeoenvironments on the west coast of Southern Africa. *Journal of Biogeography,* 5: 319-337.

Van der Merwe, C. R., and Heysteck, H., 1955: Clay minerals of South African Soil Groups: 11. Sub-tropical black clays and related soils. *Soil Science,* 79, 147-148.

Verfaille, E. J. J. 1987: *The Textural Characterization of Terrigenous Muds in various Marine Environments around Southern Africa.* Unpublished Bsc Hons project, Department of Geological Sciences, University of Cape Town. 20pp.

Vilela, G. C. 1995: Ecology of Quaternary benthic foraminiferal assemblages on the Amazon Shelf, Northern Brazil. *Geo-Marine Letters,* 15, 199-203.

Wagner, P. A. and Merensky, H. 1928: The diamond deposits on the coast of Little Namaqualand. *Transactions of the Geological Society of South Africa,* 31: 1-41.

Wang, Y., Amundson, R. and Trumbore S. *1996:* Radiocarbon Dating of Soil Organic Matter. *Quaternary Research,* 45, 282-288.

Wellington, J. H. 1933: The middle course of the Orange River. *South African Journal of Geography,* 16: 58-68.

Wellington, J. H. 1955: *Southern Africa, A geographical study.* Cambridge University press. Cambridge.

Whitaker A. 1984: *Dust Transport by Berg winds off the coast of South West Africa: direction, sources and flux to marine sediments.* Unpublished B.Sc Honours project, University of Cape Town. 31pp.

Willis, J. P. 1996: Instrumental Parameters and Data Quality for routine major and trace Elements Determinations by WDXRFS. Unpublished Information

Circular No. 14, Department of Geological Sciences, University of Cape Town.

Woodborne, M. W. 1991: The geology of the diamondiferous inner shelf off Namaqualand between Stompneus Bay and White Point, just north of the Buffels River. *Bulletin Geological Survey, South Africa,* 99: 1-68.

Wright, J. A. 1964: Gully pattern and development in wave-cut bedrock shelves north of the Orange River Mouth, South West Africa: *Trans. geol. soc. S. Africa,* 67, 163-171.

Circular No. 14, Department of Geological Sciences, University of Cape Town.

Woodborne, M. W. 1991: The geology of the diamondiferous inner shelf off Namaqualand between Stompneus Bay and White Point, just north of the Buffels River. *Bulletin Geological Survey, South Africa,* 99: 1-68.

Wright, J. A. 1964: Gully pattern and development in wave-cut bedrock shelves north of the Orange River Mouth, South West Africa: *Trans. geol. soc. S. Africa*, 67, 163-171.

APPENDIX A

COLOUR PHOTOGRAPHS OF UNDISTURBED SEDIMENT STRUCTURES

CORE H2

16° 21.298'

570 ± 35

Soft brown mud

1500 ± 45

Soft olive brown clay

6

dark laminated clays

5

White layer

White layer

4

gas

3

White layer

1350 ± 40

gas

2

White layers

dark laminated clays

White layers

1

1630 ± 40

Olive brown clay homogeneous

1290 ± 40

gas

The "White layer" near top of Section 3 (≃ 300 cm)

"Sp." Samples

"stiff"

"mottled"

1030 ± 35

mottled

CC

? mottled

CE

990 ± 40

Bioturbated Compact Olive muds / Laminated muds (≃ 460 cm)

CORE H3

28° 51·2667'
16° 21·8667'
104m.

Soft olive/brown clay

"Top"

mottled light/dk brown clay

laminated brown – dark grey clay – light brown – black & laminae

white layer

black layer

enlargement top of section 2.

plant stems

Plant stems horizon

black layer

white layer

black layer

black layer

Contains lenses of "coarser" (?) brown clay

viscous dark grey clay

CORE H5

28° 57.2583'
16° 28.7183'

118m.

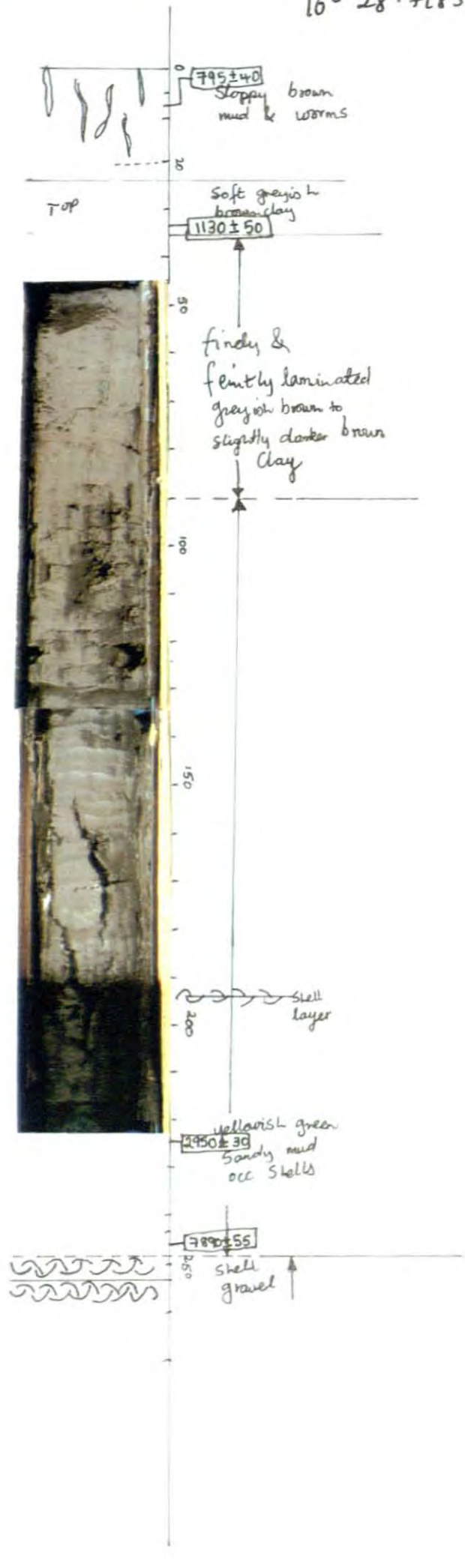

CORE H6

29° 16·0333'
16° 50·3800'
78m

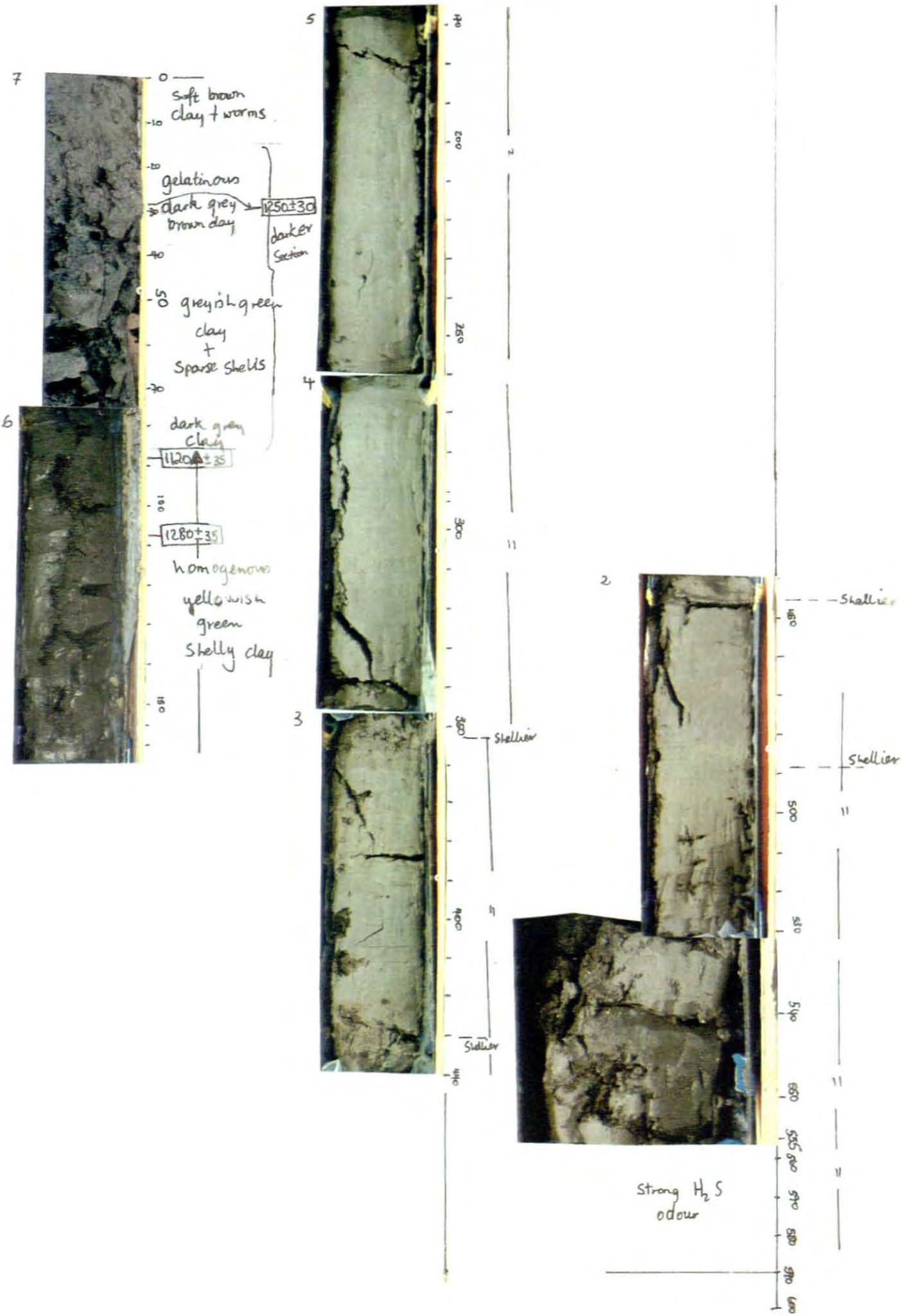

CORE H7

~~29° 42.122'~~
~~17° 00.691'~~
~~30° 40.08'~~
~~17° 23.829'~~

Depth. ~~150m.~~ 80m.

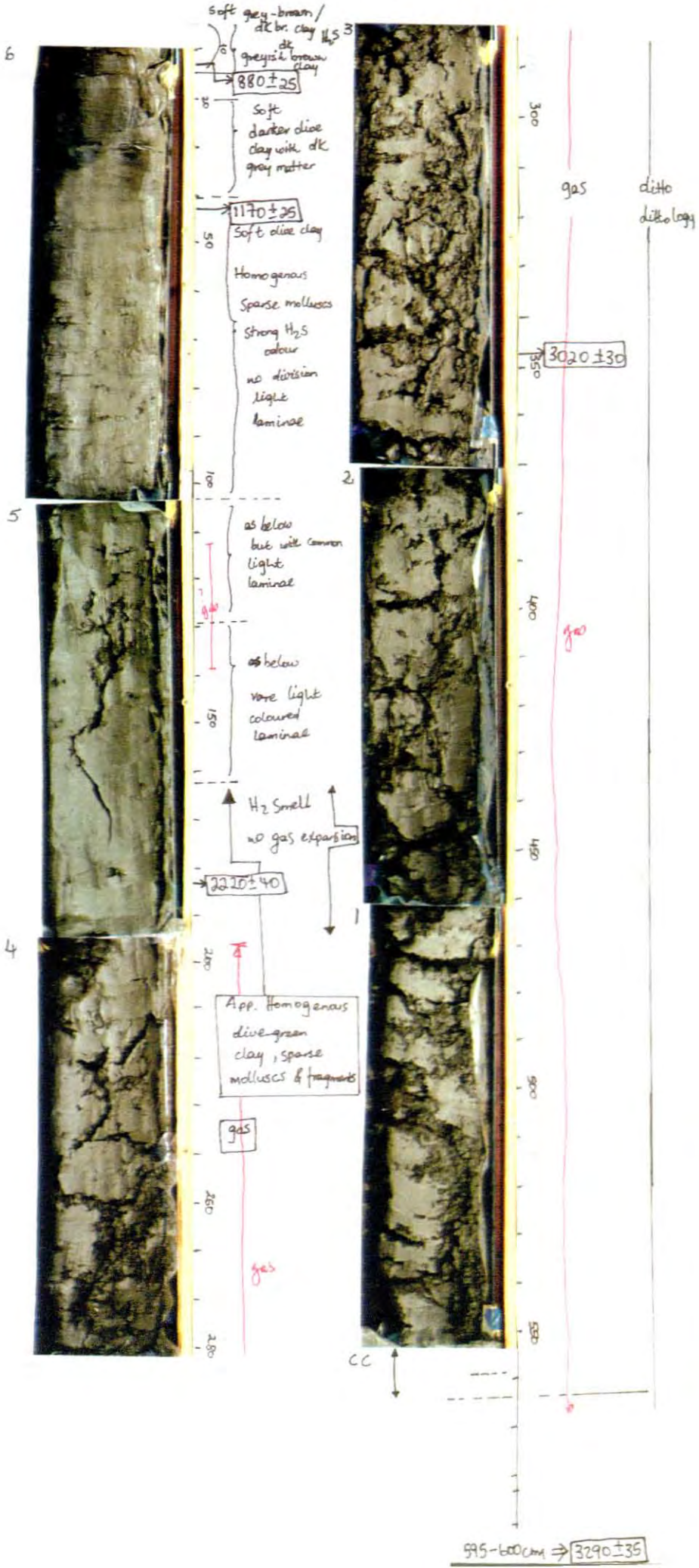

detail of top of Section 6

APPENDIX B: Lithology of cores

Site H1

0-4cm (4cm)	Soft brown mud
4-59cm (55cm)	Stiff, dark olive to dark greyish brown clay
55->60cm (>5cm)	Stiff, olive-brown clay

Site H2

0-4cm (4cm)	Soft, brown mud
4-20cm (16cm)	Soft, Olive-brown clay
20-470cm (450cm)	Dark, brown-olive, light brown, black and dark grey, laminated clays, generally stiff below c80cm. Lamination is at two scales: coarse (1-2cm) superimposed on fine (1-2mm). Boundaries between the coarse laminae are generally diffuse, while the fine laminae are generally laterally impersistent, producing streaks with elongated blebs. Particularly prominent, wide, whitish laminae occur at c130, 150, 300 (the most prominent) 410 and 450cm. Gas-charged layers occur at 200-270 and 310-365cm

Site H3

0-20cm (20cm)	Soft, Olive-brown clay
20-30cm (10cm)	Soft, mottled, light-dark clay
30-522cm (492)	Dark brown-olive, light brown, black and dark grey, laminated clays, soft above c80cm, stiffer below. Lamination is at two scales, (1-2cm) superimposed on fine (1-2mm). Boundaries between the coarse laminae are generally diffuse, while the fine laminae are generally laterally impersistent, producing streaks and elongate blebs. Particularly prominent, wide, whitish laminae occur at c75 and 345cm, and black laminae at 110, 382 and 502cm. A thin horizon with plant remains (grass or fine twigs) occurs at 287cm.
522-540cm (18cm)	Laminations similar to above but with lenses or coarser brown clay
540->576cm (>36 cm)	Viscous, dark grey clay with no laminae

Site H4

0-8cm (8cm)	Soft, olive-brown clay with live marine Gastropoda
8-108cm (100cm)	Soft, light yellowish-green clay. Very soft at top
108->540cm (>432cm)	Light yellowish-green clay with feint colour variations and subtle laminations. Occasional shells, appears also to be foram-rich

Site H5

0-22cm (22cm)	Sloppy, light brown mud with worm tubes
22-35cm (13cm)	Soft, greyish-brown clay

35-90cm (55cm)	Greyish-brown to slightly darker brown, feintly-laminated clay
90-248 (158cm)	Yellowish-green sandy mud, with sparse molluscan shell fragments. Largely homogeneous, with thin (2-3cm) shelly layer at 194cm

Site H6

0-15cm (15cm)	Soft, light-brown mottled clay with worm tubes and sparse shells
15-38cm (23cm)	Dark grey-brown, gelatinous clay, feintly laminated
38-75cm (37cm)	Greenish-gray clay with sparse shells
75-85cm (10cm)	Dark grey clay
85->590cm (>505cm)	Yellowish-green clay with scattered shells. Mainly homogenous with rare shelly layers at 352, 430, 445 and 490cm. H_2S apparent

Site H7

0-4cm (4cm)	Very soft, grey-brown/dark brown clay. H_2S odour
4-20cm (16cm)	Soft, greyish dark brown clay. H_2S odour
20-40cm (20cm)	Soft, dark olive clay with dark grey feint laminations
40-103cm (63cm)	Soft, olive clay. Homogeneous with sparse molluscs. Strong odour
103-162cm (59cm)	Olive-green clay, sparse molluscs and shell fragments, strong H_2S odour. Feint, light-coloured laminae. Gas expansion structures at 130-140cm
162->565cm (302cm)	Olive-green clay, sparse molluscs and shell fragments, H_2S odour. Apparently homogeneous. Strongly developed gas expansion structures at 197->465cm.

APPENDIX C -Storage, dialysis and grain size analyses of sediments.

After being subsampled at 5 cm onboard, the sediments were stored in air-tight containers in an unfrozen state. These sediments were subsampled again in the laboratory, with a plastic tube to obtain a vertical core through the samples. The subsamples , each consisting of approximately 50g of wet sediment, were placed directly into 400 mm lengths of cellophane tubing and hung, 20 at a time, in plastic buckets rigged with cord across their tops. All subsamples were dialysed in a running tap water for 24 hours to remove interstitial water and salts. Birch (1975) has shown that this dialysis method will effectively extract the interstitial water and salts from samples without stripping the sediment of exchangeable cations.

Size Analysis

Dialysed samples were then wet-sieved through 63μm and 2 mm screens to separate gravel and sand fractions from silt and clay (mud). The silt and clay proportions were determined using Pipette method (Anonymous, 1967; Rogers, 1971). The Pipette method is based on determining the density of a dispersed suspension at a fixed depth as a function of time (Krumbein and Pettijohn, 1938). A suspension in a 1000 ml glass measuring cylinder is thoroughly stirred with a plastic stirrer and then left to stand. Particles will then start settling and those with a particular settling velocity will settle below particular plane in the cylinder column. A calibrated Pipette is then used to pipette from specific depth in the cylinder column at a set time intervals. Only a particular size-range will be sampled as those with higher settling velocities will have settled beyond the chosen depth (Verfaille, 1987). The smaller the size to be measured, the longer the time to wait before taking samples, as the finer material takes a long time to settle (e.g. measuring size-range finer than 1μm (10 phi) would take more than 16 hours! (Krumbein and Pettijohn, 1938). The actual mass of the subsample is then determined by drying and weighing. A Pipette factor is then used to calculate how much sediment finer than the size represented by the selected depth remains in suspension. The mass of each sample can then be calculated by subtraction and expressed as a percent of the total mass of the sediment.

Sedigraph Analysis

A detailed size analysis of fine sediments (silt and clay) were made on selected samples from both cores H2 and H7, using the Sedigraph particle analyser. Just like Pipette method, the Sedigraph Particle Analyser measures the sedimentation rates of particles in suspension, however, it is relatively faster and allows a detailed analyses of finer particles. This technique is described in detail in Verfaille (1987) and will not be discussed here.

Texture and component analyses (coarse fractions)

Coarse fractions was separated into Gravel and sand fractions by dry-sieving through 2 mm screens. The actual mass of each fraction was then determined by drying and weighing. By subtraction, the mass of each fraction was calculated and then expressed as percentage of the total weight of sediment.

APPENDIX D :- H2 CLAY MINERALS PROPORTIONS (%)

Sample No.	Depth (m)	smectite	vermiculite	chlorite	mica	kaolinite	quartz	plagioglase	felspars
H2.7.4	0.0	22	20	12	35	8	3	0	0
H2.7.2	0.1	25	22	8	31	9	4	1	0
H2.7.1B	0.2	31	18	6	31	10	4	0	0
H2.7.1A	0.2	30	17	4	33	10	4	1	0
H2.6.12	0.2	24	18	9	35	8	4	1	1
H2.6.10	0.3	25	14	10	36	9	5	2	0
H2.6.8	0.4	21	24	8	32	8	4	2	0
H2.6.6	0.5	19	22	8	36	9	4	3	0
H2.6.4	0.6	30	12	8	37	9	4	0	0
H2.6.3	0.6	25	16	8	37	9	4	0	0
H2.5.20	0.8	13	25	8	36	8	4	4	1
H2.5.18	0.9	23	16	10	35	8	4	4	0
H2.5.16	1.0	18	24	8	33	9	4	4	0
H2.5.14	1.1	23	20	8	33	9	3	3	0
H2.5.12	1.2	30	14	9	33	8	4	2	1
H2.5.10	1.3	26	16	10	38	7	4	0	0
H2.5.8	1.4	22	22	8	34	8	4	3	0
H2.5.6	1.5	33	6	8	40	9	4	0	0
H2.5.4	1.6	20	21	8	34	7	4	6	0
H2.5.2	1.7	34	10	9	30	7	5	5	1
H2.4.20	1.8	28	12	10	35	8	4	3	0
H2.4.18	1.9	30	13	8	31	9	4	5	0
H2.4.16	2.0	24	19	7	32	8	4	5	0
H2.4.14	2.1	29	13	6	33	8	6	5	0
H2.4.12	2.2	23	21	6	32	9	5	3	0
H2.4.10	2.3	28	16	6	30	9	5	5	1
H2.4.8	2.4	19	26	8	32	8	5	2	0
H2.4.6	2.5	19	25	9	34	9	5	0	0
H2.4.4	2.6	24	16	10	35	7	4	3	2
H2.4.2	2.7	30	15	8	34	8	5	0	0
H2.3.20	2.8	19	20	9	33	10	4	4	2
H2.3.18	2.9	25	18	8	34	9	5	0.6	0.4
H2.3.16	3.0	23	14	10	33	8	5	6	2
H2.3.14	3.1	16	26	8	31	8	5	4	2
H2.3.12	3.2	21	25	6	30	9	4	2	3
H2.3.10	3.3	29	18	6	29	8	5	3	2
H2.3.8	3.4	22	19	6	35	8	4	4	1
H2.3.6	3.5	18	23	7	35	9	5	4	0
H2.3.4	3.6	28	18	8	33	9	4	0	0
H2.3.2	3.7	20	21	8	34	7	4	4	1
H2.2.20	3.8	33	14	6	32	9	4	1	1
H2.2.18	3.9	19	24	10	32	7	4	3	1
H2.2.16	4.0	22	21	8	37	8	4	1.6	0.4
H2.2.14	4.1	27	21	8	30	7	4	1	1
H2.2.12	4.2	15	26	6	39	8	4	2	1
H2.2.8	4.3	19	26	6	33	8	4	3	1
H2.2.10	4.4	18	25	6	33	8	4	5	0
H2.2.6	4.5	29	15	9	35	7	3	2	1
H2.2.4	4.6	27	13	8	39	7	4	2	1
H2.2.2	4.7	23	22	6	32	9	4	2	2
H2.1.20	4.8	22	14	14	31	11	5	3	0
H2.1.18	4.9	31	14	9	34	6	4	2	1
H2.1.16	5.0	24	18	10	34	7	4	1	1
H2.1.14	5.1	27	13	8	35	7	4	2	3
H2.1.12	5.2	18	19	8	33	9	4	4	4
H2.1.10	5.3	25	15	8	33	7	4	4	4
H2.1.8	5.4	28	16	10	34	8	4	0	5
H2.1.6	5.5	25	14	9	34	7	3	3	4
H2.1.4	5.6	30	14	9	30	8	4	4	0
H2.1.2	5.7	19	16	10	41	8	4	3	0
H2.SP4	5.8	28	20	10	29	6	4	3	0
H2.CC2	5.9	28	22	8	27	6	4	3	1
AVERAGE		24.29	18.34	8.18	33.6	8.15	4.18	2.55	0.85

APPENDIX E:- CORE H7 CLAY MINERALS PROPORTIONS (%)

Sample No.	Depth (m)	smectite	vermiculite	chlorite	mica	kaolinite	quartz	plagioclase	felspars
H7.G2	0.0	27	4	4	30	11	12	11	1
H7.6.20	0.1	24	7	5	32	13	8	10	0
H7.6.18	0.1	26	1	5	36	16	7	9	0
H7.6.16	0.2	15	4	2	39	26	5	6	3
H7.6.14	0.3	21	7	7	34	14	7	10	0
H7.6.12	0.4	23	5	7	36	15	5	9	0
H7.6.10	0.5	28	5	7	32	13	8	8	0
H7.6.8	0.6	25	7	8	35	16	5	4	0
H7.6.6	0.7	36	0	10	31	14	4	4	0
H7.6.4	0.8	28	2	10	34	15	5	6	0
H7.6.2	0.9	26	1	11	28	10	11	13	0
H7.5.20	1.0	26	7	6	36	16	4	4	0
H7.5.18	1.1	19	10	8	35	17	5	7	0
H7.5.16	1.2	18	7	12	36	16	5	7	0
H7.5.14	1.3	22	1	8	38	15	6	10	0
H7.5.12	1.4	14	12	11	34	17	6	5	0
H7.5.10	1.5	19	10	9	35	14	6	8	0
H7.5.8	1.6	23	3	11	33	16	6	8	0
H7.5.6	1.7	19	0	9	39	15	8	10	0
H7.5.4	1.8	20	7	10	36	15	5	7	0
H7.5.2	1.9	17	8	12	35	16	4	7	1
H7.4.20	2.0	29	2	6	38	16	5	4	0
H7.4.18	2.1	20	4	13	36	17	5	5	0
H7.4.16	2.2	29	3	7	33	13	6	9	0
H7.4.14	2.3	27	0	11	36	15	5	7	0
H7.4.12	2.4	29	3	8	34	14	5	7	0
H7.4.10	2.5	33	0	6	33	12	6	10	0
H7.4.8	2.6	21	12	8	31	16	5	6	0
H7.4.6	2.7	32	6	4	33	15	4	7	0
H7.4.4	2.8	31	3	6	32	11	6	9	2
H7.4.2	2.9	31	0	5	33	12	7	12	0
H7.3.20	3.0	33	2	7	34	15	5	4	0
H7.3.18	3.1	29	4	6	35	14	5	7	0
H7.3.16	3.2	17	2	10	37	19	5	6	3
H7.3.14	3.3	31	0	10	34	14	6	5	0
H7.3.12	3.4	28	2	10	32	15	7	6	0
H7.3.10	3.5	28	3	9	35	14	6	5	0
H7.3.8	3.6	29	7	7	32	14	5	6	0
H7.3.6	3.7	24	10	9	33	13	5	5	0
H7.3.4	3.8	16	12	10	35	15	6	6	0
H7.3.2	3.9	25	10	11	32	14	4	4	0
H7.2.20B	4.0	19	10	8	33	14	5	9	1
H7.2.18	4.1	25	7	7	32	15	7	7	0
H7.2.16	4.2	20	10	9	28	16	3	13	0
H7.2.14	4.3	26	9	6	24	9	10	15	0
H7.2.12	4.4	27	9	10	33	14	4	3	0
H7.2.10	4.5	23	8	8	34	17	4	4	2
H7.2.8	4.6	24	10	8	21	13	8	16	0
H7.2.6	4.7	25	8	8	32	13	6	6	1
H7.2.4	4.8	27	8	9	32	15	4	3	2
H7.2.2	4.9	25	10	10	34	13	5	3	0
H7.1.20B	5.0	28	6	6	33	17	5	5	0
H7.1.18	5.1	28	8	6	34	15	4	4	0
H7.1.16	5.2	26	7	6	36	17	4	4	0
H7.1.14	5.3	12	12	4	41	22	3	3	2
H7.1.12	5.4	23	10	6	30	13	8	10	0
H7.1.10	5.5	25	12	6	30	11	7	9	0
H7.1.8	5.6	23	10	6	27	10	9	13	1
H7.1.6	5.7	10	9	10	34	16	9	12	0
H7.1.4	5.8	35	8	5	27	10	8	8	0
H7.1.2	5.9	24	10	5	28	10	9	13	0
Average	**2.90**	**24.48**	**6.13**	**7.84**	**33.20**	**14.56**	**5.93**	**7.43**	**0.31**

APPENDIX F

XRF PROCEDURES FOR MAJOR & TRACE ELEMENTS (From Willis, 1996)

MAJOR ELEMENTS

Nine major elements, Fe, Mn, Ti, Ca, K, P, Si, Al and Mg (with Ni and Cr when Ni and Cr concentrations exceed ~2000 ppm or 0.2 %) are determined using fusion disks prepared according to the method of Norrish and Hutton (1969). The disks are analyzed on a Philips PW1480 wavelength dispersive XRF spectrometer with a dual target Mo/Sc x-ray tube. Fe, Mn and Ti are measured with the tube at 100 kV, 25 mA. The other elements are determined with the tube at 40 kV, 65 mA. Peak only measurements are made on the elements Fe through Mg. Sodium is determined using powder briquettes, the x-ray tube at 40 kV, 65 mA, and with backgrounds measured at -2.00 and $+2.00°2\theta$ from the peak position. Analytical conditions are given in Table 1.

Fusion disks made up with 100% Johnson Matthey Specpure SiO_2 are used as blanks for all elements except Si. Fusion disks made up from mixtures of Johnson Matthey Specpure Fe_2O_3 and $CaCO_3$ are used as blanks for Si. Intensity data are collected using the Philips X40 software. Matrix corrections are made on the elements Fe through Mg using the de Jongh model in the X40 software. Theoretical alpha coefficients used in the de Jongh model for all other elements on the analyte element are calculated using the Philips on-line ALPHAS programme. Na_2O is not included in the matrix corrections in de Jongh model, and no matrix corrections are made to the sodium intensities.

Table 1. Analytical conditions for determination of major elements using a Philips PW1480 WDXRF spectrometer.

Element/line	Collimator	Crystal	Detector	PHS LWL	PHS UPL	Counting time (s)	Concentration range *	RMS	No. of standards
FeKα	F	LiF(220)	FL	16	70	150	0 - 17	0.118	14
MnKα	F	LiF(220)	FL	15	70	150	0 - 0.22	0.005	14
TiKα	F	LiF(200)	FL	28	70	150	0 - 2.75	0.020	14
CaKα	F	LiF(200)	FL	36	70	20	0 - 12.5	0.037	14
K Kα	F	LiF(200)	FL	36	70	50	0 - 15.5	0.057	14
P Kα	C	GE(111)	FL	25	75	100	0 - 0.36	0.008	14
SiKα	C	PE(002)	FL	32	74	100	0 - 100	0.408	14
AlKα	C	PE(002)	FL	25	75	80	0 - 17.5	0.136	14
MgKα	F	PX-1	FL	30	74	150	0 - 46	0.095	14
NaKα	F	PX-1	FL	30	78	200	0 - 9	0.189	15

* = all concentrations expressed as wt% oxide

$$RMS = \sqrt{\frac{1}{n-k}\sum\left(Conc_{given} - Conc_{calc}\right)}$$

where

n = no. of standards

k = no. of calibration coefficients, *i.e.* 2, the slope and intercept of the calibration line.

$Conc_{given}$ = recommended concentration for an element in a standard

$Conc_{calc}$ = concentration of an element calculated from the best-fit calibration line

First order calibration lines, with intercept, are calculated using all data points, including blanks. Calibration plots for Fe_2O_3, CaO, SiO_2 and MgO are given in Figures 1 - 4.

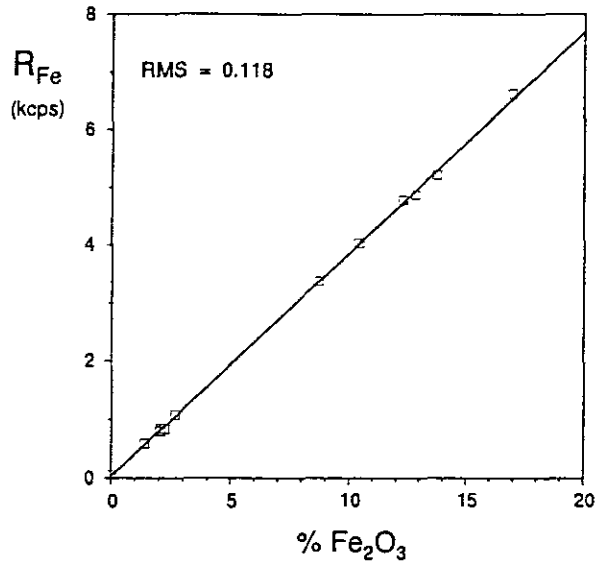

Figure 2. Calibration plot for Fe_2O_3 using "Norrish" fusion disks.

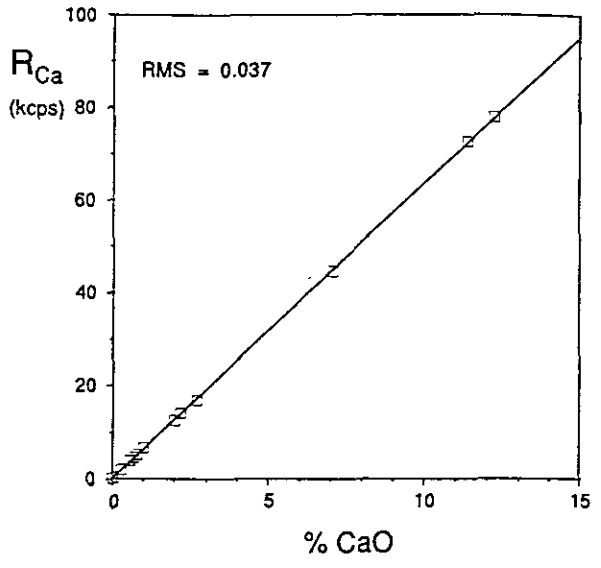

Figure 3. Calibration plot for CaO using "Norrish" fusion disks.

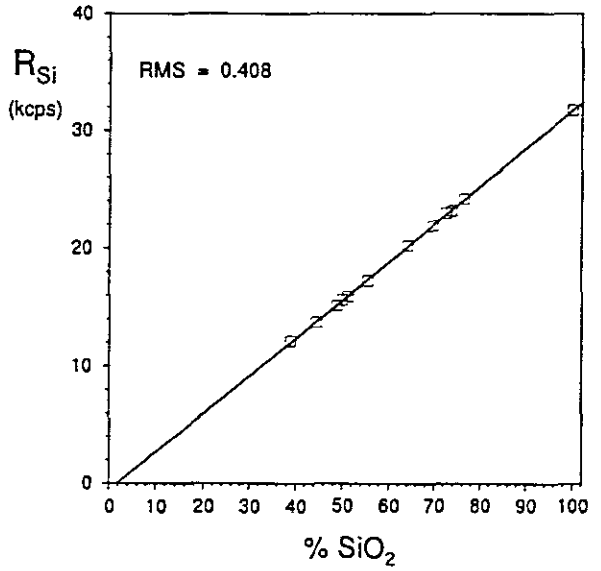

Figure 4. Calibration plot for SiO_2 using "Norrish" fusion disks.

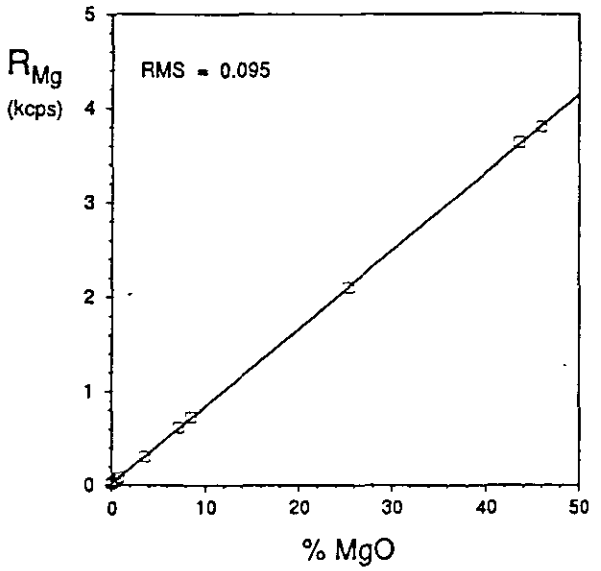

Figure 5. Calibration plot for MgO using "Norrish" fusion disks.

TRACE ELEMENTS

Trace elements are determined on powder briquettes in a series of analytical runs using a number of different x-ray tubes. Analytical conditions are listed in Tables 2 and 3.

Table 2. X-ray tubes and tube and x-ray path settings for the determination of trace elements using a Philips PW1480 WDXRF spectrometer.

Element/line	X-ray tube		X-ray path
	Target	kV - mA	
RhKαC	Rh	80 35	Vacuum
MoKαC	Mo/Sc	90 30	Vacuum
MoKα	Rh	80 35	Vacuum
NbKα	Rh	80 35	Vacuum
ZrKα	Rh	80 35	Vacuum
Y Kα	Rh	80 35	Vacuum
SrKα	Rh	80 35	Vacuum
U $L\alpha_1$	Rh	80 35	Vacuum
RbKα	Rh	80 35	Vacuum
Th $L\alpha_1$	Rh	80 35	Vacuum
Pb $L\beta_1$	Rh	80 35	Vacuum
SeKα	Mo/Sc	90 30	Vacuum
Bi $L\alpha_1$	Mo/Sc	90 30	Vacuum
AsKα	Mo/Sc	90 30	Vacuum
GaKa	Mo/Sc	90 30	Vacuum
W $L\alpha_1$	Mo/Sc	90 30	Vacuum
ZnKα	Au	60 45	Vacuum
CuKα	Au	60 45	Vacuum
NiKα	Au	60 45	Vacuum
CoKα	Au	50 55	Vacuum
MnKα	Au	50 55	Vacuum
CrKα	Au	50 55	Vacuum
V Kα	Au	50 55	Vacuum
La $L\alpha_1$	Au	50 55	Vacuum
Ce $L\beta_1$	Au	50 55	Vacuum
Nd $L\alpha_1$	Au	50 55	Vacuum
Ba $L\alpha_1$	Cr	50 55	Vacuum
ScKα	Cr	50 55	Vacuum
S Kα	Mo/Sc	40 65	Vacuum
F Kα	Mo/Sc	40 70	Vacuum

Table 3. **Instrumental conditions for determination of trace elements using a Philips PW1480 WDXRF spectrometer.**

Element /line	Collimator	Crystal	Detector	PHS LWL	PHS UPL	Counting time (s)	Background position(s) relative to peak position	Concentration range *
RhKαC	F	LiF(220)	SC	34	75	200		
MoKαC	F	LiF(220)	SC	32	74	200		
MoKα	F	LiF(200)	SC	30	74	200	−1.28 +0.54	0 - 280
NbKα	F	LiF(200)	SC	30	74	200		0 - 268
ZrKα	F	LiF(200)	SC	30	74	200		0 - 1210
Y Kα	F	LiF(200)	SC	30	74	200	−0.86 +0.74	0 - 143
SrKα	F	LiF(200)	SC	30	74	200	+0.78	0 - 440
U $L\alpha_1$	F	LiF(200)	SC	30	74	200		0 - 15
RbKα	F	LiF(200)	SC	30	74	200	+0.60	0 - 530
Th $L\alpha_1$	F	LiF(200)	SC	30	74	200		0 - 51
Pb $L\beta_1$	F	LiF(200)	SC	30	74	200	+1.52	0 - 40
SeKα	F	LiF(220)	FS	25	75	200	−3.42	
Bi $L\alpha_1$	F	LiF(220)	FS	25	75	200		
AsKα	F	LiF(220)	FS	25	75	200	+1.80	
GaKα	F	LiF(200)	FS	26	74	200	−0.50 +0.70	
W $L\alpha_1$	F	LiF(220)	FL	25	67	200	−1.00 +2.10	
ZnKα	F	LiF(220)	FS	20	80	200	−1.08 +4.24	0 - 235
CuKα	F	LiF(220)	FS	20	80	200	+4.44	0 - 227
NiKα	F	LiF(220)	FS	20	80	200	+2.52	0 - 630
CoKα	F	LiF(220)	FL	15	75	200	+1.00	0 - 116
MnKα	F	LiF(220)	FL	15	75	200	−2.30 +4.70	0 - 1700
CrKα	F	LiF(220)	FL	15	75	200	−4.10 +2.90	0 - 465
V Kα	F	LiF(220)	FL	13	67	200	+3.40	0 - 640
La $L\alpha_1$	F	LiF(220)	FL	38	68	400	−2.78 +4.22	
Ce $L\beta_1$	F	LiF(220)	FL	40	68	400	−1.64	
Nd $L\alpha_1$	F	LiF(220)	FL	40	68	400	+4.82	
Ba $L\alpha_1$	F	LiF(200)	FL	25	75	200	−5.20	0 - 2680
ScKα	F	LiF(200)	FL	25	75	200	−2.78	0 - 54
S Kα	C	Ge(111)	FL	32	72	100	−5.00 +5.00	
F Kα	C	PX-1	FL	25	80	400	+1.82	

* = all concentrations expressed as part per million (ppm or $mg.kg^{-1}$)

The RhKα Compton or the MoKα Compton peak is used to determine the mass absorption coefficients of the specimens at the RhKαC wavelength (Figure 5) or the MoKαC wavelength, and the Compton peak mass absorption coefficient values are used to correct for absorption effects on the Mo, Nb, Zr, Y, Sr, U, Rb, Th, Pb, Br, Se, Bi, As, W, Zn, Cu and Ni analyte wavelengths. Primary and secondary mass absorption coefficients for the Co, Mn, Cr, V, La, Ce, Nd, Ba, Sc, S and F analyte wavelengths are calculated from major element compositions using the tables of Heinrich (1986). Mass absorption coefficient corrections are made to the net peak intensities, (gross peak intensities corrected for dead time losses, background and spectral overlap), to correct for absorption differences between standards and specimens. No corrections are made for enhancement, which could be small but significant ($< \sim 5\%$ relative) for the elements Cr, V, Ba and Sc in certain specimens, depending on their concentrations of Fe, Mn and Ti.

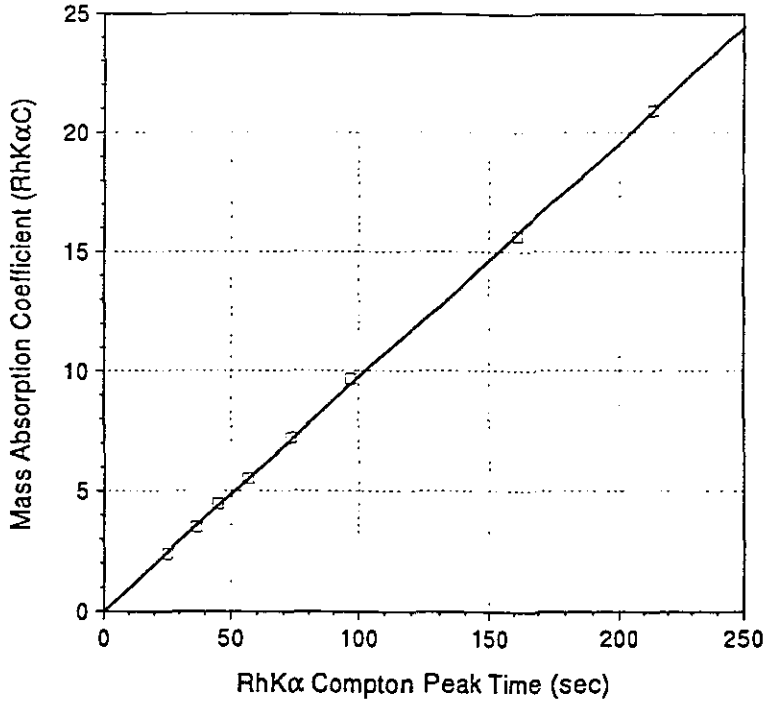

Figure 5. Calibration line for determination of mass absorption coefficients at the RhKαC wavelength. RhKαC peak time is the time required to accumulate 400 000 counts on the RhKαC peak using the fixed count method.

Measured intensity data are processed through the computer program TRACE to correct gross peak intensities for background and spectral overlap and to make mass absorption coefficient corrections according to the methods outlined in Duncan *et al.* (1984). First order calibration lines with zero intercept are calculated using six or more international rock standard reference materials (SRMs) for each element (Figs 7-14). The one standard deviation (1 σ) error due to counting statistics and the lower limit of detection is calculated for each element in each specimen.

Table 4 lists the given and calculated concentrations for selected elements in a number of rock SRMs, which give an indication of the accuracy of the trace element data. Table 5 lists the one standard deviation counting error and lower limit of detection for each of the elements in an acidic (low Fe, Ca and Mg, high Si) rock and in a mafic (high Fe, Ca and Mg, low Si) rock. Because of the difference in mass absorption coefficients between the two types of specimen the counting error and lower limit of detection will be slightly higher in mafic rock specimens. The two examples given cover the range of mass absorption coefficients found in the majority of geological rock, soil and sediment specimens.

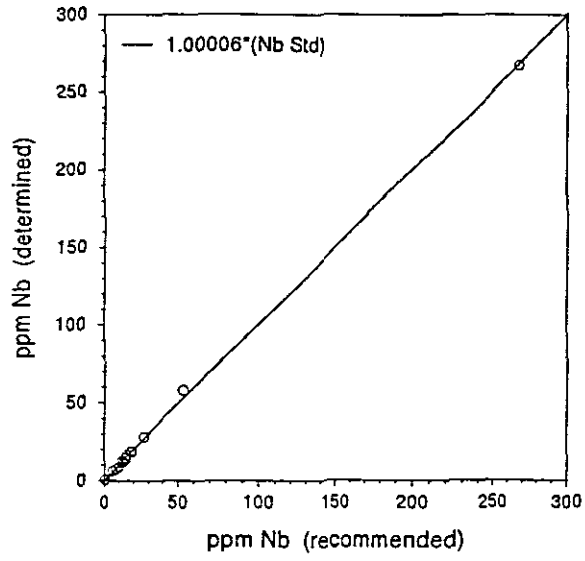

Figure 7. Comparison of recommended and determined Nb values for SRMs using powder briquettes.

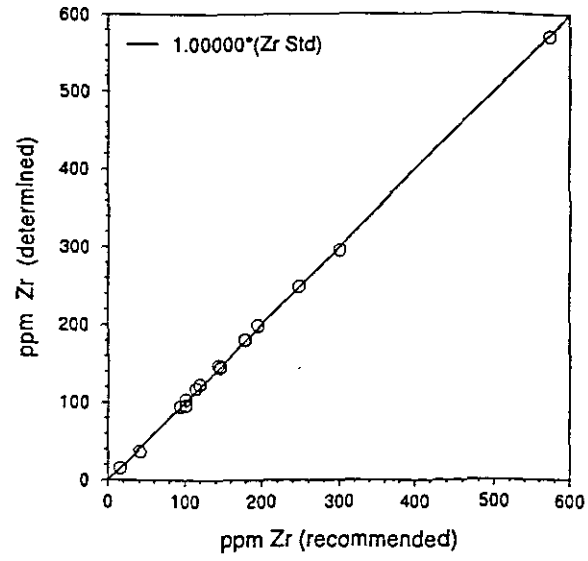

Figure 8. Comparison of recommended and determined Zr values for SRMs using powder briquettes.

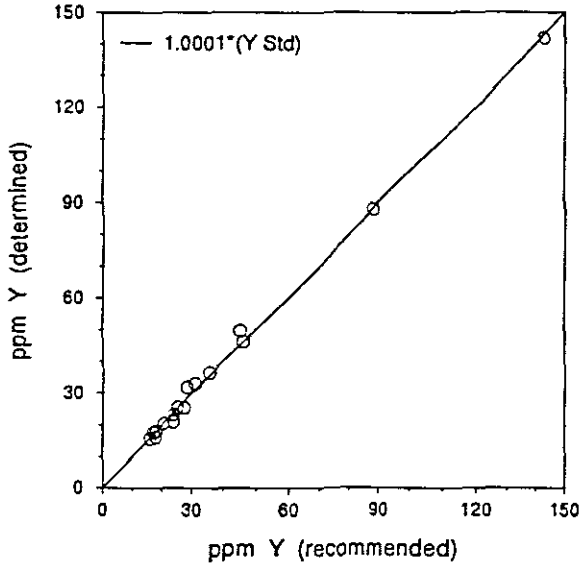

Figure 9. Comparison of recommended and determined Y values for SRMs using powder briquettes.

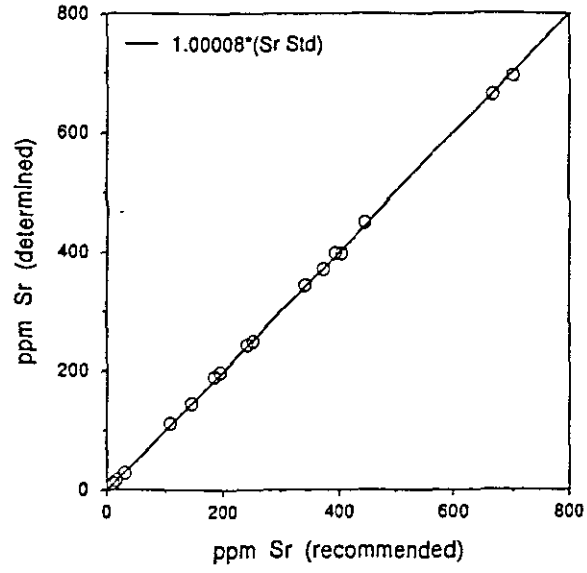

Figure 10. Comparison of recommended and determined Sr values for SRMs using powder briquettes.

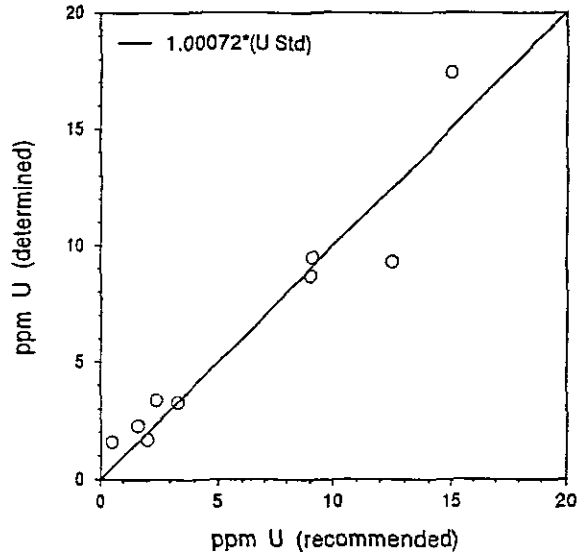

Figure 11. Comparison of recommended and determined U values for SRMs using powder briquettes.

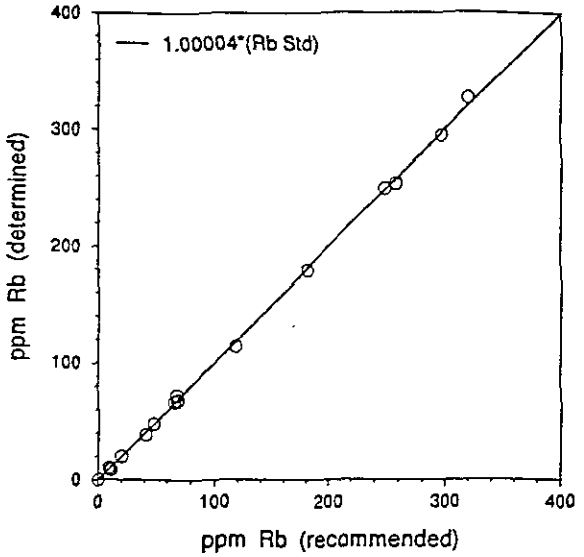

Figure 12. Comparison of recommended and determined Rb values for SRMs using powder briquettes.

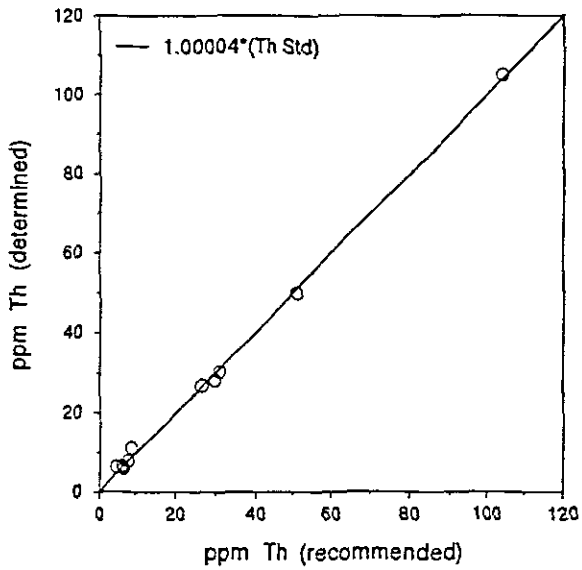

Figure 13. Comparison of recommended and determined Th values for SRMs using powder briquettes.

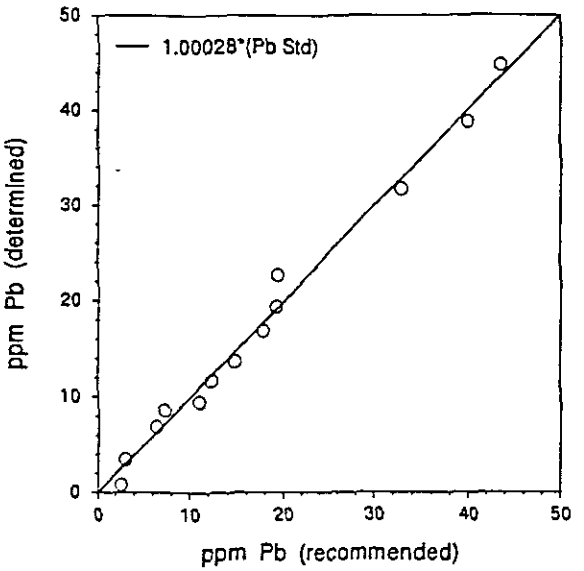

Figure 14. Comparison of recommended and determined Pb values for SRMs using powder briquettes.

Table 4. Given and calculated trace element data (all values in ppm) for some rock SRMs.

Element	QLO-1		BHVO-1		W-2		STM-1		BIR-1	
	Given	Calc	Given	Calc	Given	Calc	Given	Calc	Given	Calc
Mo	2.6	3.5	1.0	0.8	(0.6	0.5	5.2	3.1	(0.5	<0.8
Nb	10	11	19	19	7.9	7.4	268	267	0.6	0.9
Zr	185	190	179	181	94	95	1210	1220	16	19
Y	24	25	28	28	24	23	46	47	16	17
Sr	336	329	403	395	194	195	700	689	108	109
U	1.9	2.3	0.4	<1.6	0.5	<1.2	9.1	8.8	0.01	<1.2
Rb	74	71	11	9.7	20	20	118	114	0.3	<0.6
Th	4.5	4.0	1.1	1.8	2.2	2.7	31	31	0.03	<1.5
Pb	20	20	2.6	3.1	9.3	8.5	18	17	3	3.1
Zn	61	61	105	106	77	79	235	242	71	69
Cu	29	25	136	139	103	108	(4.6	2.1	126	132
Ni	(5.8	1.8	121	127	70	72	(3	1.7	166	170
Co	7.2	7.6	45	44	44	43	0.9	<1.9	51	52
Mn	720	690	1300	1290	1260	1240	1700	1600	1320	1280
Cr	(3.2	3.6	289	312	93	100	(4.3	3.2	382	404
V	54	44	317	314	262	257	(8.7	<1.6	313	306
Ba	1370	1430	139	138	182	191	560	589	7.0	10
Sc	8.9	10.3	31.8	33.9	35	36	0.6	0.5	44	39

(n.n = value given for information only

The counting error and lower limit of detection are calculated using the following formulae:

$$1\sigma \ error \ (in \ ppm) = Conc \times \frac{\sqrt{\frac{I_p}{T_p} + \frac{I_b}{T_b}}}{I_n}$$

and

$$LLD \ (in \ ppm) = \frac{6}{m}\sqrt{\frac{I_b}{T_{total}}}$$

where Conc = calculated concentration in ppm
m = net peak / concentration
I_p = gross peak count rate in cps
I_b = background count rate under the peak in cps
I_n = $I_p - I_b$ = true net peak count rate in cps
T_p = counting time for peak in seconds
T_b = total counting time for background in seconds
$T_{total} = T_p + T_b$

N.B. I_b is the calculated background *plus* any corrections for spectral interference, *i.e.* $I_b = I_p - I_n$.

Table 5. Calculated trace element data, 1 σ counting error and lower limit of detection (all values in ppm) for two rock specimens having different mass absorption coefficients.

Element	JR-2			JB-1a		
	Calc	1 σ	LLD	Calc	1 σ	LLD
Mo	4.1	0.2	0.6	1.8	0.3	0.7
Nb	19	0.1	0.4	28	0.2	0.5
Zr	87	0.1	0.3	152	0.2	0.4
Y	51	0.2	0.6	24	0.2	0.6
Sr	8.2	0.1	0.4	444	0.3	0.5
U	11	0.3	0.9	2.3	0.4	1.2
Rb	303	0.2	0.4	39	0.2	0.6
Th	34	0.4	1.1	9.8	0.5	1.4
Pb	24	0.5	1.3	7.5	0.6	1.8
Zn	28	0.2	0.6	84	0.4	0.9
Cu	1.1	0.3	0.8	55	0.5	1.1
Ni	1.3	0.3	0.8	139	0.7	1.3
Co	<1.2	0.4	1.2	37	0.9	2.3
Mn	878	1.7	1.2	1100	2.0	1.8
Cr	1.6	0.4	1.3	406	1.5	2.0
V	1.7	0.4	1.2	193	1.4	3.0
Ba	28	0.6	1.5	523	1.8	3.3
Sc	6.0	0.2	0.5	26	0.4	0.9

APPENDIX G (1) TABLE OF PARTICLE SIZE DISTRIBUTION OF SEDIMENT IN CORE H1

I.D NO.	Depth (m)	Tot. Gravel (%)	Tot. Sand((%)	Tot. Silt & Clay (%)	Texture
H1.G2	0	0.00	0.582	99.42	mud
H1.G1	0	0.00	0.147	99.85	mud
H1.1.19	0.05	0.00	0.183	99.82	mud
H1.1.18	0.1	0.00	0.143	99.86	mud
H1.1.17	0.15	0.00	0.144	99.86	mud
H1.1.16	0.2	0.00	0.120	99.88	mud
H1.1.15	0.25	0.00	0.155	99.84	mud
H1.1.14	0.3	0.00	0.063	99.94	mud
H1.1.13	0.35	0.00	0.157	99.84	mud
H1.1.12	0.4	0.00	0.392	99.61	mud
H1.1.11	0.45	0.00	0.119	99.88	mud
H1.1.10	0.5	0.00	0.877	99.12	mud
H1.1.9	0.55	0.00	0.037	99.96	mud
H1.1.8	0.6	0.00	0.047	99.95	mud
H1.1.7	0.65	0.00	0.041	99.96	mud
H1.1.6	0.7	0.00	0.126	99.87	mud
H1.1.5	0.75	0.00	0.068	99.93	mud
H1.1.4	0.8	0.00	0.027	99.97	mud
H1.1.3	0.85	0.00	0.051	99.95	mud
H1.1.2	0.9	0.00	0.122	99.88	mud
H1.1.1	0.95	0.00	0.268	99.73	mud
H1.CC2	1	0.00	0.316	99.68	mud
H1.CC1	1.05	0.00	0.216	99.78	mud
H1.CE	1.1	0.00	1.467	98.53	mud
					mud
Average		**0.00**	**0.245**	**99.76**	mud

APPENDIX G (2)TABLE OF PARTICLE SIZE DISTRIBUTION OF SEDIMENT IN CORE H2

Depth (m)	ID.No.	tot.gravel (%)	tot. sand(%)	tot.silt &clay(%)	silt (%)	cohesionless silt (%)	cohesive silt (%	Clay (%)
0.00	H2.G1	0.00	0.14	99.86	33.8	8.6	25.2	66.06
0.00	H2G2	0.00	0.25	99.75	32.7	7.27	25.43	67.05
0.05	H2.7.4	0.00	0.32	99.68	34.93	8.16	26.77	64.75
0.09	H2.7.3	0.00	0.06	99.94	27.88	7.5	20.38	72.06
0.14	H2.7.2	0.00	0.06	99.94	24.37	10.4	13.97	75.57
0.16	H2.7.1b	0.00	0.41	99.59	17.78	1.45	16.33	81.81
0.18	H2.7.1a	0.00	0.36	99.64	21.78	2.72	19.06	77.86
0.23	H2.6.12	0.00	0.29	99.71	27.3	4.16	23.14	72.41
0.27	H2.6.11	0.00	0.25	99.75	35.02	6.9	28.12	64.73
0.32	H3.6.10	0.00	0.10	99.90	37.89	8.3	29.59	62.01
0.36	H2.6.9	0.00	0.16	99.84	24.46	2.25	22.21	75.38
0.41	H2.6.8	0.00	0.29	99.71	23.25	2.13	21.12	76.46
0.45	H2.6.7	0.00	0.01	99.99	27.99	2.92	25.07	72.00
0.50	H3.6.6	0.00	0.07	99.93	22.88	3.21	19.67	77.05
0.54	H2.6.5	0.00	0.08	99.92	23.69	3.23	20.46	76.23
0.59	H2.6.4	0.00	0.32	99.68	42.95	15.68	27.27	56.73
0.63	H2.6.3	0.00	0.27	99.73	43.64	13.48	30.16	56.09
0.69	H2.6.2	0.00	0.44	99.56	41.75	14.01	27.74	57.81
0.72	H2.6.1	0.00	0.13	99.87	27.75	5.68	22.07	72.12
0.77	H2.5.20	0.00	0.02	99.98	28.5	2.43	26.07	71.48
0.82	H2.5.19	0.00	0.10	99.90	36.48	8.82	27.66	63.42
0.87	H2.5.18	0.00	0.61	99.39	28.8	5.9	22.9	70.59
0.92	H2.5.17	0.00	0.50	99.50	23.27	2.91	20.36	76.23
0.97	H2.5.16	0.00	0.11	99.89	23.66	4.69	18.97	76.23
1.02	H2.5.15	0.00	0.16	99.84	21.2	2.44	18.76	78.64
1.07	H2.5.14	0.00	0.08	99.92	23.92	3.32	20.6	76.00
1.12	H2.5.13	0.00	0.22	99.78	22	2.81	19.19	77.78
1.17	H2.5.12	0.00	1.27	98.73	22.38	2.89	19.49	76.35
1.22	H2.5.11	0.00	0.13	99.87	19.64	1.76	17.88	80.23
1.27	H2.5.10	0.00	0.11	99.89	26.97	3.89	23.08	72.92
1.32	H2.5.9	0.00	0.19	99.81	11.08	8.06	3.02	88.73
1.37	H2.5.8	0.00	0.55	99.45	40.65	17.09	23.56	58.80
1.42	H2.5.7	0.00	0.37	99.63	46.44	17.39	29.05	53.19
1.47	H2.5.6	0.00	0.04	99.96	20.12	1.75	18.37	79.84
1.52	H2.5.5	0.00	0.29	99.71	27.06	5.45	21.61	72.65
1.57	H2.5.4	0.00	0.16	99.84	26.83	4.61	22.22	73.01
1.62	H2.5.3	0.00	0.05	99.95	33.51	4.78	28.73	66.44
1.67	H2.5.2	0.00	0.19	99.81	33.05	10.52	22.53	66.76
1.72	H2.5.1	0.00	0.21	99.79	43.18	18	25.18	56.61
1.77	H2.4.20	0.00	0.70	99.30	33.65	7.64	26.01	65.65
1.82	H2.4.19	0.00	0.17	99.83	24.18	2.05	22.13	75.65
1.87	H2.4.18	0.00	0.06	99.94	18.63	1.56	17.07	81.31
1.92	H2.4.17	0 00	0.31	99.69	31.08	2.24	28.84	68.61
1.97	H2.4.16	0.00	0.13	99 87	34.95	5.82	29.13	64.92
2.02	H2.4.15	0.00	0.36	99.64	30.98	8.31	22.67	68.66
2.07	H2.4.14	0.00	0.30	99.70	28.03	8.22	19.81	71.67
2.12	H2.4.13	0.00	0.07	99.93	42.77	17.9	24.87	57.16
2.17	H2.4.12	0.00	0.13	99.87	33.79	8.85	24.94	66.08
2.22	H2.4.11	0.00	0.03	99.97	29.5	4.57	24.93	70.47
2.27	H2.4.10	0.00	0.14	99.86	24.92	2.23	22.69	74.94
2.32	H2.4.9	0.00	0 07	99 93	25.06	3.11	21.95	74.87
2.37	H2.4.8	0.00	0.10	99.90	27.92	1.36	26.56	71.98
2.42	H2.4.7	0.00	0.11	99.89	22.28	1.26	21.02	77.61
2.47	H2.4.6	0.00	0 03	99.97	24.78	1.36	23.42	75.19
2.52	H2.4.5	0.00	0.14	99.86	24.18	2.35	21.83	75.68
2.57	H2.4.4	0.00	0.06	99.94	35.83	5.39	30.44	64.11
2.62	H2.4.3	0.00	0.09	99.91	21.48	3.23	18.25	78.43
2.67	H2.4.2	0.00	0.09	99.91	15.37	1.36	14.01	84.54
2.72	H2.4.1	0.00	0.20	99.80	15.63	1.17	14 46	84.17
2.77	H2.3.20	0.00	0.16	99.84	29.46	7.33	22.13	70.38
2.82	H2.3.19	0.00	0 06	99.94	30.78	4.38	26.4	69.16
2.87	H2.3.18	0.00	0.06	99.94	30.62	4.87	25.75	69.32
2 92	H2.3.17	0.00	0.56	99.44	25.69	3.38	22.31	73.75
2.97	H2.3.16	0.00	0.09	99.91	21.87	2.44	19.43	78.04
3.02	H2.3.15	0.00	0 04	99.96	19.99	0.87	19.12	79.97

3.07	H2.3.14	0.00	0.03	99.97	25.14	1.27	23.87	74.83
3.12	H2.3.13	0.00	0.07	99.93	25.02	1.66	23.36	74.91
3.17	H2.3.12	0.00	0.32	99.68	23.62	3.4	20.22	76.06
3.22	H2.3.11	0.00	0.03	99.97	23.95	0.78	23.17	76.02
3.27	H2.3.10	0.00	0.04	99.96	22.78	2.23	20.55	77.18
3.32	H2.3.9	0.00	0.06	99.94	20.42	0.39	20.03	79.52
3.37	H2.3.8	0.00	0.14	99.86	25.66	2.89	22.77	74.20
3.42	H2.3.7	0.00	0.04	99.96	20.02	1.85	18.17	79.94
3.47	H2.3.6	0.00	0.03	99.97	33.63	12.95	20.68	66.34
3.52	H2.3.5	0.00	0.06	99.94	18.57	1.66	16.91	81.37
3.57	H2.3.4	0.00	0.07	99.93	20.73	2.24	18.49	79.20
3.62	H2.3.3	0.00	0.37	99.63	28.19	6.64	21.55	71.44
3.67	H2.3.2	0.00	0.16	99.84	29.18	9.57	19.61	70.66
3.72	H2.3.1	0.00	0.06	99.94	37.75	13.56	24.19	62.19
3.77	H2.2.20	0.00	0.10	99.90	32.56	12.45	20.11	67.34
3.82	H2.2.19	0.00	0.14	99.86	41.03	24.81	16.22	58.83
3.87	H2.2.18	0.00	0.12	99.88	29.14	10.41	18.73	70.74
3.92	H2.2.17	0.00	0.07	99.93	28.94	10.29	18.65	70.99
4.02	H2.2.16	0.00	0.09	99.91	13.37	0.77	12.6	86.54
4.07	H2.2.15	0.00	0.04	99.96	41.16	1.17	39.99	58.80
4.12	H2.2.14	0.00	0.22	99.78	18.78	0.94	17.84	81.00
4.17	H2.2.13	0.00	3.32	96.68	16.79	0.84	15.95	79.89
4.17	H2.2.12	0.00	0.49	99.51	24.09	0.97	23.12	75.42
4.22	H2.2.11	0.00	1.43	98.57	21.1	1.54	19.56	77.47
4.27	H2.2.10	0.00	1.71	98.29	49.06	17.39	31.67	49.23
4.32	H2.2.9	0.00	1.57	98.43	38.48	10.68	27.8	59.95
4.37	H2.2.8	0.00	1.79	98.21	20.44	4.32	16.12	77.77
4.42	H2.2.7	0.00	1.57	98.43	15.09	0.67	14.42	83.34
4.47	H2.2.6	0.00	2.26	97.74	19.73	1.52	18.21	78.01
4.52	H2.2.5	0.00	1.50	98.50	18.57	1.53	17.04	79.93
4.57	H2.2.4	0.00	3.11	96.89	28.6	8.56	20.04	68.29
4.62	H2.2.3	0.00	1.97	98.03	38.62	15.8	22.82	59.41
4.67	H2.2.2	0.00	0.33	99.67	20.61	1.55	19.06	79.06
4.72	H2.2.1	0.00	0.28	99.72	29.94	3.21	26.73	69.78
4.77	H2.1.20	0.00	1.21	98.79	15.67	0	15.67	83.12
4.82	H2.1.19	0.00	4.79	95.21	14.9	0.93	13.97	80.31
4.87	H2.1.18	0.00	3.26	96.74	21.91	3.4	18.51	74.83
4.92	H2.1.17	0.00	6 80	93.20				
4.97	H2.1.16	0.00	2.87	97.13				
5.02	H2.1.15	0.00	2.80	97.20				
5.07	H2.1.14	0.00	2.70	97.30				
5.12	H2.1.13	0.00	4.49	95.51				
5.17	H2.1.12	0.00	4.35	95.65				
5.22	H2.1.11	0.00	5.10	94.90				
5.27	H2.1.10	0.00	5.44	94.56				
5.32	H2.1.9	0.00	12.36	87.64				
5.37	H2.1.8	0.00	18.65	81.35				
5.42	H2.1.7	0.00	8.12	91.88				
5.47	H2.1.6	0.00	12.31	87.69				
5.52	H2.1.5	0.00	13.12	86.88				
5.57	H2.1.4	0.00	11.55	88.45				
5.62	H2.1.3	0.00	1.27	98.73				
5.67	H2.1.2	0.00	7.35	92.65				
5.72	H2.1.1	0.00	7.51	92.49				
5.77	H2SP4	0.00	4.44	95.56				
5 82	H2SP3	0.00	6.41	93.59				
5.87	H2SP2	0.00	3.05	96.95				
5.92	H2SP1	0 00	2.77	97.23				
5 97	H2CC2	0.00	6.75	93.25				
6.02	H2CC1	0.00	9.92	90.08				
	Average	**0.00**	**1.65**	**98.35**	**27.33**	**5.55**	**21.78**	**72.22**

APPENDIX G (3) PARTICLE SIZE DISTRIBUTION OF SEDIMENT IN CORE H3

Depth (m)	I.D. No	tot. Gravel (%	Tot. sand (%	Tot. silt & clay (%	Texture
0.00	H3.G2	0.00	0.38	99.62	mud
0.00	H3.G1	0.00	0.08	99.92	mud
0.00	H3TOP	0.00	0.49	99.51	mud
0.05	H3.6.12	0.00	0.45	99.55	mud
0.10	H3.611	0.00	0.16	99.84	mud
0.15	H3.610	0.00	0.07	99.93	mud
0.20	H3.6.9	0.00	0.16	99.84	mud
0.25	H3.6.8	0.00	0.12	99.88	mud
0.30	H3.6.7	0.00	0.14	99.86	mud
0.35	H3.6.6	0.00	0.07	99.93	mud
0.40	H3.6.5	0.00	0.10	99.90	mud
0.45	H3.6.4	0.00	0.24	99.76	mud
0.50	H3.6.3	0.00	0.09	99.91	mud
0.55	H3.6.2	0.00	0.07	99.93	mud
0.60	H3.6.1	0.00	0.13	99.87	mud
0.65	H3.5.20B	0.00	0.25	99.75	mud
0.70	H3.5.20A	0.00	1.02	98.98	mud
0.75	H3.5.19	0.00	0.02	99.98	mud
0.80	H3.5.18	0.00	0.41	99.59	mud
0.85	H3.5.17	0.00	0.15	99.85	mud
0.90	H3.5.16	0.00	0.09	99.91	mud
0.95	H3.5.15	0.00	0.15	99.85	mud
1.00	H3.5.14	0.00	0.23	99.77	mud
1.05	H3.5.13	0.00	0.12	99.88	mud
1.10	H3.5.12	0.00	0.14	99.86	mud
1.15	H3.5.11	0.00	0.19	99.81	mud
1.20	H3.5.10	0.00	0.38	99.62	mud
1.25	H3.5.9	0.00	0.06	99.94	mud
1.30	H3.5.8	0.00	0.19	99.81	mud
1.35	H3.5.7	0.00	0.50	99.50	mud
1.40	H3.5.6	0.00	0.31	99.69	mud
1.45	H3.5.5	0.00	0.25	99.75	mud
1.50	H3.5.4	0.00	0.15	99.85	mud
1.55	H3.5.3	0.00	1.14	98.86	mud
1.60	H3.5.2	0.00	0.22	99.78	mud
1.65	H3.5.1	0.00	0.54	99.46	mud
1.68	H3.4.20B	0.00	0.84	99.16	mud
1.70	H3.4.20A	0.00	0.65	99.35	mud
1.73	H3.4.19B	0.00	0.19	99.81	mud
1.75	H3.4.19A	0.00	0.22	99.78	mud
1.80	H3.4.18	0.00	0.11	99.89	mud
1.85	H3.4.17	0.00	0.46	99.54	mud
1.90	H3.4.16	0.00	0.11	99.89	mud
1.95	H3.4.15	0.05	0.14	99.81	mud
2.00	H3.4.14	0.00	0.15	99.85	mud
2.05	H3.3.13	0.33	0.37	99.30	mud
2.10	H3.4.12	0.13	0.26	99.61	mud
2.15	H3.4.11	0.00	0.28	99.72	mud

2.20	H3.4.10	0.00	0.24	99.76	mud
2.25	H3.4.9	0.00	0.09	99.91	mud
2.30	H3.4.8	0.00	0.64	99.36	mud
2.35	H3.4.7	0.00	0.05	99.95	mud
2.40	H3.4.6	0.00	0.13	99.87	mud
2.45	H3.4.5	0.00	0.22	99.78	mud
2.50	H3.4.4	0.00	0.29	99.71	mud
2.55	H3.4.3	0.00	0.19	99.81	mud
2.60	H3.4.2	0.00	0.79	99.21	mud
2.65	H3.4.1	0.00	0.47	99.53	mud
2.68	H3.3.20B	0.00	0.74	99.26	mud
2.70	H3.320A	0.00	5.81	94.19	mud
2.73	H3.3.19B	0.00	0.43	99.57	mud
2.75	H3.3.19A	0.00	0.11	99.89	mud
2.80	H3.3.18	0.00	0.11	99.89	mud
2.85	H3.3.17	0.00	0.06	99.94	mud
2.90	H3.3.16	0.00	0.05	99.95	mud
2.95	H3.3.15	0.00	0.10	99.90	mud
3.00	H3.3.14	0.00	0.04	99.96	mud
3.05	H3.3.13	0.00	0.07	99.93	mud
3.10	H3.3.12	0.00	0.04	99.96	mud
3.15	H3.3.11	0.00	0.17	99.83	mud
3.20	H3.3.10	0.00	0.07	99.93	mud
3.25	H3.3.9	0.00	0.09	99.91	mud
3.30	H3.3.8	0.00	0.03	99.97	mud
3.35	H3.3.7	0.00	0.05	99.95	mud
3.40	H3.3.6	0.00	0.02	99.98	mud
3.45	H3.3.5	0.00	0.31	99.69	mud
3.50	H3.3.4	0.00	0.05	99.95	mud
3.55	H3.3.3	0.00	0.02	99.98	mud
3.60	H3.3.2	0.00	0.03	99.97	mud
3.65	H3.3.1	0.00	0.05	99.95	mud
3.68	H3.2.20B	0.00	0.08	99.92	mud
3.70	H3.2.20A	0.00	0.14	99.86	mud
3.73	H3.2.19B	0.00	0.06	99.94	mud
3.75	H3.2.19A	0.00	0.09	99.91	mud
3.78	H3.2.18B	0.00	0.01	99.99	mud
3.80	H3.2.18A	0.00	0.06	99.94	mud
3.83	H3.2.17B	0.00	0.05	99.95	mud
3.85	H3.2.17A	0.00	0.10	99.90	mud
3.90	H3.2.16	0.00	0.10	99.90	mud
3.95	H3.2.15	0.00	0.11	99.89	mud
4.00	H3.2.14	0.00	0.19	99.81	mud
4.05	H3.2.13	0.00	0.38	99.62	mud
4.10	H3.2.12	0.00	0.08	99.92	mud
4.15	H3.2.11	0.00	0.33	99.67	mud
4.20	H3.2.10	0.00	0.28	99.72	mud
4.25	H3.2.9	0.00	0.04	99.96	mud
4.30	H3.2.8	0.00	0.86	99.14	mud
4.35	H3.2.7	0.00	0.73	99.27	mud
4.40	H3.2.6	0.00	0.13	99.87	mud

4.45	H3.2.5	0.00	0.26	99.74	mud
4.50	H3.2.4	0.00	0.17	99.83	mud
4.55	H3.2.3	0.00	0.18	99.82	mud
4.60	H3.2.2	0.00	0.08	99.92	mud
4.65	H3.2.1	0.00	0.05	99.95	mud
4.68	H3.1.20B	0.00	0.06	99.94	mud
4.70	H3.1.20A	0.89	0.08	99.03	mud
4.75	H3.1.19	0.00	0.43	99.57	mud
4.80	H3.1.18	0.00	0.10	99.90	mud
4.85	H3.1.17	0.06	0.13	99.81	mud
4.90	H3.1.16	0.00	0.10	99.90	mud
4.95	H3.1.15	0.00	0.02	99.98	mud
5.00	H3.1.1.14	0.00	0.02	99.98	mud
5.05	H3.1.13	0.00	0.04	99.96	mud
5.10	H3.1.12	0.00	0.01	99.99	mud
5.15	H3.1.11	0.00	0.04	99.96	mud
5.20	H3.1.10	0.00	0.08	99.92	mud
5.25	H3.1.9	0.00	0.03	99.97	mud
5.30	H3.1.8	0.00	0.13	99.87	mud
5.35	H3.1.7	0.04	0.14	99.82	mud
5.40	H3.1.6	0.00	0.03	99.97	mud
5.45	H3.1.5	0.00	0.04	99.96	mud
5.50	H3.1.4	0.00	0.15	99.85	mud
5.55	H3.1.3	0.00	0.02	99.98	mud
5.60	H3.1.2	0.00	0.09	99.91	mud
5.65	H3.1.1	0.00	0.04	99.96	mud
5.70	H3.CC2	0.00	0.02	99.98	mud
5.75	H3.CC1	0.00	0.00	100.00	mud
5.80	H3.CCE	0.00	0.02	99.98	mud
	average	**0.01**	**0.24**	**99.75**	mud

APPENDIX G (4) TABLE OF PARTICLE SIZE DISTRIBUTION OF SEDIMENT IN CORE H5

Depth (m)	I.D No	Tot. gravel (%)	Tot. sand (%)	Tot, silt & clay (%)	Texture
0.0	H5.GA2	0.00	1.06	98.94	mud
0.0	H5.GA1	0.00	0.81	99.19	mud
0.0	H5.GB2	0.00	0.33	99.67	mud
0.0	H5.GB1	0.00	0.33	99.67	mud
0.0	H5.GC2	0.00	0.08	99.92	mud
0.0	H5.GC1	0.00	0.04	99.96	mud
0.0	H5.3.6	0.00	0.55	99.45	mud
0.1	H5.3.5	0.00	0.15	99.85	mud
0.1	H5.3.4	0.00	0.18	99.82	mud
0.2	H5.3.3	0.00	0.16	99.84	mud
0.2	H5.3.2	0.00	0.17	99.83	mud
0.3	H5.3.1	0.12	0.16	99.72	mud
0.3	H5.2.20B	0.00	0.18	99.82	mud
0.3	H5.2.20A	0.00	0.28	99.72	mud
0.4	H5.2.19	0.00	0.34	99.66	mud
0.4	H5.2.18	0.00	0.33	99.67	mud
0.5	H5.2.17	0.00	0.41	99.59	mud
0.5	H5.2.16	0.00	0.61	99.39	mud
0.6	H5.2.15	0.00	0.67	99.33	mud
0.6	H5.2.14	0.00	0.71	99.29	mud
0.7	H5.2.13	0.00	1.41	98.59	mud
0.7	H5.2.12	0.00	1.28	98.72	mud
0.8	H5.2.11	0.00	1.23	98.77	mud
0.8	H5.2.10	0.00	1.75	98.25	mud
0.9	H5.2.9	0.00	1.88	98.12	mud
0.9	H5.2.8	0.00	2.19	97.81	mud
1.0	H5.2.7	0.00	2.77	97.23	mud
1.0	H5.2.6	0.00	3.11	96.89	mud
1.1	H5.2.5	0.00	3.65	96.35	mud
1.1	H5.2.4	0.00	3.57	96.43	mud
1.2	H5.2.3	0.00	4.68	95.32	mud
1.2	H5.2.2	0.00	7.67	92.33	mud
1.3	H5.2.1	0.00	5.28	94.72	mud
1.3	H5.1.20B	0.00	4.93	95.07	mud
1.3	H5.1.20A	0.00	5.03	94.97	mud
1.3	H5.1.19B	0.60	5.64	93.76	mud
1.4	H5.1.19A	0.00	5.81	94.19	mud
1.4	H5.1.18	0.26	6.52	93.22	mud
1.5	H5.1.17	0.00	8.94	91.06	mud
1.5	H5.1.16	0.00	12.98	87.02	sandy mud
1.6	H5.1.15	0.20	18.47	81.33	sandy mud (g)
1.6	H5.1.14	0.00	20.25	79.75	sandy mud
1.7	H5.1.13	0.00	23.32	76.68	sandy mud
1.7	H5.1.12	0.46	21.93	77.61	sandy mud (g)
1.8	H5.1.11	1.23	24.38	74.39	sandy mud (g)
1.8	H5.1.10	0.00	21.71	78.29	sandy mud
1.9	H5.1.9	0.39	20.21	79.40	sandy mud (g)
1.9	H5.1.8	2 18	20.75	77.07	sandy mud (g)
2.0	H5.1.7	0.86	19.57	79.57	sandy mud (g)
2.0	H5.1.6	0.51	22.01	77.48	sandy mud (g)
2.1	H5.1.5	1.32	23.39	75.28	sandy mud (g)
2.1	H5.1.4	0.70	21.95	77.35	sandy mud (g)
2.2	H5.1.3	0.83	23.02	76.15	sandy mud (g)
2.2	H5.1.2	0.70	25.60	73.71	sandy mud (g)
2.3	H5.1.1	1.31	28.44	70.25	sandy mud (g)
2.3	H5.CC4	1.10	23.83	75.07	sandy mud (g)
2.4	H5CC3	2.17	25.89	71.94	sandy mud (g)
2.4	H5.CC2	4.80	28.62	66.58	sandy mud (g)
2.5	H5.CC1	21.02	34.09	44.89	gravelly mud
2.5	H5.CE	49.84	31.81	18.35	muddy sandy gravel
average		**1.51**	**9.62**	**88.87**	**sandy mud (g)**

Key: (g) =slightly gravelly

APPENDIX G (5) TABLE OF PARTICLE SIZE DISTRIBUTION OF SEDIMENT IN CORE H4

Depth (m)	I.D No.	tot. gravel (%)	Tot. sand (%)	tot. silt & clay (	Texture
0.0	H4.G2	0.00	0.28	99.72	mud
0.0	H4.G1	0.00	0.25	99.75	mud
0.0	H4.5.20B	0.00	0.24	99.76	mud
0.1	H4.5.20A	0.23	0.47	99.29	mud
0.1	H4.5.19B	0.00	0.19	99.81	mud
0.1	H4.5.19A	0.00	0.15	99.85	mud
0.2	H4.5.18	0.00	0.53	99.47	mud
0.2	H4..5.17	0.00	0.23	99.77	mud
0.3	H4.5.16	0.00	0.24	99.76	mud
0.3	H4.5.15	0.00	0.23	99.77	mud
0.4	H4.5.14	0.09	0.22	99.69	mud
0.4	H4.5.13	0.00	0.22	99.78	mud
0.5	H4.5.12	0.00	0.20	99.80	mud
0.5	H4.5.11	0.00	0.20	99.80	mud
0.6	H4.5.10	0.00	0.19	99.81	mud
0.6	H4.5.9	0.00	0.25	99.75	mud
0.7	H4.5.8	0.00	0.22	99.78	mud
0.7	H4.5.7	0.00	0.30	99.70	mud
0.8	H4.5.6	0.03	0.31	99.66	mud
0.8	H4.5.5	0.00	0.34	99.66	mud
0.9	H4.5.4	0.00	0.42	99.58	mud
0.9	H4.5.3	0.00	0.28	99.72	mud
1.0	H4.5.2	0.00	0.43	99.57	mud
1.0	H4.5.1	0.00	0.50	99.50	mud
1.0	H4.4.20B	0.00	0.39	99.61	mud
1.1	H4.4.20A	0.12	0.41	99.47	mud
1.1	H4.4.19	0.00	0.35	99.65	mud
1.2	H4.4.18	0.13	0.38	99.49	mud
1.2	H4.4.17	0.15	0.40	99.45	mud
1.3	H4.4.16	0.00	0.58	99.42	mud
1.3	H4.4.15	0.13	0.29	99.58	mud
1.4	H4.4.14	0.10	0.28	99.62	mud
1.4	H4.4.13	0.00	0.47	99.53	mud
1.5	H4.4.12	0.00	0.23	99.77	mud
1.5	H4.4.11	0.06	0.28	99.66	mud
1.6	H4.4.10	0.10	0.28	99.61	mud
1.6	H4.4.9	0.00	0.30	99.70	mud
1.7	H4.4.8	0.00	0.32	99.68	mud
1.7	H4.4.7	0.25	0.58	99.18	mud
1.8	H4.4.6	0.00	0.20	99.80	mud
1.8	H4.4.5	0.00	0.26	99.74	mud
1.9	H4.4.4	0.11	0.44	99.46	mud
1.9	H4.4.3	0.00	0.25	99.75	mud
2.0	H4.4.2	0.42	0.27	99.32	mud
2.0	H4.4.1	0.13	0.52	99.35	mud
2.0	4.3.20.	0.00	0.28	99.72	mud
2.1	H4.3.20A	0.06	0.31	99.64	mud
2.1	H4.3.19B	0.11	0.45	99.45	mud
2.1	H4.3.19A	0.00	0.30	99.70	mud
2.2	H4.3.17	0.00	0.25	99.75	mud
2.3	H4.3.16	0.11	0.46	99.43	mud
2.3	H4.3.15	0.00	0.43	99.57	mud
2.4	H4.3.14	0.00	0.38	99.62	mud
2.4	H4.3.13	0.00	1.02	98.98	mud

2.5	H4.3.12	0.00	0.40	99.60	mud
2.5	H4.3.11	0.39	0.36	99.24	mud
2.6	H4.3.10	0.01	0.41	99.58	mud
2.6	H4.3.9	0.16	1.01	98.83	mud
2.7	H4.3.8	0.21	0.76	99.03	mud
2.7	H4.3.7	0.04	0.66	99.31	mud
2.8	H4.3.6	0.06	0.54	99.40	mud
2.8	H4.3.5	0.03	0.78	99.19	mud
2.9	H4.3.4	0.35	0.65	99.00	mud
2.9	H4.3.3	0.33	0.79	98.88	mud
3.0	H4.3.2	0.22	0.44	99.34	mud
3.0	H4.3.1	0.83	1.09	98.08	mud
3.0	H4.2.20B	0.00	0.32	99.68	mud
3.1	H4.2.20A	0.33	0.49	99.18	mud
3.1	H4.2.19	0.00	0.30	99.70	mud
3.2	H4.2.18	0.00	0.30	99.70	mud
3.2	H4.2.17	0.19	0.75	99.05	mud
3.3	H4.2.16	0.00	0.04	99.96	mud
3.3	H4.2.15	0.00	0.27	99.73	mud
3.4	H4.2.14	0.00	0.25	99.75	mud
3.5	H4.2.12	0.24	0.60	99.16	mud
3.5	H4.2.11	0.00	0.26	99.74	mud
3.6	H4.2.10	0.02	0.27	99.71	mud
3.6	H4.2.9	0.34	0.73	98.93	mud
3.7	H4.2.8	0.58	0.60	98.82	mud
3.7	H4.2.7	0.58	0.81	98.61	mud
3.8	H4.2.6	0.33	0.87	98.80	mud
3.8	H4.2.5	0.00	0.91	99.09	mud
3.9	H4.2.4	0.45	0.97	98.58	mud
3.9	H4.2.3	0.13	0.54	99.32	mud
4.0	H4.2.2	0.09	0.95	98.96	mud
4.0	H4.2.1	0.00	0.38	99.62	mud
4.0	H4.1.20B	0.16	1.34	98.50	mud
4.1	H4.1.20A	0.49	1.18	98.33	mud
4.1	H4.1.19	0.00	0.46	99.54	mud
4.2	H4.1.18	0.00	0.43	99.57	mud
4.2	H4.1.17	0.12	1.08	98.80	mud
4.3	H4.1.16	0.16	0.65	99.19	mud
4.3	H4.1.15	0.00	0.60	99.40	mud
4.4	H4.1.14	0.27	0.79	98.93	mud
4.4	H4.1.13	0.08	0.72	99.20	mud
4.5	H4.1.12	0.23	0.72	99.05	mud
4.5	H4.1.11	0.03	0.90	99.07	mud
4.6	H4.1.10	0.00	1.11	98.89	mud
4.6	H4.1.9	0.40	1.13	98.47	mud
4.7	H4.1.8	0.00	1.03	98.97	mud
4.7	H4.1.7	0.00	2.07	97.93	mud
4.8	H4.1.6	0.00	1.10	98.90	mud
4.8	H4.1.5	0.11	1.25	98.64	mud
4.9	H4.1.4	0.76	1.64	97.60	mud
4.9	H4.1.3	0.41	1.68	97.91	mud
5.0	H4.1.2	0.41	2.33	97.27	mud
5.0	H4.1.1	1.45	2.24	96.32	mud
5.0	H4.CC2	0.46	2.04	97.50	mud
5.1	H4.CC1	0.25	2.60	97.15	mud
5.1	H4.CE2	0.17	3.09	96.74	mud
5.2	H4.CE1	0.16	3.03	96.81	mud
					mud
Average		**0.13**	**0.65**	**99.22**	mud

APPENDIX G (6) TABLE OF PARTICLE SIZE DISTRIBUTION OF SEDIMENT IN CORE H6

Depth(cm)	I.D No	Tot. gravel (%)	Tot. Sand (%)	Tot. silt & clay (%)	Texture
0	G1	0.00	4.49	95.51	mud
0	G2	0.00	16.52	83.48	sandy mud
10	H6.7.15	0.00	21.21	78.79	sandy mud
15	H6.7.14	0.00	10.53	89.47	sandy mud
20	H6.7.13	0.00	9.81	90.19	sandy mud
25	H6.7.12	0.00	5.17	94.83	mud
30	H6.7.11	0.00	6.21	93.79	mud
35	H6.7.10	0.00	5.63	94.37	mud
40	H6..7.9	0.00	7.64	92.36	mud
45	H6.7.8	0.00	8.18	91.82	mud
50	H 6.7.7	0.00	13.74	86.26	sandy mud
55	H6.7.6	0.00	27.16	72.84	sandy mud
60	H6.7.5	0.00	30.41	69.59	sandy mud
65	H6.7.4	0.00	48.73	51.27	sandy mud
70	H6.7.3	0.00	30.80	69.20	sandy mud
75	H6.7.2	0.00	20.57	79.43	sandy mud
80	H6.7.1B	0.00	44.81	55.19	sandy mud
85	H6.7.1A	0.00	20.23	79.77	sandy mud
90	H6.6.20	0.00	46.44	53.56	sandy mud
95	H6.6.19	0.00	44.52	55.48	sandy mud
100	H6.6.18	0.00	32.72	67.28	sandy mud
105	H6.6.17	0.00	37.01	62.99	sandy mud
110	H6.6.16	0.00	46.94	53.06	sandy mud
115	H6.6.15	0.00	45.56	54.44	sandy mud
120	H6.6.14	0.00	43.20	56.80	sandy mud
125	H6.6.13	0.00	44.16	55.84	sandy mud
130	H6.6.12	0.00	46.34	53.66	sandy mud
135	H6.6.11	0.00	42.49	57.51	sandy mud
140	H6.6.10	0.00	34.22	65.78	sandy mud
145	H6.6.9	0.00	43.09	56.91	sandy mud
150	H6.6.8	0.00	41.03	58.97	sandy mud
155	H6.6.7	0.00	38.84	61.16	sandy mud
160	H6.6.6	0.00	36.20	63.80	sandy mud
165	H6.6.5	0.00	40.72	59.28	sandy mud
170	H6.6.4	0.00	38.25	61.75	sandy mud
175	H6.6.3	0.00	37.55	62.45	sandy mud
180	H6.6.2	0.00	30.74	69.26	sandy mud
185	H6.6.1	0.00	33.23	66.77	sandy mud
187.5	H6.5.20B	0.00	32.18	67.82	sandy mud
190	H6.5.20A	0.00	32.44	67.56	sandy mud
195	H6.5.19	0.00	39.59	60.41	sandy mud
200	H6.5.18	0.00	40.62	59.38	sandy mud
205	H6.5.17	0.00	42.57	57.43	sandy mud
210	H6.5.16	0.00	39.11	60.89	sandy mud
215	H6.5.15	0.00	29.04	70.96	sandy mud
220	H6.5.14	0.00	23.91	76.09	sandy mud
225	H6.5.13	0.00	33.83	66.17	sandy mud
230	H6.5.12	0.00	27.30	72.70	sandy mud
235	H6.5.11	0.00	22.85	77.15	sandy mud
240	H6.5.10	0.00	26.60	73.40	sandy mud
245	H6.5.9	0.00	27.72	72.28	sandy mud
250	H6.5.8	0.00	27.14	72.86	sandy mud
255	H6.5.7	0.00	26.73	73.27	sandy mud

260	H6.5.6	0.00	9.44	90.56	sandy mud
265	H6.5.5	0.00	12.97	87.03	sandy mud
270	H6.5.4	0.00	11.79	88.21	sandy mud
275	H6.5.3	0.00	23.48	76.52	sandy mud
280	H6.5.2	0.00	21.64	78.36	sandy mud
285	H6.5.1	0.00	41.36	58.64	sandy mud
290	H6.4.20	0.00	22.95	77.05	sandy mud
295	H6.4.19	0.00	24.14	75.86	sandy mud
300	H6.4.18	0.00	23.43	76.57	sandy mud
305	H6.4.17	0.00	13.76	86.24	sandy mud
310	H6.4.16	0.23	16.10	83.66	sandy mud
315	H6.4.15	0.00	17.18	82.82	sandy mud
320	H6.4.14	0.20	18.77	81.03	sandy mud
325	H6.4..13	0.00	15.73	84.27	sandy mud
330	H6.4.12	0.00	26.39	73.61	sandy mud
335	H6.4.11	0.00	33.85	66.15	sandy mud
340	H6.4.10	0.00	45.57	54.43	sandy mud
345	H6.4.9	0.00	44.23	55.77	sandy mud
350	H6.4.8	0.00	38.68	61.32	sandy mud
355	H6.4.7	0.00	37.92	62.08	sandy mud
360	H6.4.6	0.00	45.60	54.40	sandy mud
365	H6.4.5	0.00	50.20	49.80	muddy sand
370	H6.4.4	0.00	51.21	48.79	muddy sand
375	H6.4.3	0.00	53.82	46.18	muddy sand
380	H6.4.2	0.00	51.44	48.56	muddy sand
385	H6.6.1	0.00	50.59	49.41	muddy sand
390	H6.3.20	0.00	61.35	38.65	muddy sand
395	H6.3.19	0.00	58.26	41.74	muddy sand
400	H6.3.18	0.00	52.85	47.15	muddy sand
405	H6.3.17	0.00	40.05	59.95	sandy mud
410	H6.3.16	0.00	39.55	60.45	sandy mud
415	H6.3.15	0.00	49.35	50.65	sandy mud
420	H6.3.14	0.00	38.95	61.05	sandy mud
425	H6.3.13	0.00	51.10	48.90	sandy mud
430	H6.3.12	0.00	48.35	51.65	sandy mud
435	H6.3.11	0.13	29.39	70.48	sandy mud (g)
400	H6.3.10	0.00	16.45	83.55	sandy mud
445	H6.3.9	0.00	20.84	79.16	sandy mud
450	H6.3..8	0.00	28.62	71.38	sandy mud
455	H6.3.7	0.00	40.36	59.64	sandy mud
460	H63.6	0.00	41.66	58.34	sandy mud
465	H6.3.5	0.00	58.29	41.71	muddy sand
470	H6.3.4	0.00	66.79	33.21	muddy sand
475	H6.3.3	0.00	62.14	37.86	muddy sand
480	H6.3.2	0.00	50.60	49.40	muddy sand
485	H6.3.1	0.00	52.03	47.97	muddy sand
487.5	H6.2.20B	0.00	46.03	53.97	sandy mud
490	H6.2.20A	0.00	11.21	88.79	sandy mud
495	6.2.19	0.00	22.62	77.38	sandy mud
500	H6.2.18	0.00	25.11	74.89	sandy mud
505	H6.2.17	0.00	20.12	79.88	sandy mud
510	H6.2.16	0.72	20.36	78.92	sandy mud (g)
515	H6.2.15	0.00	20.06	79.94	sandy mud
520	H6.2.14	0.00	32.96	67.04	sandy mud
525	H6.2.13	0.00	54.11	45.89	muddy sand
530	H6.2.12	0.00	36.58	63.42	sandy mud

535	H6.2.11	0.00	40.80	59.20	sandy mud
540	H6.2.10	0.00	58.85	41.15	muddy sand
545	H6.2.9	0.00	48.18	51.82	sandy mud
550	H6.2.8	0.00	52.21	47.79	muddy sand
555	H6.2.7	0.00	57.91	42.09	muddy sand
560	H6.2.6	0.04	52.82	47.14	muddy sand (g)
565	H6.2.5	0.00	57.47	42.53	muddy sand
570	H6.2.4	0.11	61.23	38.66	muddy sand (g)
575	H6.2.3	0.06	56.14	43.80	muddy sand (g)
580	H6.2.2	0.38	58.51	41.11	muddy sand (g)
585	H6.2.1	0.00	66.76	33.24	muddy sand
595	H6.1.6	0.09	65.27	34.64	muddy sand (g)
600	H6.1.5	0.22	59.10	40.68	muddy sand (g)
605	H6.1.4	0.14	67.11	32.75	muddy sand (g)
610	H6.1.3	0.00	69.26	30.74	muddy sand
615	H6.1.2	0.32	60.65	39.03	muddy sand (g)
620	H6.1.1	0.19	55.62	44.19	muddy sand (g)
625	H6CC2	0.09	56.25	43.66	muddy sand (g)
630	H6CC1	0.00	62.78	37.22	muddy sand
Average	**Average**	**0.02**	**36.81**	**63.16**	**muddy sand (g)**

Key: (g) =slightly gravelly

APPENDIX G (7) TABLE OF PARTICLE SIZE OF SEDIMENT IN CORE H7

DEPTH (CM)	I.D. No.	Tot.gravel (%)	Tot.sand (%)	Tot silt & clay (%)	Silt (%)	cohesionless silt (%)	cohesive Silt (%)	clay (%)	Texture
0	H7.G2	0.00	5.09	94.91					
0	H7.G1	0.00	1.98	98.02					
5	H7.6.20	0.00	2.87	97.13	28.09	12.58	15.51	69.04	mud
10	H7.6.19	0.00	1.23	98.77	15.07	14.09	0.98	83.70	mud
11	H7.6.18	0.00	2.10	97.90	38.90	16.49	22.41	59.00	mud
20	H7.6.17	0.00	1.87	98.13	44.33	16.09	28.24	53.80	mud
25	H7.6.16	0.00	1.48	98.52	45.94	11.89	34.05	52.58	mud
30	H7.6.15	0.00	4.68	95.32	33.50	13.20	20.30	61.82	mud
35	H7.6.14	0.00	3.60	96.40	29.31	12.45	16.86	67.09	mud
40	H7.6.13	0.00	6.41	93.59	34.37	16.63	17.74	59.22	mud
45	H7.6.12	0.00	5.54	94.46	34.28	15.51	18.77	60.18	mud
50	H7.6.11	0.00	9.13	90.87	33.04	10.60	22.44	57.83	mud
55	H7.6.10	0.00	5.90	94.10	30.92	11.27	19.65	63.18	mud
60	H7.6.9	0.00	8.41	91.59	29.31	11.48	17.83	62.28	mud
65	H7.6.8	0.00	7.74	92.26	33.77	16.81	16.96	58.49	mud
70	H7.6.7	0 00	6.62	93.38	32.75	10.63	22.12	60.63	mud
75	H7.6.6	0.00	5 22	94.78	33.89	11.43	22.46	60.89	mud
80	H7.6.5	0.00	5.02	94.98	37.35	14.01	23.34	57.63	mud
85	H7.6.4	0.00	4.99	95.01	39.55	16.81	22.74	55.46	mud
90	H7.6.3	0.00	5.20	94.80	35.88	13.68	22.20	58.92	mud
95	H7.6.2	0.00	7.93	92.07	38.95	16.31	22.64	53.12	mud
100	H7.6.1	0.00	11.05	88.95	49.25	29.99	19.26	39.70	mud
105	H7.5.20	0.00	5.34	94.66	42.16	14.45	27.71	52.50	mud
110	H7.5.19	0.00	4.32	95.68	38.35	11.68	26.67	57.33	mud
115	H7.5.18	0.00	1.33	98.67	42.29	16.72	25.57	56.38	mud
120	H7.5.17	0.00	4 04	95.96	41.90	16.57	25.33	54.06	mud
125	H7.5.16	0.00	5.61	94.39	34.54	11.60	22.94	59.85	mud
130	H7.5.15	0.00	4.89	95.11	36.90	14.51	22.39	58.21	mud
135	H7.5.14	0.00	4.45	95.55	37.28	11.81	25.47	58.27	mud
140	H7.5.13	0.00	7.26	92.74	33.85	10.22	23.63	58.89	mud
145	H7.5.12	0.00	8.67	91.33	38.76	12.72	26.04	52.57	mud
150	H7.5.11	0 00	10.11	89.89	32 39	19.54	12.85	57.50	mud
155	H7.5.10	0.00	8.12	91.88	34.08	13.68	20.40	57.80	mud
160	H7.5.9	0.00	4.23	95.77	37.93	11.35	26.58	57.84	mud
165	H7.5.8	0.00	9.33	90.67	33.70	12.35	21.35	56.97	mud
170	H7.5.7	0.00	9.79	90.21	32.69	10.65	22.04	57.52	mud
175	H7.5.6	0.00	9.02	90.98	34.04	12.66	21.38	56.94	mud
180	H7.5.5	0.00	6.55	93.45	35.45	11.92	23.53	58.00	mud
185	H7.5.4	0.00	5.94	94.06	33.92	12.26	21.66	60.14	mud
190	H7.5.3	0.00	5.55	94.45	32.96	11.32	21.64	61.49	mud
195	H7.5.2	0.00	4.75	95.25	36.73	11.44	25.29	58.52	mud
200	H7.5.1	0.00	4.08	95 92	34.55	11.85	22.70	61.37	mud
205	H7.4.20	0.00	4.36	95.64	33.88	9.47	24.41	61.76	mud
210	H7.4.19	0.00	1.74	98.26	35.45	11.01	24.44	62.81	mud
215	H7.4.18	0.00	5.32	94.68	29.10	9.12	19.98	65.58	mud
220	H7.4.17	0.07	6.38	93.54	29.13	13.39	15.74	64.41	mud (g)
225	H7.4.16	0 00	6.18	93.82	31.61	11.44	20.17	62.21	mud
230	H7.4.15	0.00	7.41	92.59	36.51	13.15	23.36	56.08	mud
235	H7.4.14	0.00	8.34	91.66	35.61	13.29	22.32	56.05	mud
240	H7.4.13	0.00	6.44	93.56	30.87	10.97	19.90	62 69	mud
245	H7.4.12	0.00	6.89	93 11	35.80	12.23	23.57	57.31	mud
250	H7.4.11	0.00	6.23	93.77	36.35	14.25	22.10	57.42	mud
255	H7.4.10	0.00	4.87	95.13	20.53	12.48	8 05	74.60	mud
260	H7.4.9	0 00	3.65	96 35	27.18	5.00	22.18	69.17	mud
265	H7.4.8	0.00	1.13	98.87	26 63	4.74	21.89	72.24	mud
270	H7.4.7	0.00	2.35	97.65	27.69	4.67	23.02	69.96	mud
275	H7.4.6	0.00	2.60	97.40	35.37	10.71	24.66	62.03	mud
280	H7.4.5	0.00	2.48	97.52	29.95	10.85	19.10	67.57	mud
285	H7.4.4	0.00	2.43	97.57	39 99	11.70	28.29	57.58	mud
290	H7.4.3	0 00	2.09	97.91	40 22	10.95	29 27	57.69	mud
295	H7.4.2	0.00	1.73	98.27	45.59	20.20	25.39	52.68	mud
300	H7.4.1	0.11	1.87	98.02	40.22	17 37	22.85	57.80	mud (g)
305	H7.3.20	0.06	2.45	97.48	46.23	24.46	21.77	51.25	mud (g)
310	H7.3.19	0 00	2.35	97.65	46.31	24.50	21.81	51.34	mud
315	H7.3.18	0.00	1.44	98.56	47.48	24.41	23.07	51.08	mud
320	H7.3.17	0.00	0.95	99.05	49.40	22.81	26.59	49.65	mud
325	H7.3.16	0 00	1.04	98.96	44.17	20.16	24.01	54.79	mud
330	H7.3.15	0 00	0.73	99.27	41.04	9 83	31.21	58.23	mud
335	H7.3.14	0.00	1.42	98.58	39.54	13.39	26.15	59.04	mud
340	H7.3.13	0.00	1.19	98.81	41.27	16.30	24.97	57.54	mud
345	H7.3.12	0.00	2.60	97.40	32.74	13.26	19.48	64.66	mud
350	H7.3.11	0.00	2.99	97.01			0.00	97.01	mud
355	H7.3.10	0.15	3 90	95.96			0.00	95.96	mud (g)
360	H7.3 9	0.17	4.24	95.59			0.00	95.59	mud (g)
365	H7.3.8	0.20	2.85	96 95			0.00	96.95	mud (g)

370	H7.3.7	0.00	22.28	77.72			0.00	77.72	mud
375	H7.3.6	0.00	2.34	97.66			0 00	97.66	mud
380	H7.3.5	0.00	4.34	95.66			0.00	95.66	mud
385	H7.3.4	0.00	4 41	95.59			0.00	95.59	mud
390	H7.3.3	0.00	6 03	93.97			0.00	93.97	mud
395	H7.3.2	0.25	3.18	96.56	27.61	11.24	16.37	68.95	mud (g)
400.	H7.3.1	0.00	1.07	98.93	47.41	21.60	25.81	51.52	mud
402.5	H7.2.20b	0.00	2.27	97.73	38.45	12.91	25.54	59.28	mud
405	H7.2.20a	0.00	1.17	98.83	45.65	15.20	30.45	53.18	mud
410	H7.2.19	0.04	2.35	97.61	39.87	12.73	27.14	57.74	mud (g)
415	H7.2.18	0.00	1.91	98.09			0.00	98.09	mud
420	H7.2.17	0.00	3.04	96.96	32.39	9 83	22.56	64.57	mud
425	H7.2.16	0.00	3.36	96.64	31.34	9.29	22.05	65.30	mud
430	H7.2.15	0.13	4.84	95.03	30.69	8.77	21.92	64.34	mud (g)
435	H7.2.14	0.00	8.67	91.33	31.03	9.53	21.50	60.30	mud
440	H7.2.13	0.06	5.74	94.20	33.73	11.73	22.00	60.47	mud (g)
445	H7.2.12	0.48	7.48	92.04	11.16	6.00	5.16	80.88	mud (g)
450	H7.2.11	0.00	13.36	86.64			0.00	86.64	mud
455	H7.2.10	0.00	5.59	94.41			0.00	94.41	mud
460	H7.2.9	0.00	7.30	92.70			0.00	92.70	mud
465	H7.2.8	0.03	10.84	89.13			0.00	89.13	mud (g)
470	H7.2.7	0.00	18.68	81.32	34.85	12.01	22.84	46.47	mud
475	H7.2.6	0.25	9.33	90.42	34.28	13.73	20.55	56.14	mud (g)
480	H7.2.5	0.00	10.72	89.28			0.00	89.28	mud
485	H7.2.4	0.00	4.87	95.13	34.42	11.59	22.83	60.71	mud
490	H7.2.3	0.00	4.91	95.09			0.00	95.09	mud
495	H7.2.2	0.00	6.16	93.84	34.45	14.21	20.24	59.39	mud
500	H7.2.1	0.00	8.84	91.16	36.21	15.87	20.34	54.95	mud
502.5	H7.1.20a	0.00	11.51	88.49	46.65	15.94	30.71	41.84	mud
505	H7.1.20b	0.00	7.33	92.67	48.14	16.01	32.13	44.53	mud
507.5	H7.1.19b	0.00	6.35	93.65	47.26		47.26	46.39	mud
510	H7.1.19a	0.44	8.60	90.95			0.00	90.95	mud (g)
515	H7.1.18	0.19	7.18	92.64			0.00	92.64	mud (g)
520	H7.1.17	0.00	10.66	89.34			0.00	89.34	mud
525	H7.1.16	0.45	6.67	92.89			0.00	92.89	mud (g)
530	H7.1.15	0.00	3.78	96.22	44.14	18.58	25.56	52.08	mud
535	H7.1.14	0.00	8.96	91.04	38.66	13.48	25.18	52.38	mud
540	H7.1.13	0.00	12.90	87.10	44.70	14.89	29.81	42.40	mud
545	H7.1.12	0.00	7.19	92.81	41.57	17.60	23.97	51.24	mud
550	H7.1.11	0.52	9.67	89.81	43.17	16.25	26.92	46.64	mud (g)
555	H7.1.10	0.00	7.58	92.42			0.00	92.42	mud
560	H7.1.9	0.00	8.50	91.50			0.00	91.50	mud
565	H7.1.8	0.14	4.94	94.92			0.00	94.92	mud (g)
570	H7.1.7	0.00	8.85	91.15			0.00	91.15	mud
575	H7.1.6	0.00	4.97	95.03			0.00	95.03	mud
580	H7.1.5	0.00	8.45	91.55			0.00	91.55	mud
585	H7.1.4	0.00	7.56	92.44			0.00	92.44	mud
590	H7.1.3	0.00	12.14	87.86			0.00	87.86	mud
595	H7.1.2	0.00	4.63	95.37			0.00	95.37	mud
600	H7.1.1	0.00	6.50	93.50			0.00	93.50	mud
605	H7CC2	0.00	9.30	90.70			0.00	90.70	mud
610	H7CC1	0.00	6.07	93.93			0.00	93.93	mud
615	H7CE	0.00	3.72	96.28			0.00	96.28	mud
	Average	**0.03**	**5.70**	**94.27**	**36.31**	**13.66**	**16.83**	**67.44**	**mud (g)**

Key: (g) =slightly gravelly